ELECTRO-OPTIC ARCHITECTURE (EOA) FOR SENSORS AND ACTUATORS IN AIRCRAFT PROPULSION SYSTEMS

FINAL TECHNICAL REPORT

by
W. L. Glomb, Jr.

June 1989

United Technologies Research Center
East Hartford, CT 06108

Prepared for
NASA-Lewis Research Center
Cleveland, OH 44135
NASA Contract # NAS3-25343

1. Report No.	2. Government Accession No.	3. Recipient's Catalog No.
NASA CR 182270		

4. Title and Subtitle	5. Report Date
Electro-Optic Architecture (EOA) for Sensors and Actuators in Aircraft Propulsion Systems	April 1989
	6. Performing Organization Code

7. Author(s)	8. Performing Organization Report No.
W. L. Glomb, Jr.	UTRC R89-927889
	10. Work Unit No.

9. Performing Organization Name and Address	11. Contract or Grant No.
United Technologies Research Center East Hartford, CT 06108	NAS3-25343
	13. Type of Report and Period Covered Final Report April 1988 - January 1989
12. Sponsoring Agency Name and Address	14. Sponsoring Agency Code
National Aeronautics and Space Administration Lewis Research Center Cleveland, OH 44135	

15. Supplementary Notes

NASA Project Manager: Mr. Robert Baumbick

16. Abstract

This report describes results of a study to design an optimal architecture for electro-optical sensing and control in advanced aircraft and space systems. The propulsion full authority digital Electronic Engine Control (EEC) was the focus for the study.

The recommended architecture is an on-engine EEC which contains electro-optic interface circuits for fiber-optic sensors on the engine. Size and weight are reduced by multiplexing arrays of functionally similar sensors on a pairs of optical fibers to common electro-optical interfaces. The architecture contains common, multiplex interfaces to seven sensor groups: (1) self luminous sensors; (2) high temperatures; (3) low temperatures; (4) speeds and flows; (5) vibration; (6) pressures; and (7) mechanical positions. Nine distinct fiber-optic sensor types were found to provide these sensing functions: (1) CW intensity modulators; (2) TDM digital optic codeplates; (3) TDM analog self-referenced sensors; (4) WDM digital optic code plates; (5) WDM analog self-referenced intensity modulators; (6) analog optical spectral shifters; (7) self-luminous bodies; (8) coherent optical interferometers; and (9) remote electrical sensors.

The report includes the results of a trade study including engine sensor requirements, environment, the basic sensor types and relevant evaluation criteria. These figures of merit for the candidate interface types were calculated from the data supplied by leading manufacturers of fiber-optic sensors.

17. Key Words (Suggested by Author(s))	18. Distribution Statement
Fiber Optic Sensors, Fly-by-Light, Digital Electronic Control Electronic Engine Control Optic Multiplex	Unclassified - unlimited

19. Security Classif. (of this report)	20. Security Classif. (of this page)	21. No. of pages	22. Price*
Unclassified	Unclassified		

*For sale by the National Technical Information Service, Springfield, Virginia 22161

ACKNOWLEDGEMENT

The author gratefully acknowledges the important contributions from individuals at United Technologies and the fiber-optic sensor suppliers. Jim Birdsall and Bob Bartle at Pratt & Whitney provided engine requirements and guidance in establishing the evaluation criteria. Tony Martin was instrumental in establishing links with technical specialists at Hamilton Standard. At United Technologies Research Center, Paul Suchoski and Bruce Hockaday contributed the studies of optical switch technology. Bruce Hockaday also contributed descriptions of the Opto-Hydraulic Servovalve. Denise Francis provided input on coherent optical sensors. Deepak Varshneya at Teledyne Ryan Electronics contributed a design for digital optical time division multiplex. Randy Morton, Tom Lindsay, and Bill Little at Eldec provided descriptions of analog optic sensors and remote electronic sensors. Norris Lewis and Mike Miller at Litton Polyscientific contributed designs for optical wavelength multiplex sensors and networks.

NASA Contract # NAS3-25343

Electro-Optic Architecture (EOA) for Sensors and Actuators in Aircraft Propulsion Systems

TABLE OF CONTENTS

TABLE OF CONTENTS (continued)

LIST OF TABLES

LIST OF FIGURES

1.0 SUMMARY

This report describes results of a study by the United Technologies Research Center (UTRC) to design a preferred architecture for electro-optical sensing and control in advanced aircraft and space systems. The propulsion full authority digital Electronic Engine Control (EEC) was the focus for the study. Consideration of this system provided a concrete example for evaluation of a variety of sensors and multiplexing techniques. Unlike earlier studies, the emphasis of this program was on the EEC interface design rather than on the transducer technology itself. UTRC evaluated a variety of electro-optic architectures and completed a conceptual design of an all-optic aircraft propulsion control system by: establishing criteria for the comparative evaluation of various optic architectures; identifying and characterizing candidate optic systems; then selecting an overall architecture for optical sensing and control.

The subject of the study was the sensor complement for the EEC on an advanced technology military turbine engine with variable turbine geometry, variable nozzle geometry, and a 2-D thrust vectoring nozzle. The program considered the variety of multiplexing techniques which can be employed to interconnect a number of sensors on a single optical fiber. These were compared on the basis of criteria relevant to EEC design. Based on tabulation of these criteria, a preferred architecture was selected. The goal was to select the best minimal set of interface types, the assignment of sensors to interfaces, and to determine the hierarchy of coding or multiplexing methods.

The recommended architecture is an on-engine EEC which contains electro-optic interface circuits for fiber-optic sensors on the engine. Size and weight are reduced by multiplexing arrays of functionally similar sensors on a pairs of optical fibers to common electro-optical interfaces. The architecture contains common, multiplex interfaces to seven sensor groups: (1) self luminous sensors; (2) high temperatures; (3) low temperatures; (4) speeds and flows; (5) vibration; (6) pressures; and (7) mechanical positions. Nine distinct fiber-optic sensor types were found to provide these sensing functions: (1) CW intensity modulators; (2) TDM digital optic codeplates; (3) TDM analog self-referenced sensors; (4) WDM digital optic code plates; (5) WDM analog self-referenced intensity modulators; (6) analog optical spectral shifters; (7) self-luminous bodies; (8) coherent optical interferometers; and (9) remote electrical sensors.

The report includes the results a trade study including engine sensor requirements, environment, the basic sensor types and relevant evaluation criteria. These figures of merit for the candidate interface types were calculated from the data supplied by leading manufacturers of fiber-optic sensors.

In most areas little or no significant difference could be discerned between the candidate sensing methods. The areas in which there is some discrimination are the types of sensors which can be accommodated, the effectiveness of drift compensation, the numbers of sources and detectors required, the optical power margin, the number of multiplex channels, and reliability. However in most of these areas the differences between designs is not great. These results indicate that a flight demonstration/validation is needed to determine preferred optical modulation methods for an electro-optic architecture. Such a program would provide more realistic on-engine performance data

and may reveal discriminators to guide the selection of a preferred architecture. Section 5 of this report describes a configuration of the electro–optic sensor interfaces that is suited to a flight test program.

2.0 INTRODUCTION

Optical fibers have been proposed for signal paths in aerospace propulsion and flight controls as a means to achieve electromagnetic immunity, to reduce control system weight, and to provide advanced sensing functions not available in electronic systems. Optical fiber data busses and a broad array of sensors have been developed for this application (refs. 1–8). The use of fiber–optic technology in these applications is motivated by the weight of large cable harnesses and by problems with signal transmission through electrical cables, poor contacts at connectors, electrical shorts, lightning, and the need for improved sensors for advanced control and condition monitoring. In view of these potential benefits to aerospace systems the subject study was required to determine the preferred architecture for the application of optics to aircraft. The propulsion system full authority digital electronic engine control was the focus for the study. The engine control includes a variety of sensors that provide a concrete vehicle for evaluation of a variety of sensors and multiplexing techniques.

Starting points for the study were the conceptual designs and fiber–optic sensors for the engine control system identified in the previous FOCSI and FACTS engine study programs (refs. 6–8). This program considered the variety of techniques which can be employed to interface to a number of sensors on an optical fiber. The goal was to select the best minimal set of interface types, the preferred assignment of sensors to interfaces, and to determine the hierarchy of coding or multiplexing methods. The fiber–optic sensor and multiplexing technologies were compared on the basis of criteria set by the engine manufacturer. Based on tabulation of these criteria, a preferred architecture is suggested to optimize these criteria.

A six–member team was assembled to include first–hand expertise in a variety of optical sensor and networking technologies including wavelength division multiplexing, time division multiplexing, fiber–optic couplers, linear optic data bus, integrated optics, and coherent sensors as well as knowledge of advanced engine control and diagnostic systems. This team included the propulsion and research divisions of United Technologies Corporation: Pratt & Whitney, Hamilton Standard, and the Research Center; along with leading vendors of fiber–optic sensors, namely Teledyne Ryan Electronics, Litton Polyscientific, and Eldec. The work drew heavily from fiber–optic technology assessments and conceptual designs done by the individual team members in previous Government and internal studies. Among these were FOCSI, Helicopter Subsystems, Advanced ADOCS, and commercial engine control programs as well as the experiences of Teledyne Ryan, Litton Polyscientific, and Eldec in production of fiber–optic sensors and networks.

Each team member contributed unique knowledge and experience to the effort. UTRC managed the program, assembled the trade study, tabulated the trade factors and issued the final report. UTRC also provided experience with advanced optical sensor and processor technologies, especially coherent systems, integrated optics, and environmental effects on electro–optic components. Pratt & Whitney contributed specifications and requirements for next generation aircraft engine controls. The three fiber–optic sensor manufacturers contributed data on the size, weight, producibility, and relative cost factors for the specified sensors.

2.1 Engine Sensor Requirements

This section presents the requirements for the electro-optic architecture. The types and numbers of sensors on the engine are specified and criteria for comparison of the various electro-optic architectures are defined.

The subject of this study was the sensor complement for the EEC on an advanced technology military turbine engine with variable turbine geometry, variable nozzle geometry, and a 2-D thrust vectoring nozzle. For this program an effort was made to identify common sensor ranges and accuracies for a composite of advanced engine designs. Shown in Table 2.1-1 are generic sensor requirements derived in this manner. The system includes a total of 44 sensors for the following measurements: 19 linear positions, 1 rotary position, 7 temperatures, 6 fuel flows, 3 gas pressures, 1 hydraulic pressure, 1 fuel pressure, 2 rotary speeds, 1 flame light off detector, 1 vibration, and 2 fluid level.

The accuracies shown in the table are for the complete sensor including the interface electronics. The operating temperatures for the sensors are generally higher than those considered in previous studies: -54 to 230 C ambient air temperature, with transients to 300 C. The high temperature represents operation during a supersonic dash. The duration at this temperature extreme will get longer for supersonic cruise. The temperatures at specific sensor locations are shown in the table. The sensor interface electronics, including the optical sources, detectors, and filters must operate on a heat sink temperature ranging from -54 to 125 C. The ambient temperatures specified for the optical sensors are representative of current aircraft. This leaves just two temperature ranges for sensors on the engine: -54 to + 200 C for the inlet, fan and compressor regions; and -54 to + 350 C for the burner, turbine, augmenter, and exhaust nozzle. For a more extensive discussion of sensor requirements the reader is referred to the FOCSI and FACTS reports (refs. 6-8).

Two sets of criteria will be considered for evaluation of electro-optic architectures: (1) sensor interface design features and (2) system impacts. The sensor design criteria are listed in Table 2.1-2. These features are meant to indicate the scalability, and operating margin of the candidate approaches. In addition to these circuit-level criteria, the candidates will be judged on the system impacts in Table 2.1-3. These represent the most important system qualities identified in previous EEC technology development programs. In selecting the preferred system, both system level criteria 1 and circuit level criteria were considered.

TABLE 2.1-1 - EEC SENSOR SET (SINGLE CHANNEL, NO REDUNDANCY)

Number of Sensors	Measurement	Update Time	Accuracy	Range	Ambient
4	Linear position	5 ms	± 0.36 cm	0 to 36 cm	-54 to 200 C
2	Linear position	10 ms	± 0.26 cm	0 to 26 cm	-54 to 200 C
4	Linear position	5 ms	± 0.18 cm	0 to 18 cm	-54 to 200 C
2	Linear position	10 ms	± 0.09 cm	0 to 9 cm	-54 to 200 C
5	Linear position	5 ms	± 0.05 cm	0 to 5 cm	-54 to 200 C
2	Linear position	10 ms	± 0.05 cm	0 to 5 cm	-54 to 200 C
1	Rotary position	10 ms	± 0.2 deg	0 to 130 deg	-54 to 200 C
1	Gas temperature	120ms	± 2 C	-54 to 260 C	-54 to 200 C
4	Gas temperature	20 ms	± 11 C	0 to 1500 C	0 to 350 C
1	Fuel temperature	120 ms	± 3 C	-54 to 180 C	-54 to 200 C
1	Turbine blade temperature	20 ms	± 10 C	500 to 1500 C	-54 to 350 C
1	Light off detector	20 ms	± 5 %	< 290 nm (optical wavelength)	-54 to 350 C
3	Fuel flow	10 ms	± 100 kg/hr	200 to 6000 kg/hr.	-54 to 200 C
3	Fuel flow	40 ms	± 100 kg/hr	5000 to 16000 kg/hr. (1 inch diameter)	-54 to 200 C
1	Gas pressure	10 ms	± 4.0 kPa	7 to 830 kPa	-54 to 350 C
1	Gas pressure	120 ms	± 1.0 kPa	7 to 280 kPa	-54 to 200 C
1	Gas pressure	10 ms	± 40 kPa	35 to 5000 kPa	-54 to 350 C
1	Hydraulic pressure	40 ms	± 40 kPa	500 to 8000 kPa	-54 to 200 C
1	Fuel pressure	120 ms	± 40 kPa	0 to 690 kPa	-54 to 200 C
1	Rotary speed	10 ms	± 7 rpm	650 to 16000 rpm	-54 to 200 C
1	Rotary speed	10 ms	± 7 rpm	1600 to 19000 rpm	-54 to 200 C
1	Vibration	120 ms	± 2.5 g	0 to 50 g (10 Hz to 1 kHz)	-54 to 350 C
2	Fluid Level	120 ms	± 2 %		-54 to 200 C

TABLE 2.1-2 – CIRCUIT FEATURES

1. Optical power margin (dB)
2. Signal processing time (microseconds)
3. Complexity (number of circuit elements)
4. Number of channels
5. Number of distinct sources
6. Number of detectors
7. Number of fibers
8. Types of sensors
9. Signal compensation or calibration
10. Redundancy

TABLE 2.1-3 – SYSTEM FEATURES

1. Weight (lbs)
2. Reliability (failures per million hours)
3. Maintainability
4. I/O circuit area (square inches)
5. I/O pincount
6. EMI immunity (dB attenuation)
7. Power consumption (Watts)
8. Availability or development schedule (months or years)

For comparison each candidate was assigned a quantitative measure for each criterion (such as size in square inches, power in watts, complexity in number of components and software operations, power margin in dB, or reliability in failures per million hours) based on the state of the art forecast for the late 1990's. The preferred methods of optical modulation will be those having the best overall measures.

2.2 The Present Electronic Sensor Architecture

A prerequisite to the comparative study of novel electro-optic architectures is an understanding of the existing electronic sensor interfaces. The present electronic architecture has evolved to economically and reliably meet the control requirements. Therefore it serves to illustrate key aspects of the problem. A key feature of this architecture is that signals of a common type are multiplexed through a single digital interface. The engine parameter interfaces are comprised of three main groups: frequency type signals, analog signals, and LVDT/resolver signals. Each of these groups is interfaced to the EEC processor through a common decoder and digitizer block as shown in figure 2.2-1. This electronic architecture provides a guide to developing an electro-optic architecture.

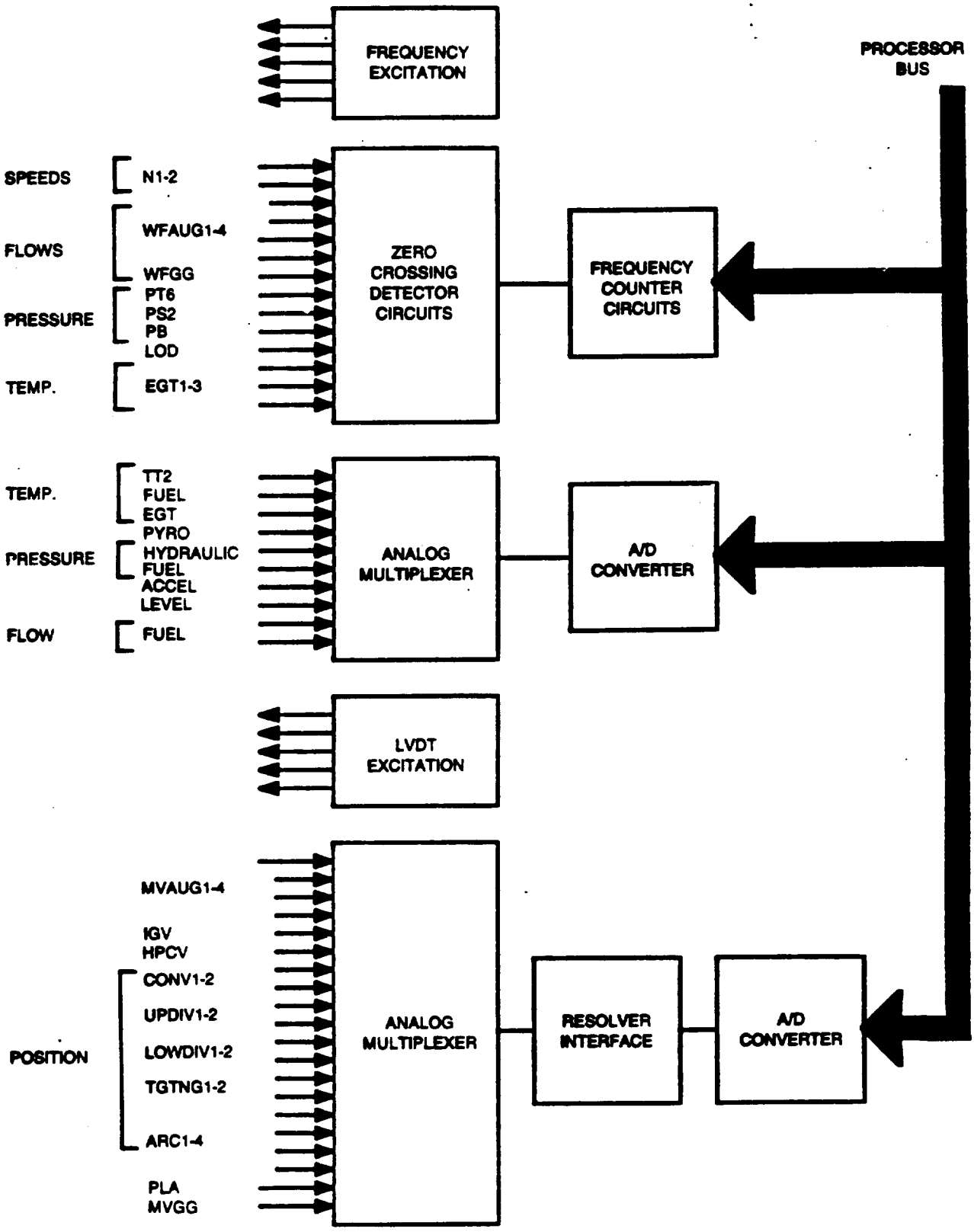

Figure 2.2-1. – EEC electronic sensor input interfaces.

The electronic architecture allows for a variety of sensor output types, and for different applications, a particular quantity may be sensed in different ways. For example, some flows and temperatures are sensed as frequencies while others are sensed as analog levels. Likewise, it is reasonable to expect some variety of interface types in the electro-optic sensor architecture.

The control processor in the electro-optical control system will continue to be a central digital electronic computer so the electro-optic interfaces must convert the sensor signals from the optic domain to digital values on the processor bus, just as is done by the present electronic system. The electronic architecture features multiplexing techniques to achieve system economy in electronic circuit size and power consumption. A part of the electro-optic design is to develop techniques which move the multiplex function out of the electronic enclosure, off of the electronic circuit boards and out into the fiber- optic network. The motivations for this change in the architecture are (1) reduction in I/O pincount on the electronic enclosure and (2) lack of suitable optical switches to replace the analog electronic multiplexers. The EEC then contains a multiplex decoder/electro-optic demultiplexer in place of the analog electronic multiplexers to convert the optical multiplex format into a low speed serial electronic sequence.

2.3 Strawman Fiber-Optic System Designs

Strawman electro-optic architectures for the EEC sensors and actuators were defined according to the guidelines in Appendix A. These were based on: pulse time delay multiplexing, wavelength coding or multiplexing, local electrical power, normalized analog ratiometric transduction, and coherent optical techniques. UTRC provided designs for coherent systems, and optic switches. Teledyne Ryan Electronics designed a time delay multiplex system. Litton Polyscientific designed a wavelength division multiplex system. Eldec contributed designs for analog sensors and remote electric power.

Teledyne Ryan Electronics report no. TRE/SD29065-21 entitled "Time Division Multiplexed NASA Electro-Optic System Architecture for Advanced Aircraft Engines" is attached as Appendix B. The report describes an electro-optical architecture that may be used to service all engine sensors using optical time division multiplexing (TDM). The sensors are separated into six sub groups according to sensing concept. Each of the six subgroups has separate transmitters, receivers, and a data pre-processor to present data to the controller in a common parallel digital format. Position sensing and fluid level measurements (21 measurements in all) are performed with digital optical code plates on a common electro-optical interface. Pressure and fluid flow measurements use microbend sensors on a common analog interface. Turbine blade temperature, light-off, vibration, and engine speeds each require a separate interface.

Eldec report no. 011-0880-701 entitled "Electro-Optic Architecture Study for Advanced Aircraft Sensing Systems" is presented in Appendix C. The report describes two architectures: one based on electrically active sensors with fiber optic signal communication; the other based on passive fiber-optic sensors using time domain intensity normalization (TDIN). The electrically active approach is comprised of conventional sensors with local electrical power (such as a battery or a photocell) and electronic circuitry. The sensor circuits transmit digitally coded parameter values from the sensors to the EEC through optical fibers. There are no electrical attachments to the sensors.

The TDIN architecture described by ELDEC uses a pulse TDM method to analyze the intensity of the light returned from a sensor to determine the measurand. Therefore, all sensors in the architecture are intensity modulated types. In operation, a pulse is sent to each sensor where it is separated into two legs, a sensor leg and a reference leg. A delay line is included in one of the legs. The pulses are reflected and recombined on the return link to the EEC interface where the ratio of the pulse amplitudes provides a normalized measure of the intensity modulation in the sensor. The TDIN technique compensates for variations in link transmission and provides a common interface technique for all intensity type sensors. TDIN is best suited to the moderate accuracy, static measurands: position, temperature, and pressure given the availability of suitably designed optical intensity modulators.

A Litton Polyscientific report titled "Fiber Optic Wavelength Division Multiplexing Sensor Techniques in Aircraft Engine Control Systems" is attached as Appendix D. The report describes the design of sensors for position, speed, pressure, and temperature. The position sensors are based on wavelength multiplexing the tracks of a digital transmissive optical code plate onto a single optical fiber. The speed sensor is based on sensing the frequency of reflections from a pattern on the rotating part. The pressure and temperature sensors are based on analog wavelength coding scheme. The excitation to the sensors is comprised of banks of light emitting diodes combined to form optically broadband sources. The receiver proposed for the wavelength sensors is a CCD detector on a fiber, lens, and grating assembly.

These reports form the basis for the system analysis presented in the following sections of this report.

2.4 The Electro-Optic Architecture (EOA) for Propulsion Control

The propulsion EOA sensor network is illustrated in figure 2.4-1. The recommended architecture is an on-engine EEC which contains electro-optic interface circuits for fiber-optic sensors on the engine. The purpose of this design is to reduce the size and weight attributed to inputs and outputs by multiplexing arrays of functionally similar sensors on a single pair of optical fibers through common electro-optical interfaces.

Sensors interface to the engine control computer through electro-optic circuit boards contained in the EEC enclosure. These circuits feature passive optical multiplex of groups of sensors through a common electro-optic interface. The internal architecture proposed for the EEC is illustrated in figure 2.4-2 where the sensor and actuator interface boards are shown connected to the control processor bus. Each interface is standardized to multiplex a set number of measurements of a given parameter through a single circuit card in a modular mechanical design. Each multiplexed sensor interface would include a CPU bus interface, sensor decoder, electro-optic interface (LED or photodiodes) and power conditioning. To meet the stringent size constraints in the boxes the electro-optic interfaces themselves would be fabricated in pigtailed fiber-optic hybrid packages.

Each optic sensor interface type is suited to a subset of the EEC sensor complement. The sensor circuits are comprised of the seven standard EO interface types shown in Table 2.4-1.

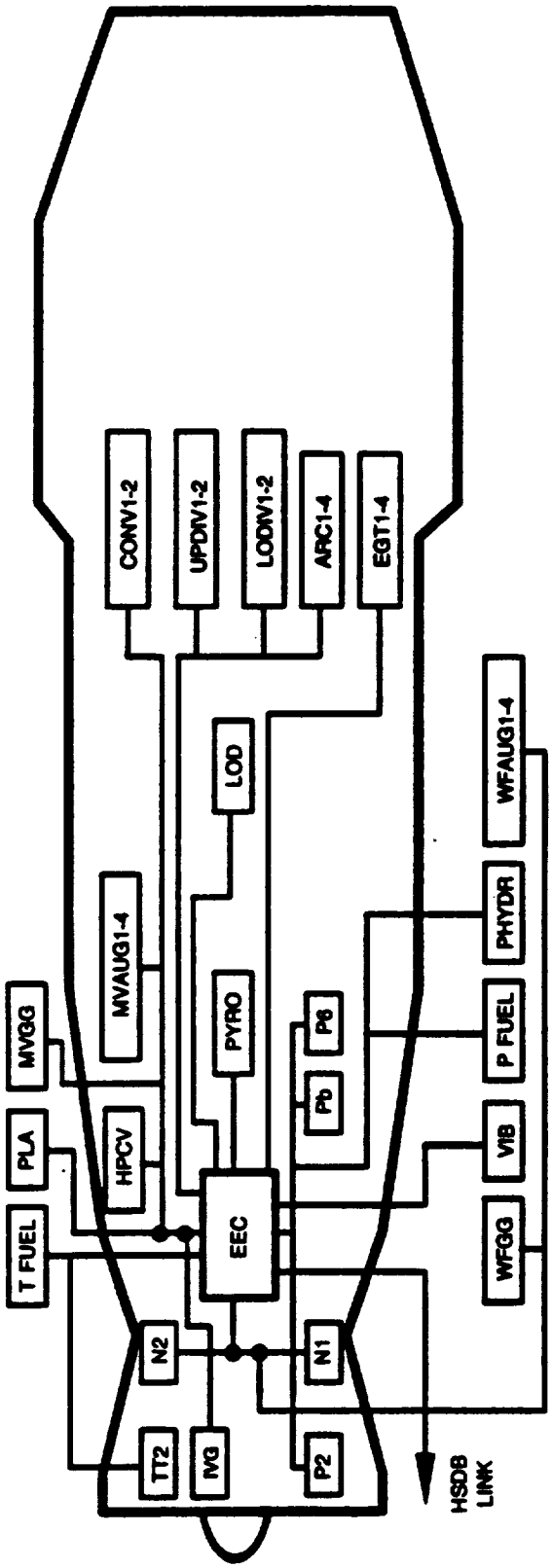

Figure 2.4-1. — The engine EOA features an engine-mounted EEC with multiplexed fiber-optic sensors and a fiber-optic data bus link.

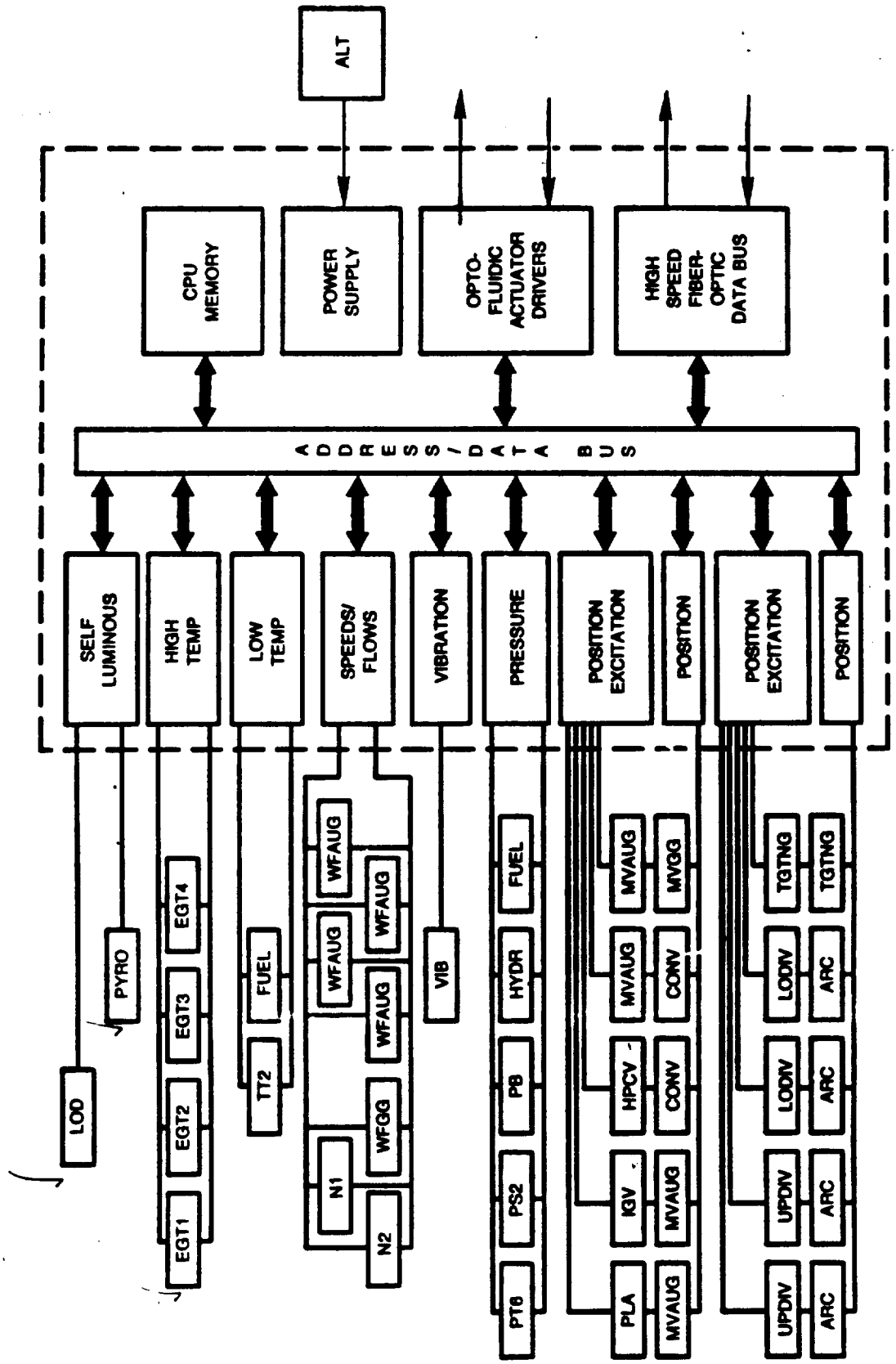

Figure 2.4-2. — The EEC EOA includes multiplex fiber-optic sensor interfaces to 8 sensor groups.

TABLE 2.4-1 - EOA SENSOR GROUPS

Number of Sensors	Measurement	Update Time	Accuracy	Range	Sensor Ambient
Self luminous sensor interface: (2 parameters)					
1	Turbine blade temp	20 ms	± 10 C	500 to 1500 C	-54 to 350 C
1	Light off detector	20 ms	± 5 %	< 290 nm	-54 to 350 C
High temperature sensor interface: (4 parameters)					
4	Gas temperature	20 ms	± 11 C	0 to 1500 C	0 to 350 C
Low temperature sensor interface: (2 parameters)					
1	Gas temperature	120 ms	± 2 C	-54 to 260 C	-54 to 200 C
1	Fuel temperature	120 ms	± 3 C	-54 to 180 C	-54 to 200 C
Speed and flow sensor interface: (8 parameters)					
1	Rotary speed	10 ms	± 7 rpm	650 to 16000 rpm	-54 to 200 C
1	Rotary speed	10 ms	± 7 rpm	1600 to 19000 rpm	-54 to 200 C
3	Fuel flow	10 ms	± 100 kg/hr	200 to 6000 kg/hr.	-54 to 200 C
3	Fuel flow	40 ms	± 100 kg/hr	5000 to 16000 kg/hr	-54 to 200 C
Vibration sensor interface: (1 parameter)					
1	Vibration	120 ms	± 2.5 g	0 to 50 g (10 Hz to 1 kHz)	-54 to 350 C
Pressure sensor interface: (5 parameters)					
1	Gas pressure	10 ms	± 4.0 kPa	7 to 830 kPa	-54 to 350 C
1	Gas pressure	120 ms	± 1.0 kPa	7 to 280 kPa	-54 to 200 C
1	Gas pressure	10 ms	± 40 kPa	35 to 5000 kPa	-54 to 350 C
1	Hydraulic pressuure	40 ms	± 40 kPa	500 to 8000 kPa	-54 to 200 C
1	Fuel pressure	120 ms	± 40 kPa	0 to 690 kPa	-54 to 200 C
Five Position sensor interfaces: (22 parameters total)					
4	Linear position	5 ms	± 0.36 cm	0 to 36 cm	-54 to 200 C
4	Linear position	5 ms	± 0.18 cm	0 to 18 cm	-54 to 200 C
2	Linear position	10 ms	± 0.26 cm	0 to 26 cm	-54 to 200 C
2	Linear position	10 ms	± 0.09 cm	0 to 9 cm	-54 to 200 C
5	Linear position	5 ms	± 0.05 cm	0 to 5 cm	-54 to 200 C
2	Linear position	10 ms	± 0.05 cm	0 to 5 cm	-54 to 200 C
1	Rotary position	10 ms	± 0.2 deg	0 to 130 deg	-55 to 200 C
2	Fluid level	120 ms	± 2 %		-54 to 200 C

The turbine blade temperature sensor and the flame light-off detector (LOD) both require an interface to self luminous fiber-optic sensors. The LOD self luminous sensor interface requires a

detector with 170 nm to 290 nm passband multiplexed to an A/D converter. The turbine blade pyrometer requires a near infra-red dual-wavelength detector multiplexed to an A/D converter.

The 4 high temperatures can also be measured using a blackbody spectral analyzer similar to that used for the turbine blade temperature. The alternative for these gas temperatures is a variable spectral transmittance sensor on a wavelength measurement interface, a time domain intensity analog interface, or a two-wavelength analog interface.

The two low temperatures also can be measured by a wavelength measurement interface, a time domain intensity analog interface, or a two-wavelength analog interface. These could be handled by a common circuit.

The flows, speeds, and vibration measurements can be done by any of the analog interface types. A logical grouping would have the flows and speeds together on a common interface and the vibration measurement processed independently.

The five pressures can be measured through any of the analog interface types. It is recommended that these be multiplexed through a common interface.

The rotary position, linear positions, and fluid level can be measured by any of the digital or normalized analog techniques. It is recommended that these be grouped together in sets of four measurements through a common multiplex interface.

3.0 ANALYSIS OF ELECTRO–OPTIC ARCHITECTURES

Previous optic flight control studies identified a great number of optic sensors currently available or in development for application to aircraft propulsion control (refs. 1–8). These sensors use a variety of mechanisms to measure the temperatures, pressures, speeds, flows, and positions required for control and condition monitoring. One problem addressed in the study is to determine the best way to combine these various mechanisms into a network. The focus of the study then is on the selection of multiplexing and networking technology for the sensor interfaces.

3.1 Sensor Categorization

Nine distinct fiber–optic sensor types were identified in the strawman electro–optic architectures presented in the appendices. These are: (1) baseband continuous wave intensity modulators, (2) time division multiplex (TDM) digital optical codeplates, (3) analog TDM self–referenced intensity modulators, (4) wavelength division multiplex (WDM) digital optical codeplates, (5) analog WDM self–referenced intensity modulators (6) analog wavelength measurement, (7) self–luminous sensors, (8) coherent optical frequency modulated continuous wave (FMCW), and (9) remote electrically powered sensors. This classification provides a useful guide for discussion of the various sensor types according to categories. These categories are discussed in the following sections.

3.2 Electro–Optic Architecture (EOA) Designs

Following are brief descriptions of the operation of each of these electro–optic interfaces. More detailed discussion of the designs and the associated fiber–optic sensors are presented in the references and Appendices B–D.

In each electro–optic interface design, the optical signals are detected and digitized with a minimum of signal processing in the interface. All normalization and calibration functions are performed on the digitized optical signal values in the microprocessor. This separation of functions is motivated by the requirement to minimize the size and part count in the electro–optic interface.

In the following discussion all values apply to the optical interface, therefore power levels refer to optical power and decibel units refer to optical power ratios. These are meant to apply to LED type multimode systems in which a relatively broadband optical spectrum is modulated by a passive sensor or sensors.

For meaningful specification of optical power levels a standard waveguide aperture must be specified. The selection of a standard waveguide dimension involves consideration of losses, fiber mechanical properties, coupling efficiency, and dispersion. Consideration of efficient source power coupling and low loss connections favors large core fibers; while cost and strength favor small diameter fibers. For control applications the dispersion is not a significant problem because distances are relatively short. The 100 micron, step index waveguide currently used by many sensor manufacturers is a practical compromise and is consistent with the source power levels specified in this program. Fiber specifications are thus:

Core Diameter:	100 microns
Numerical Aperture:	0.22
Index Profile:	step index

In general there is no need to match cladding diameter across an interface if the core parameters and connector types are the same. The cladding diameter would be specified to be compatible with the connector. The specifications in this document do not depend on the cladding diameter selected.

Optic connectors should be in accordance with MIL-C-38999, or an approved equivalent. The electro-optic interface board should employ a fiber optic pigtail to a fiber optic MIL 38999 Series IV connector receptacle with pins. The contacts should be #16 in accordance with MIL-T-29504/4. According to SAE AS-3 fiber-optics committee recommendations, butt termini are preferred over lensed termini. The pigtail should have proper strain relief to the backshell of the connector. The number of fibers, the fiber bend radius, and length will be specified. The harness would contain at least three connectors between the sensor and the electro-optic interface. The optical power budget for system connectors and fiber should not be less than the formula $2(n + 1)$ dB where n is the number of connectors in the system. This is based on 100/140 micron fiber where as smaller fibers will require a larger margin.

3.2.1 The simple CW modulation interface.- The simplest electro-optical interface for fiber-optic sensors is illustrated in figure 3.2.1-1. This interface provides no calibration from optical power measurements so it is useful only with sensors that produce frequency modulation. A single light emitting diode (LED) illuminates the fiber-optic sensor continuously. The sensor modulates the light at a frequency proportional to the measurand. The modulated optical signal is detected in a photo diode and processed through electronic circuits that measure the frequency of the modulation.

The electronic circuits required for the interface consist of a constant current source to drive the LED, a pre-amplifier (transimpedance amplifier) with automatic gain control (AGC) for the photo diode, bandpass filters, frequency counter, and digital interface to the microprocessor bus.

3.2.2 The analog TDM interface.- Fiber-optic sensors that produce analog intensity modulation can be used with the analog TDM sensor interface illustrated in figure 3.2.2-1 (See Appendix C). This interface provides a normalized optical loss measurement that can be used to read microbend, macrobend, variable absorption, or variable transmittance type fiber-optic sensors. A single LED in the interface produces a short pulse of light to interrogate the sensor. The remote sensor includes means to split the pulse into two parts. One serves as an intensity reference level while the other is delayed in time and propagates through the sensing element. Two pulses of light, separated by the delay time, return to the optical receiver. The ratio of the amplitudes of the two pulses is proportional to the measurand. The two returning pulses are detected by a photo diode and processed through electronic circuits that measure the frequency of modulation.

The delay between pulses would typically be less than 100 nanoseconds. Detection averaging, performed in the lowpass filters in figure 3.2.2-1, provides more than 20 dB (optical) improvement in sensitivity.

The electronic circuits required for this interface consist of a pulser for the LED, a transimpedance amplifier with AGC for the photo diode, time base trigger and synchronization, analog multiplexes, lowpass filters, analog to digital converter, and digital interface to the microprocessor bus. Both pulse amplitudes are digitized. The ratio of the amplitudes is calculated in the microprocessor.

An alternative to the pulse processing circuit shown here is the radio frequency (RF) interferometer where the LED pulser is replaced with a cw two-tone RF source and the receiver electronics measure the ratio of two frequencies.

3.2.3 **The digital TDM interface:** The digital optical interface illustrated in figure 3.2.3-1 would be used to read digital optical code plates in sensors such as those developed in the Army ADOCS program (refs. 3,4,11 and see Appendix A). The interface reproduces the pattern on a remote optical codeplate as a digital output word to the processor. Teledyne Ryan Electronics has successfully implemented the time delay multiplexed architecture for high accuracy position feedback in the Army ADOCS flight demonstrator. This technique dramatically reduces the number of fibers and connector contacts required to interface to a number of binary optical sensors.

A single LED produces a a short pulse of light to read the sensor. The remote sensor includes means to split the pulse into many, one for each bit in the optical code. Each pulse is delayed by a different amount in time and combined into a single return path. A serial binary pulse train returns to the optical receiver. The returning pulses are detected by a photo diode and processed through electronic circuits that convert the serial pulse train to a paralleled digital word.

The length of the pulse train would typically be less than 240 nanoseconds while the sensor update time is greater than 5 ms. Therefore, many serial digital optical words can be averaged to produce a single sensor reading. This post detection averaging is performed in digital circuits between the shift register and the processor interface, and can provide more than 10 dB (optical) improvement in signal-to-noise ratio.

The electronic circuits required for the interface consist of a pulser for the LED, a transimpedance amplifier for the photo diode, time base trigger and synchronization, comparator, shift register, digital averaging, and interface to the micro-processor bus.

The TDM transmitter produces a narrow pulse of light to interrogate a network or delay lines. A proposed TDM optical pulse waveform is illustrated in figure 3.2.3-2. The standard pulse width is a compromise between the length of the delays which are achievable using fiber-optic delay lines in practical geometries and the speeds achievable in practical optoelectronic transmitters and receivers. The 10 ns width corresponds to a 4 meter delay which is quite practical in small, 2 cm diameter, coils. This pulse width is also producible in high speed, high radiance light emitting diodes.

The standard delay length (about 4 meters in optical silica fiber) is that which sensor manufacturers must provide for the excitation pulse.

The pulse risetime and fall time are selected to for practical transmitter time constants and receiver filtering for the specified pulse width.

The minimum peak pulse power level is specified to accommodate the losses and receiver sensitivities typically found in state-of-the-art fiber-optic sensors. This level is also within the range of lasers and low duty cycle LEDs.

The suggested TDM specifications are:

Pulse Width:	10 ns
Risetime/Falltime:	3 ns/4 ns
Peak Pulse Power:	1 mW (0 dBm)
Interference:	-30 dB (optical)
Slot Spacing:	20 ns
Receiver Sensitivity:	-51 dBm noise floor in 50 MHz bandwidth

(-74 dBm noise floor may be achieved using post-detection averaging).

3.2.4 **The analog WDM interface.-** The analog WDM sensor interface illustrated in figure 3.2.4-1 would be used to read fiber-optic sensors that produce analog intensity modulation such as: microbend, macrobend, absorption, or transmittance types. The interface produces normalized optical loss measurement using wavelength division multiplex (see Appendices D-1 and D-2).

An array of LED's illuminate the sensor with a broadband spectrum as illustrated in the figure. The remote sensor includes means to filter two spectral components from the source spectrum. The intensity of one spectral component is varied in proportion to the measurand while the other serves as a reference. The ratio of the amplitudes of the two spectral components is proportional to the measurand. The receiver includes means to disperse the optical spectrum on a photo diode array. The optical spectrum returning from the sensor is detected in a photodiode array, and processed through electronic circuits that calculate the spectral power ratio.

The components required in this interface are: a constant current source for the photo diode array a source power monitor, a wavelength dispersing element on a photo diode array, analog multiplexer, transimpedance amplifier, A/D converter, and microprocessor bus interface.

3.2.5 **The Digital WDM Interface.-** The digital wavelength division multiplex (WDM) interface illustrated in figure 3.2.5-1 would be used to read digital optical codeplates (ref. 12 and Appendix D). An array of LED's illuminate the sensor with a broadband spectrum as illustrated in the figure. The remote sensor includes means to filter the spectrum into many components, one for each bit in the optical code. Each spectral component illuminates a track on the code place, then the intensities from all tracks are combined into a single return path. A broadband spectral pattern returns to the optical receiver. The receiver includes means to disperse the optical spectrum on a photo diode array. The spectral power distribution is detected and processed through electronic circuits that produce the digital output.

The components required in this interface are the constant current source for the LED array, dispersive element coupled to the photodiode array, analog multiplexer, source monitor, comparator, shift register, and microprocessor bus interface.

Litton Polyscientific Fiber-optic Products and NASA Lewis Research Center are developing the wavelength division multiplexed interface also as an interface to an optical code plate. This interface uses optical wavelength dispersing elements in the EEC to isolate sensor signals in distinct wavelength bands. For use in the EEC, the stability of the source spectrum and the dispersing elements over a wide temperature range must be considered.

3.2.6 The spectral measurement interface.- Some fiber-optic sensors act as variable narrowband optical filters that produce a single spectral component in which the center wavelength is proportional to the measurand. The electro-optic interface to these sensors is illustrated in figure 3.2.6-1. Sensors in this class include Fabry-Perot cavities, absorption edge shift, and spectral transmittance (movable grating) types.

An array of LED's illuminate the sensor with a broadband spectrum as illustrated in the figure. The remote sensor contains means to filter a single spectral component at a wavelength proportional to the measurand. The receiver includes means to disperse the optical spectrum on a photodiode array. The spectral component is detected by an element of the array and processed through electronic circuits that determine the wavelength.

The components required for this interface include a constant current source for the LED array, a dispersive element coupled to the photo diode array, analog multiplexer, transimpedance amplifier, A/D converter, and microprocessor bus interface.

The WDM transmitter must provide a broad spectrum of light to be filtered by the sensor network. The minimum acceptable power density must be consistent with that obtainable from state-of-the-art light emitting diodes and with the losses or power budgets of present WDM codeplate and spectral filtering sensors. The total width of the spectrum emitted by the transmitter depends upon the type and number of sensors in the application. A typical WDM optical spectrum is illustrated in figure 3.2.6-2. A realistic specification which meets these requirements is:

Minimum power density:	2 microwatt/nanometer
Ripple:	Maximum 3dB variation across the specified band
Spectral Coverage:	750 nm - 950 nm

The WDM receiver filters the wavelength coded sensor signals into discrete bands for analysis. The channel spacing must be consistent with state-of-the-art WDM components and with the source power density specified above. With the specified channel spacing, the system must have a useful number of digital channels in a realizable source bandwidth or have sufficient wavelength resolution to decode an analog wavelength sensor.

Channel width and channel spacing are here consistent with common fiber sizes in a grating-type WDM unit. The channel spacing corresponds to fiber diameter while channel width is determined by core diameter. Note that maximum channel width is specified, actual width may be smaller depending on core size. The presence of guard bands assures good channel separation over environment and manufacturing tolerances. Standard channel locations allow interchangeable sensors, and intermatability of encoders and decoders.

The implementation of the spectrum analyzer in the receiver requires further discussion, development and analysis. This function is now performed in several different ways: grating coupled CCD or miniature Fabry-Perot interferometer. In either case, the system specification may be affected by component performance, e.g. finesse and stability of the Fabry Perot or size of the CCD.

The suggested WDM specification is:

Channel spacing:	10 nm spacing between center of bands
Maximum Channel width:	8.7 nm width occupied by signal power
Guard band width:	(Channel Spacing - Channel Width) /2 = 0.65 nm

Channel locations: Bands shall be centered at wavelengths of 600 nm +- n (Channel spacing) with integer n. Allowable channels within the AlGaAs band are thus 730, 740, 750, ... , 940, 950, so about 25 channels are accessible using AlGaAs sources.

Interference: -30 dB of the excitation power or 17 nanowatts (maximum). Note present state-of-the-art WDM components have as much as -15 dB cross talk. This specification places a limit on the magnitude of the spurious reflections allowed in a single fiber system. The interference specification limits the maximum allowable power level in any other band. The -30 dB level is chosen to assure compatibility with high accuracy, 0.1%, analog intensity type sensors.

Receiver sensitivity: -78 dBm noise floor in 200 Hz bandwidth.

3.2.7 The self luminous sensor interface.- Three of the fiber-optic sensors considered for engine control radiate light without any optical excitation. These are the turbine blade pyrometer, the black body temperature sensor, and the augmenter flame detector. For these reasons, the spectrum analyzer receiver illustrated in figure 3.2.7-1 is required.

The electro-optic circuit contains just the receiver portion of the WDM interfaces described previously. The electronics serve to produced digitized representation of the optical power spectral density to be processed by the micro computer.

Though the blackbody temperature sensor is not compatible with external multiplexing schemes it is still a candidate sensor in the EOA. There may be unique sensing demands for which the optimal architecture would include sensors which are not multiplexed. A blackbody probe is well suited to the measurement of very high temperatures (such as exhaust gas) where few alternatives are compatible with multiplexing. Furthermore, significant improvements could still be realized by replacing wire connections with optical fibers without multiplexing. Therefore it is expected that the optimal architecture may still include a variety of sensor types with some multiplexed and others not.

3.2.8 Coherent fiber-optic sensor technology.- Ultimately the greatest sensitivity and flexibility in fiber-optic sensors will be achieved through the use of integrated optics and singlemode coherent systems. Use of this technology is the current trend in commercial telecommunications which has been the source of the technology for fiber-optic flight controls. The generic form a coherent

interferometric interface is shown in figure 3.2.8–1. The interface includes a frequency swept cw laser source illuminating a sensor probe through an input/output coupler. In the sensor probe the parameter of interest (e.g. speed, flow, position) modulates the optical field on reflection. In the receiver a reference field is mixed with the probe field to produce a heterodyne signal at the offset frequency of the reference field. The receiver consists of a high speed photodiode with a low noise transimpedance amplifier and a bandpass filter to isolate the heterodyne frequency. The output from the receiver is a sinusoidal voltage carrier with amplitude and phase proportional to the optical field returned from the probe. Therefore, a radio receiver tuned to the heterodyne frequency can detect amplitude, phase, or frequency modulation modulation of the complex optical field.

Coherent sensor types for engine parameters are as follows:

Speed – a fiber–optic interferometric magnetic field sensor to serve as an eddy current probe similar to present speed sensors. This has the advantage that light is contained in the fiber at the sensor so it is not sensitive to contamination of optic surfaces.

Flow – an a.c. coupled interferometric fiber strain sensor in a vortex shedding flowmeter provides an f.m. signal proportional to flow.

Pressure – two options: (1) coherent detection in a microbend–type diaphragm pressure sensor, or (2) coherent phase detection in a photoelastic crystal.

Temperature – frequency modulated carrier wave readout of silicon carbide or optical fiber Fabry–Perot resonators.

Position – frequency modulated carrier wave readout of reflecting piston.

Coherent sensors would be grouped on common frequency modulated carrier wave laser sources. Temperature and pressure sensors would use a common phase reading receiver. Speed and flow would use a common frequency discriminator receiver. Position sensors would use a common, high accuracy, fringe counting receiver.

Laser sources will be required for the coherent interferometric optical receivers. The temperature variations in the EEC electronics module will cause extreme variations in the output power and spectral characteristics of presently available commercial semiconductor laser diodes. However, new low threshold devices show promise of reducing the magnitude of this problem. The primary effect of temperature on the operation of a laser diode is to increase the threshold current. The magnitude of this effect is a doubling of threshold current for a 100 C rise in temperature. In the present generation of commercial semiconductor laser diodes the threshold current is typically 30% to 50% of the maximum cw operating current so the effect of the 180 C temperature range of the EEC is a severe drop in laser power. Closed loop, constant optical power operation is not feasible since this would drive the injection current to excessive levels at the higher temperatures. Recently developed

laser diode, however, have very low threshold current. In these devices, the threshold may be less than ten per cent of the allowable cw injection current so the twofold increase in threshold current would result in only a ten percent power reduction.

Fiber-optic links to electronic sensors.– Many of the benefits of fiber-optic signal transmission in aircraft control systems may be realized in networks of electronic sensors interconnected by optical fibers (Appendix C). The electro-optic circuit in figure 3.2.9-1 illustrates a fiber-optic data bus terminal to interface with remote electronic sensors. The data bus protocol logic, fiber-optic transmitter and fiber-optic receiver circuits would be replicated for each sensor. This interface would transmit digital commands to the sensors to request data, then the remote terminals would transmit digital data words back to the controller.

3.3 Assessment of Evaluation Criteria

In this section the various optical modulation techniques will be evaluated on the basis of the criteria identified in Section 2.1. These criteria include applicability to engine sensors, calibration, size, optical power budget, multiplex technique, and reliability. Each technique is assigned a quantitative measure for each feature (such as size in square inches, power in watts, complexity in number of components and software operations, power margin in dB, or reliability in failures per million hours) based on the state of the art forecast for the mid' 1990's. The preferred methods of optical modulation will be those which can be realized in the systems having the best overall measure.

In attempting to substitute optic sensors into this architecture one must consider the suitability of optic sensing methods to the multiplex and sensor transmission techniques. For example frequency type sensors are well suited to optic transmission while analog signals are not unless compensation and referencing are provided. Also, due to the size and cost of optic transmitters, receivers, and connectors it is desirable to minimize the number of these.

The most desirable multiplexing technique and network architecture would be one which is compatible with all or at least the greatest number of sensors while reducing EEC size and complexity. Any multiplexing technique or network architecture which cannot be used for certain measurements or excludes some measurements or sensor types would be judged undesirable. Similarly those sensor types which are compatible with optical multiplexing are more desirable than those which cannot be easily incorporated into a multiplexed network.

Applicability to engine sensors.– The continuous wave modulator interface is applicable only to simple intensity-type sensors which produce a frequency-output such as a variable frequency light chopper. This measurement can be used for speed, flow, and vibration sensing on the engine.

The TDM, and WDM codeplate interfaces are applicable to absolute displacement sensors requiring better than 1% accuracy. In the engine control system these are the linear position, rotary position, and fluid level measurements.

The analog TDM and WDM interfaces are applicable to absolute fiber loss measurements requiring no better than 1% accuracy. In the engine control system this measurement technique can be applied to linear position, fluid level, pressure, and temperature.

The analog wavelength interface measures the wavelength returned from the sensor which is typically varied by displacement of a dispersive element in the sensor. This type of interface is applicable to linear and rotary position, fluid level, speed, pressure, and temperature.

The self-luminous sensor interface is needed for sensors which emit their own optical radiation: the light-off detector, turbine blade pyrometer, and blackbody temperature sensors.

The FMCW interface measures the beat frequency produced in an unbalanced interferometer. This technique can be used for measurement of position, fluid level, pressure, temperature, and speed.

The remote electrically powered sensor interface is an optical data link transceiver which can be used with all of the conventional electronic sensors.

A matrix showing the measurands for each of the nine interface types is shown in Table 3.3.1-1.

3.3.2 **Signal compensation or calibration.**- The continuous wave modulator interface provides no optical loss compensation or intensity calibration. Therefore it is applicable only to measurements, such as the frequency of modulation, which are insensitive to signal level.

The TDM, and WDM codeplate interfaces provide a direct reading of an optical codeplate pattern. The measurement calibration is provided by the codeplate assembly and is independent of optical power levels and link losses.

The analog TDM and WDM interfaces provide a normalized optical power measurement which cancels source power and link loss drifts. The TDM interface does the normalization in the time domain by forming a ratio of pulse amplitudes. The WDM interface does the normalization in the optical spectral domain by forming a ratio of spectral amplitudes.

The analog wavelength interface reads the wavelength of the light transmitted by the sensor independently of optical power level or link transmission loss.

The self-luminous sensor interface for the pyrometer and blackbody temperature sensor forms a ratio of optical spectral components to determine the peak wavelength radiated by the probe. The light-off detector interface produces a binary output indicating whether the total power is above or below a threshold.

The coherent interface measures the frequency or phase of a heterodyne intermediate frequency independently of optical power level or link transmission loss. The remote interferometer design assures that the sensor will be insensitive to phase noise in the optical harness.

The remote electrically powered sensor interface transmits sensor data in digital codes complete with error detection bits.

3.3.3 **Size.**- In Table 3.4-1 these candidate multiplexing techniques are compared on the basis of the size of the interface circuitry and harness. Here size is represented by the number of distinct sources, detectors, and fibers required to service a number of sensors. With the more advanced optic multiplexing methods (namely WDM, TDM, FDM) the physical size of the interface is independent of the number of sensors.

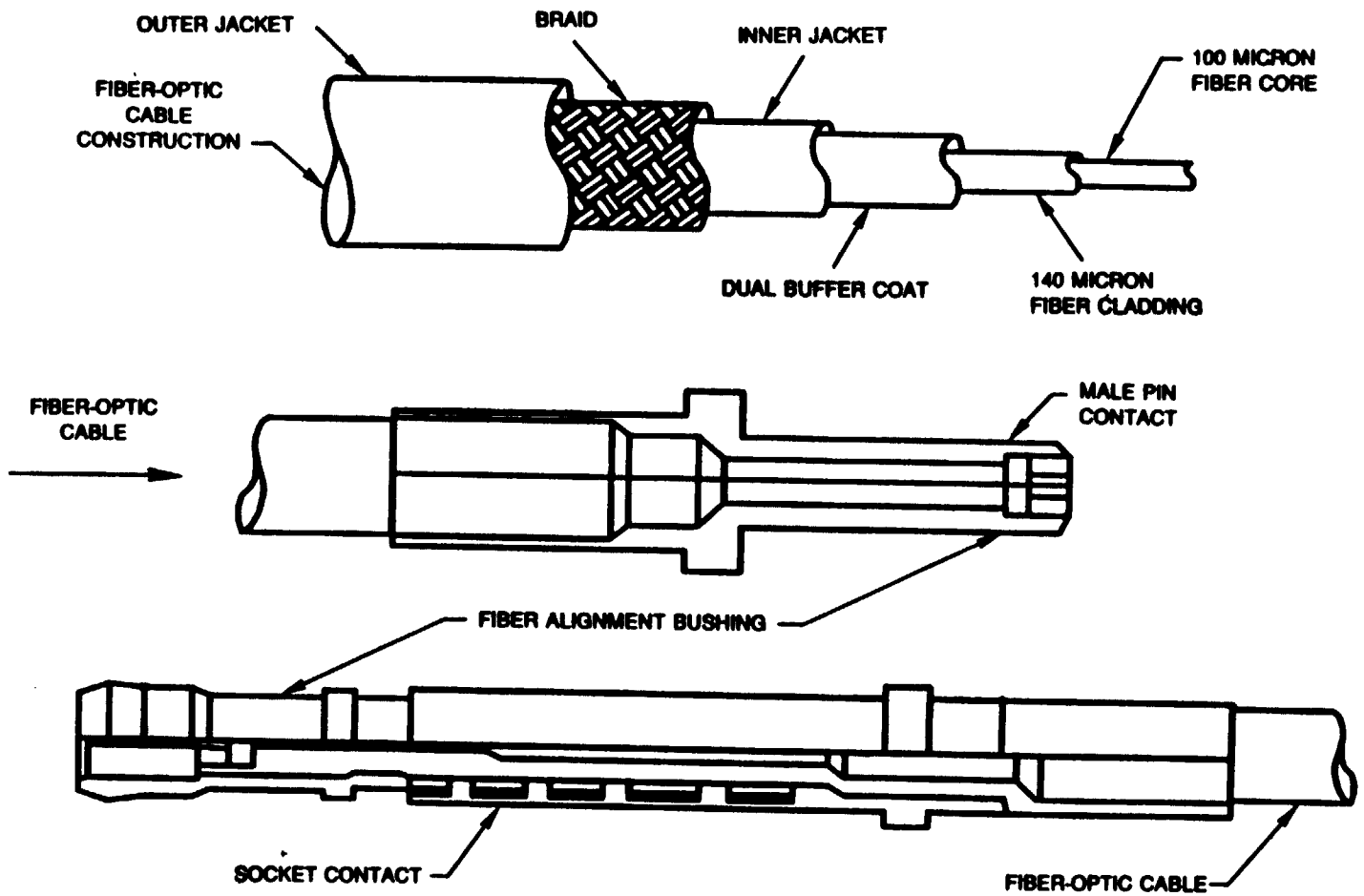

Figure 3.2-1. — The FOCSI interconnect standard uses 100/140 micron optical fiber in a # 16 MIL-C-38999 contact.

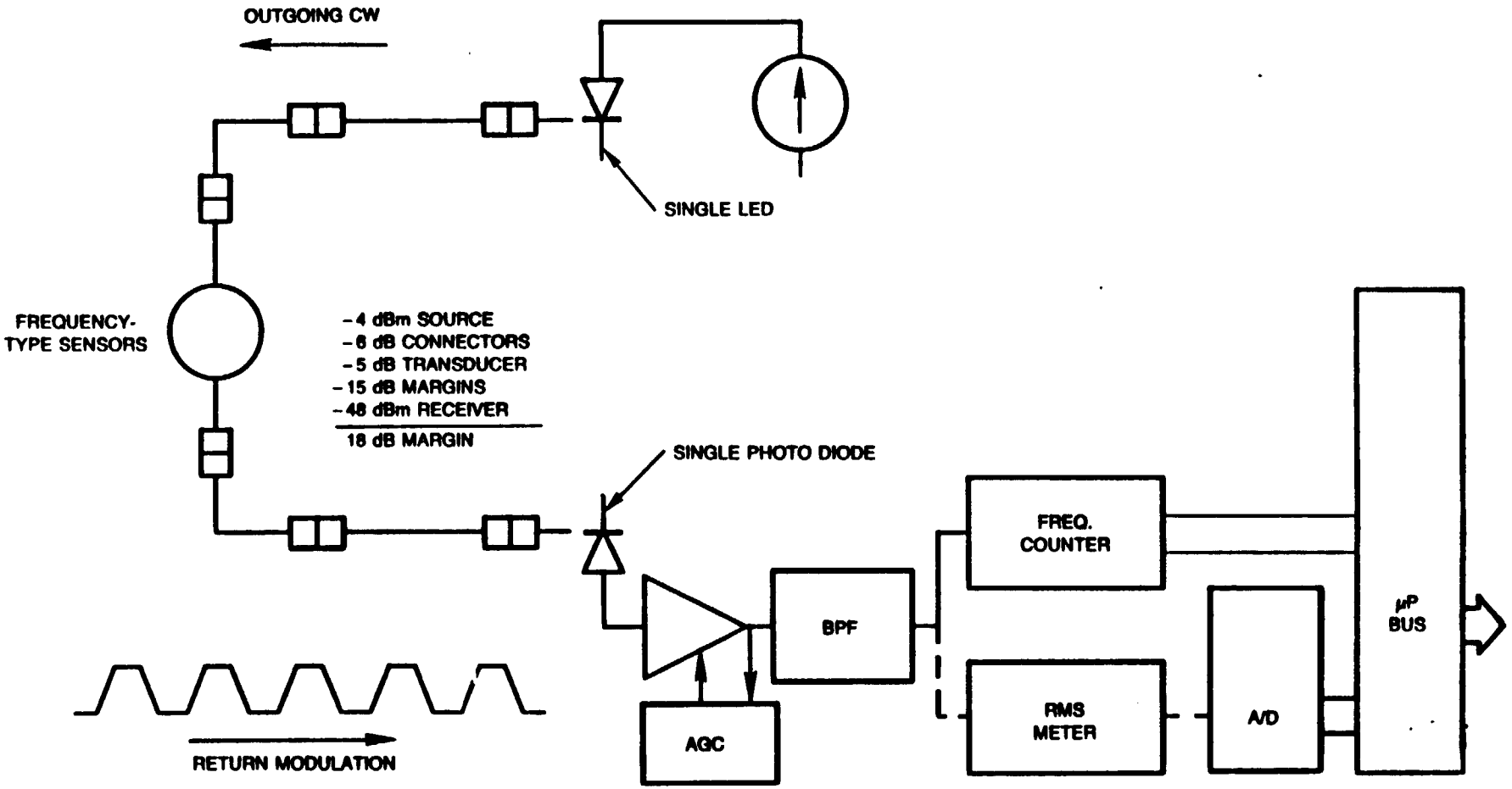

Figure 3.2.1-1. — The continuous wave (CW) modulation interface:

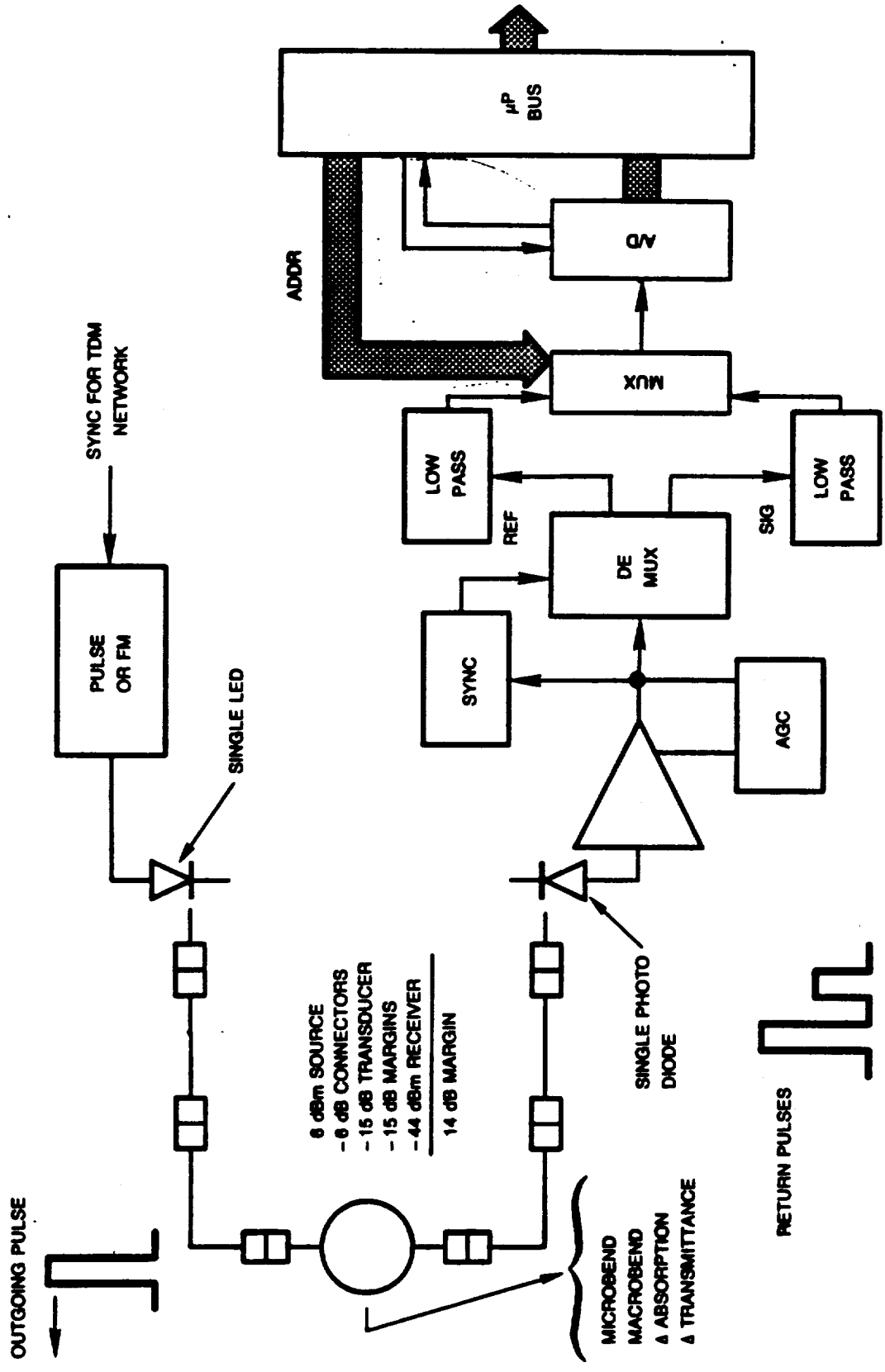

Figure 3.2.2-1. — The analog TDM sensor...

89—3—15—6

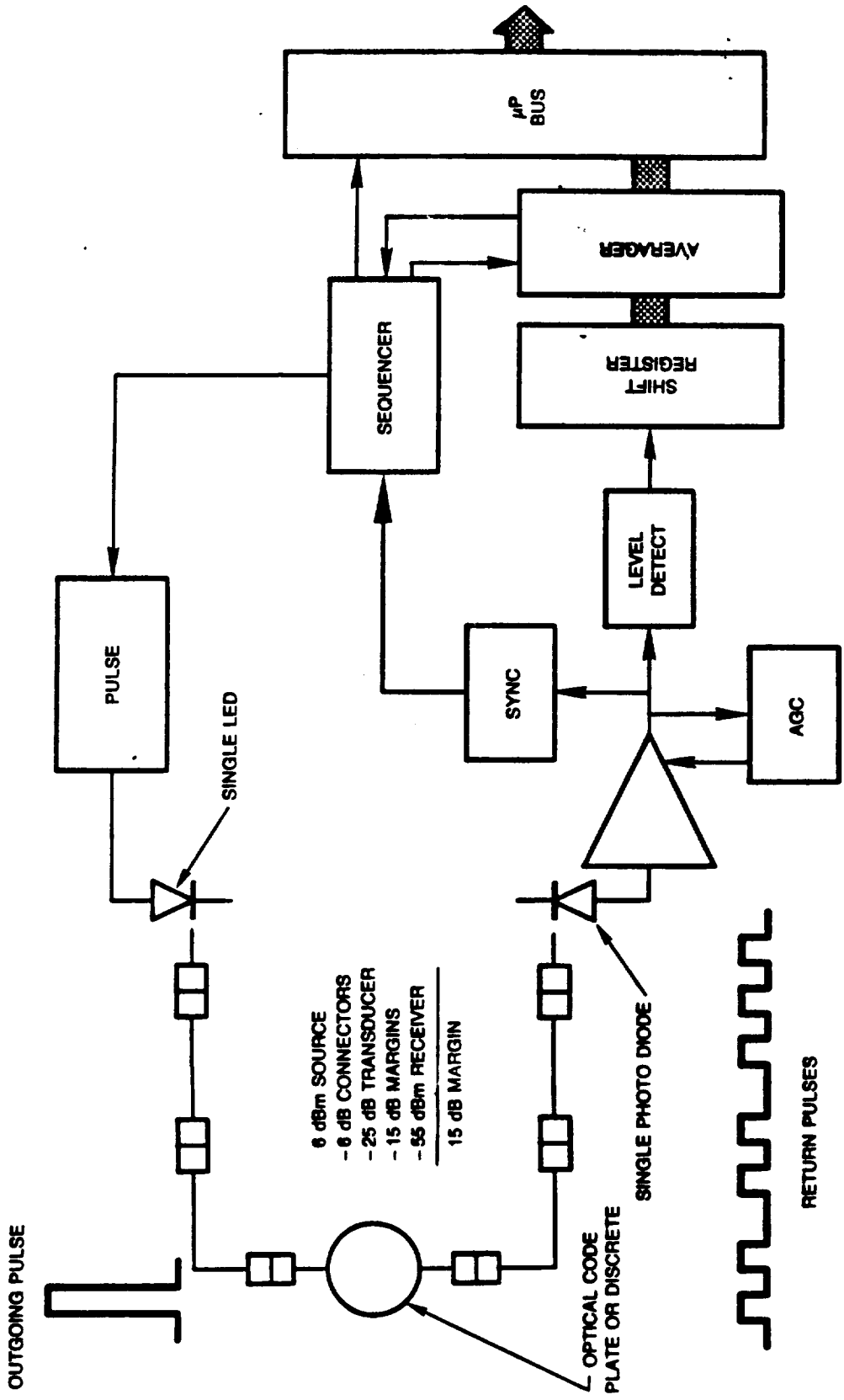

Figure 3.2.3-1. — The digital TDM sensor...

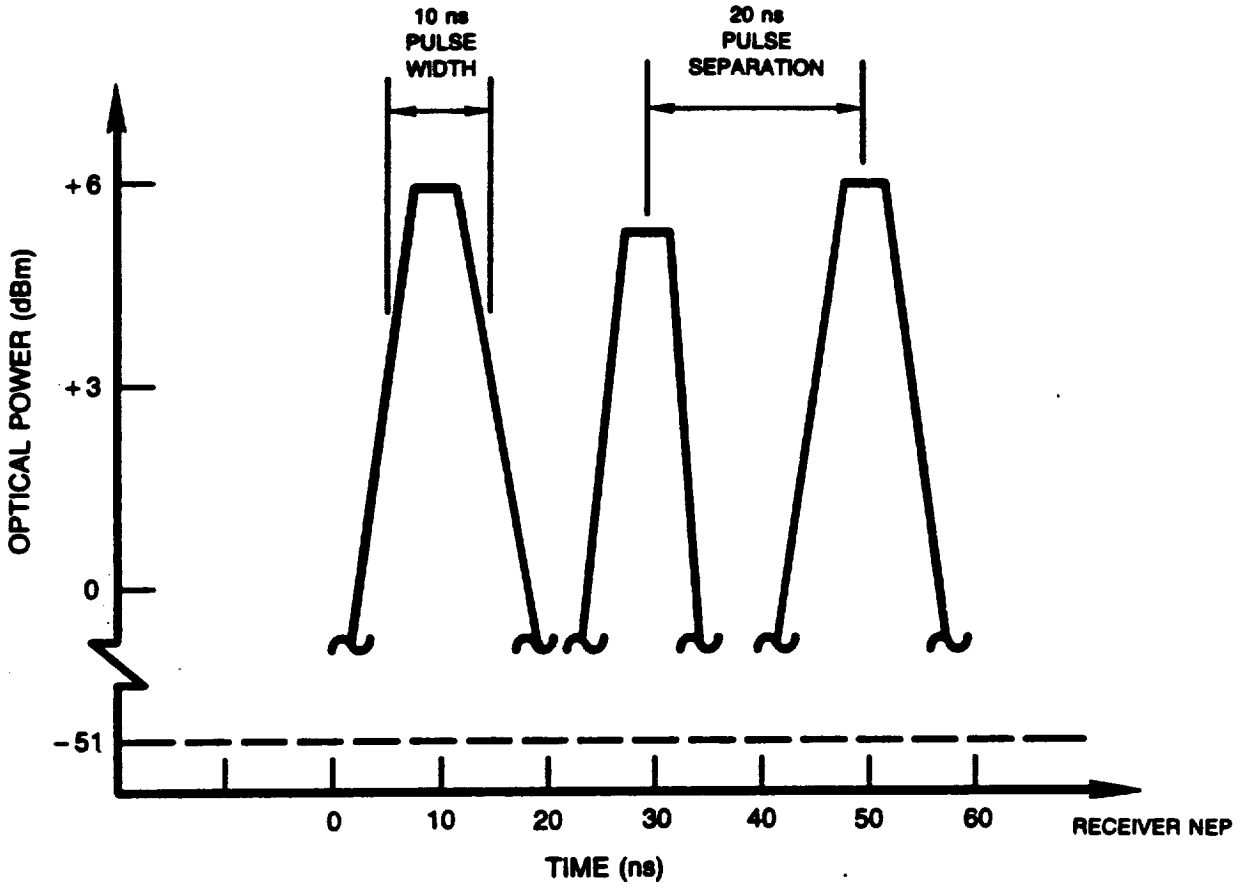

Figure 3.2.3-2. — The EOA TDM puse standard.

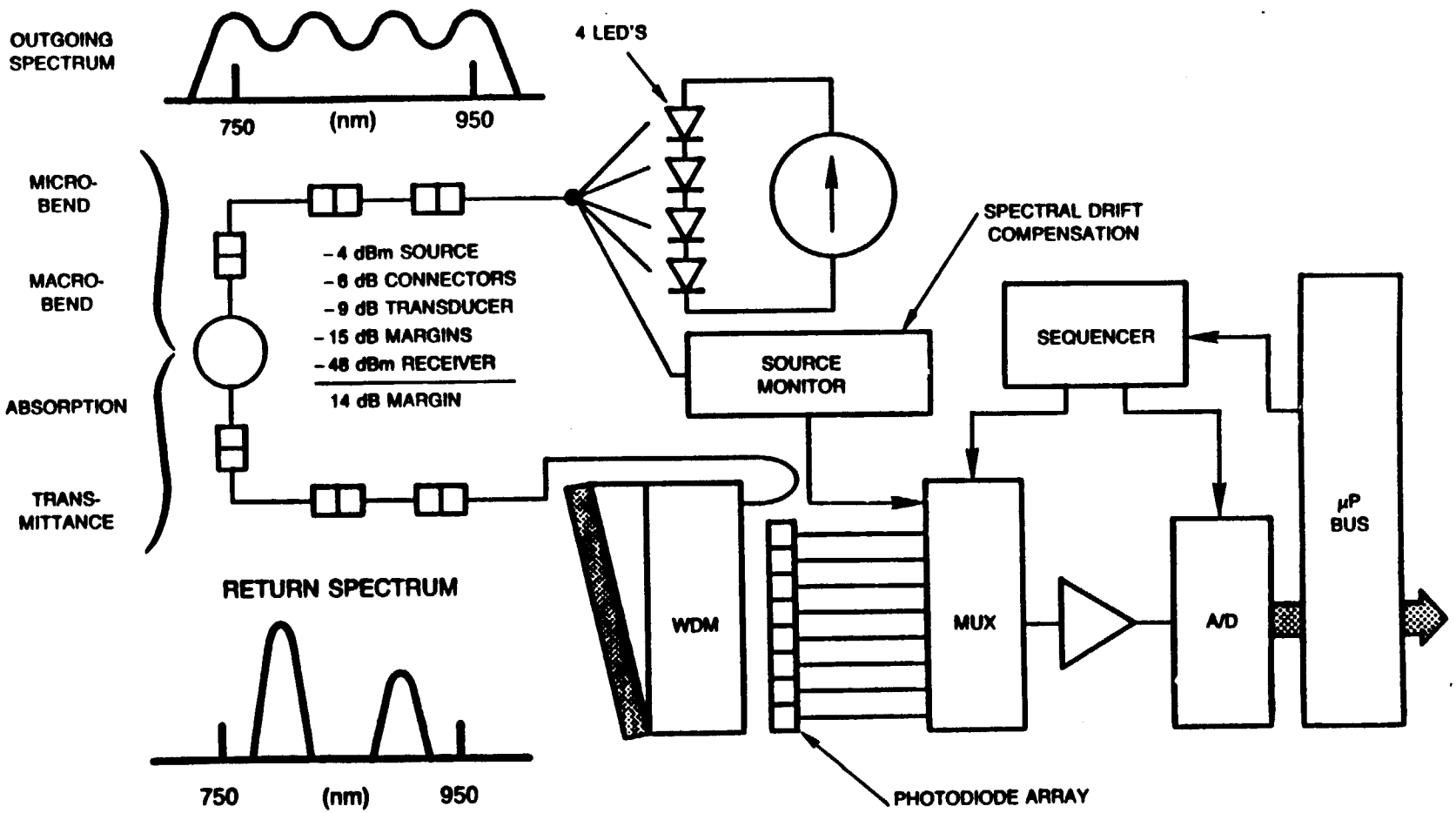

Figure 3.2.4-1. — The analog WDM interface:

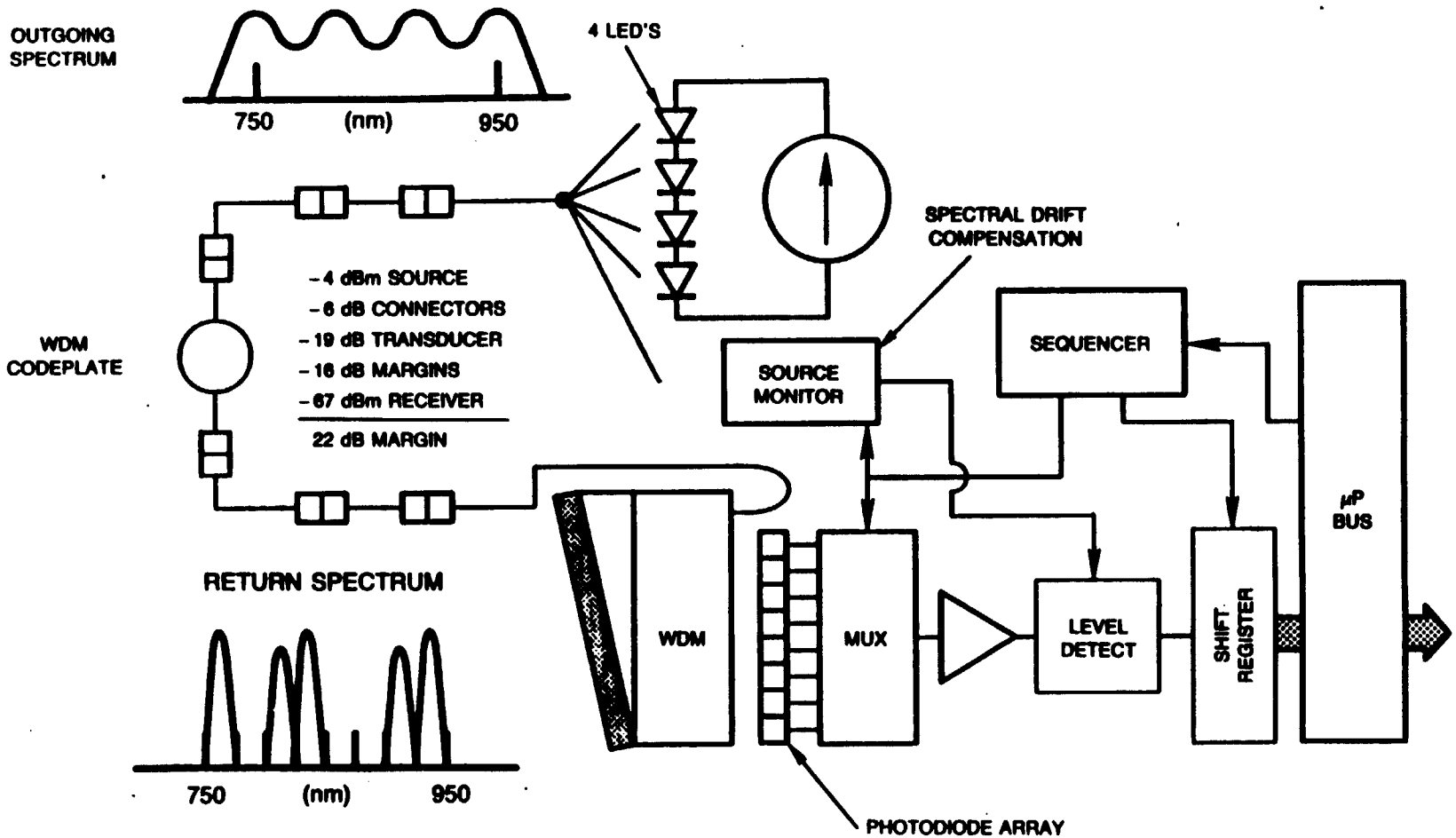

Figure 3.2.5-1. — The digital WDM interface:

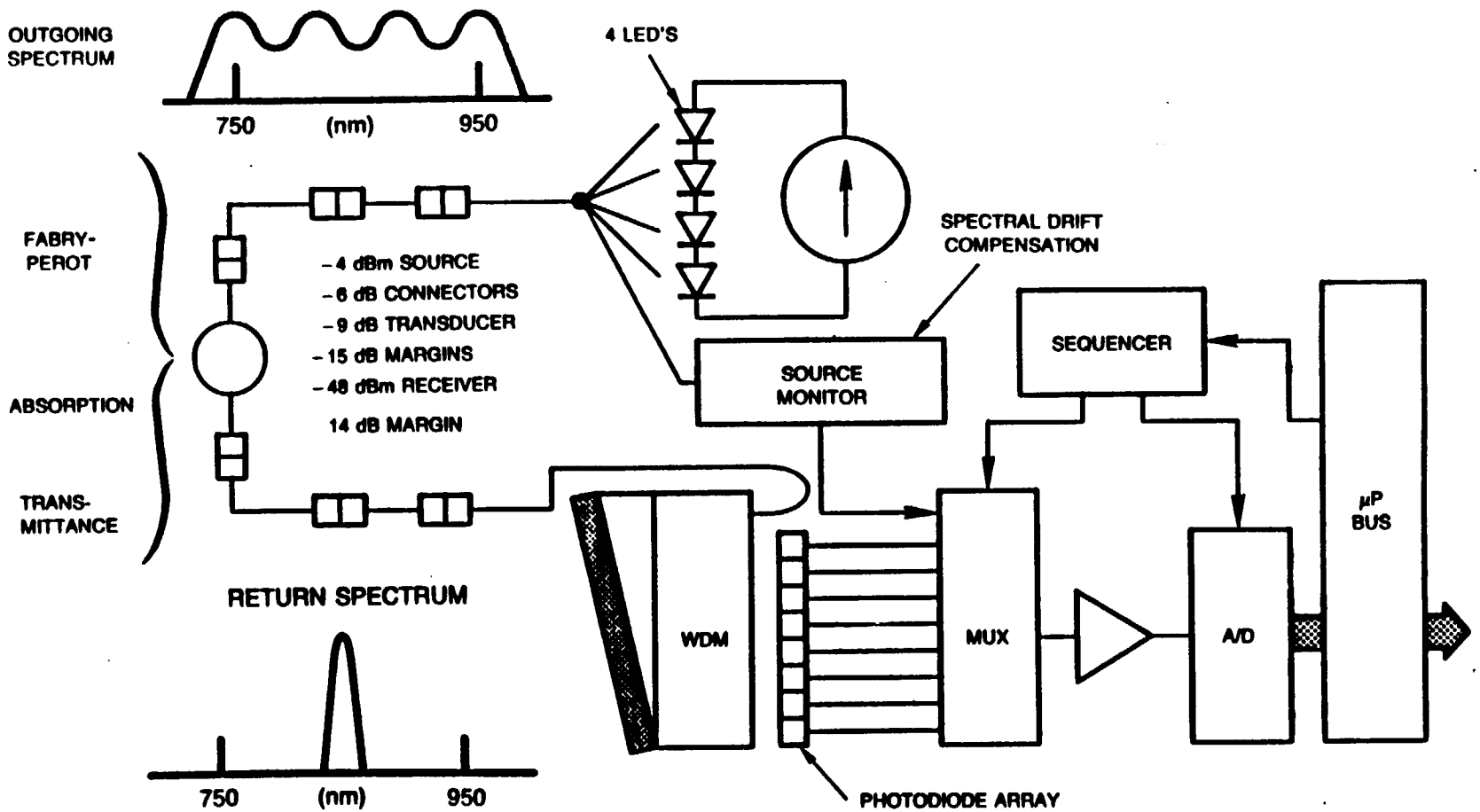

Figure 3.2.6-1. — The spectral measurement interface:

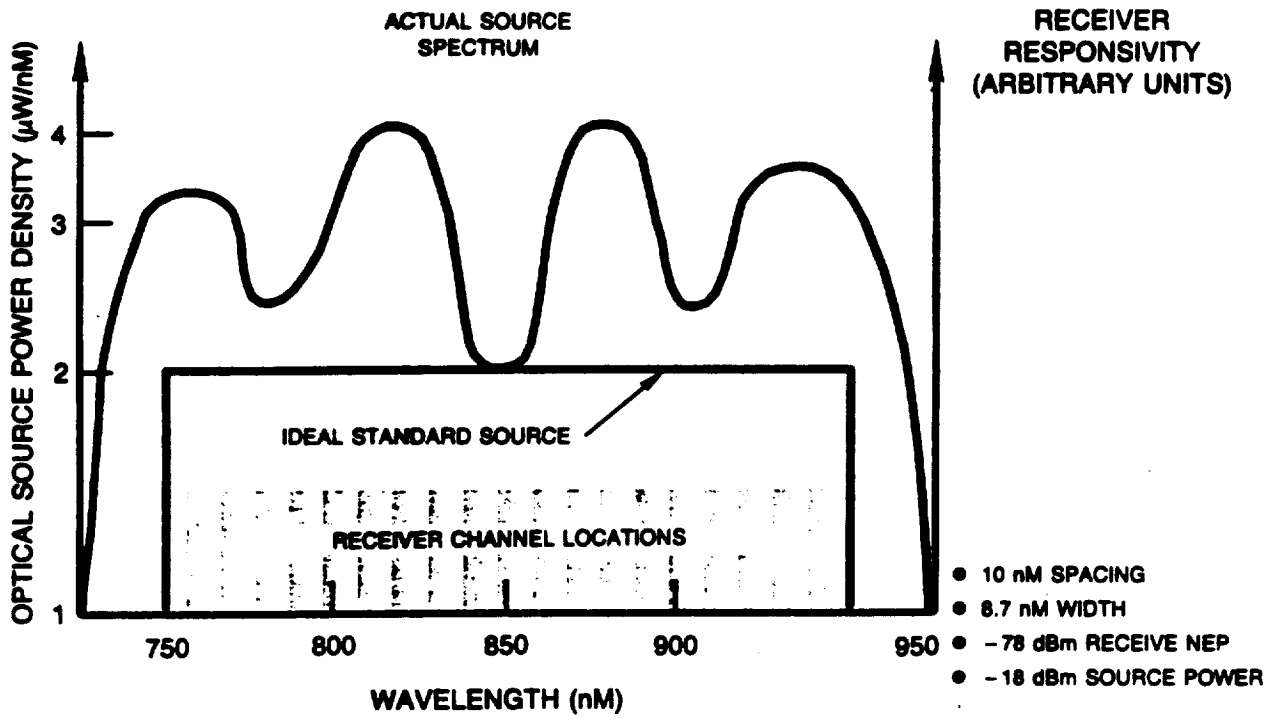

Figure 3.2.6-2. — The EOA WDM spectral standard.

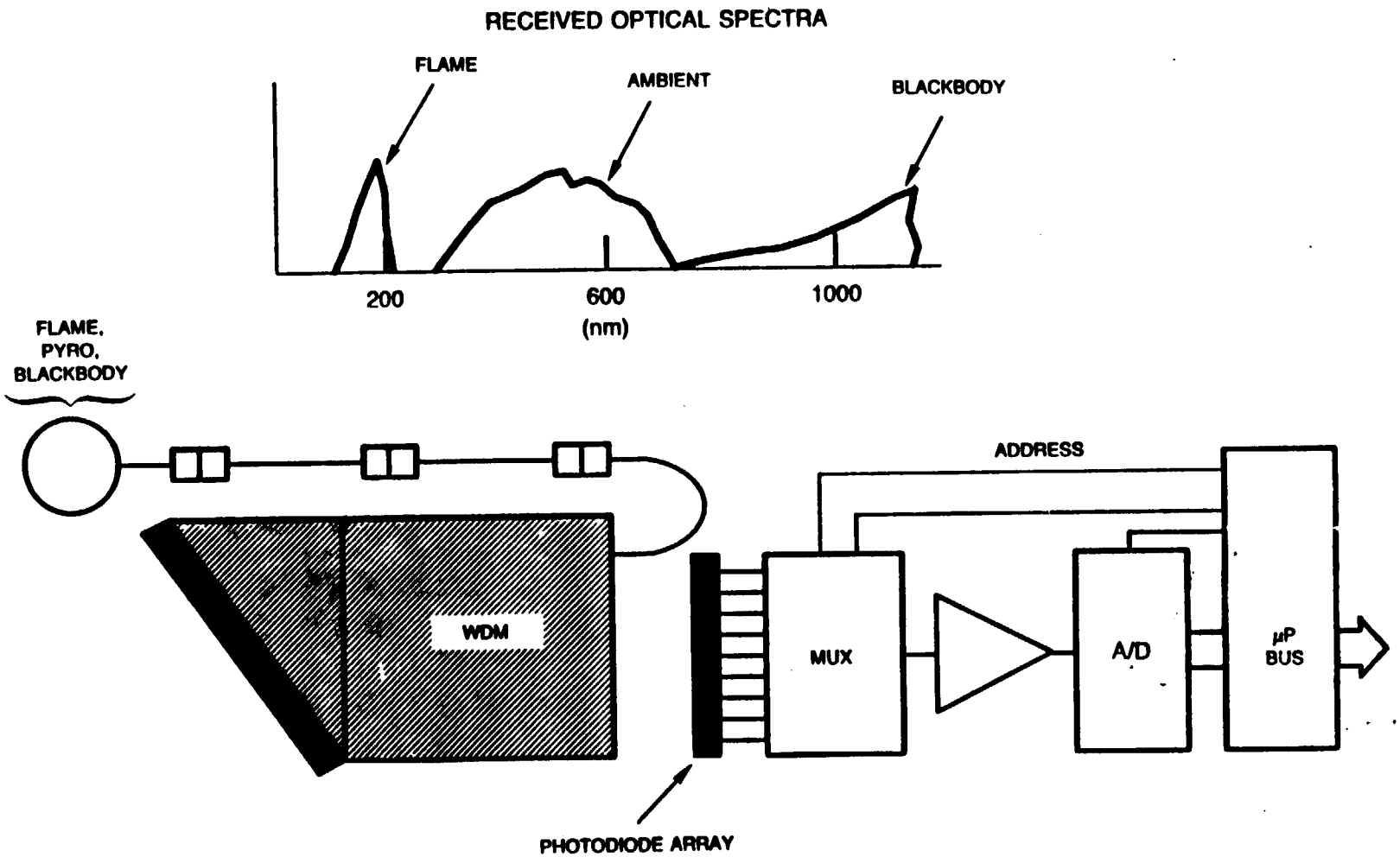

Figure 3.2.7-1. — The self luminous optical sensor interface:

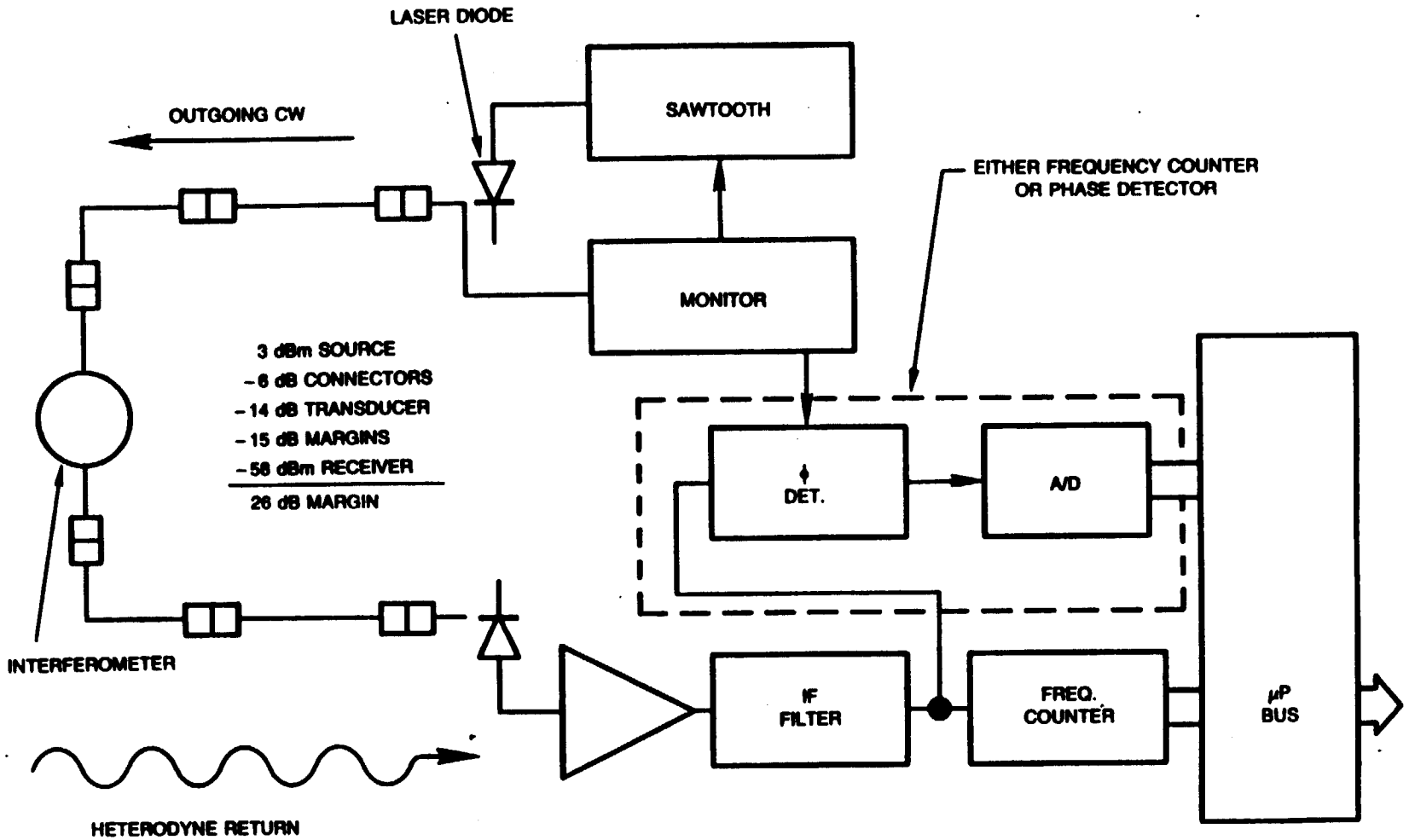

Figure 3.2.8-1. — The coherent optical FMCW sensor interface:

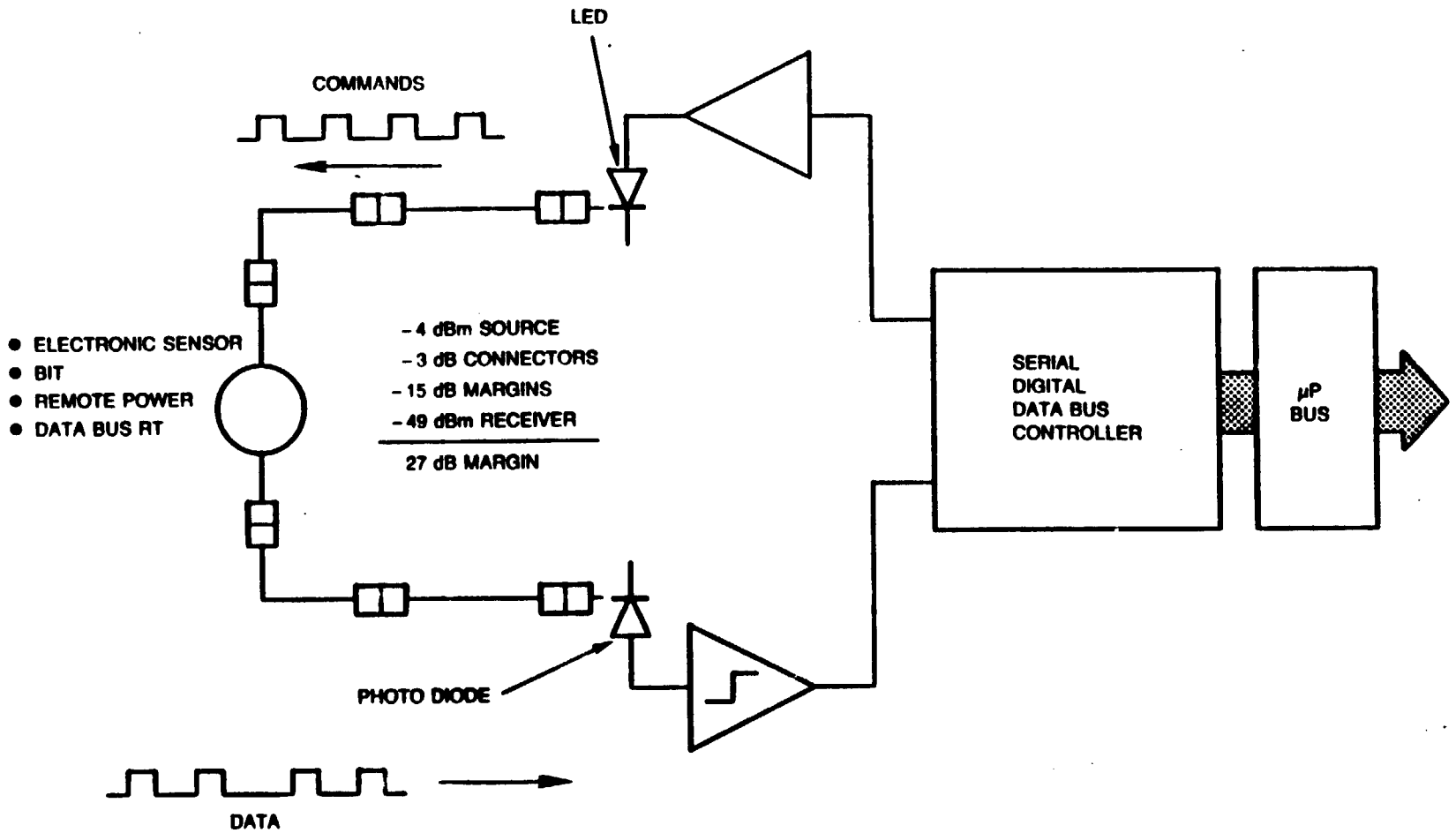

Figure 3.2.9-1. — The fiber-optic link to an electronic sensor...

TABLE 3.3.1-1 – APPLICABILITY OF FIBER-OPTICS TO ENGINE SENSORS

	Digital TDM	Analog TDM	CW Mod.	Digital WDM	Analog 2 Wavelength Ref.	Analog wv lngth Meas.	Self Lum.	FMCW	Electric PBL
Linear position	✓	✓		✓	✓	✓		✓	✓
Rotary position	✓	✓		✓	✓	✓		✓	✓
Gas temperature		✓			✓	✓	✓	✓	✓
Fuel temperature		✓			✓	✓	✓	✓	✓
Turbine blade temp							✓		
Light off detector							✓		
Fuel flow			✓		✓	✓		✓	✓
Gas pressure		✓			✓	✓		✓	✓
Hydraulic pressure		✓			✓	✓		✓	✓
Fuel pressure		✓			✓	✓		✓	✓
Rotary speed			✓	✓	✓	✓		✓	✓
Vibration			✓	✓	✓	✓		✓	✓
Fluid level	✓	✓		✓	✓	✓		✓	✓

TABLE 3.4–1 – SUMMARY OF EOA EVALUATION CRITERIA

	Digital TDM	Analog TDM	CW mod.	Digital WDM	Analog WDM	Analog Wavelength	FMCW
Types of sensors	3	8	3	5	11	11	11
Compensation	Good	Good	None	Good	Poor *	Good	Good
Signal processing time (ms)	1.6	1.6	1.6	1.6	1.6	1.6	1.6
Number of sources	1	1	1	4	4	4	1
Number of detectors	1	1	1	20	2	20 *	1
Number of fibers	2	2	2	2	2	2	2
I/O pincount	2	2	2	2	2	2	2
Complexity	8	8	8	8	8	8	8
Power consumption (Watts)	1	1	1	1	1	1	1
I/O circuit area (cm^2)	26	26	26	26	26	26	26
Weight (g)	50	50	50	50	50	50	50
Optical power margin (dB)	5	4	8	12	3	3	16
Number of channels	4	4	8	8	4	4	10
Reliability (failures/10^6 hours)	9.6	7.2	7.8	15.6	15.6 *	15.6 *	361 *

The WDM spectral slicing techniques require 4 LEDs and N low bandwidth optical receivers for N sensors while the TDM systems require only one high bandwidth receiver with one source. Given the same level of component integration, the TDM receiver is physically smaller than the WDM. The continuous wave modulator, FMCW, and the remote electrically powered sensor interfaces each require a single source and single detector. The self-luminous sensor interfaces require a single receiver for each sensor. An optical source may also be required if optical fiber fault detection is implemented.

For the continuous wave modulator interface a two-fiber interconnect is recommended. This design avoids the 6 dB power penalty in the input/output coupler and produces a higher contrast signal for the frequency measurement.

For the digital TDM, analog TDM, and FMCW interfaces, the preferred interconnect is a single bidirectional optical fiber link because the sensors proposed for this interface tend to work in reflection and spurious back reflections can be separated in the time domain. The 6 dB loss penalty incurred in the reflective arrangement is included in the transducer loss estimates.

For the digital WDM, analog WDM, and analog wavelength interfaces, a two-fiber interconnect is recommended to eliminate the effects of spurious reflections from connectors. One fiber connects to the transmitter, the other to the receiver.

For the self-luminous sensor interface a single fiber is required for each probe. A two-fiber bus structure is recommended for the remote electrically powered sensor interface. A single I/O connector pin is required for each interconnect fiber on each interface.

All of the candidate interface designs require approximately the same number of circuit elements (exclusive of optoelectronic devices): a 100 mA driver for the LEDs, three or four analog amplifiers (transimpedance amplifier, active filter, AGC circuit, A/D converter), plus three or four digital logic elements (frequency counter, shift register, sequencer, bus interface). Electronic circuit complexity is not a significant discriminator.

The electrical power required for the TDM and WDM multiplexed sensor interfaces designed by Eldec and Litton respectively is approximately 6 Watts. This level does not represent a low-power CMOS design which is expected to reduce the power consumption to approximately one Watt.

Estimates of the circuit board area required for a multiplexed sensor interface range from 26 cm^2 (4 sq in.) to 77 cm^2 (12 sq in.) despite the fact that each design requires approximately the same number and variety of components. Therefore, the 26 cm^2 estimate is taken as a high density approach representative of what can be achieved in all of the designs with maximum utilization of gate-arrays, ASICs, and surface mount technology.

Estimates of the weight of an electro-optic interface ranged from 50 g (1.76 oz) to 128 g (4.5 oz). The weight of the fiber optic cable in the system is determined by the network topology and is the same for each of the interface designs.

3.3.4 Optical power budgets.- A physical limitation which is common to all fiber-optic networks is the optical power budget. The elements of the optical power budget are the source power

level, the network losses, the receiver noise level, and the signal to noise ratio required to achieve the required level of sensor performance/sensitivity.

The power budgets shown in Table 3.3.4–1 include source powers, transmission losses, and receiver sensitivities. The source in each system is assumed to be a high radiance AlGaAs light emitting diode (LED) or laser diode (LD). At room temperature the LED provides 4.0 microwatts optical power per milliampere of injection current into an optical fiber pigtail having 100 μm diameter core and 0.29 numerical aperture. The maximum power output is assumed to be limited to the maximum average power dissipation of 200 milliwatts (ref. 17). In the WDM and CW systems the LED is operated at a high duty cycle and provides 400 microwatts. For the TDM system the LED is pulsed in a low duty cycle providing 4 mW peak optical power in a 10 ns pulse. WDM spectral slicing techniques require 4 LEDs having 63 nm spectral width and 4 uW/nM power spectral density. The laser diode source for the coherent system is assumed to provide a total of 4 mW into the same aperture.

The losses seen by the sensor interface arise from connectors and the transducer itself. Connector loss is estimated to be one decibel for the 100/140 fiber. A sensor interconnect would require at least six connectors. Transducers losses range from 5 to 25 dB based on manufacturer's data. The total loss seen by the interface thus ranges from 11 to 31 dB as shown in the table.

In addition to the anticipated losses, system margins and component deratings must also be included in the power budget. System margins account for repair splices, added connector, and connector aging (such as fiber "pistoning", scratching of the fiber end, or wear of connector surfaces). Component deratings include source aging, source power drift over temperature, wavelength drift over temperature, and noise drift over temperature (ref. 19). Source lifetime is commonly specified as the time when the power has dropped to half its value so an additional -3 dB derating factor should be applied to account for degradation over time. The temperature drift of source power is about -1 dB per 100°C. In the broadband sources for the WDM techniques, the 250 nm spectrum shifts by 50 nm over the temperature range leaving 200 nm available spectrum.

For fiber-optic sensors a wide dynamic range receiver is usually required so a PIN photodiode with a transimpedance type preamplifier is the receiver design of choice. The performance of this type of receiver is well understood and there is a generally accepted model for the sensitivity (ref. 18). The optical noise equivalent power, excluding 1/f noise, achieved in state-of-the-art PIN photodiode transimpedance amplifiers is typically:

$$NEP = (4 \times 10^{-16} \text{ Joules}) \times BW \text{ Watts} \quad (1)$$

where BW is the effective bandwidth of the receiver. As discussed in reference 1, the receiver noise is directly proportional to bandwidth in optimized designs. This value is very close to the theoretical minimum so significant improvements in receiver sensitivity are not expected.

TABLE 3.3.4-1 - OPTICAL POWER BUDGETS

	Digital TDM	Analog TDM	CW mod.	Digital WDM	Analog WDM	Analog wvingth meas.	FMCW	Elec.
Source power (dBm)	6	6	-4	-4	-4	-4	3	-4
Losses (dB)								
Connectors (3 ea. way)	6	6	6	6	6	6	6	3
Transducer loss	25	15	5	19	9	19	14	NA
Total losses (dB)	31	21	11	25	15	25	20	3
Margins and deratings (dB)								
Repair splices	3	3	3	3	3	3	3	3
Added connector	2	2	2	2	2	2	2	2
Connector aging	3	3	3	3	3	3	3	3
Source aging	3	3	3	3	3	3	3	3
Source power drift/T	2	2	2	2	2	2	2	2
Wavelength drift/T**	NA	NA	NA	1	1	1	NA	NA
Noise drift	2	2	2	2	2	2	2	2
Total derating (dBm)	15	15	15	16	16	16	15	15
Received power (dBm)	-40	-30	-30	-45	-35	-45	-32	-22
Receivier NEP (pW $\sqrt{Hz}$)	10	10	10	10	10	10	10	10
Receiver BW (Hz)	50M	50M	200	200	200	200	200	1M
Processing gain (dB)	15	23	NA	NA	NA	NA	NA	NA
S/N required (dB)	11	30	30	11	30	20	20	11
Sensitivity (dBm)	-45	-34	-38	-57	-38	-48	-48	-39
Net power margin (dB)	5	4	8	12	3	3	16	7

With the receiver noise level known, the optical power level required to achieve a given sensor accuracy can be calculated. For analog sensors, the signal to noise ratio required is inversely proportional to the sensor accuracy. As a general rule, to provide adequate phase margin at the control loop bandwidth, the sensor time constants must be less than one third the sampling interval specified for the sensor.

For digital sensors the signal to noise ratio must be at least 12 to achieve a bit error rate better than 10^{-9}, so the received signal must have at least 24×10^{-16} Joules per bit assuming NRZ format and the bandwidth weighting given in reference 18. The number of bits in a single reading is proportional to the logarithm of the analog accuracy so the total energy required for a single sensor reading can be calculated. The digital readings must be completed within the sensor time constant.

Two limitations to these theoretical estimates must be noted. First, the analog analysis assumes the use of optimized, low-bandwidth receivers with low 1/f noise. Such receivers are uncommon. In practice, the analog noise levels may be higher than estimated. Second, the bit rate in practical digital optical sensors is typically at least three orders of magnitude higher than the minimum estimated here because low bit rates require excessive length in fiber delay lines. For the higher bit rates, proportionally higher power levels will be required.

The estimates for receiver sensitivity assume the use of a state-of-the-art photodiode receiver equivalent to a 50 kilo-ohm transimpedance amplifier. This assumption is consistent with data supplied by manufacturers and allows a unified treatment of receiver sensitivity for all sensor types. The minimum receiver bandwidth of 200 Hz is chosen to be consistent with the update interval in the fastest control loop. The TDM systems require wider bandwidth in the receiver front end, however post-receiver averaging of the TDM pulse trains increases the signal-to-noise ratio by 15 to 23 dB.

In conclusion, the net power margins for a single sensor range from 4 to 16 dB if an LED source is used with a PIN photodiode receiver.

To insure adequate optical signal levels at the electro-optic interface, the fiber-optic link loss must be controlled within limits. This analysis included manufacturers estimates of the optical insertion loss of their sensors. Conversely, the sensor losses used in the optical power budget can be used as specifications for the maximum allowable loss in a sensor. Using this approach, the optical loss budget for each of the nine sensor types is:

Sensor type	Maximum loss (dB)
Digital TDM	25
Analog TDM	15
CW modulation	5
Digital WDM	19
Analog WDM	9
Analog wavelength	19
FMCW	14
Self luminous	NA
Electronic	NA

3.3.5 **Optic multiplex topologies and switch technology.**– Multiplexing sensors on common sources and receivers is a method for minimizing the number of circuit elements, the circuit board area and the I/O pincount. The number of sensors on a common interface is ultimately limited by the optical power budget so the impact of sharing sources and receivers on the optical power budget was analyzed. Multiplex operation effects the optical power budget in two ways: (1) by dividing power among sensors and (2) by reducing the receiver integration time where data must be multiplexed in a serial format. Five network topologies were considered: (a) the non–multiplex (parallel) baseline architecture; (b) a single shared source; (c) a single shared receiver; (d) shared source and receiver; and (e) a matrix of sensors with shared sources and receivers.

The parallel architecture illustrated in figure 3.3.5–1 serves as a baseline for comparison. Here an optical source and receiver are dedicated to each sensor. There are no network losses associated with the number of sensors. All of the sources illuminate all of the sensors continuously and the receivers have the maximum integration time of 1/3 update interval. The theoretical minimum optical power required at the receivers in this topology was calculated in Section 3.3.4.

TABLE 3.3.5–1 – SIZE OF MULTIPLEX TOPOLOGIES

	MSMD (baseline)	SSMD	MSSD	SSSD	Matrix	Switch
Sources	N	1	N	1	$\sqrt{N}$	1
Detectors	N	N	1	1	$\sqrt{N}$	1
Fibers	2N	N + 1	N + 1	2	$2\sqrt{N}$	2
Pincount	2N	N + 1	N + 2	2	$2\sqrt{N}$	N + 1

In the topology illustrated in figure 3.3.5–2, a single source illuminates N sensors in the network continuously so the power is divided. Receivers still integrate over the full 1/3 update interval. The source illuminates all sensors continuously, or quasi– continuously in the case of repetitively pulsed sources. (The case of repetitively pulsed sources will be treated in detail in a later analysis of optically pulse TDM networks.) The total impact on the power budget in this topology is a loss of –10 Log N dB.

In the case of the shared receiver, figure 3.3.5–3, a single optical receiver is shared by N sensors. The sources are turned on sequentially to produce serial optical sensor inputs at the receiver. In this mode of operation the source power can be increased in inverse proportion to the duty cycle. To obtain serial data from the receiver each of the N sensors is sampled in 1/N of the allowable integration time. Therefore the receiver bandwidth and noise level are increased. This increase in receiver noise is compensated by the increase in source power. There is still a slight penalty for sensors with long update intervals because all sensors in the network must be sampled at the shortest update interval.

Where a receiver is shared there is also a potential for excess loss due to reciprocal loss in power combining. So the net impact where a receiver is shared by N sensors is an additional link loss 0f –10 Log N due to reciprocal coupling losses. If the fiber size is larger for receivers than it is for transmitters

and sensors, as in bundle couplers, asymmetric directional couplers, or WDM demultiplexers this reciprocal loss can be avoided at the expense of the added complexity of having a multiplicity of fiber sizes installed on the engine.

The fourth topology, shown in figure 3.3.5–4, is the case where a single source and a single receiver are shared by a group of sensors. In this case three effects impact the power budget: power division, reciprocal loss in power combining, and reduced receiver integration time. Therefore the net impact on sensor signal–to–noise ratio is –30Log N dB if a common fiber size is used on the receiver, or –20 Log N dB if a larger receiver aperture or non–reciprocal power combiner is used.

Finally, the matrix architecture in figure 3.3.5–5 can be considered (ref. 20). In this case each receiver is shared by $\sqrt{N}$ sensors so there is an increase in receiver noise of $\sqrt{N}$ and a potential reciprocal loss of $\sqrt{N}$. Each source illuminates $\sqrt{N}$ sensors and the sources are switched on in sequence. Therefore there is a power division loss of –5 Log N dB and the sources can be operated at $\sqrt{N}$ times the cw power level. The increased source power compensates for the increase in receiver noise so the net impact on the network loss is –10 Log N if a common fiber size is used on the receiver and – 5 Log N if a non–reciprocal power combiner is used.

In conclusion, multiplexing a groups of sensors on common sources and receivers will reduce the power margin by an amount which depends on the topology. In topologies with a shared receiver there is a potential benefit if the network uses a non–reciprocal power combining technique such as wavelength demultiplexer or asymmetric fiber couplers. After estimates of the sensor insertion losses are received from the vendor consultants, the power budget can be used to determine the maximum number of sensors which can be supported in each topology.

The number of sensors which can share a single interface circuit is determined by the power budget and the number of available "addresses", i.e. the number of wavelength bands or the number of time slots. The power budget limits the number according to the loss penalties discussed in previous reports. For a group of N sensors, the loss penalty ranges from 5 log N dB to 20 log N dB depending on the multiplex technique. Figure 3.3.5–7 shows the single–sensor power margin required to support a number of sensors. This figure can be used to determine the number of sensors from the net power margin estimated in Table 3.3.5–1. Excess loss is a significant factor. This analysis assumes excess loss in decibels directly proportional to the number of sensors in the network. Hence a four–sensor network includes four decibels of excess loss.

The number of electro–optic interface circuits required to service the 44 sensors on the engine depends on the number of sensors which can be multiplexed on a common interface. The two self luminous probes, LOD and turbine blade temperature, are not compatible with any multiplex technique. Figure 3.3.5–7 indicates that 4 to 15 interface circuits would be needed to access the remaining 42 measurands, depending upon the topology selected and the multiplex technique.

3.3.5-1 Optical switch multiplexer technology: The advantages of the optical switch multiplexer are reduced circuit board area, reduced parts count, and possibly lower power consumption. Use of the optical switch would not reduce the I/O pincount nor the number of fibers required to service the sensors. The architecture would feature optical switching of a single source or receiver among an array of fibers. The purpose of the optical switch in this application is to replace electronic analog multiplexers by performing that function directly on optical signals. Presently, electronic sensors in an engine control are interfaced to digital control logic through low-level analog multiplexers. In a fiber-optic sensor system it is desirable to provide a similar function, i.e. switch light to a single output fiber from any one of N input fibers. Switch specifications are summarized in Table 3.3.5-2.

TABLE 3.3.5-2 - OPTICAL SWITCH SPECIFICATIONS

Requirement		Multi-mode	Single mode
Fanout	16:1	4 x 2:1	4 x 2:1
Loss	1 dB	3.2 dB	4.5 dB
Crosstalk	-30 dB	-50 dB	-30 dB
Speed	< 100 μ sec	1 ms	1- nsec
Wavelength	750-950 nm	Broadband	$\lambda_0 \pm 2\%$
Environment	-55 to 125 C	TBD	TBD
Improvement in loss, speed, wavelength sensitivity and environmental data are needed			

Analog electronic multiplexers typically provide 8:1 or 16:1 fanout. A useful optical switch would address the same number of channels. Other parameters of interest are optical insertion loss, linearity, crosstalk, switching time, and optical wavelength sensitivity. Typically, 1 dB would be budgeted for the insertion loss. The optical linearity must be better than 0.1% over the optical power range from 10 picowatts to 100 microwatts. The crosstalk from inputs other than the one selected must be less than 30 dB (optical) to permit accurate analog sensing. A switching time less than 1 microsecond is desirable. Broadband operation over 750 to 900 nm or 1250 to 1350 nm is also desirable. If the design is sensitive to wavelength, then a wavelength tolerance must be specified. Both multimode and singlemode designs are needed.

Three types of optic switch can be considered for this design: optomechanical, electro-optical, and integrated optic. Optomechanical switches are now commercially available. These devices rely on electromechanical movement of precisely aligned fiber arrays. They are subject to microphonic pickup and vibration so they are not desirable in an engine mounted EEC. Bulk electro-optical switches have been proposed and demonstrated. Because these devices require complex alignment to discrete micro-optic components and high voltage for operation they are generally not desirable in the

EEC. The integrated optic waveguide switch is based on optical waveguide modulator technology being developed by UTRC. It features low voltage operation at extremely high speeds and the potential for small, lightweight, ruggedized package.

Numerous configurations of multimode optical switches have been fabricated, tested and reported in the literature. These switch configurations fall into three categories; moving fiber, scanning optical beam and multimode integrated optic devices. The moving fiber system employed electro-magnetic force to move the input fiber between one of two, closely spaced, output fibers. The scanning optical beam switches moved a collimated input optical beam between two or more output fibers placed beyond a lens. The scanning mechanisms, in general, involve ether moving optical elements, liquid crystal shutter/mirror elements, or electrooptic birefringent shutter elements. The multimode integrated optic switch directed the optical signal in the input waveguide of a Y branch structure to one of the two outputs. These devices functioned by modulating an electric field at the junction of the Y branch which switched the optical signal from one output to the other.

The present multimode optical switch technologies have at least one of two fundamental problems which preclude their use in high speed multiplexer systems for aerospace applications. These fundamental limitations are high insertion loss or slow switching speed. Of all the switch configurations considered in this investigation, the moving fiber switches are the most promising technology with insertion losses of 0.5 and 0.8 dB as well as switching speeds of 1 and 13 msec (refs. 21, 22). The 1 msec device was achieved by magnetically moving a fiber that was coated with a ferromagnetic film, whereas the slower device moved a ferromagnetic reed with an attached optical fiber. These switches also had output channel crosstalk isolation levels of less than -70 and -50 dB and no optical wavelength sensitivity. The only other candidate technology is a scanning optical beam switch that employed a galvanometer movement equipped with a spherical mirror to switch the input signal to one of five outputs (ref. 23). This system has a typical insertion loss of 1.5 dB and a scanning frequency of 300 Hz. The crosstalk levels ranged from -23 to -38 dB and there was no wavelength sensitivity stated. The moving fiber switch that manipulated the coated fiber is the best technology of the multimode switches since it had the best performance and provided high reliability potential due to the lowest parts count.

All the other multimode switch technologies had lower performance characteristics than the preceding systems. The mechanical scanning optical beam switches which moved lenses (ref. 24) or prisms (ref. 25) or mirrors (ref. 26) all had similar insertion losses, 1.5 dB, and switching speeds of 8–10 msec. A liquid crystal optical beam scanning system was reported, having a 15 dB insertion loss and a 4 msec switching speed, furthermore the temperature range of this liquid crystal devices was from 7 to 84 deg C (ref. 27). Another reported beam scanning switch employed the electrooptic effect in PLZT ceramic to rotate the polarization vector of the input beam by 90 degs to produce a shutter mechanism (ref. 28). This system was reported to have an insertion loss of 1.9 dB, but the 3 dB loss from polarizing the input beam was neglected. The switching speed was 70 nsec. The multimode integrated optic switches were not fiber compatible since the waveguides were 1.5 microns deep by 8–40 microns wide, producing high insertion losses which were not reported (refs. 29–31). The attainable switching speeds were reported to be 1 GHz when optimized electron designs are used.

Single mode switching structures are capable of switching optical signals in one microsecond or less. Both LiNbO3 and semiconductor waveguide devices can be used for this purpose. LiNbO3 is the more mature of the two technologies since it has been studied extensively in recent years for telecommunication switching applications (ref. 32). Several research laboratories have demonstrated 4x4 and 8x8 switch arrays in LiNbO3 and these structures are currently becoming commercially available from several vendors.

Regardless of the specific waveguide technology used to implement the integrated optical switch array, the N-1 switch elements are arranged in a K-stage binary tree configuration. To switch from the input port to the desired output port, K switches need to be activated. As a result of reciprocity, this structure can also function as an 8x1 analog multiplexer by operating it in reverse.

Hogert et. al. (ref. 40) demonstrated a 4x4 crossbar array which consisted of sixteen reversed delta beta directional couplers. The device operated at 1.3 microns and had a pigtailed fiber-to- fiber insertion loss of 5.2 dB. The switch elements with 5.5-mm- long electrodes required 8.0 + 1.8 Volts for the cross state and 13.4 + 1.7 Volts for the bar state. The optical crosstalk in the switch array was <-35 dB for all switch elements.

Woges et. al. (ref. 42) demonstrated a 4x4 crossbar array which consisted of sixteen X-switches. No value for insertion loss was given for the 1.3 micron device. The 1-mm-long electrodes required +25 Volts for the bar state and -35 Volts for the cross state. The optical crosstalk ranged form -25 to <-35 dB.

Sawaki et. al. (ref. 33) demonstrated a rectangularly configured switch array which consisted of 16 reversed delta beta directional couplers. The device operated at 1.3 micron and exhibited a fiber-to-fiber insertion loss of 4.7 + 0.3 dB. The switch array had very uniform voltage requirements with 9 + 0.5 Volts for the cross state and 20 + 0.5 Volts for the bar state. Optical crosstalk ranged from -15 to - 30 dB.

Milbrodt et. al. (ref. 41) demonstrated a 4x4 switch array which utilized a non-blocking Benes-Banyan architecture. Their architecture required 3 banks of four reversed delta beta directional couplers. The fiber-to-fiber insertion loss in their 1.3 micron device ranged from 2.9 to 4.8 dB. The 8.55-mm-long electrodes required 4 + 1.5 Volts for the cross state and 11.5 + 1.5 Volts for the bar state. Optical crosstalk was extremely low and ranged from -36 to <-44 dB.

Duthie et. al. (ref. 35) demonstrated an 8x8 re-arrangably nonblocking switch array which utilized 28 reversed delta beta directional couplers. The average fiber-to-fiber insertion loss in their array was 5.5 dB. The 4.25-mm-long electrodes required 25.7 Volts for switching. Optical crosstalk was less than -20 dB.

Granestrand et. al. (ref. 34) demonstrated an 8x8 crossbar array which utilized 64 directional couplers. The 1.3 micron device had a fiber-to-fiber insertion loss of 5.3-6.8 dB. The 3-mm-long electrodes required 18.6 + 3.6 Volts for the bar state and 26.4 + 1.6 Volts for the cross state. Optical crosstalk is currently <-30 dB.

Nishimoto et. al. (ref. 36) demonstrated a polarization- independent strictly-nonblocking 4x4 switch array consisting of twelve polarization-independent directional couplers. The device operated

at 1.3 micron and exhibited a fiber-to-fiber insertion loss of 4.0-6.0 dB independent of input polarization. Switching voltages for the twelve elements ranged from 21 to 32 Volts. Optical crosstalk levels ranged from -15.5 to -45.8 Db with an average crosstalk level of -28 dB for the TM mode and -29.6 dB for the TE mode.

Granestrand et. al. (ref. 37) demonstrated a polarization independent strictly-nonblocking 4x4 switch array which was configured in a tree architecture. The array required 24 switching elements. The 1.3 micron device had a fiber-to-fiber insertion loss of 8.4 + 1.4 dB for the TE mode and 8.4 + 0.6 dB for the TM mode. The device required 50 Volts for switching between the cross and bar states. Optical crosstalk was <-29 dB for all switch elements.

A near-term (within one year) realistic estimate of the performance of 1x8 and 1x16 multiplexers/demultiplexers is presented:

Optical Insertion Loss: Assuming an electrode length of 10 mm, a 1x8 circuit will be approximately 4 cm long while a 1x16 circuit will be approximately 5 cm long. Included in these lengths are 1 mm for bends into and out of each switch element and an additional 4 mm on one end of the crystal to separate the waveguides to the typical 250 micron center to center fiber spacing. A conservative estimate for propagation loss is 0.3 dB/cm at both 0.8 and 1.3 micron so that the 1x8 and 1x16 circuits will have 1.2 and 1.5 dB propagation loss, respectively.

The total fiber-to-fiber insertion loss in the 1x8 and 1x16 devices should be approximately 4 and 4.5 dB, respectively. In addition to propagation loss, these values include excess device loss of 0.3 dB per device rank, Fresnel loss of 0.1 dB per fiber/waveguide interface, fiber coupling loss of 0.3 dB per interface, and excess pigtailing loss of 0.5 dB per interface. These estimates are slightly conservative based on current technology; however, they should represent values which can be easily achieved once the LiNbO3 technology is transferred from the research laboratories to manufacturing divisions. Champion devices should exhibit 2.5-3 dB insertion loss.

Optical Linearity: Devices operating at 1.3 micron should exhibit an optical linearity of better than 0.1% for optical powers ranging from 10 pW to 100 μW. At 0.8 micron, optical damage (photorefractive effect) will place an upper limit on optical power handling of 10 μW for Ti-diffused waveguides. For power < 10 μW, the linearity should be comparable to the 1.3 micron devices. The power handling capabilities can be increased to 100 μW at 0.8 micron if proton-exchanged waveguides are used.

Optical Crosstalk: At least two laboratories have demonstrated polarization- dependent switch arrays with <-35 dB optical crosstalk. As fabrication processes become better controlled, achieving crosstalk levels of -35 dB should become routine in 1x8 and 1x16 circuits. Due to tighter fabrication requirements, polarization- independent circuits will likely exhibit crosstalk levels of -25 dB.

Switching Time: Electrode capacitance is typically 5 pF or less for most device structures. For 50-ohm termination, switching times of 10 nsec are easily achieved.

Drive Voltage: The drive voltage in the polarization-dependent circuits should be <5 Volts at 0.8 micron and <8 Volts at 1.3 micron for 10-mm-long electrodes. The drive voltages will be approximately 3 times larger at each wavelength.

Wavelength Sensitivity: All of the devices described in this work are wavelength sensitive. Varying the wavelength changes both the coupling length and the voltage-induced in the directional coupler-type devices. To maintain <-30 dB optical crosstalk, the wavelength must be controlled to within +/- 2%.

3.3.6 Reliability.- The failure rates of the electro-optic interfaces were calculated based on the number of electronic circuit elements and electro-optic components using MIL-HDBK-217E procedures with the following assumptions:

- Aux environment, 65°C ambient temperature

- JAN quality for optoelectronics, MIL-M-38510 Class S for electronics

- 20 volt, 50°C stress

- gate and transistor counts > 100 per package

- 16-pin hermetic DIP packages

- AlGaAs Laser Diode, 100% duty factor, fixed 100 mA current source, 50% degradation

The failure rates calculated for key electro-optic interface components using these assumptions are shown in Table 3.3.6-1. Also shown in the table are the calculated failure rates for each of the nine candidate sensor interface types. Except for the coherent sensor, all of the candidates have failure rates which fall between 7.2 to 19.2 failures per million hours. The differences in failure rates arise mainly from the optical sources or detectors.

For all sensors, redundancy would be implemented by duplicating the sensor, optical fiber interconnect, and electro-optic interface in each of the two channels of the engine control. In a multiplexed architecture the size, weight, performance, and component reliability advantages are purchased at the price of a single point failure potential which did not exist in the original non-multiplexed electrical system. This potential may affect the system redundancy or fault tolerance, hence the number and types of sensors which can in practice be allocated to a multiplexed interface may not be limited by optic technology but rather by system fault tolerance requirements. This aspect of the problem will be considered in Task II of the proposed program.

More experience is needed to determine fault isolation and maintenance strategies for fiber-optic sensors.

TABLE 3.3.6-1 - ELECTRO-OPTIC INTERFACE RELIABILITY DATA

Part	Failure Rate/10^6 Hr
Light Emitting Diode (LED)	0.8
LED driver amplifier	0.6
LD	360.0
PIN photodiode	0.4
CCD photodiode array	8.0
Photodiode pre-amplifier	0.2
Analog amplifier	0.2
Analog multiplexer	0.2
A/D converter	1.8
TTL frequency counter	1.5
Digital gate array	1.5
Power supply regulation	0.6

Candidate	Single sensor failure rate/10^6 hours (UTRC estimates per MIL-HDBK-217E)
Analog TDM	7.2
CW modulation	7.8
Digital TDM	9.6
Self luminous	10.8
Coherent	361.0
Analog WDM	15.6
Digital WDM	15.6
Spectral measurement	15.6
Electronic	19.2

3.3.7 **EEC location.**- The location of a EEC processor with electro-optic input and output interfaces effects the the evaluation criteria established for this study as described below.

Types of sensors: EEC location cannot compromise the types of sensors which can be accommodated in the design, however a remote EEC may restrict the optical sensing mechanisms employed for each quantity if higher degree of multiplexing is required to support the off-engine location.

Signal compensation or calibration: EEC location should not effect signal compensation or calibration methods or whether the sensing mechanism is digital or analog.

Number of channels: Location of the EEC does not effect how many sensors can share a single optical source or receiver. Remote location may be more feasible if many sensors share common sources and receivers.

Number of distinct sources and detectors: Location of the EEC does not directly effect the number of optical sources and detectors required to service all of the sensors. However, a remote EEC would place more emphasis on minimizing the I/O fiber count and thereby may influence the number of sources and detectors.

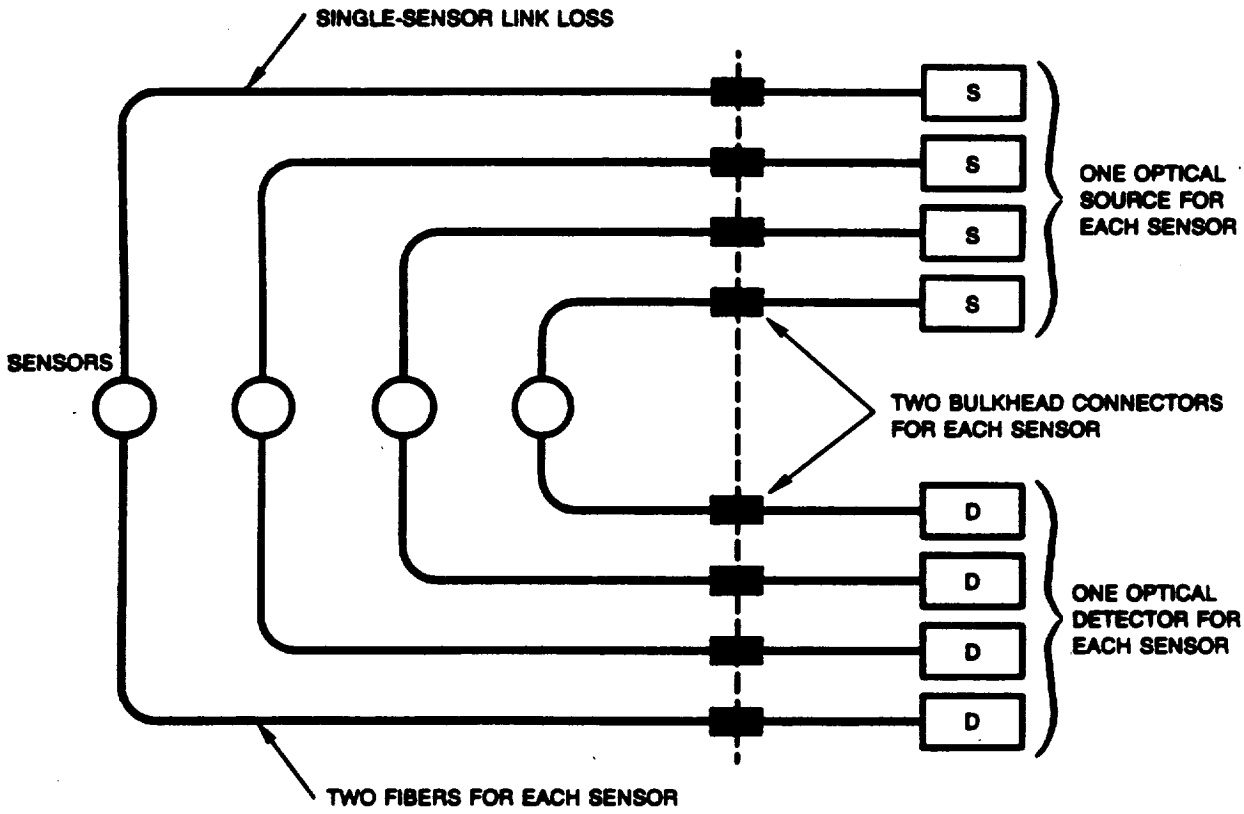

Figure 3.3.5-1. — The multiple source, multiple detector (MSMD) topology:

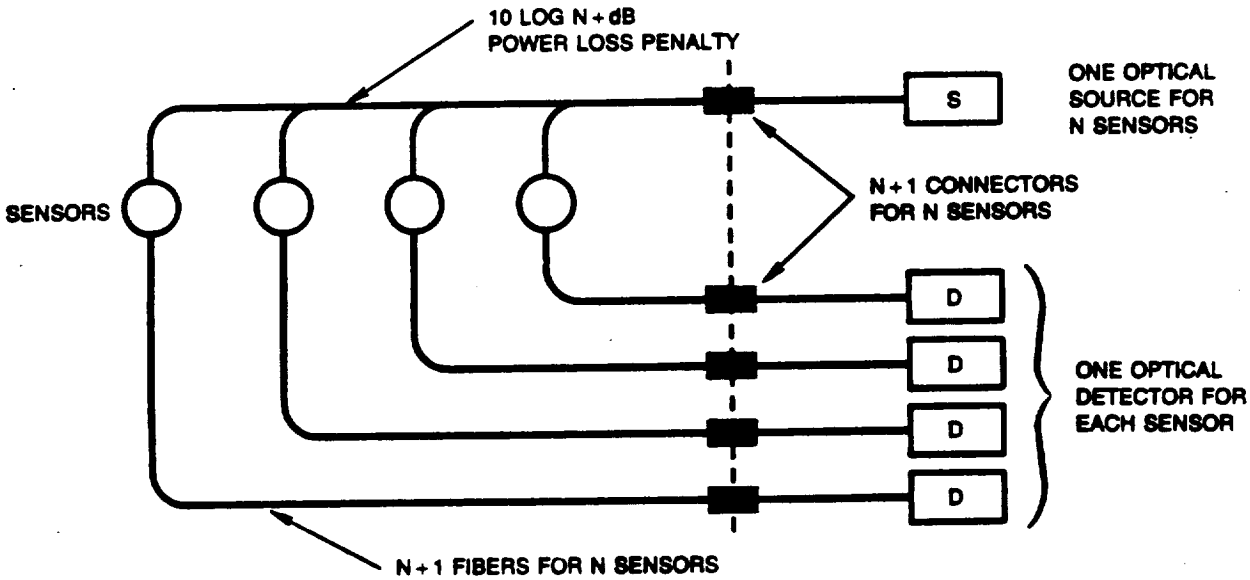

Figure 3.3.5-2. — The single source, multiple detector (SSMD) topology:

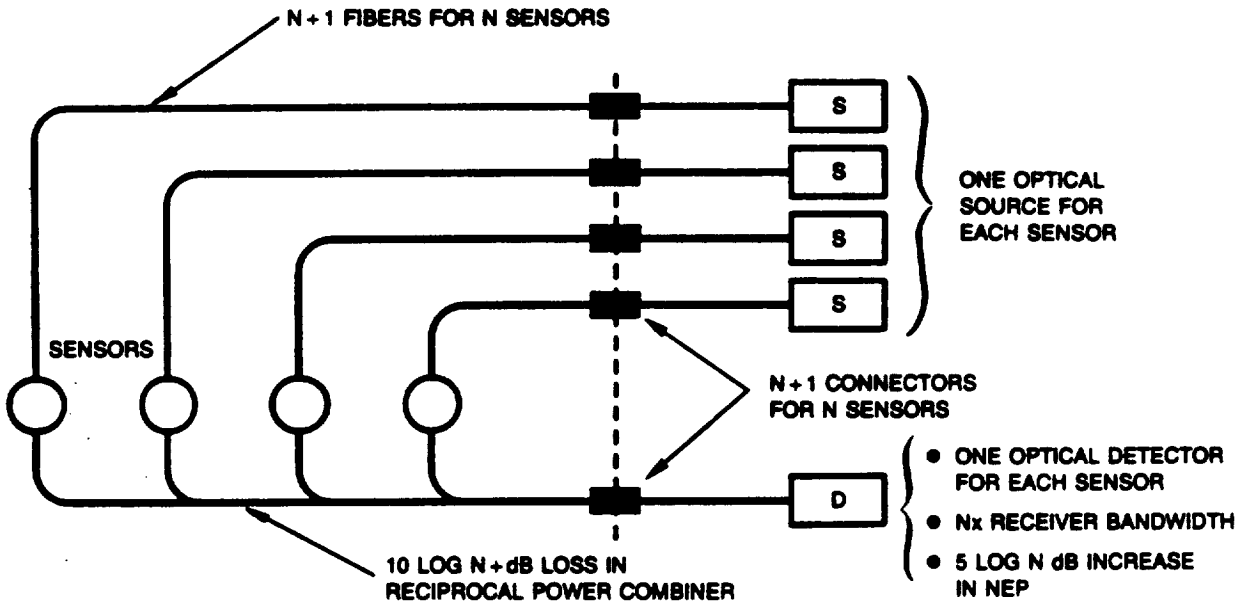

Figure 3.3.5-3. — The multiple source, single detector (MSSD) topology:

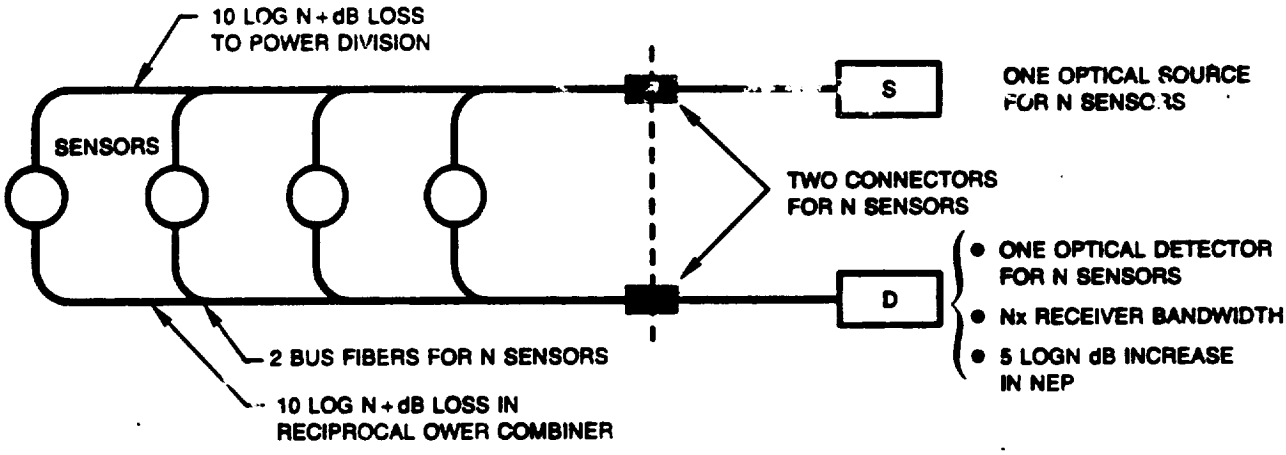

Figure 3.3.5-4. — The single source, single detector (SSSD) topology:

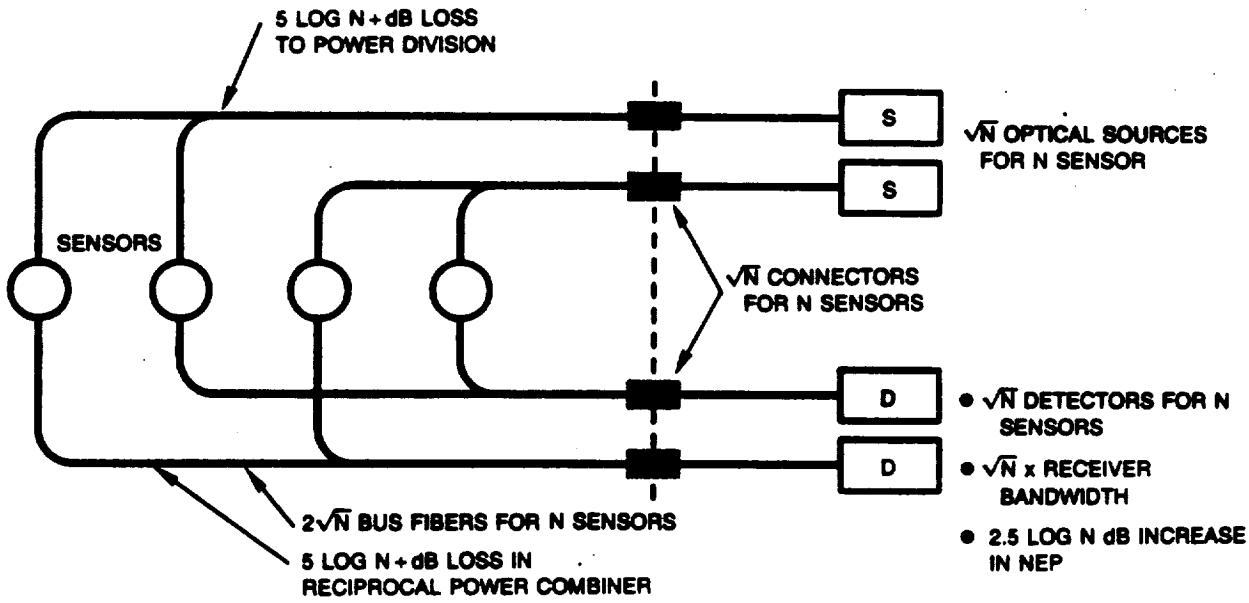

Figure 3.3.5-5. — The fiber-optic matrix multiplex topology:

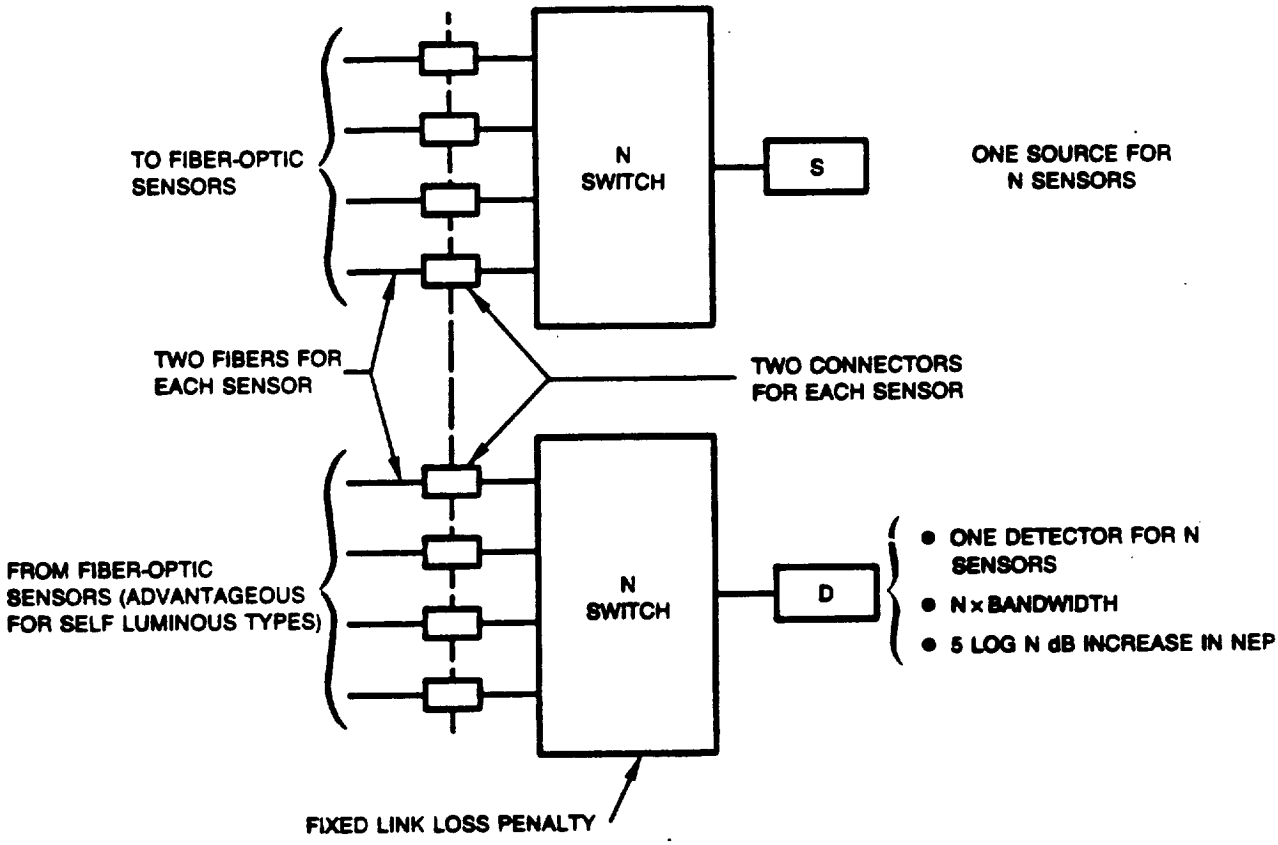

Figure 3.3.5-6. — The optical switch topology:

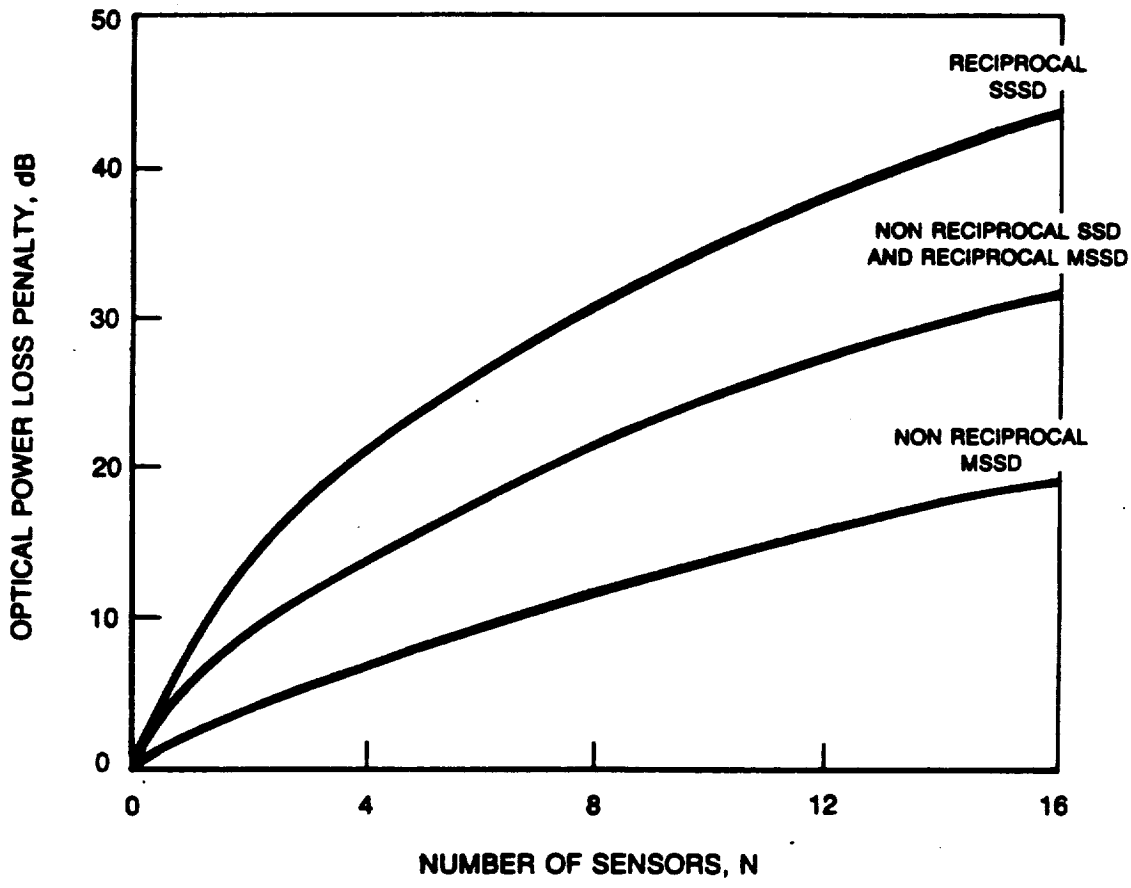

Figure 3.3.5-7. — The optical power budget limits the number of sensors on a common multiplex interface.

Number of fibers and I/O pincount: A remotely located EEC would naturally tend to favor architecture having the minimum number of parallel optical fibers and I/O connections to service all of the sensors. Note that this is primarily a size and maintainability issue, system weight is not significantly increased by adding more fibers to the cable. Note that it is desirable to minimize the I/O pincount for any location of the EEC.

Optical power margin: A remote EEC impacts the optical power margin by inserting additional optical connectors between the EEC sensor interface transmitters and receivers. This impact is estimated to be an additional two connectors in each direction or about 4 dB in additional loss. The power margin is also effected if a higher degree of multiplexing is required to support an off-engine EEC.

Signal processing time: Location of the EEC does not impact the signal processing time for the electronic interface to compute the sensor value or the bandwidth of the analog portion of the receiver.

Complexity: The location of the EEC effects the number of circuit elements in the electronic interface only if higher degree of multiplexing is required to support an off-engine EEC.

Electrical power consumption: Additional electrical power may be required for the interface circuitry if additional multiplexing is needed for an off-engine location.

I/O circuit area: The location of the EEC should not effect the circuit board area required for the electro-optic interface.

Weight: Application of fiber-optic data links and fiber-optic sensors reduces the harness weight thereby changing the tradeoff between harness weight and EEC location. The total length of cable in the sensor system is estimated to be 400 feet per channel. The weight of the optical fiber cable is 0.0045 lb/ft compared to 0.0372 lb/ft for wire. If the wire is replaced with optical fiber cable then the weight of the optical harness would be less than 2 lb. Assuming that an additional 4 lb of electronics plus 4.5 lb of composite connectors would be required to support the optical interface to the sensors, the total weight of an optical control harness would be 10.5 lb. Assuming a worst case of 88 fibers in the harness the additional weight required to extend the harness 10 feet from the engine is only 4 lb. This requires, of course, that ALL sensing and actuation functions on the engine can be accomplished with optical signals alone. The conclusion reached through this comparison is that harness weight is not a significant factor in design of the all-optic control system. Therefore, location of the EEC in the electro-optic architecture does not significantly impact the weight of the system.

Reliability: The location of the EEC effects its reliability mainly by the environment. Previous studies concluded that the thermal and vibration environment for optimum airframe and engine mounting locations are essentially the same. In both cases the EEC electronics must be rated for operation over the -55 C to 125 C temperature range and high vibration levels. On the engine itself, a relatively cool location away from the core is preferred. Note the the MTBF the commercial engine-mounted EEC in service now exceeds 20,000 hr. Therefore, the reliability factor favors a EEC location in the cooler, lower vibration locations in the airframe or on the engine but does not effect the choice of engine versus off-engine location.

Redundancy: Since the EEC location does not strongly influence EEC reliability, redundancy requirements would not be effected.

EMI immunity: By design, the electro-optic architecture will use no metal wires for signal transmission so the EMI susceptibility of the system will be unaffected by the harness length or routing to different EEC locations.

Maintainability: EEC location effects maintainability through accessibility. Fault detection, and isolation, and electronic components replacement may be easier in an airframe location.

Availability or development schedule: Since an all-optic architecture is assumed wherever the EEC is located, the development issues are not effected by location.

The choice of location for the EEC is influenced primarily by maintainability, complexity (in the form of multiplexing), and optical power budget. In general this means a location away from hot spots and extreme vibration levels. In the airframe this implies locating the EEC in a central bay. On the engine the EEC must be located forward outside the fan. Improved maintainability favors the central location with other aircraft electronics. Reduced system complexity and maximum optical power budget favor the location on the engine. Other factors (sensor types, sensing mechanisms, fibers, sources, detectors, processing, power consumption, size, weight, reliability, redundancy, EMI immunity, and development schedule) are not strongly effected by the location of the EEC.

In conclusion, the electro-optic architecture will support either the engine or airframe locations but the use of this architecture does not influence this selection. None of the evaluation factors are effected by where the sensors are distributed around the engine. This is because the fiber-optic cable weight is insignificant. EEC location (within the confines of the aircraft) can be determined without consideration of the sensor locations.

3.4 Summary of Electro-Optic Architectures

The 14 figures of merit for the nine candidate interface types are summarized in Table 3.4-1. In most areas little or no significant difference can be discerned between the candidate sensing methods. The areas in which there is some discrimination are the types of sensors which can be accommodated, the effectiveness of drift compensation, the numbers of sources and detectors required, the optical power margin, the number of multiplex channels, and reliability.

All of the candidate interface designs are capable of computing multiple sensor values within the 5 millisecond control loop. The fiber-optic receiver bandwidths can all be matched to the data acquisition rate. Signal processing time is not a significant discriminator between interface designs.

All of the candidate systems are presently in prototype stage, except for the coherent system which is still in laboratory development and lags the multimode, incoherent designs by an estimated five years. None of the fiber-optic sensor designs have been proven in the aircraft engine environment.

While the simplicity of the transducer design and the interface electronics recommend the analog designs over the digital approaches, the limited accuracy of analog compensation schemes in the

engine environment may dictate use of the more complex digital methods to insure sensor accuracy. This selection depends on real performance data in the target environment. Of particular concern are the effects of spectral drift in analog wavelength domain intensity referencing and drift of delay coil loss in analog time domain intensity referencing. Therefore, both analog and digital optical sensor types should be evaluated in system demonstration. The architecture for the demonstration/evaluation should accommodate both types for the appropriate groups of sensors.

The wavelength multiplex methods in general require a larger number of sources and detectors than the time domain techniques. However, the use of more efficient packaging such as LED or photodetector arrays may reduce the size of multiple receivers or transmitters.

The optical power margin in passive multimode optical fiber sensor links ranges from 13 dB to 22 dB. However there is a large uncertainty in these estimates due to unknown performance of fiber-optic sensors in the engine environment. The number of multiplex channels on a common shared interface, as determined by this optical power margin, ranges between four and eight.

Estimates of failure rates range from 7.2 to 15.6 failures per million hours, with the exception of coherent systems and remote electronics. Note the laser source alone has a failure rate two orders of magnitude higher (360 failures per million hours). There is a small reliability penalty in wavelength multiplex systems due to the larger numbers of sources and detectors, however the magnitude of this difference may not be significant.

In conclusion, the analysis shows no strong discriminator (except reliability of laser diodes and remote electronics) on which to base a selection of preferred common interface type. Therefore a hardware test program is recommended to assess the relative maturity of the technologies and to determine real performance in the engine environment.

4.0 OPTICAL ACTUATION

Optical actuation of fluidic devices has been proposed as an alternative to electrical controls. Optical power sources, glass fiber transmission lines, and optical connector technology are all well developed and available for this application. The essential element of a complete optically controlled actuator which still requires development is the opto–fluidic interface where optical intensity is converted to fluidic pressure.

A number of attempts to build opto–fluidic or opto–mechanic interfaces have been made. In 1885, Alexander Graham Bell used the opto–acoustic effect to produce sound in a gas with a chopped beam of sunlight (ref. 43). For most of the century following Bell's experiment, the opto–acoustic effect was used only to study the absorption of light by materials. In 1976, an optoacoustic telephone was demonstrated at Bell Telephone Laboratories (ref. 44). In 1980, an optically controlled fluidic actuator was built. This device used the opto–acoustic effect to generate a pressure signal in the control port of a fluidic laminar proportional amplifier (ref. 45). Optical actuation of electro– mechanical devices via photoelectric cells has also been demonstrated (refs. 46–48).

The optical hydraulic servovalve (OSV) proposed for the EOA is made up of a hydromechanical subsystem and an opto–fluidic subsystem as shown in figure 4.0–1. The OSV employs an optical command signal to generate a fluidic pressure signal that is used to control a hydraulic servovalve. The optical command signal, generated via solid–state laser, is conveyed to the opto–hydraulic interface (OHI) through fiber optics. The OHI is a modified fluidic laminar proportional amplifier (LPA) which transforms the optical signal into a differential pressure signal. The OHI is followed by hydraulic amplification with a fluidic gain block assembled from laminar proportional amplifiers. The OHI and LPAs are fluidic devices that function in the same manner except that the OHI is modified to accommodate the optical input signal.

The Opto–Hydraulic Interface (OHI) illustrated in figures 4.0–1 and 4.0–2 converts an optical signal into a hydraulic pressure via thermal manipulation of boundary layer flow in a fluidic device (refs. 49–51). Pressurized fluid is accelerated through a nozzle forming a fluid jet (represented by three arrows) which creates a pressure at the outputs via jet stagnation. The signal conversion is performed by optically heating one side of the nozzle back plane causing a localized reduction in the hydraulic oil viscosity, deflecting the jet off center and producing a differential pressure between the output ports.

The OHI driver module consists of a commercial pulse width modulator circuit and a current amplifier for the laser diodes. The pulse width modulator circuit accepts a digital signal input and produces an output pulse train with duty cycle proportional to the input level. The laser diode delivers 50 mW continuous output power from a step index 100/140 fiber optic pigtail. The OHI/hydraulic amplifier was connected to the laser diode with a 100/140 step index optical fiber to provide the optical command signal to the OHI. The connection with the OHI is made with a 0.48 pitch graded index rod lens. The graded index rod lens serves as the window and focusing element. The focused optical energy has a 35 micron diameter spot. The rod lens is potted into the fluidic top cover plate whereas the fiber–optic termination is bolted to this cover plate. The OHI top cover plate is the physical boundary between the optical and fluidic portions of the assembly. The top cover plate provided a smooth and flat surface for sealing to the fluidic laminates while housing the optical components.

60 INTENTIONALLY BLANK

In the opto–fluidic interface light is focused onto the flow boundary layer of the power jet in a laminar proportional amplifier. This interface has produced a larger fluidic response than previous opto–acoustic interfaces and can be operated from dc to 100 Hz without appreciable signal loss. This optical actuator system successfully demonstrated that the OFI can be combined with fluidic amplifiers to build an actuator system.

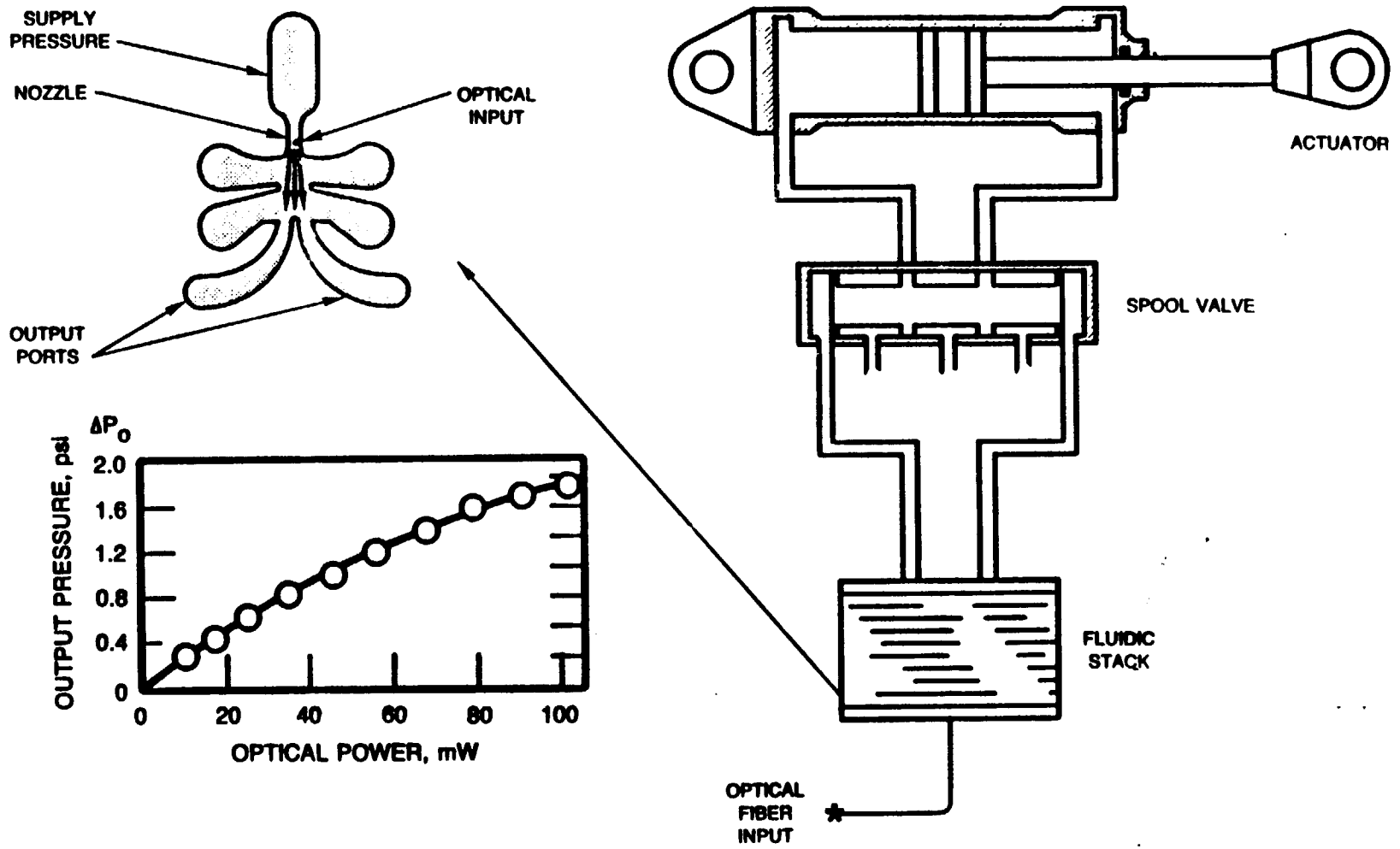

Figure 4.0–1. — The UTRC optical servovalve complements the electro-optic sensor architecture.

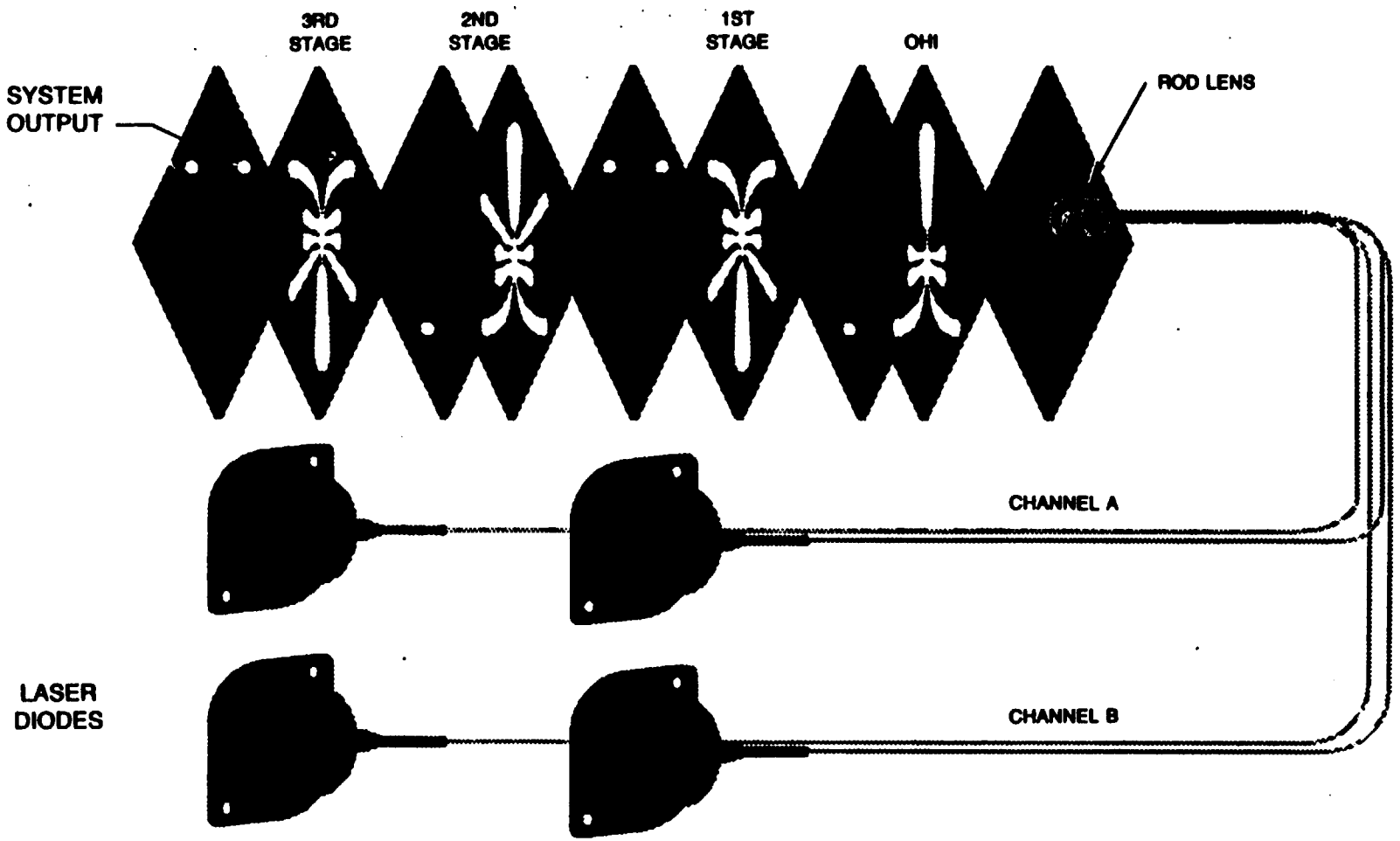

Figure 4.0–2. —Double redundant; push/pull opto-fluidic system.

5.0 SYSTEM DEVELOPMENT RECOMMENDATIONS

Analysis of the candidate electro-optic interfaces concluded that a flight demonstration/validation is needed to determine preferred optical modulation methods for an optimal electro-optic architecture. Such a program would provide more realistic on-engine performance data and may reveal discriminators to guide the selection of a preferred architecture. This section describes a configuration of the electro-optic sensor interfaces that is suited to a flight test program. The purpose of the program is to design, fabricate, and test an electro-optic architecture (EOA) and integrated it with a set of representative sensors for the propulsion control system in a military aircraft. The recommended architecture is an on-engine EEC which contains electro-optic interface circuits for fiber-optic sensors on the engine. These circuits would feature passive optical multiplex of groups of sensors through a common electro-optic interface.

An attractive configuration for the flight test is a generic, modular testbed which will provide for evaluation of a number of different electro-optic interface technologies and is suitable for installation on the aircraft test platforms. A block diagram of such a system is shown in figure 5.0-1. The testbed would consist of an engine mountable electronic enclosure containing microprocessor, power supply, fiber-optic data bus interface, and electro-optical interface boards. The microprocessor would be programmed to acquire and analyze sensor data. The fiber-optic data bus would provide a link to the integrated flight/propulsion control system. An illustration of the engine mountable unit is shown in figure 5.0-2.

A single electro-optic board would acquire all of the sensor values in one of the groups in Table 2.4-1. Boards would be procured for each of the seven sensor groups: Self luminous interface, High temperature interface, Low temperature interface, Speed and flow interface, Vibration interface, Pressure interface, and Position interfaces. These circuit boards would all be fabricated to common electrical, mechanical, and optical interface specifications to allow interchangeability. Figure 5.0-3 illustrates a generic specification for an electro-optic circuit board.

Following are relevant documents, typical design requirements, typical environmental data, and typical reliability goals for the demonstration optical sensor and opto-electrical interface electronics. These requirements are supplied as a general guide only. It is suggested that the suppliers of sensors and electro-optic interface boards be familiar with the following government and industry documents as they pertain to aircraft engine control hardware:

U.S. GOVERNMENT DOCUMENTS:

MIL-E-5007D	Engine, Aircraft, Turbojet and Turbofan, General Specifications for
MIL-B-5087B With Amend 1	Bonding, Electrical, and Lightning Protection for Aerospace Systems
MIL-L-7808	Lubricating Oil, Aircraft Turbine engine, Synthetic
MIL-L-236998-2	Lubricating Oil, Aircraft Turbine Engine, Synthetic
MIL-C-38999H	Electrical Connectors For Severe Environment

MIL-T-29504/4	Termini, Fiber Optic, Pin Terminus (Preliminary)
MIL-T-5624L	Turbine fuel, aviation: Grades JP-4 and JP-5
MIL-STD-461B	Electromagnetic Interference Characteristics, Requirements for Equipment
MIL-STD-462	Electromagnetic Interference Characteristics, With Notice 1 Measurements of
MIL-STD-704B	Electrical Power, Aircraft, Characteristics and Utilization of
MIL-STD-785A	Reliability Program for Systems and Equipment, Development and Production
MIL-STD-810C	Environmental Test Methods
MIL-HDBK-235-1	Electromagnetic (Radiated) Environment considerations for Design and Procurement of Electrical and Electronic Equipment - Part 1

INDUSTRY DOCUMENTS:

D6-16050-2	Electromagnetic Interference (The Boeing Company)
D6-44588N	Electrical Requirements for Utilization Equipment Installed on Commercial Transport Airplanes (The Boeing Company)
WZZ7000	(Douglas Aircraft)
RTCA DO16OB	Environmental Condition and Test Procedures for Airborne Electronic/ Electrical Equipment and Instruments (Radio Technical Commission for Aeronautics)

The general design objectives for the demonstration hardware are low weight, high reliability, simple design, low cost, and minimum size. The hardware will be required to meet specific requirements for sensor performance, as well as optical, electronic, and mechanical interfacing within the engine control system. The sensors and electro-optic circuit boards should be designed in accordance with the general requirements of MIL-E-5007.

Each sensor should provide a digital representation of the measured parameter. The digital data output refresh rate should be faster than or equal to values in Table 2.1-1. The response time of the sensors should be minimized, goals being less than 1/3 that shown in Table 2.1-1. The interface board electrical connector and voltages available at the connector will be specified. The interface board electrical power requirement should be specified by the sensor vendor.

The electro-optic interface board will be mounted in, and interfaced to, an engine mountable enclosure. The electro-optical interface board should not exceed specified dimensions. The board should mount via a flange around its edges using screws of size, number, and location, as specified. The weight of each proposed sensor design should be minimized. The electro-optic interface board weight should not exceed 1.0 lbs. The board should be designed for engine mounting on vibration isolators. The unit would be air cooled by natural convection.

Ambient light effects due to pick-up in fibers and connectors must be negligible.

The sensors should be electromagnetically in compliance with MIL-B-5087B, MIL-STD-461B, MIL-STD-462 and MIL-HDBK-235-1. The vendor would be responsible for determining the interface board EMI criteria to insure sensor interface board and EEC compatibility. The optical sensor system should also comply with the requirements of specifications WZZ7000, D6-16050-2, and D6-44588N.

The demonstration sensors should be capable of operating throughout the ambient temperature range of -55 degrees C to 180 degrees C. Suppliers should indicate the maximum temperature capability of proposed sensor and the source of this limit. The flight ambient temperature for most sensors is expected to be 55 to 260 degrees C, with fifteen minute excursions to 290 degrees C. The sensor interface electronics must be designed to operate through the range of EEC temperatures: from -55 degrees C to 125 degrees C. It must operate in this range for ambient pressures between 2 and 20 PSIA.

The sensors should be compatible with the following fluids: Fuels - MIL-T-5624L, grades JP4 and JP5; Oils - MIL-L-236998-2, Chlorotrifluoroethylene (CTFE).

Tests should be performed on each sensor system to ensure compliance with the performance specification. Suppliers should recommend specific procedures or analysis for design verification, environment compatibility, reliability, and endurance tests. Environmental stress screening should include: electromagnetic compatibility and lightning protection test; thermal cycling; vibration test; operational shocks test; crash safety shocks test; explosion proof test; humidity test; and fungus test per MIL-STD-454.

After completion of the certification tests the units should be completely disassembled to the subassembly level for examination of all parts. Measurements should be taken as necessary to disclose excessively worn, distorted or weakened parts. These measurements should be compared with the applicable drawings, dimensions and tolerances or with similar measurements made prior to the tests. After completion of the tests a final report should be provided.

The fully developed flight reliability of the sensor should be a Mean Time Between Failure (MTBF) of 30,000 hours at a maturity of 20,000 flight hours, and 90,000 hours at a maturity of one million flight hours. MTBF is defined as flight hours divided by the total number of sensor failures. The service life of the sensor should be 10,000 hours, indicating approximately 8,000 flight hours.

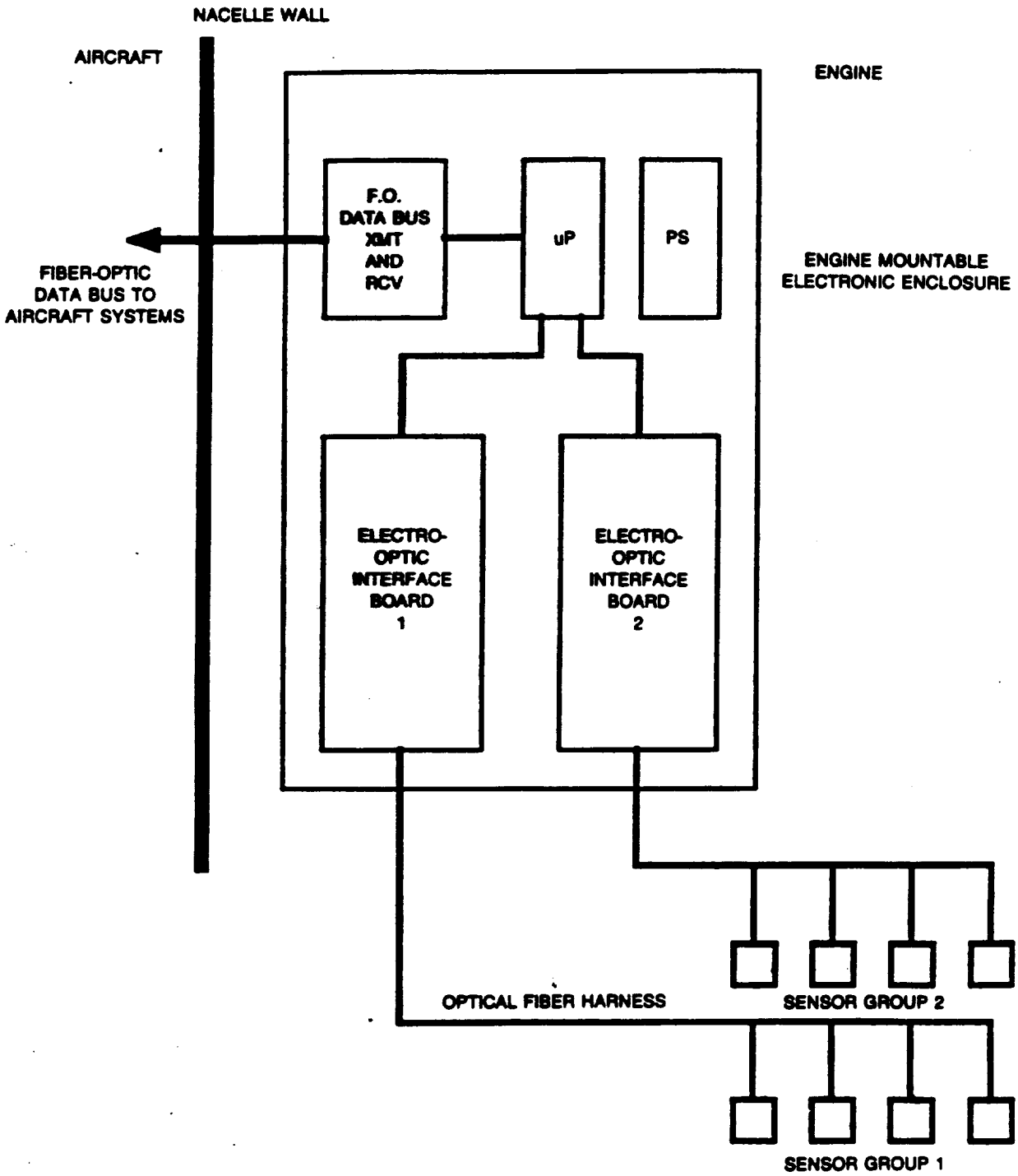

Figure 5.0-1. — A configuration for the FOCSI II testbed would consist of an engine-mountable enclosure containing a power supply (PS), microprocessor (uP), fiber-optic data bus, and electro-optic interface boards.

89—3—15—25

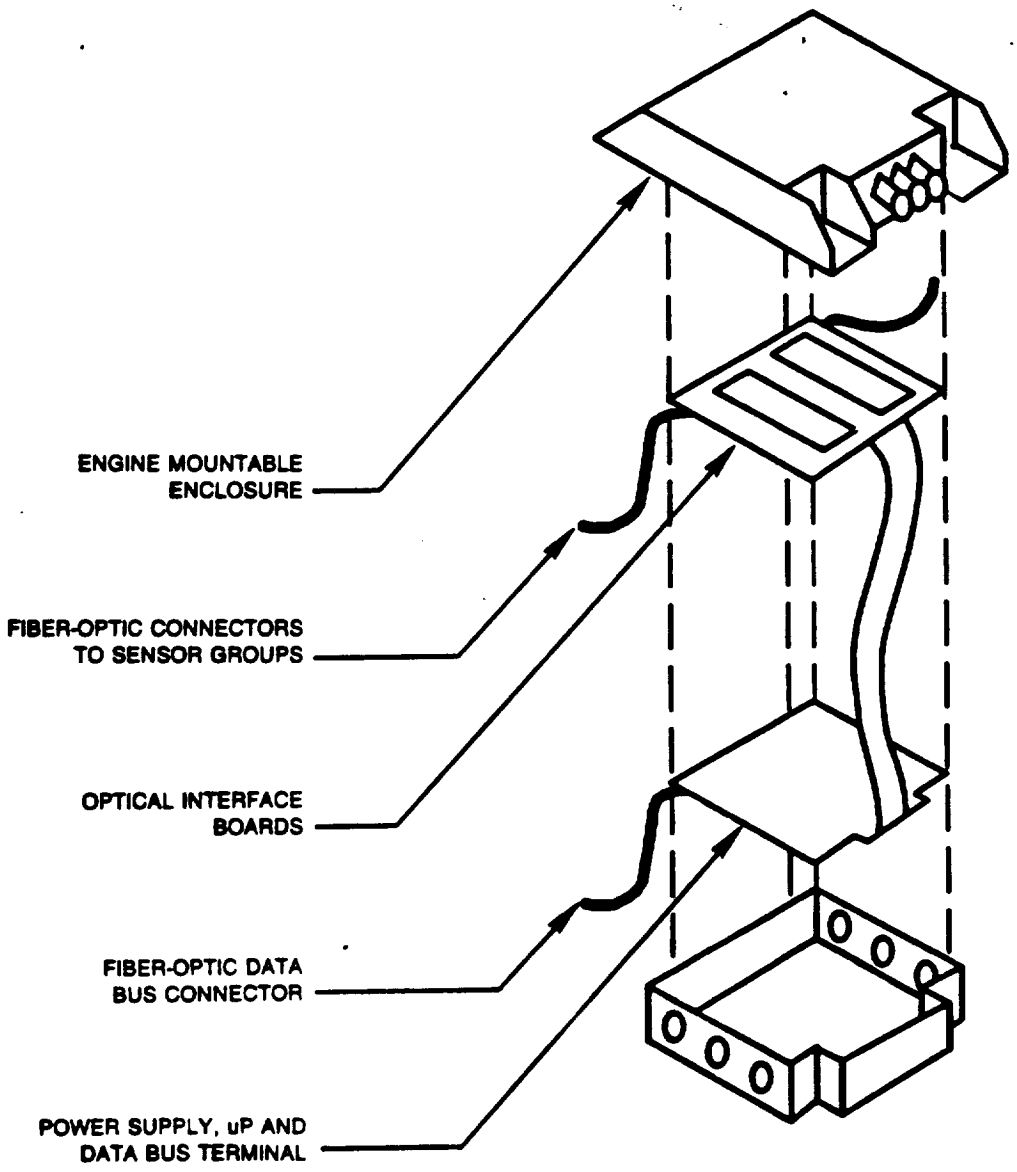

Figure 5.0-2. — Electro-optic interface boards will be mounted in an engine mountable enclosure.

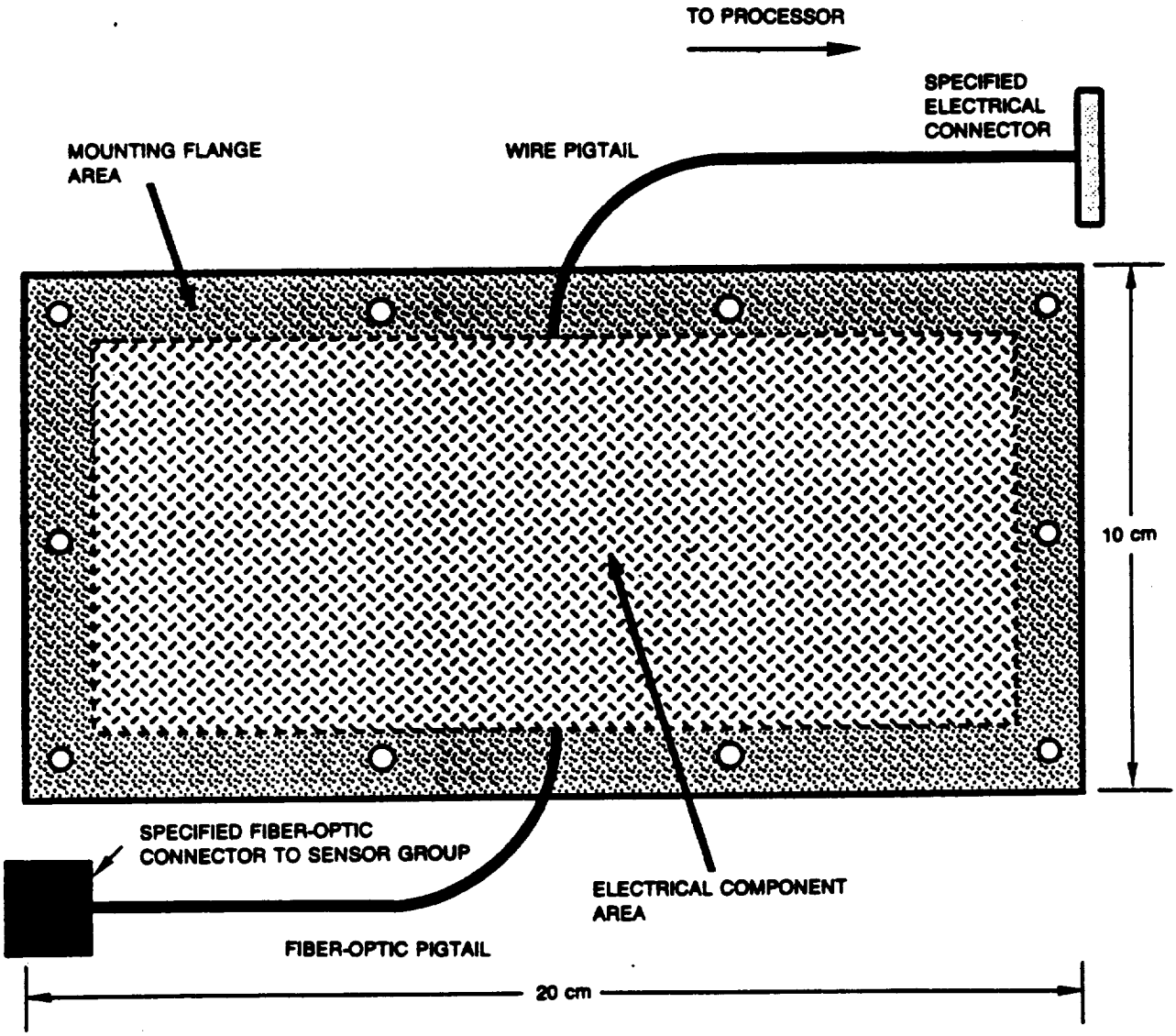

Figure 5.0-3. — Electro-optic interface boards would be fabricated to common electrical, mechanical, and optical interface specifications.

6.0 CRITICAL COMPONENT DEVELOPMENT NEEDS

Accelerated development of electro-optic components is required to meet the size and environmental requirements for the electro-optic architecture in propulsion control systems. Five areas of technology must be addressed: optical sources, optoelectronic device integration and packaging, optical switches, fiber-optic component reliability, and interface standards.

The FOCSI program concluded that optical cable, connectors, and fiber-optic sensors are now available for EOA development. The FOCSI cable and connector hardware were presented in Section 3.2, figure 3.2-1. Evaluation of this hardware in long term exposure to the engine environment is still required.

In the area of optical sources, development should address increased optical power for all applications, broader spectra for WDM systems, and lasers for operation at 125 C.

In the area of optoelectronic device integration and packaging, the outstanding need for further EOA development is for pigtailed functional modules for key EOA interface functions. As stated in Section 3.3.3 on the subject of size, maximum utilization of hybrid optoelectronic packaging and monolithic integrated electronic circuit arrays will be required to produce electro-optic interfaces that fit within the confines of the EEC enclosure. These components will be in the form of multi-application, general purpose pigtailed functional modules (PFM) to ease electrical and mechanical design.

Three module designs are proposed: a broadband optical source module, a WDM receiver module, and a dual LED TDM pulse transmitter. These modules will perform the fiber-optic sensor excitation and detection functions in the EOA. These functions will allow optical multiplex to interface multiple optic sensors to the EEC processor. The broadband optical source module includes an LED array, current source drive, and optical feedback circuits. This component will provide the 2 μW/nm optical power density over the 200 nm wavelength range required for the WDM EOA discussed in Section 3.2. The WDM receiver module consists of a PIN photodiode array, analog multiplexer, and A/D converter. The WDM receiver will detect the optical signals in the ten spectral bands for the WDM EOAs discussed in Section 3.2. The TDM transmitter module consists of two LEDs with high speed pulse circuits. This component will produce the narrow, high intensity pulses required for the TDM EOA presented in Section 3.2.

Optical switches for the EOA were described in Section 3.3.5. Presently available optical switch technology does not satisfy system requirements. Improvements in loss, speed, wavelength sensitivity, and environmental capabilities are needed.

As stated in Sections 3.3.4 and 3.3.6 (on optical power budgets and reliability respectively), the performance of optical components (e.g. optical power levels, spectral properties, noise levels, optical loss, and failure rates) must be maintained over the environment. In particular, the performance models used for the electro-optic architecture require that over the lifetime (typically on the order of 10,000 hours) and the environment the following conditions must be maintained:

Optical source power must not drift more three decibels.

Optical spectra must not drift more than 50 nm.

Receiver noise levels must not drift more than one decibel.

Optical link loss must not drift by more than three decibels.

Failure rate of an interface circuit must be less than $4x10^{-6}$/hour.

For each of the electro-optic designs an optical interface specification must be provided to insure compatibility in fiber sizes, connectors, optical power levels, and optical spectral characteristics. Each specification must indicate the sensors to which that interface is applicable, properties of the optical source (optical power, spectral components), properties of the receiver (sensitivity, bandwidth, timing, spectral filtering), and properties of the sensor (loss, delays).

Standard interfaces will be required also for economical design of future aircraft systems employing optical sensors. These standards would allow a modular system architecture providing greater flexibility in design, upgrades, and maintenance. The basic interface specifications would include waveguide parameters (such as core size and numerical aperture), wavelengths, optical power levels, and component losses. If a common TDM interface is to be used for a variety of sensors, then a common time delay standard and pulse waveform must be set. If WDM is to be used with a variety of sensors, then realistic standard wavelength bands need to be specified. In either case the fundamental link characteristics: core diameter, numerical aperture, and loss must be specified. The five multimode, passive fiber-optic sensor types can be covered by four general specifications: Optical interconnect, Spectral properties, Time domain properties, and Sensor insertion loss.

It must be noted here that it is presently very difficult to impose common standards on producers of fiber-optic sensors. This is true for two reasons: (1) Many sensor designs have been optimized for a specific fiber type (e.g. 50/85, 50/125, or 200/230 in particular cases) so producers may claim their design cannot be made compatible with common interface using a standard fiber size (e.g. 100/140); and (2) some producers do not wish to sell fiber-optic sensors separately from their electro-optic circuits because proprietary signal processing or electro-optic components are used or sale of the complete system is more profitable.

Standards for optical fiber sensors have been discussed in industry committees. A white paper outlining areas requiring standardization in TDM and WDM sensor interfaces was presented to a meeting of interested industry specialists. Comments were received and the drafts were revised accordingly. The revised drafts will be presented to the SAE AS3 Fiber-Optics committee sensor task group. A desire for a rational selection of a standard fiber for aircraft was expressed by most, though there were some feelings that it is too early to standardize the fiber size. Instead, fiber types may be specific to the application. Also, standard optical measurement techniques are needed: e.g. optical power and loss in short links and optical signal to noise ratios.

The commercial aircraft and engine companies are presently seeking standards for a fiber-optic interface between the engine control and the airframe. For example, environmental requirements, fiber sizes, and connector types to implement optic data bus and throttle position sensing are needed. Also needed are recommended practices for testing and installation.

REFERENCES

1. Mongeon, R., et al., *Digital Aircraft Function Monitors Utilizing Passive Fiber-Optic Sensors.* UTRC R78-922820, March 1979.

2. Glenn, W. H., et al, *Analysis and Preliminary Design of Optical Sensors for Propulsion Control.* NASA CR-159468, NASA Lewis Research Center, Cleveland, March 1979.

3. Stanton, R. O., "Digital Optical Transducers for Helicopter Flight Control Systems." Proc. SPIE, Vol. 412, p. 122, April 1983.

4. Farina, J., R. Hubbard, P. Lefkowitz, *Development and Test of a Digital/Optical Rotary Position Transducer.* USAAVRADCOM TR 83-D-15, U. S. Army Research and Technology Laboratories, Ft. Eustis, VA, 1983.

5. Zavednak, D., *Helicopter Optical Subsystem Sensors.* Sikorsky Aircraft, December 1983.

6. Poumakis, D. J. and W. J. Davies, *Fiber Optic Control System Integration Final Report.* Pratt & Whitney report no. CR 179569, December 1986.

7. Russell, J. C., et al., "Protocol Branch Optimization Method used in FOCSI Program Fiber-Optic Control System." IECE Japan OFS'86 Technical Digest , p. 3, 1986.

8. Hoskin, R., *FACTS: Fiber Optic Sensors Report to Industry and Government.* Allison Gas Turbine Division of General Motors, April 1987.

9. Glenn, W. H., et al, *Development of a Fiber Optic High Temperature Sensor.* NAC-TR-2343, Naval Avionics Center, Indianapolis, October 1983.

10. Meltz, G., et al, "Cross-talk fiber-optic temperature sensor." Applied Optics, Vol. 22, No. 3, pp. 464 - 477, 1 February 1983.

11. *Fiber Optic Measurement Devices for a Fiber Optic Control System Integration Program.* Teledyne Ryan Electronics, January 1986.

12. Fritsch, K. and G. Beheim, "Wavelength-division multiplexed digital optical position transducer." Optics Letters, Vol. 11, No. 1, p. 1, (1986).

13. Glomb, W. L., Jr., "Passive Fiber-Optic Coherence for Aircraft Sensors." AIAA/IEEE 7th Digital Avionics Systems Conference, October, 1986, Fort Worth, p. 437.

14. Glomb, W. L., Jr., "General Purpose Electro-optical Interfaces for Fiber-optic Sensors on Aircraft." IGI MFOC'87, Vol. 2, April 1987.

15. Glomb, W. L., Jr., "Fiber-optic coherence multiplexing for passive binary optical data networks." IEEE/OSA Optical Fiber Communication Conference, January 1987, Reno, paper THG4.

16. Walter L. Glomb, Jr. "Optical heterodyne interferometric receivers for fiber optic sensor networks." SPIE Conference 844, Coherent Technology in Fiber Optic Systems II, paper 844-04, August 1987.

17. Deepak Varshneya and Walter L. Glomb, Jr. "Application of TDM and WDM to digital optical code plates." SPIE Conference 838, Fiber Optic and Laser Sensors V, paper 838-58, August 1987.

18. R. G. Smith and S. D. Personick, "Receiver Design for Optical Fiber Communication Systems." in Semiconductor Devices for Optical Communication, H. Kressel Ed., Springer-Verlag, NY, 1982.

19. Glomb, W. L., Jr., "Fiber-optic circuits for aircraft engine controls." to be presented at SPIE O-E/Fibers'87, San Diego, CA, paper number 840-15, August 1987.

20. U. S. Patent no. 4,117,460, Sensing Device, by K. S. Walworth and A. N. Martin, assigned to United Technologies Corporation, Sept. 26, 1978.

21. Stockman, M., G. Winzer, E. Grassl: Rigid Reed-Type Routing Switch for Multimode Optical Fibers. Fiber and Integrated Optics, Volume 3, Number 2-3, 1980.

22. Nagaoka, S., I. Nishi: Small Sized Optical Switch Using Magnetic Alloy Coated Fiber. Conference on Optical Fiber Communications, Proceedings, New Orleans, LA, January 23-25, 1984

23 Spillman, W. B. Jr.: Mechanical One-to-Many Fiber-Optic Switch. Applied Optics, Volume 18, Number 12, 1979.

24 Numoshita, M., Y. Nomura, T. Matsui, T. Nakayama: Optical Switch For Multimode Optical-Fiber Systems. Optical Letters, Volume 4, Number 1, 1979.

25 Fujii, Y., J. Minowa, T. Aoyama, K. Doi: Low-Loss 4x4 Matrix Switch for Fiber Optic Communication. Electronic Letters, Volume 15, Number 14, 1979.

26 Nunoshita, M., Y. Nomura: Optical Bypass Switch for Fiber-Optic Data Bus Systems. Applied Optics, Volume 19, Number 15, 1980.

27 Soref, R. A.: Electrooptic 4x4 Matrix Switch for Multimode Fiber-Optic Systems. Applied Optics, Volume 21, Number 8, 1982.

28 Sampei, Y., S. Naito, Y. Kurita: PLZT Fiber-Optic Switch. Journal of Lightwave Technology, Volume LT-5, Number 9, 1987.

29 Ishida, K., H. Nakamura, H. Matsumura, T. Kado, H. Inoue: InGaAsP/InP Optical Switches Using Carrier Induced Refractive Index Change. Applied Physics Letters, Volume 50, Number 3, 1987.

30. Tonchev, S., I. Savatinova: Optical Multimode X-Switch in Ti-Diffused LiNbO3. Journal of Optical Communications, Volume 6, Number 3, 1985

31. Lorenzo, J. P., R. A. Soref: 1.3 Micron Electro-Optic Silicon Switch. Applied Physics Letters, Volume 51, Number 1, 1987.

32 R.C. Alferness, "Waveguide electrooptic switch arrays," IEEE J. Selected Areas in Comm. 6, pp. 1117-1130 (1988).

33 I. Sawaki et. al., "Rectangularly configured 4x4 Ti: LiNbO3 matrix switch with low drive voltage," IEEE J. Selected Areas in Comm. 6, pp. 1267-1272 (1988).

34 P. Granestrand et. al., "Strictly nonblocking 8x8 integrated-optic switch matrix in Ti: LiNbO3," in Proc. OFC/IGWO '86, Atlanta, GA.

35 P.J. Duthie and M.J. Wale, "Rearrangeably nonblocking 8x8 guided wave optical switch," Electron. Lett. 24, pp. 594- 596 (1988).

36 H. Nishimoto et. al., "Polarization independent LiNbO3 4x4 matrix switch," in Proc. IGWO '88, Santa Fe, NM.

37 P.Granestrand et. al., "Polarization independent 4x4 switch matrix in LiNbO3 for communicative and distributive switching," in Proc. IGWO '88, Santa Fe, NM.

38 H. Inoue et. al., "An 8 mm length nonblocking 4x4 optical switch array," IEEE J. Selected Areas in Comm. 6, pp. 1262- 1265 (1988).

39. K.E. Petersen, "Silicon as a mechanical material," Proc. IEEE 70, pp. 420-454 (1982).

40. G. Bogert et. al., "Low crosstalk 4x4 Ti: LiNbO3 optical switch with permanently attached polarization maintaining fiber array," J. Lightwave Tech. LT-4, pp. 1542-1545 (1986).

41. M. Milbrodt et. al., "A tree-structured 4x4 switch array in lithium niobate with attached fibers and proton-exchanged polarizers," in Proc. IGWO '88, Santa Fe, NM.

42. E. Voges and A. Neyer, "Integrated-optic devices for optical communication," J. Lightwave Tech. LT-5, pp. 1229-1238 (1987).

43 A. G. Bell. "Upon the Production of Sound by Radiant Energy," Philos. Mag., Vol. 11, 1981, p. 510.

44 D. F. Nelson, K. W. Wecht and D. A. Kleinman. "Photophone Performance," J. Acoust. Soc. Am., Vol. 60, 1976, p. 251.

45 J. O. Gurney. "Photofluidic Interface," ASME J. Dynamics Sys. Meas. Control, March 1984 (to be published).

46 R. C. Miller and R. B. Lawry. "Optically Powered Speech Communication Over a Fiber Lightguide," Bell Syst. Tech. J., Vol. 58, 1979, p. 1735.

47 M. J. Collier, et. al. "The Optical Actuation of a Process Control Valve," First International Conferences on Optical Fiber Sensors, IEEE Conference Pub. No. 221, April 1983, p. 57.

48. Berak, J. M., et al., High-Temperature Optically Activated GaAs Power Switching for Aircraft Digital Electronic Control. *NASA CR-174711, 1983.*

49. Hockaday, B. D., and J. P. Waters: "An Optical to Hydraulic Interface." Presented to the Military and Government Fiber Optics and Communications Exposition, Washington, D.C., March 19, 1987.

50. Hockaday, B. D., and J. P. Waters: "Opto-Mechanical Smart Actuator." presented to the American Controls Conference, Minneapolis, MI, June 11, 1987.

51. Hockaday, B. D., and J. P. Waters: "The Opto-Hydraulic Servo Valve." presented to SAE Aerospace Control and Guidance Systems Committee, Galveston, TX, October 30, 1987.

APPENDIX A

VENDOR INFORMATION REQUEST

APPENDIX A.
VENDOR INFORMATION REQUEST

This attachment describes technical data requested by the United Technologies Research Center (UTRC) for NASA Contract NAS3-25343 to design an optimal architecture for electro-optical sensing and control in advanced aircraft and space systems. The propulsion system Full Authority Digital Electronic Control (FADEC) will be the focus for the study. Consideration of this system provides a concrete example for evaluation of a variety of sensors and multiplexing techniques. Unlike earlier studies, the emphasis of this program will be on the FADEC interface design rather than on the transducer technology itself.

The program will evaluate a variety of electro-optic architectures and complete a conceptual design of an all-optic aircraft propulsion control system by: (1) establishing criteria for the comparative evaluation of various optic architectures; (2) identifying and characterizing candidate optic systems in a trade study matrix format; then (3) performing a evaluation of the impact of the selected system on the control.

Designs for candidate fiber optic systems for measurement of the parameters listed in the attached Table A.1 are required for item (2) above. The accuracy and operating environment for the sensors are as shown in the table. The sensor interface electronics, including the optical sources, detectors, and filters must operate on a heat sink temperature ranging from -54 to 125 C. The designs should reflect the state-of-the art forecast for the late 1990's.

In addition to a system block diagram and general description, the design reports should include the following 17 items:

1. *Types of sensors*: Which of the sensors listed in Table A.1 can be accommodated in the design? Which cannot? What optical sensing mechanism is employed for each quantity?

2. *Signal compensation or calibration*: Is the sensing mechanism digital or analog? If analog, then what compensation or referencing method is employed?

3. *Number of channels*: How many sensors can share a single optical source or receiver?

4. *Number of distinct sources*: How many optical sources, light emitting diodes or laser diodes, are required to service all of the sensors shown in Table A.1?

5. *Number of detectors*: How many optical detectors are required to service all of the sensors shown in Table A.1?

6. *Number of fibers*: How many parallel optical fibers are required to service all of the sensors shown in Table A.1?

7. *I/O pincount*: How many optical connector contacts are required to connect the FADEC to the optic sensors?

8. *Optical power margin*: What is the optical power level of each source in the design? What is the receiver noise level? What are the sensor and link losses?

9. *Signal processing time*: How much time is required for the electronic interface to compute the sensor value? What is the bandwidth of the analog portion of the receiver?

10. *Complexity*: How many circuit elements (transistors, amplifiers, logic elements) are in the electronic interface?

11. *Electrical power consumption*: How many watts of electrical power are required for the interface circuitry?

12. *I/O circuit area*: Estimate the circuit board area required for the electro–optic interface. Specify where electro–optic hybrids or custom monolithic integrated circuits could be used to minimize the size of the interface.

13. *Weight*: Estimate the weight of the electro–optic interface and the fiber optic cable in the system.

14. *Reliability*: Estimate the mean time to failure of the electro–optic interface based on the number of electronic circuit elements and electro–optic components.

15. *Redundancy*: How would redundancy be implemented for the sensor network?

16. *Maintainability*: When the system fails, how are faults isolated? What components would be repaired or replaced?

17. *Availability or development schedule*: Are all of the components in the system available today in flight quality? What components are lacking? What new developments are needed for this design?

TABLE A.1 – FADEC SENSOR SET WITH UNIFORM TEMPERATURE SPECIFICATIONS

Number of Sensors	Measurement	Update Time	Accuracy	Range	Ambient
4	Linear position	5 ms	± 0.36 cm	0 to 36 cm	-54 to 200 C
2	Linear position	10 ms	± 0.26 cm	0 to 26 cm	-54 to 200 C
4	Linear position	5 ms	± 0.18 cm	0 to 18 cm	-54 to 200 C
2	Linear position	10 ms	± 0.09 cm	0 to 9 cm	-54 to 200 C
5	Linear position	5 ms	± 0.05 cm	0 to 5 cm	-54 to 200 C
2	Linear position	10 ms	± 0.05 cm	0 to 5 cm	-54 to 200 C
1	Rotary position	10 ms	± 0.2 deg	0 to 130 deg	-54 to 200 C
1	Gas temperature	120ms	± 2 C	-54 to 260 C	-54 to 200 C
4	Gas temperature	20 ms	± 11 C	0 to 1500 C	0 to 350 C
1	Fuel temperature	120 ms	± 3 C	-54 to 180 C	-54 to 200 C
1	Turbine blade temperature	20 ms	± 10 C	500 to 1500 C	-54 to 350 C
1	Light off detector	20 ms	± 5 %	< 290 nm (optical wavelength)	-54 to 350 C
3	Fuel flow	10 ms	± 100 kg/hr	200 tc 5000 kg/hr.	-54 to 200 C
3	Fuel flow	40 ms	± 100 kg/hr	5000 to 16000 kg/hr. (1 inch diameter)	-54 to 200 C
1	Gas pressure	10 ms	± 4.0 kPa	7 to 830 kPa	-54 to 350 C
1	Gas pressure	120 ms	± 1.0 kPa	7 to 280 kPa	-54 to 200 C
1	Gas pressure	10 ms	± 40 kPa	35 to 5000 kPa	-54 to 350 C
1	Hydraulic pressure	40 ms	± 40 kPa	500 to 8000 kPa	-54 to 200 C
1	Fuel pressure	120 ms	± 40 kPa	0 to 690 kPa	-54 to 200 C
1	Rotary speed	10 ms	± 7 rpm	650 to 16000 rpm	-54 to 200 C
1	Rotary speed	10 ms	± 7 rpm	1600 to 19000 rpm	-54 to 200 C
1	Vibration	120 ms	± 2.5 g	0 to 50 g (10 Hz to 1 kHz)	-54 to 350 C
2	Fluid Level	120 ms	± 2 %		-54 to 200 C

APPENDIX B

TELEDYNE RYAN ELECTRONICS TDM EOA

REPORT NO. TRE/SD29065-21

TIME DIVISION MULTIPLEXED

NASA ELECTRO-OPTIC SYSTEM ARCHITECTURE

FOR

ADVANCED AIRCRAFT ENGINES

3 AUGUST 1988

PREPARED FOR: UNITED TECHNOLOGIES CORPORATION
RESEARCH CENTER
SILVER LANE
EAST HARTFORD, CT 06108

PURCHASE ORDER 171372

TELEDYNE RYAN ELECTRONICS
8650 BALBOA AVENUE
SAN DIEGO, CALIFORNIA 92123

TABLE OF CONTENTS

LIST OF ILLLUSTRATIONS

SECTION 1

INTRODUCTION

Use of fly-by-wire systems in aircraft to monitor and control the propulsion and flight, has been recognized to limit the performance, maneuverability and safety of the aircraft in a flight critical application. Lighting, EMI and EMP (electromagnetic effects) affect the electrical signals in the sensor, electronic control units (ECU) and/or the signal transmission on the electrical wiring between the sensor and the ECU. Interference induced in the signals by the electromagnetic effects can lead to inappropriate control system response or catastrophic failure of the control system. The EMI and EMP problems are exacerbated in aircraft whose structures are fabricated with advanced composite materials that have poor electrical insulation properties. Such systems may be shielded from lighting, EMI and EMP by using metallic enclosures and braided wire mesh to enclose them in an electromagnetically sealed envelope. However, electromagnetic shielding of wiring, sensors and ECU adds weight and bulk to the control system and therefore does not offer any advantage.

In an effort to improve this situation, NASA Lewis Research Center has planned a study to implement fiber-optics in advanced aircrafts that provides advantages not realized in a conventional system architecture. This technology will allow complete replacement of the fly-by-wire system by a fly-by-light one. Introduction of fiber-optic data links and multiplexed optic-sensor arrays will provide reduction in harness and system weight, system size and added advantage of high temperature capability, wide bandwidth, immunity to EMI, EMP and RFI.

Teledyne Ryan Electronics (TRE), under subcontract to United Technologies have studied Time Division Multiplexing (TDM) techniques as applied to the fiber-optic sensors and electro-optic (EO) system architecture. A description of the optimum EO architecture to multiplex 43 sensors is provided based on the most promising TDM scheme of the three TDM schemes studied. In Section 2, the standard (EO) sensor system architecture is described using six separate system interfaces. In Section 3, six common optical sensing concepts are identified and described to group 43 sensors. Section 4 provides the description of primarily two of the six interfaces required followed by a description of the

three TDM schemes in Section 5. In Section 6, a brief description of the seventeen items per UTRC request is provided along with references in Section 7.

SECTION 2

ELECTRO-OPTIC SENSOR SYSTEM ARCHITECTURE OVERVIEW

Figure 2-1 shows a block diagram of the sensor system electro-optical architecture that may be used to service all 43 sensors listed in Table 2-1 using time division multiplexing (TDM). The architecture contains the circuitry necessary to interrogate each sensor process and translate the data as required, store the data, send the data to the host system and control the operation of the entire interface.

The group of 43 sensors are separated into six sub-groups according the type of processing required for that sensing concept. Each of the six sub-groups has separate transmitters, receivers and a data preprocessing section to perform data conversion and/or averaging so that the data presented to the controller is in a common parallel, digital format. Due to the speed of the interrogation cycle for some of the sensor types it is advantageous to incorporate some discrete data preprocessing in separate circuitry in each of the six interface subsections. The preprocessing includes averaging of the data over several samples or some specific time duration in the case of the frequency measurement and conversion of the data from one format to another. The sensor measurement concepts, interface configurations and operation of each of the six types of interface sections are described in a later section of this report.

As mentioned above, six interface sections are required to address the six subgroups of sensors. For the digital sensors such as the linear, rotary and fluid level (incorporates a position sensor with bellows) one common interface is allocated to multiplex 21 of these sensors. All of these sensors utilize a digital code scale and fiber optic delay lines to create a serial digital code that represents the position of the code scale. This concept has been demonstrated on the Advanced Digital Optical Control System (ADOCS) program that TRE has been involved in for the past six years. Thirty sensors using this concept have been flight tested in a helicopter flight control system with a total flight time of over 500 hours.

Pressure and fluid flow sensors that employ the microbend measurement concept are combined on a second analog interface section. The microbend measurement concept has been used widely and prototypes of pressure, vibration and other sensors have been tested and demonstrated for high temperature applications.

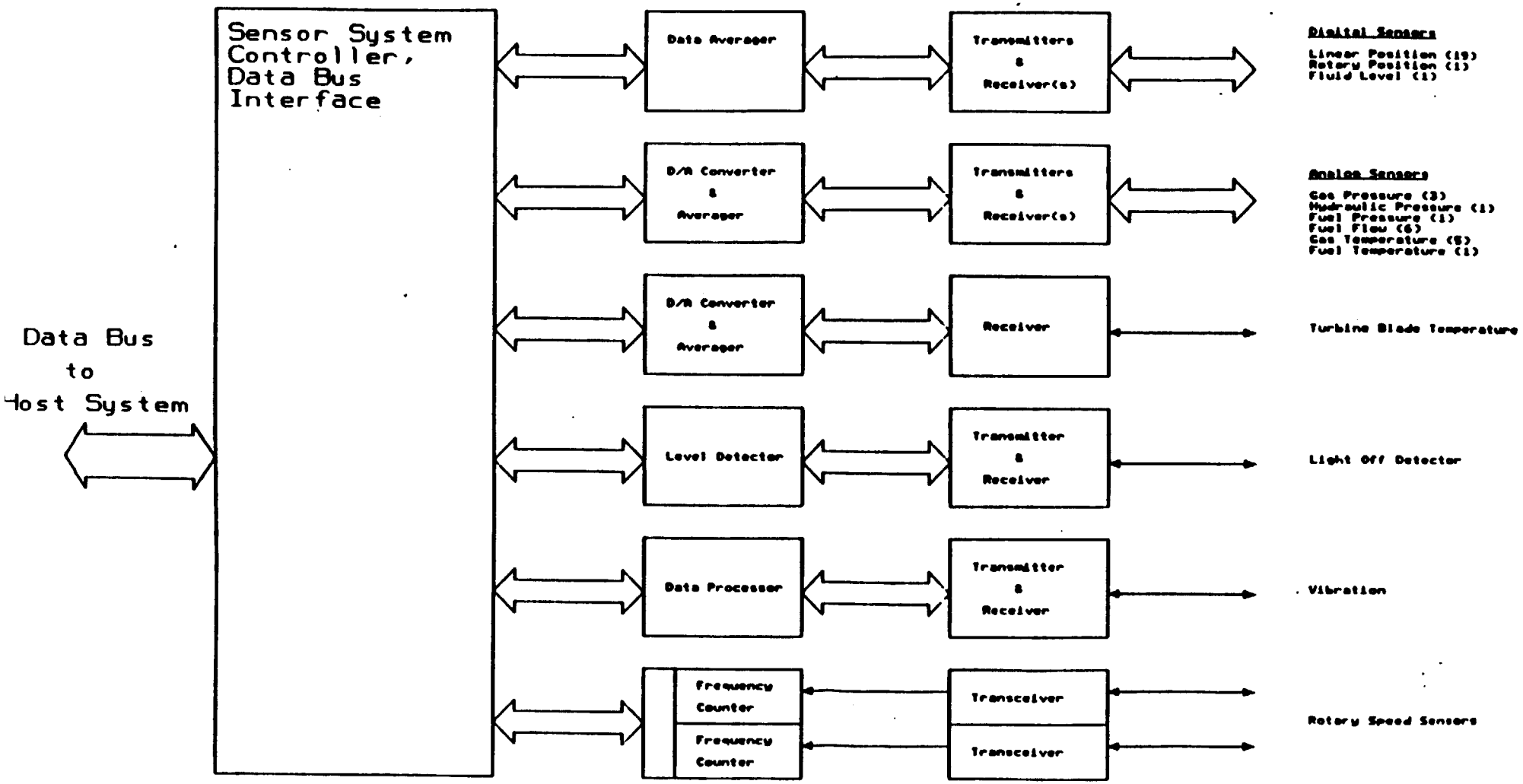

Figure 2-1. Sensor System Electro-Optic Interface Block Diagram

Table 2-1. FADEC Sensor Set with Uniform Temperature Specifications

Number of Sensors	Measurement	Update Time	Accuracy	Range	Ambient
4	Linear position	5 ms	+/- 0.36 cm	0 to 36 cm	-54 to 200 C
2	Linear position	10 ms	+/- 0.26 cm	0 to 26 cm	-54 to 200 C
4	Linear position	5 ms	+/- 0.18 cm	0 to 18 cm	-54 to 200 C
2	Linear position	10 ms	+/- 0.09 cm	0 to 9 cm	-54 to 200 C
5	Linear position	5 ms	+/- 0.05 cm	0 to 5 cm	-54 to 200 C
2	Linear position	10 ms	+/- 0.05 cm	0 to 5 cm	-54 to 200 C
1	Rotary position	10 ms	+/- 0.2 deg	0 to 130 deg	-54 to 200 C
1	Gas temperature	120 ms	+/- 2 C	-54 to 260 C	-54 to 200 C
4	Gas temperature	20 ms	+/-11 C	0 to 1500 C	0 to 350 C
1	Fuel temperature	120 ms	+/- 3 C	-54 to 180 C	-54 to 200 C
1	Turbine blade temperature	20 ms	+/-10 C	500 to 1500 C	-54 to 350 C
1	Light off detector	20 ms	+/-5 %	< 290 nm (optical wavelength)	-54 to 350 C
3	Fuel flow	10 ms	+/-100 kg/hr	200 to 6000 kg/hr	-54 to 200 C
3	Fuel flow	40 ms	+/-100kg/hr	5000 to 16000 kg/hr (1 inch diameter)	-54 to 200 C
1	Gas pressure	10 ms	+/-4.0 kPa	7 to 830 kPa	-54 to 350 C
1	Gas pressure	120 ms	+/-1.0 kPa	7 to 280 kPa	-54 to 200 C
1	Gas pressure	10 ms	+/-40 kPa	35 to 5000 kPa	-54 to 350 C
1	Hydraulic pressure	40 ms	+/-40 kPa	500 to 8000 kPa	-54 to 200 C
1	Fuel pressure	120 ms	+/-40 kPa	0 to 690 kPa	-54 to 200 C
1	Rotary speed	10 ms	+/- 7 rpm	650 to 16000 rpm	-54 to 200 C
1	Rotary speed	10 ms	+/- 7 rpm	1600 to 19000 rpm	-54 to 200 C
1	Vibration	120 ms	+/- 2.5g	0 to 50 g (10 Hz to 1 kHz)	-54 to 350 C
1	Fluid level	120 ms	+/-2%	0 to 15 cm	-54 to 200 C

The temperature sensors that use the absorption concept may be designed in to a very similar optical configuration compared to the microbend sensors. The return signals and the processing required is sufficiently similar that these may be multiplexed into the same interface section. These sensors are designed using the concept of light absorption in material which has a well defined temperature dependence. The light amplitude returned to the interface is measured and converted to a digital word that represents the temperature.

The turbine blade temperature sensor, which is based on a noncontact measurement technique, is used for the turbine blade section. This sensor monitors the blackbody radiation from the turbine blades at two closely spaced wavelengths and from the ratio of the amplitudes at these two wavelengths the temperature is determined. Since the radiation being monitored is continuous and the processing required is unique, this sensor cannot be multiplexed with others. Therefore, a separate interface is required for this sensor.

The light off detector uses a measurement technique that monitors a continuous source of radiation to determine when it has exceeded a predetermined level. Periodically a reference signal is sent to the sensor and a portion of this signal is reflected back to the interface. This reflected return signal is used to calibrate the sensor. The interface measures the target radiation level and compares it to the return reference level. Since the radiation source being monitored for this sensor is also continuous and the processing unique, it also cannot be multiplexed with other sensors.

The vibration sensor is also a continuous measurement system. The sensor is a microbend accelerometer in which one of the microbend gratings is fixed and the other acts as an inertial mass which moves with applied acceleration. The light transmission through the fiber is modulated at the rate of the applied acceleration. The processing of the output data depends on the type of information required at the output of the sensor interface. If the rms value of the acceleration over the frequency range of interest is required then the processing is relatively simple. If a data set is required which gives the acceleration amplitude as a function of frequency, then an FFT processor is used in the interface design. This should be feasible within the bounds of a single circuit card of moderate size.

The rotary speed sensors use an optical reflective light chopper to monitor the speed of rotating shafts. The processing required for these two sensors is to count the pulse

frequencies over the data update time interval. Further study is required to determine if they can be time multiplexed into a single receiver and frequency counter.

Figure 2-2 shows a timing diagram of the sensor interrogation sequence. The group of 43 sensors is divided into six subgroups according to the data update time required for each sensor. The sensor interrogation process is divided into frames of 120 ms each. Each frame is divided into 12 subframes of 5 ms each. During each subframe the sensor group with the update period requirement less than or equal to the update period for that sensor group is interrogated.

The interrogation of the digital and analog sensor types shown in Figure 2-1 is performed sequentially with relatively short sample times. The interrogation of the temperature and frequency measurement types may use sample times that are longer than the 5 ms. This means that the sampling of these sensors may be done concurrently with the sampling of other sensors in other groups. For the most efficient use of the circuitry the sensors within each of the sensor groups should be completely multiplexed or sequentially sampled using as much common circuitry as possible.

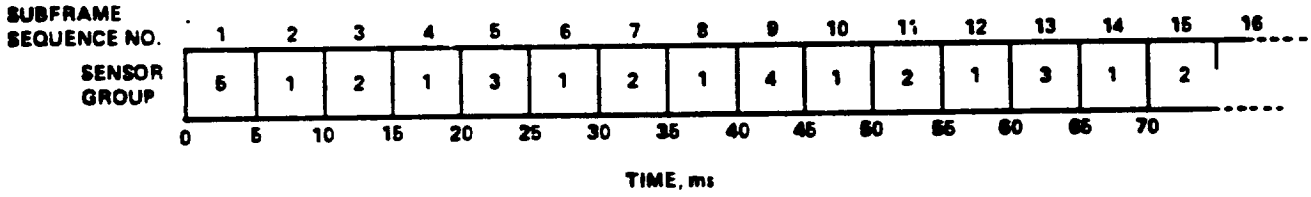

GROUP	UPDATE PERIOD
1	5 ms
2	10 ms
3	20 ms
4	40 ms
5	120 ms

Figure 2-2. Sensor Interrogation Timing Diagram

SECTION 3

OPTICAL SENSING CONCEPTS

The list of sensors in the data requirements package of UTRC may be designed using six optical sensing concepts. Table 3-1 summarizes the types of sensors and the corresponding mechanism used to perform the measurement.

Table 3-1. Types of Sensors

Sensor	No. of Sensors	Specific Concept
Position	20	(1) Gray-code/Digital Optical TDM
Temperature	6	(2) Absorption/fluorescence
	1	(3) Black-body radiation
Light Off	1	(4) Digital Optical TDM
Fuel Flow	6	(2) Δp sensor/vortex shedding frequency with microbend sensor
Pressure	5	(2) Microbend sensor/amplitude
Rotary Speed	2	(5) Rotor Reflection Frequency
Vibration	1	(6) Microbend Accelerometer
Fluid Level	1	(1) Bellows + Position Sensor (Digital TDM)

3.1 DIGITAL OPTICAL TIME DIVISION MULTIPLEXING (TDM) CONCEPT

The digital optical TDM method of measuring position has been demonstrated on the ADOCS program and a second generation of such a transducer is being developed at TRE under the Advanced Optical Position Transducer (AOPT) program sponsored by the U.S Army.

The measurement method may be described by referring to Figure 3-1. The Figure shows a reflective digital code scale with a linear array of fibers used to interrogate the code scale. Each of the fibers in the array or read head is connected through a delay line to the interconnect cable. The electro-optical interface at the other end of the cable contains a transmitter and receiver. The transmitter produces an interrogation pulse about 20 ns wide which is coupled to the transducer through the interconnect cable. Each successive delay line in the transducer is progressively delayed by an amount sufficient to provide a round

trip delay time of 20 ns, which is the width of the interrogation pulse. In this manner, a single interrogation pulse 20 ns wide generates a serial pulse train that represents the state of each data bit on the code scale by a unique time cell.

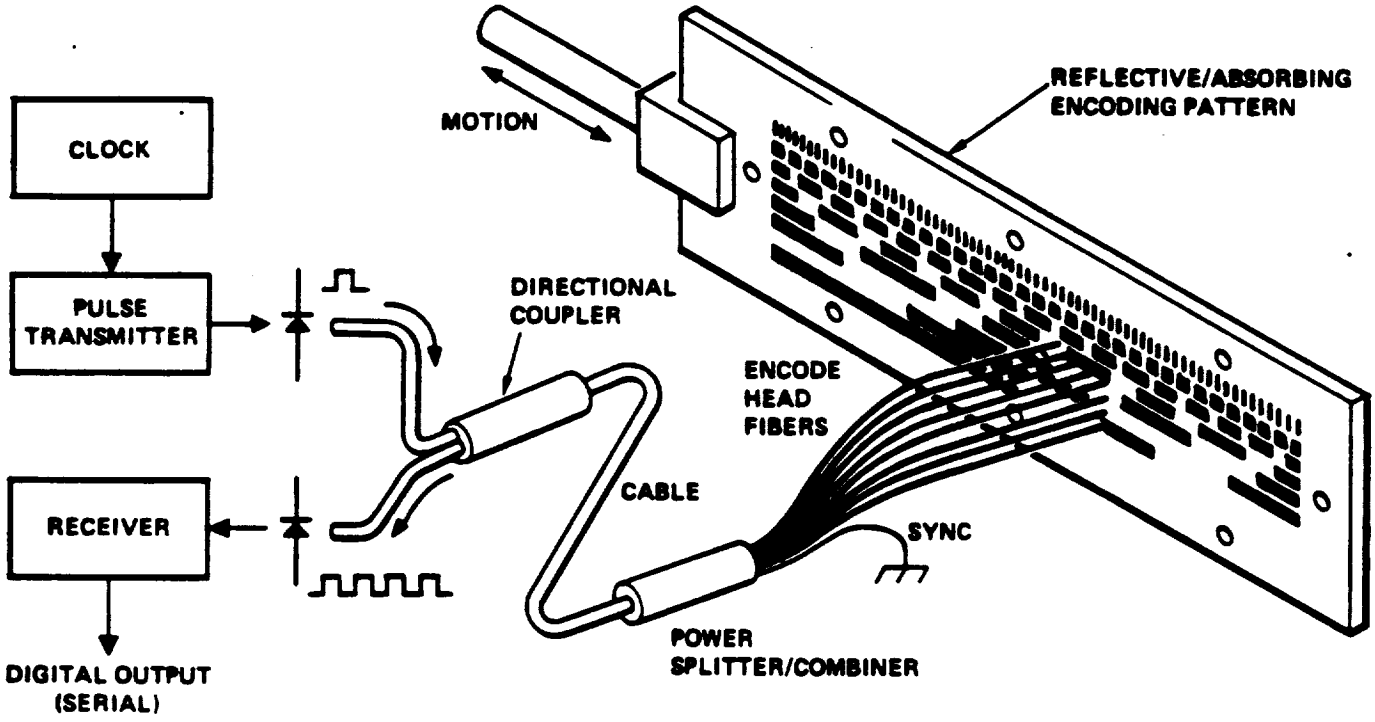

Figure 3-1. Digital Displacement Transducer Element with Reflective Gray-Code Scale

Figure 3-2 shows the timing sequence for the interrogation operation. The received signal on the second line shows Fresnel reflections from connectors, followed by the signals from the digital code scale in the transducer. The first bit to return is always high and is used for an amplitude and timing reference in the recovery of the data bits.

3.2 ANALOG MICROBEND CONCEPT

Figure 3-3 shows an illustration of the analog microbend concept which may be used for measuring small displacements of diaphragm and beams. A fiber is placed between two complementary gratings which is displaced as the gratings are moved closer together. The displacement of the fiber causes bending that exhibits excess optical loss that is a well defined function of the displacement. This method of sensing displacement has been well documented in the literature[1] and has been used in the industry for pressure, flow and acceleration measurements.

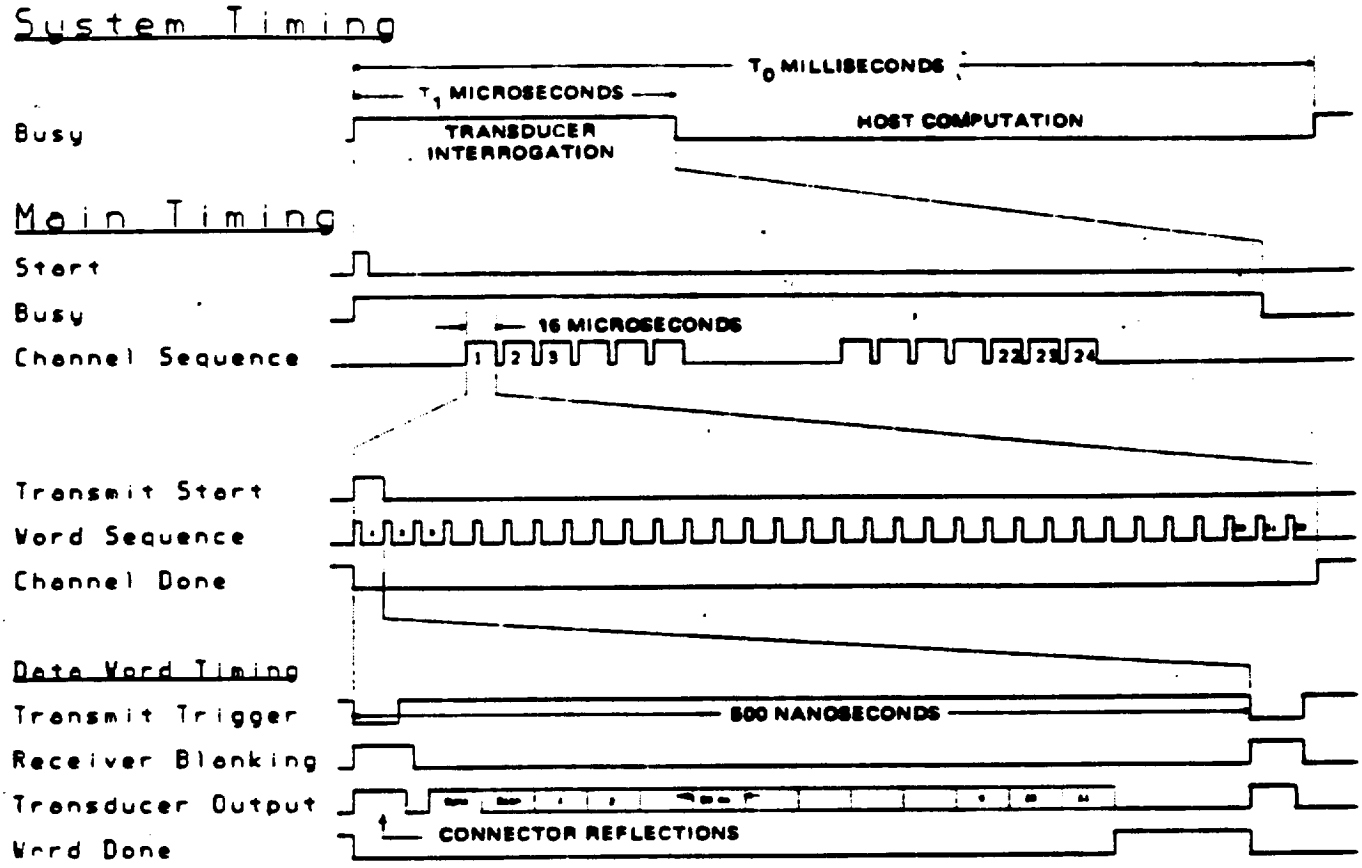

Figure 3-2. Digital Optical TDM Sensor System Timing Diagram

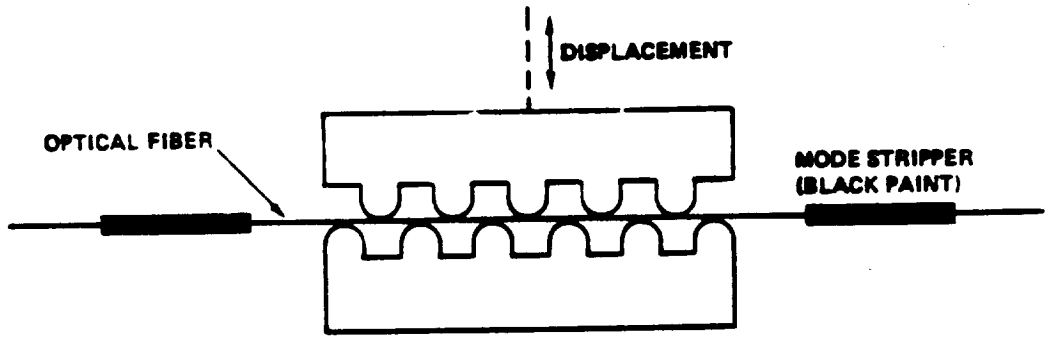

Figure 3-3. Schematic Representation of Microbending Sensor

Figure 3-4 shows the complete fiber-optic circuit of a microbend sensor. Two mirrored fiber ends are used to give reflected signals back to the electro- optical interface. One delay line is placed in the common path for the two reflections to separate the first mirror

Figure 3-4 shows the complete fiber-optic circuit of a microbend sensor. Two mirrored fiber ends are used to give reflected signals back to the electro- optical interface. One delay line is placed in the common path for the two reflections to separate the first mirror reflection in time from the connector reflections. A second fiber is routed through the microbend gratings and a second delay line to the second mirrored end. The first reflection provides a timing and amplitude reference and the second reflection provides a measure of the attenuation due to displacement through the gratings.

Figure 3-5 shows the timing diagram of the interrogation cycle. A transmit pulse of 100 ns duration is used which requires a receiver bandwidth of about 10 MHz. The third line shows the two return signals for the reference pulse and the measurement pulse. During processing, gates sample the amplitudes of the two pulses from which the grating displacement is calculated.

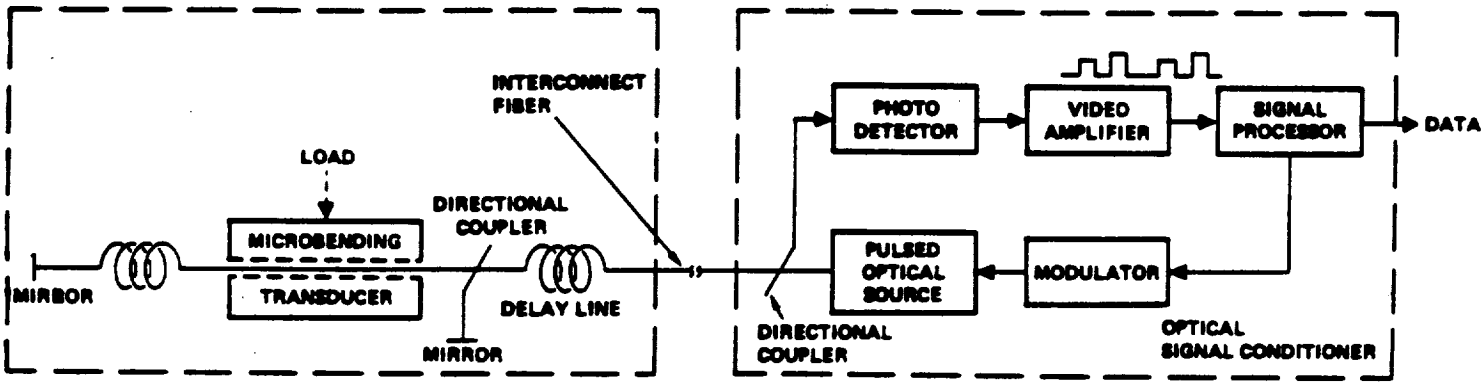

Figure 3-4. Time Division Multiplexed Microbending Optical Transducer

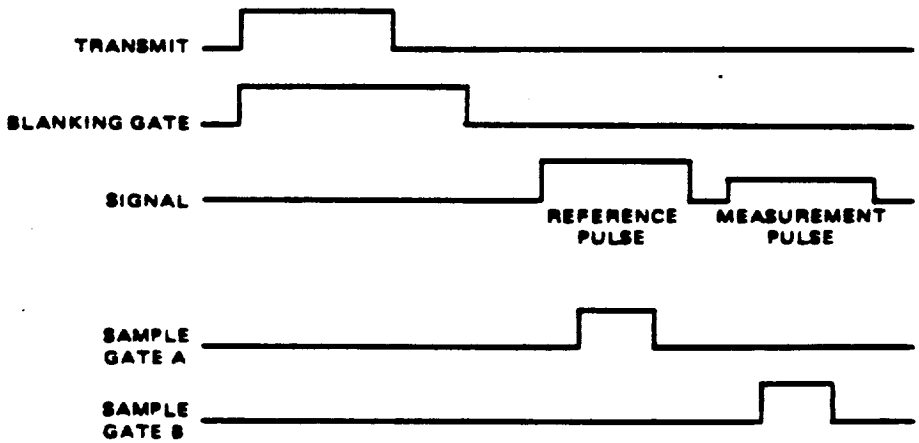

Figure 3-5. Signal Timing Diagram for Microbending Transducer

3.3 BLACK-BODY RADIATION MEASUREMENT CONCEPT

Figure 3-6 shows the Black-Body Radiation measurement concept which may be used in two modes of operation. The mode more suitable for the turbine temperature application is the non-contact type where the sensor is brought in proximity of the turbine. Using optical imaging, radiation from the turbine blade is collected and transported via an optical fiber light chopper to electro-optic unit where it is detected processed and formatted. Details on the description are provided in reference (2).

Because of the nature of the sensing concept, this sensor cannot be multiplexed. However, several such sensors could be operated from a common electro-optic unit, but at the expense of bigger interface volume.

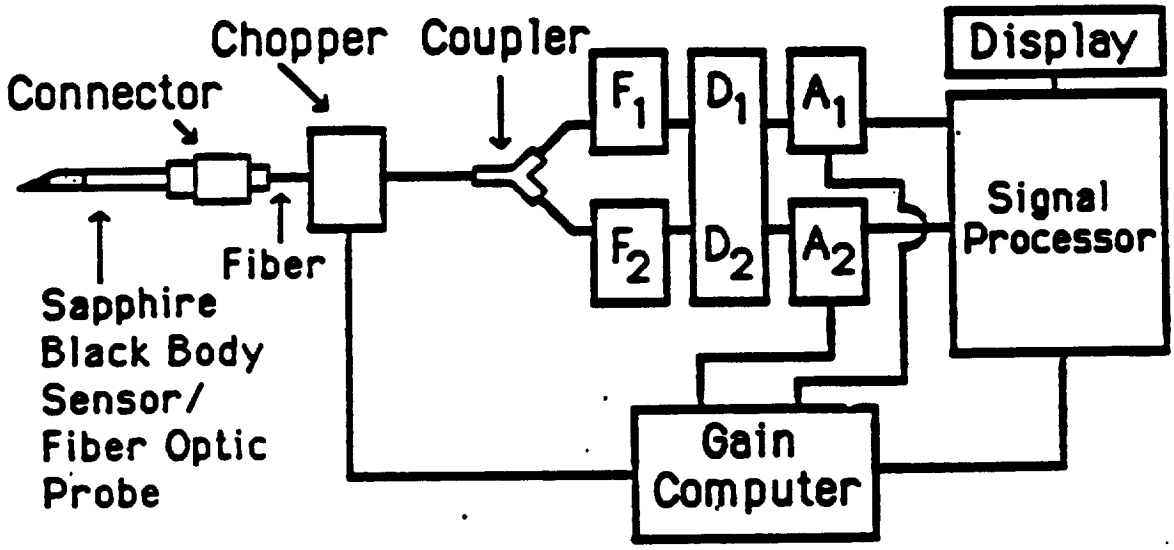

F_1 & F_2 - Filters
D_1 & D_2 - Detectors
A_1 & A_2 - Amplifiers

Figure 3-6. Fiber Optic Temperature Sensor System

3.4 LIGHT-OFF DETECTOR CONCEPT

Figure 3-7 shows a block diagram and timing diagram for the light-off detector. Since this sensor is always active and (light coming in from the object that is being monitored), it needs to be calibrated only occasionally. The calibration is performed by sending a reference light pulse to the sensor which is reflected back to the interface from the reference mirror. This return pulse is used to calibrate the fiber optic link to the sensor and compensate for variations in the link losses. The amplitude of the light being emitted from the object may then be precisely measured and compared to a predetermined level. A measurement higher than a threshold level indicates that the light is on.

This measurement concept is sufficiently different from the others to preclude multiplexing it with any other sensor proposed in this report. It is possible to multiplex this sensor with others of the same type, but separate receiver preamplifiers must be used with each sensor with electrical switching at the output of the preamplifiers.

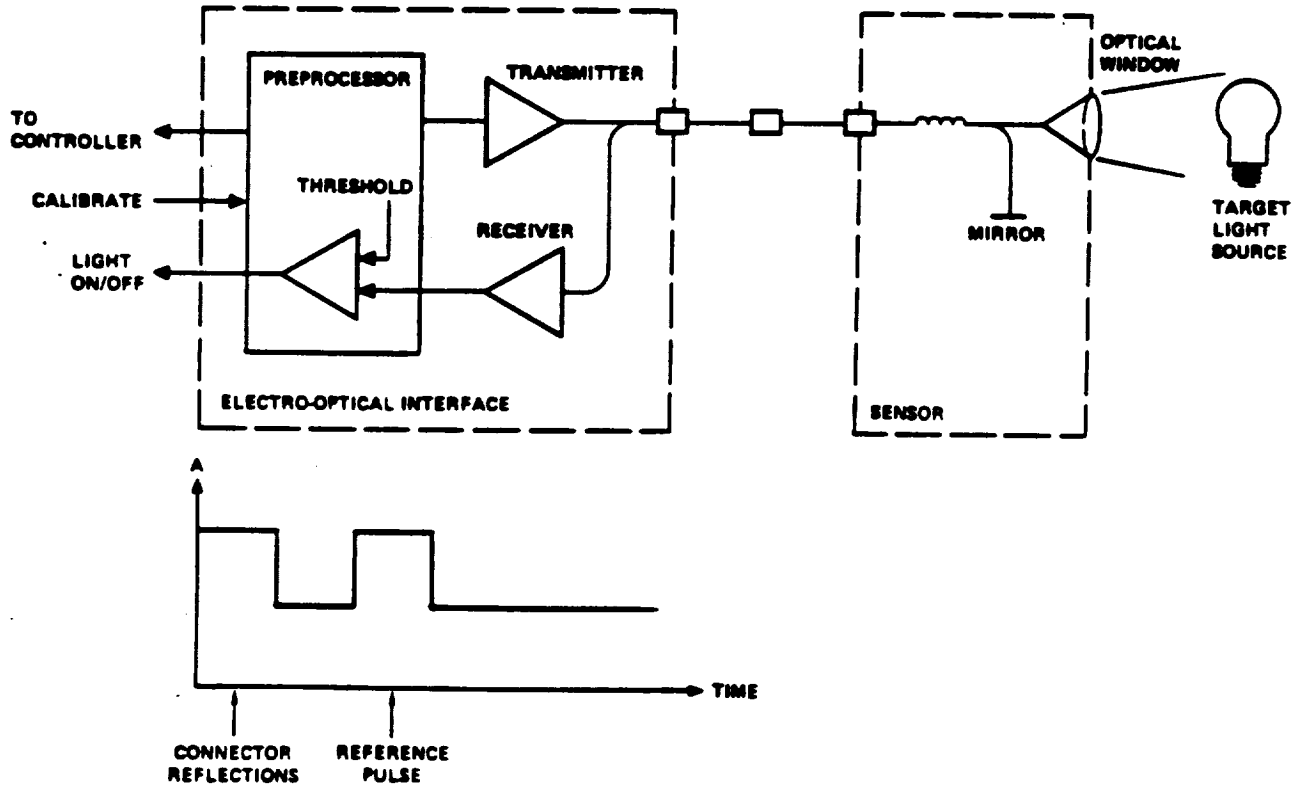

Figure 3.7 Block Diagram and Timing Diagram for Light Off Detector

3.5 ROTARY SPEED SENSOR CONCEPT

Figure 3-8 shows a system block diagram of a sub-system with two speed sensors. The principle used for determining speed is to modulate the light amplitude in the sensor at a rate directly proportional to the speed of the shaft being monitored. The processor measures this frequency of the modulation and calculates the rotary speed.

Another approach that is currently under development at TRE can also be used to measure the gasifier turbine speed of an engine. In this approach the pressure fluctuations frequency at the trailing edge of the turbine blades is measured by a microbend modulator through a diaphragm. This approach is suitable for applications where the sensor service temperature requirements exceed 200°C. Therefore, this technique is not recommended for this application.

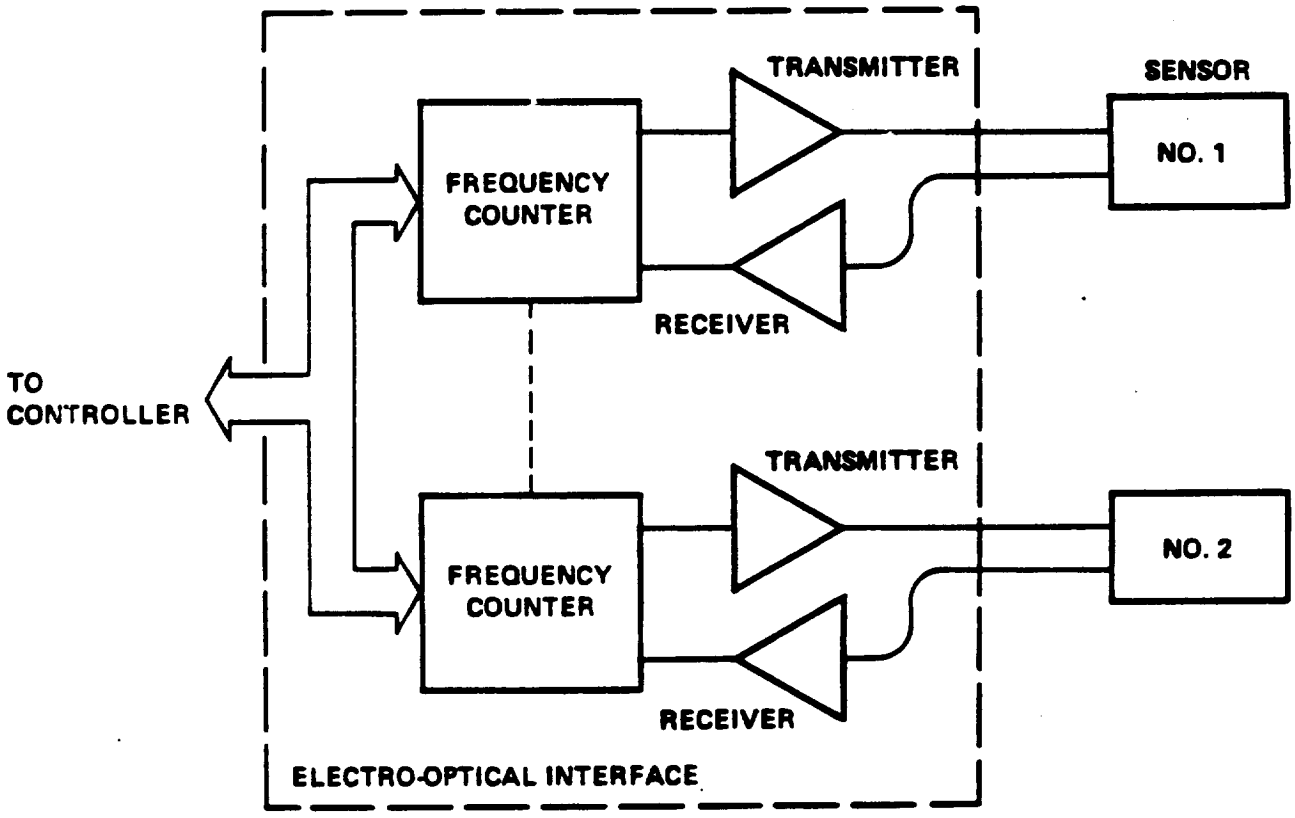

Figure 3-8. System Block Diagram for Frequency Measurment Sensors with No Multiplexing

The light amplitude modulation technique that is used in the proposed sensor is shown in Figure 3-9. Two fibers are focused onto a disk coupled to the shaft being monitored. The disk has alternating reflective and non-reflective areas that pass under the two fibers. When a reflective area is under the fibers, light is coupled from the input fiber. This system forms a reflective optical chopper.

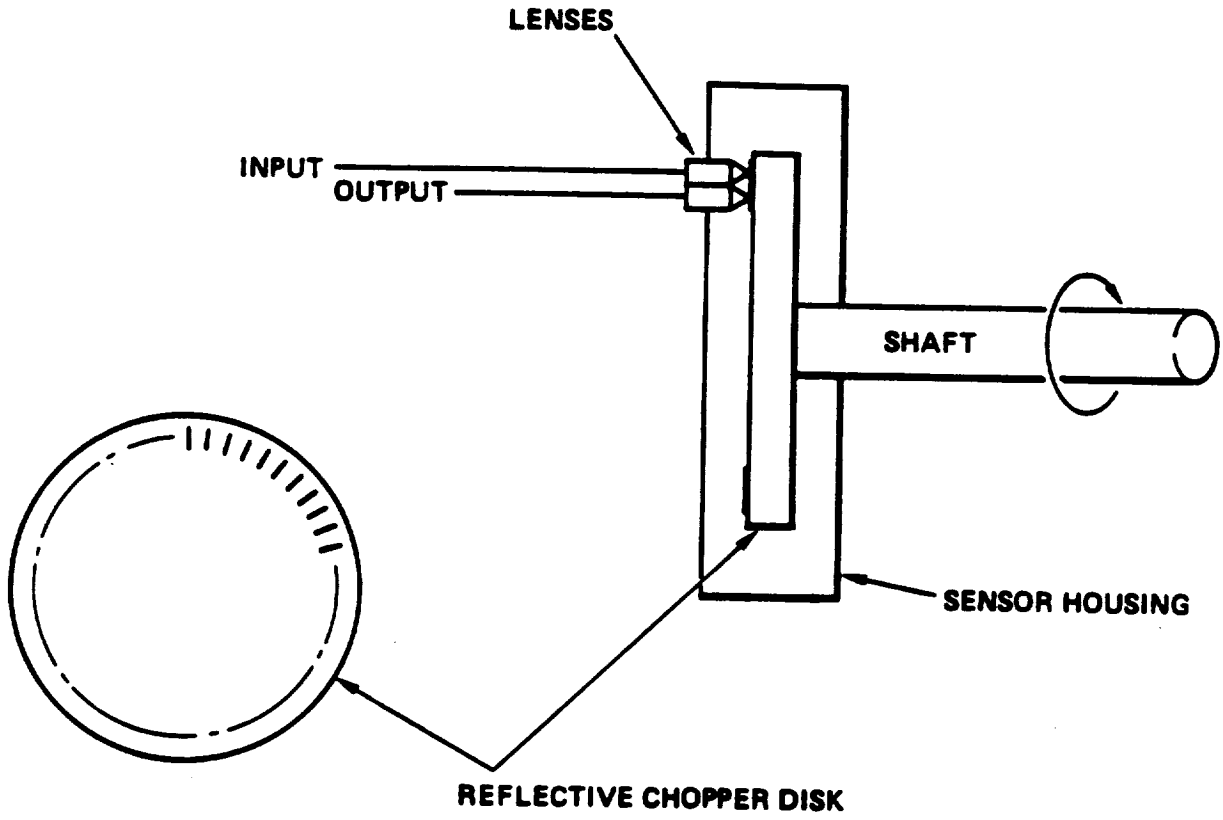

Figure 3-9. Conceptual Diagram of Optical Rotary Speed Sensor

Several signal processing methods are considered for measuring speed. The simplest is a digital counter which simply counts the pulses generated as a result of reflective and non-reflective areas. This processor requires the highest signal-to-noise ratio of all the processors considered. For the optical chopper type of sensor this processor should be adequate.

The second type of processor that may be considered for measuring speed is a tracking filter such as a phase locked loop matched to the signal bandwidth and dynamics, followed by a counter. This has the advantage of being able to eliminate much of the

noise within the total receiver bandwidth required to accommodate the total frequency range of the incoming signal. The potential disadvantage of this system is the difficulty in identifying the appropriate signal from spurious signals with similar amplitudes in the frequency range of interest.

A third type of processor that is being considered is an FFT processor. This is the most universal processor and provides the best performance since it may easily be programmed to adapt to a wide range of signal conditions. With current technology it is also the most complex and largest in size. As the state-of-art in electronics changes, the level of integration and design of more complex digital signal processors will be feasible and it will be possible to build a programmable high speed FFT processor with very few components. The attractive feature of this system is that it provides much additional information on the status of the engine or system being monitored.

A detailed system analysis needs to be performed to determine the feasibility of multiplexing the two sensors into a single receiver and frequency counter. If there is sufficient signal-to-noise ratio or contrast ratio and a sufficient number of pulses to determine the speed to the required accuracy in half of the update period then the multiplexing should be feasible.

3.6 VIBRATION MEASUREMENT CONCEPT

Vibration may be measured using an accelerometer which employs a fiber-optic microbend sensor that measures the force required to accelerate a mass. The mass is mounted to a thin, wide beam and contains corrugations on its lower surface. The base of the accelerometer contains mating corrugations and a support for the ends of the beam. A fiber loop is clamped between the two sets of corrugations. Accelerations of the base cause a relative motion between the mass and the base, resulting in microbending and an intensity modulation of the optical power in the fiber loop. The accelerometer range and sensitivity are determined by the stiffness of the beam and by the quantity of mass mounted on the beam. These parameters can be adjusted to tailor the accelerometer to specific measurement requirements. A detail study on this matter is provided in reference (3).

SECTION 4

ELECTRO-OPTICAL INTERFACE DESCRIPTION

A total of six electro-optic interfaces are required to address the list of 43 sensors. Description of primarily two types, digital and analog interfaces which were examined at TRE are provided in this section. The rest four EO interfaces require additional evaluation and analysis and therefore, is beyond the scope of this work.

4.1 DIGITAL OPTICAL TDM SENSOR INTERFACE

Figure 4-1 is a block diagram of the electronic interface for digital optical TDM sensors. This block diagram is representative of the functions required for aircraft sensor systems including a dual interface to the host system. The main elements of this interface are as follows:

1. Separate transmitter for each sensor
2. Common receiver for a group of sensors
3. Serial to parallel converter
4. Digital data averager
5. Gray to binary converter
6. Two dual port memories for the host interface
7. Transmitter sequencer
8. Transmitter auto level control (ALC) circuit
9. System controller

Figure 4-2 shows a timing diagram of the sensor interrogation sequence. This timing diagram shows a group of 24 sensors being interrogated in a sequence after a single start command is received from the host system. After receiving the start command from the host system the controller selects the first sensor and sends a transmit pulse to that sensor. The received signal is shown on the second line from the bottom. The serial received signal is converted to parallel format then averaged in the digital averager. This data word interrogation cycle is repeated 32 times for each sensor before the data is converted to binary format and stored in the interface memory. The 32 sample averaging gives an improvement in the optical link sensitivity of about 13 dB.

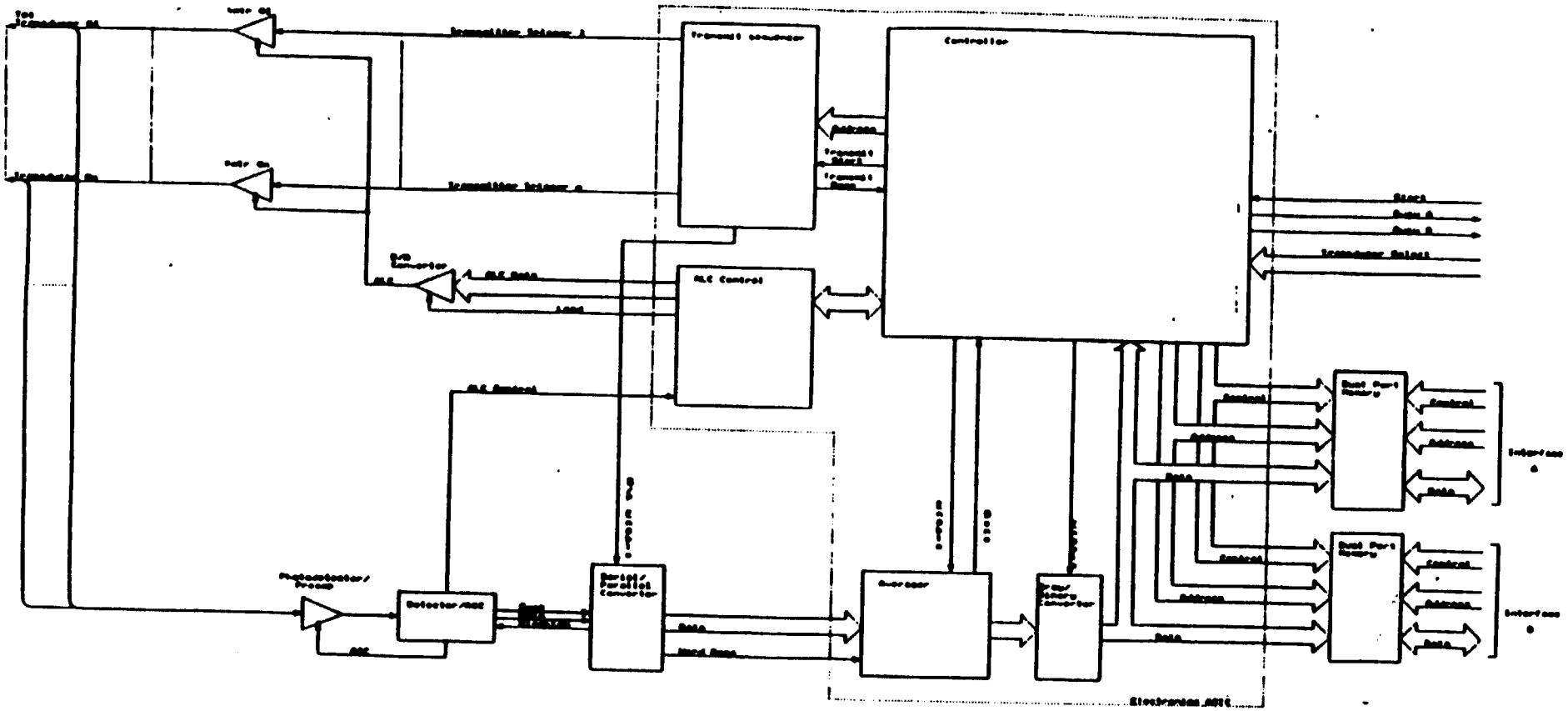

Figure 4-1. Block Diagram of Electronic Interface for Digital TDM Sensors

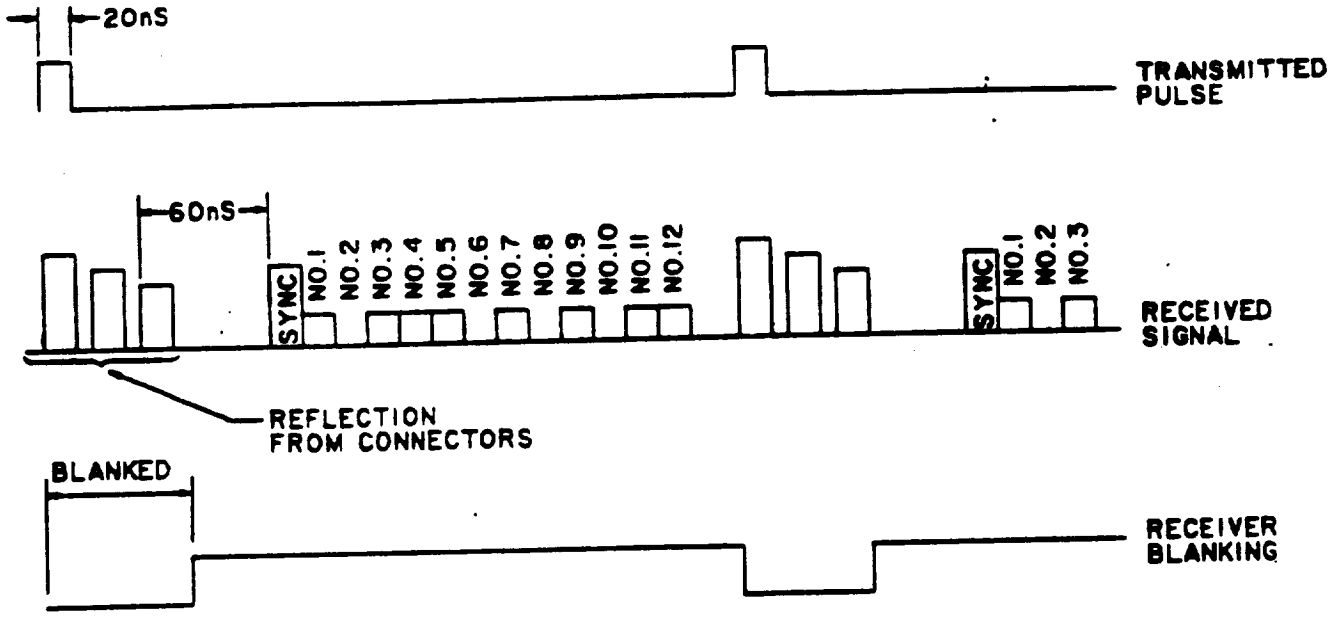

Figure 4-2. Transmitted and Encoded Reflected Signals in Time Division Multiplexed Optical Transducer

4.2 ANALOG MICROBEND SENSOR INTERFACE

Figure 4-3 is a block diagram of the electronic interface for an analog microbend sensor system. The main elements of this interface are:

1. System controller, data processor and interface
2. Transmit timing controller
3. One transmitter per sensor
4. Receiver
5. Sample and hold timer
6. Two sample and hold circuits
7. Analog data selector

The block diagram shows that the essential difference from the digital system is the signal processing/data recovery section. Although the details are not shown here, the interface to the host system is identical to the interface for the digital sensor system including the dual data bus if required. Refer to the timing diagram in Figure 3-5 for this discussion of the operation of this system. A sensor channel is selected and a single transmit pulse is generated upon initiation of the interrogation process by command from the host system. The return signals consist of a reference signal and a measurement signal. The amplitude

of each of these signals is sampled and converted to digital format by the A/D converter and then read into the data processor. Since this transmit/receive cycle takes less than 500 ns, this cycle is repeated 32 times and the amplitude data is averaged in the data processor to provide additional SNR margin. At the end of the interrogation of one sensor channel the next sensor is selected and the interrogation process is repeated for that sensor until all sensors have been interrogated.

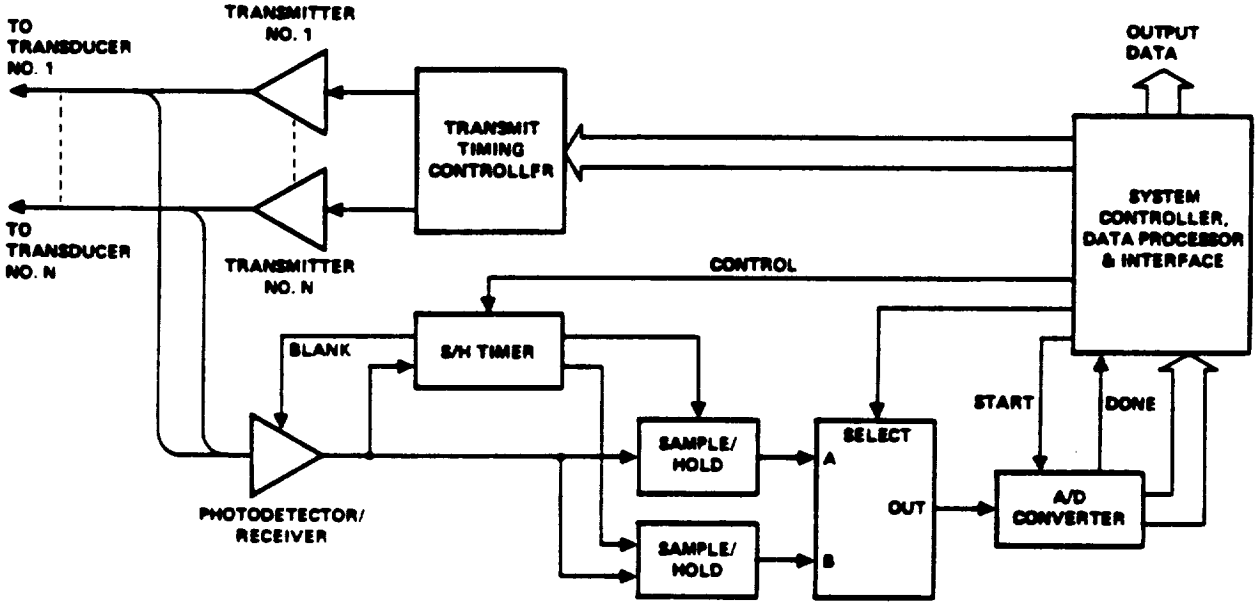

Figure 4-3. Block Diagram of Electronic Interface for Analog Microbend Sensors

SECTION 5

TIME DIVISION MULTIPLEXING SCHEMES

There are three sensor system multiplexing architectures that are considered for evaluation. The previous electro-optical interface descriptions are based on one of these three concepts but the operation of the interface is easily adapted to the other two methods by altering the method of selecting the individual sensors.

5.1 SYSTEM CONCEPTA

Figure 5-1 is a block diagram of a sensor system using the multiplexing concept with one common receiver for a group of sensors and a separate transmitter for each sensor. As described previously, the selection of the individual sensors is done by selecting the appropriate transmitter. The main advantage of this system is that it provides the most efficient use the available optical power. This will be discussed further in the section on the SNR budgets.

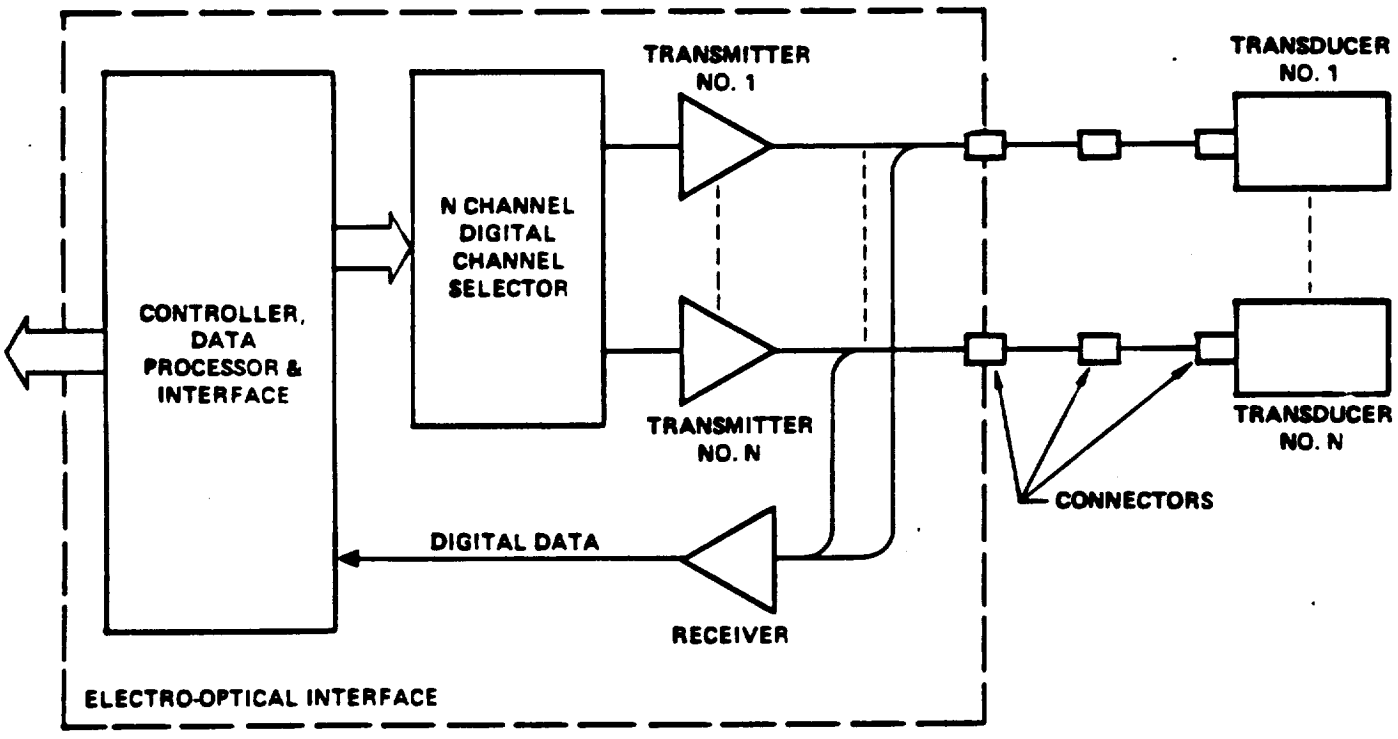

Figure 5-1. TDM Sensor System Using One Receiver with Multiple Transmitters

5.2 SYSTEM CONCEPT B

Figure 5-2 is a block diagram of a sensor system using one common transmitter and separate receivers for each sensor. The individual sensors are selected by selecting the appropriate receiver. The main advantage of this system is that only one optical transmitter is required for a group of sensors. Optical sources in the past have been expensive and major limiting factors in the system reliability. The reliability issues have been addressed and predicted lifetimes of >300 years for cw operation at 25 degrees C and 17 years at 80 degrees C have been reported[4]. Costs are still high but as production volumes increase these should come down to a level of <$100 for a fiber pigtailed device. The major disadvantage of this configuration is that the optical source power must be split into several paths which reduces the system SNR budget by the number of sensors multiplexed from a single source. This is examined further in the discussion on the SNR budget.

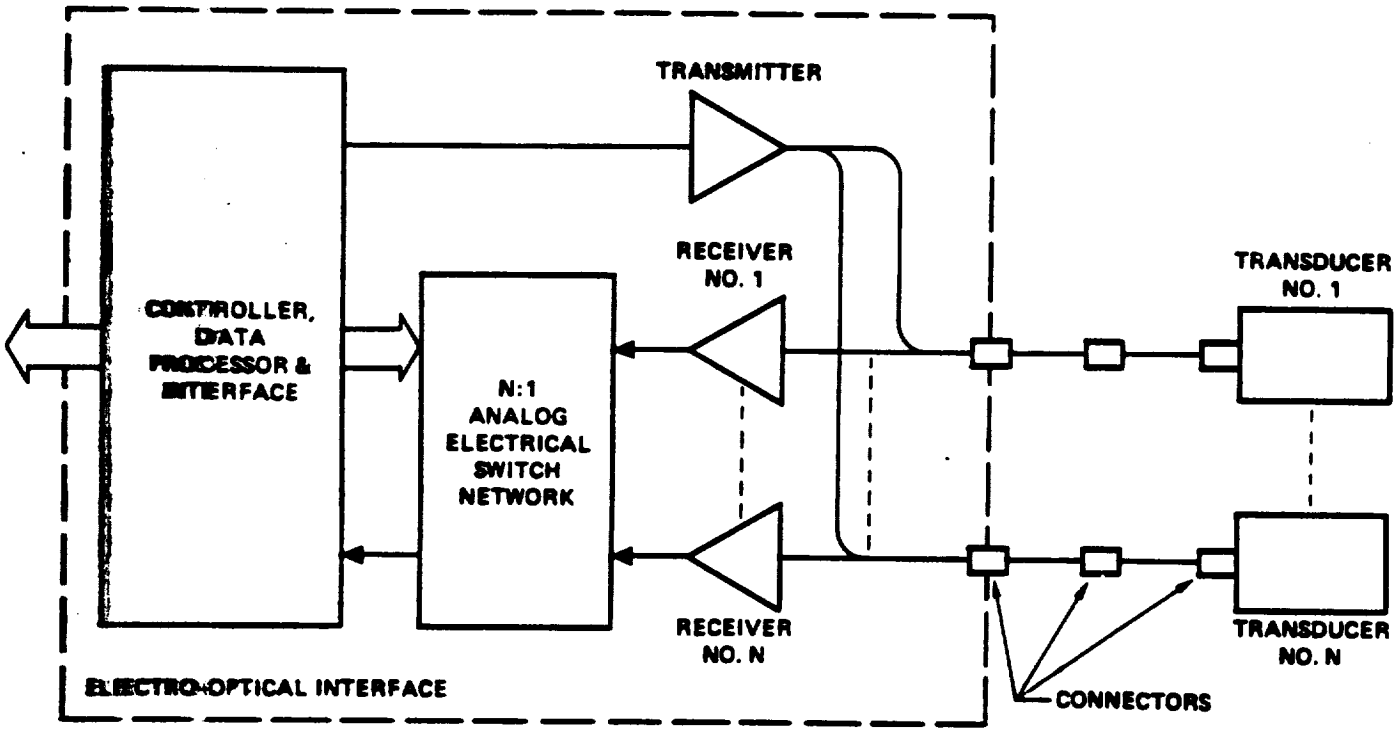

Figure 5-2. TDM Sensor System Using One Transmitter with Multiple Receivers

5.3 SYSTEM CONCEPT C

Figure 5-3 is a block diagram of a sensor multiplexing system using a single transmitter and a single receiver with an optical 1:N switching network. This system provides the minimum possible complexity but at this time cannot be considered practical since a high speed, multimode optical switch is not available. The single mode waveguide switches that are presently available suffer high losses when coupled to multimode fibers because of core area mismatch. Current techniques for multimode switches such as liquid crystals, piezos, or mechanical fiber displacement are too slow to be practical for these applications.

A technology that shows promise for a 1:N optical switch network is the use of Multiple Quantum Well (MQW) electro-optic absorption switches coupled to laser cavities for optical amplification that compensates the losses. This has been described in recent literature[5] and it appears that both the switches and the amplifiers way be fabricated on a common substrate. Since this is a relatively new concept additional study is required to determine its ultimate feasibility, particularly with regard to the receive mode sensitivity and a substantial development lead time should be anticipated. Figure 5-4 shows a block diagram of a switch network using this concept.

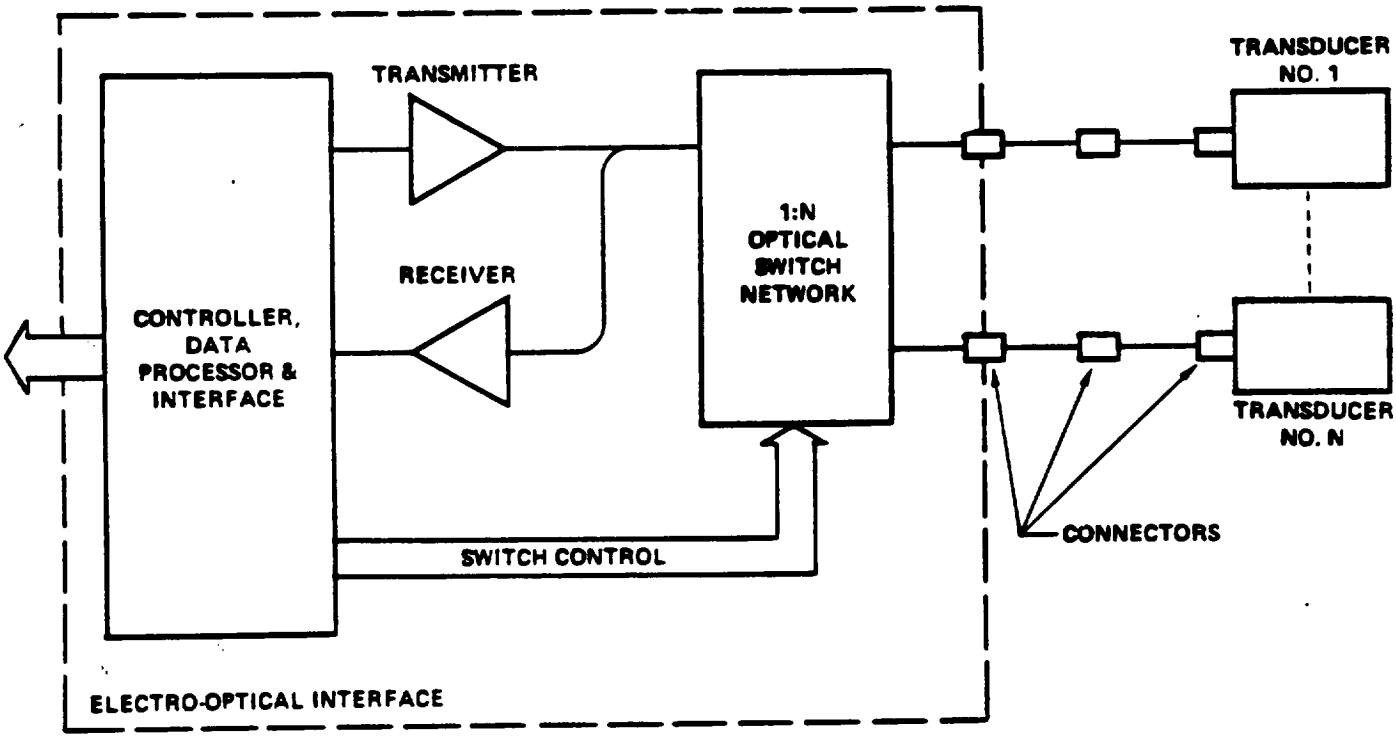

Figure 5-3. TDM Sensor System Using One Transmitter, One Receiver and a 1:N Optical Switch Network

The receiver sensitivities used are taken from manufacturers data on monolithic GaAs receiver amplifiers coupled to 1300 nm detectors. The actual value may vary depending on factors such as the detector area required for a particular multiplexing configuration. The receiver sensitivity for the digital sensor is based on a bandwidth of 50 MHz and for the analog system 10 MHz. The SNR margin required to achieve the stated system performance for both sensor types assumes averaging over 32 samples.

5.5 NUMBER OF SENSORS PER INTERFACE CARD

The number of sensors that may be multiplexed per single interface card depends, in general, on the interface card size requirements, the type of TDM scheme used and reliability. The more the number sensors the more the electronic components, i.e. larger the interface card. The reliability of the system card is quite complex, but one can safely state that it reduces with increasing number of components. There are, however, three common factors in the three proposed TDM schemes, such as the optical connector density (number of connectors per unit area), sampling rate/processing time and complexity of controller/data processing/Interface electronics that can influence the card size and these are discussed first. Following this, the three proposed multiplexing systems are discussed to understand the factors specific to that configuration.

5.5.1 Common Factors

5.5.1.1 Optical Connector Density

All the sensor types included in this report use reflective sensing mechanisms which allow the use of a single interconnect cable with a single optical connector on the interface electronics assembly. As fiber-optic connector technology progresses the required optical connector density will become less of a limiting factor than the complexity of the related electronics. Card edge connectors with mixed electrical/optical contacts are currently available with optical contact spacings of 0.156 inches. However, this spacing may be reduced by using the silicon v-groove alignment blocks that provide an order of magnitude closer spacing. A number of issues including alignment and temperature stability need to be addressed prior to commercialization of connector system for the aircraft market.

5.5.1.2 Sample Rate/Processing Time

This factor can influence the number of sensors to be multiplexed in situations where the sampling rate is approximately equal to the required update rate. Parallel processing may provide the required update rate, but the major advantage of multiplexing is reduced. The processing time used to interrogate each sensor is directly related to the accuracy required

and SNR available for each fiber-optic sensor link. This implies that if the system is deficient in one of these parameters the other two may be altered to overcome the deficiency. In the ADOCS case, however, this factor was not a problem.

The ADOCS fiber-optic sensor system uses a sample time of 16 microseconds with a processing time of about 10 microseconds for each sensor. The overlapping of the sampling and data processing operations with parallel processing circuitry allows the total interrogation time to be reduced to essentially 16 microseconds. The total interrogation time for the analog sensor types has been estimated to be approximately the same. As an example if a 5 ms data update period is required for each sensor then 312 sensors may be interrogated in each update period. This is clearly not the case because the complexity of the electronics is an overriding factor limiting the number of sensors multiplexed into a single card.

5.3.1.3 Complexity of Controller/Data Processing/Interface Electronics

The ADOCS system interface electronics excluding the optical transmitters/ modulators occupies 40 cubic inches of space using standard components and PC board construction. With the use of ASIC and hybrid technology it is possible to reduce this volume to less than 10 cubic inches for this portion of the electronics. This implies a savings of approximately 30 cubic inches of space common to the three proposed schemes.

5.5.2 Multiplexing Scheme Dependent Factors

5.5.2.1 Scheme A - Separate Transmitters/Common Receiver

This is the TDM scheme used in the ADOCS program and has proven quite effective. Using this scheme the total volume to multiplex 24 sensors is approximately 242 cubic inches of which 63 cubic inches is allocated to the power supplies, 44 cubic inches to 2 circuit boards, 30 cubic inches to optical transmitters and modulators, 30 cubic inches for the receiver, and the rest for interconnect boards, fiber-optic connectors and harnesses. It is clear that with the use of ASIC and hybrid technology, substantial volume savings may be achieved. The factors that are particularly of interest for this multiplexing are:

- Complexity of transmitter electronics/packaging density
- Maximum practical detector area

Laser diodes are currently available in 0.15 cubic inch packages with fiber pigtails. There appears to be room in these packages for the hybrid packaged drive electronics necessary

to create a narrow pulse and provide an automatic level control input. If this is achievable, a volume savings of approximately 25 cubic inches may be realized.

The factor of maximum practical detector area that may be accommodated by a receiver preamplifier is dependent on several amplifiers and system design factors. These factors include the system bandwidth and sensitivity requirements and the forward gain and feedback capacitance of the amplifier. Simulations have been done using an electronic circuit analysis program to determine the sensitivity of a typical amplifier designed for a 90 MHz bandwidth to the detector capacitance. Figure 5-4 shows the circuit with the values used for this analysis and the resulting frequency response plots for five values of detector capacitance. The following table shows typical values of capacitance v/s detector size for a square detector made from GaInAs material:

Detector Size, microns	Capacitance, pf
75	.3
150	1.2
300	4.8
500	13.3
1500	120.0

Figure 5-5 shows that a bandwidth of 50 MHz is achievable with a detector capacitance of 10 pf. From the table above we can see that the capacitance/ area quotient is 5.33×10^{-5} pf/micron^2. A 10 pf capacitance is found in a square detector element with a side dimension of 433 microns. With a fiber clad diameter of 110 microns, 16 fibers (or sensors) could be butt coupled to the detector without optimizing the packing of the fibers. If a lower receiver sensitivity could be tolerated then a larger detector could be used and more sensors may be multiplexed.

5.5.2.2 System B - Separate Receivers/Common Transmitter

The factors that determine the maximum number of channels that may be multiplexed into a single interface card for this multiplexing system are:

- System loss budget margin
- Receiver circuit complexity/packaging density

The primary limitation of this multiplexing technique is that the power from a single optical source is divided among the channels that are multiplexed into the interface card. For the

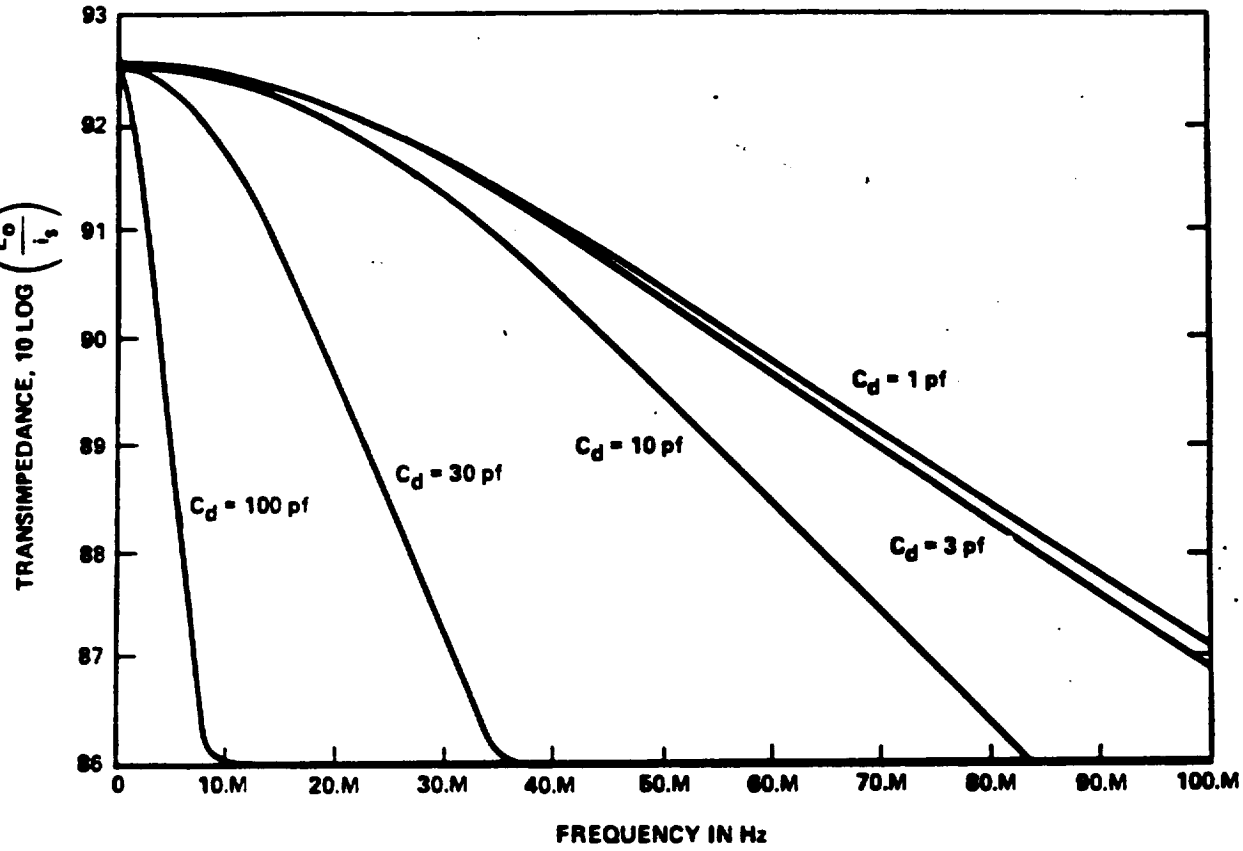

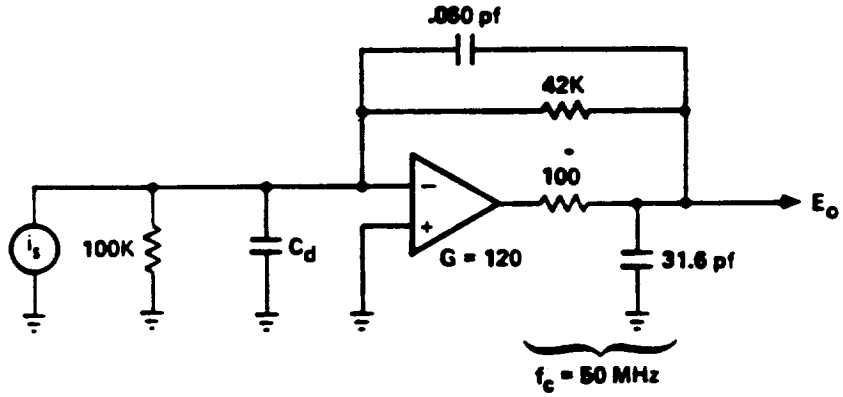

Figure 5-5. Preamplifier Frequency Response

SNR budget shown in Table 5-1, 24 channels give a SNR penalty of 15 dB. This system requires an optical source level that is not easily achievable today. In addition, the higher power levels reduce the life of the optical source.

Although the complexity of the entire receiver is significantly greater than the complexity of the transmitter circuit, the actual circuitry that needs to be duplicated for each channel is just the detector and preamplifier. These are currently available in 0.075 cubic inch packages with fiber pigtails. There is some added complexity to the remainder of the receiver to accommodate the switching and baseline stabilization required for this system configuration.

5.5.2.3 System C - Common Transmitter and Receiver/Optical Switch Network

The primary factor that determines the maximum number of channels that may be multiplexed into a single interface card for this multiplexing system is:

- Gain/noise performance of optical switch/amplifier network

Kingston[6] has shown that the noise bandwidth of a system with a laser cavity used as an optical amplifier coupled to an incoherent detector is equal to the optical bandwidth of the system. This imposes a severe limitation on the application of optical amplifiers unless a very narrowband optical filter is used. This would limit the optical system bandwidth to something close to the optical switch/amplifier network shown in Figure 5-3 modified to include T/R couplers at the transducer ports with the receive legs coupled together into a single receiver port. With this approach the optical amplifiers would be used in the transmit direction only. Much work remains to be done to determine the tradeoffs of system performance, complexity, reliability and cost for these various configurations.

SECTION 6

RESPONSE TO QUESTIONS

1. Type of Sensors

All of the sensors listed in the table have been incorporated into the system design.

2. Signal Compensation or Calibration

The sensing mechanism for the position sensors is digital and for all of the others it is analog. The sensor calibration methods are listed in the table below.

Sensor Type	Calibration Method
Digital	Internally generated reference signal time multiplexed.
Analog	Internally generated reference signal time multiplexed.
Turbine Blade Temperature	Two wavelength ratio.
Light Off Detector	Reference generated in the interface and transmitted through the sensor.
Vibration	Reference generated in the interface and transmitted through the sensor.
Rotary Speed Sensors	Time base in interface for frequency measurement.

3. Number of Channels

Each sensor has its own optical source. The digital and analog sensors share a common receiver within their respective groups. All other sensors have separate receivers.

4. Number of Optical Sources

One source is required for each sensor except for the turbine blade sensor which is a passive system. Forty-two sources are required for the complete system.

5. Number of Detectors

Approximately 10 detectors are required for the complete interface. The considerations for this number are discussed in the section on multiplexing.

6. Number of Fibers

Each sensor requires one interconnect fiber.

7. I/O Pincount

One optical connector is required for each interconnect fiber.

8. Optical Power Margin

The optical power budgets for the digital and analog sensors are discussed in Section 5.4. More study needs to be performed to determine the power margins for the other types of sensors.

9. Signal Processing Time and Receiver Bandwidth

Sensor Type	Processing Time	Receiver Bandwidth
Digital	16 microseconds	50 MHz
Analog	16 microseconds	10 MHz
Turbine Blade Temperature	<3 microseconds	<2 kHz
Light Off Detector	16 microseconds	10 MHz
Vibration	16 microseconds	10 MHz
Rotary Speed Sensors	5 microseconds	<50 kHz

10. Complexity

Further study is required to evaluate this factor.

11. Electrical Power Consumption

It is anticipated that the power requirements should not exceed 25 watts. Additional study is required to determine this more accurately.

12. I/O Circuit Area

Further design work is required to evaluate this factor.

13. Weight

This cannot be evaluated at this time.

14. Reliability

It is anticipated that the reliability requirements for flight critical aircraft systems can be met with this sensor system. More design work is required to give an accurate MTBF figure.

15. Redundancy

The redundancy requirements must be considered from the top level system performance requirements. Redundancy can be provided internally in each sensor housing or by incorporating duplicate identical sensor systems.

16. Maintainability

Fault isolation can be provided for each of the sensors to locate the fault to the replaceable assembly. In the sensors that use time division multiplexing for calibration, an analysis of the return signals will provide most of the information necessary for isolating the faults. Studies have been done of fault isolation methods to identify one that gives complete isolation of all possible faults for the digital sensor types. It may be necessary, depending on the system requirements, to add a source at a second wavelength to provide complete fault detection and isolation.

17. Availability or Development Schedule

Developmental models of the position sensors have been extensively flight tested on the ADOCS program. Additional work is required to make them into production items. All of the concepts used in the other sensors have been demonstrated but additional work is required to develop production units.

SECTION 7

REFERENCES

(1) J. W. Berthold, W. L. Ghering, and D. Varshneya, "Design and Characterization of a High Temperature Fiber-Optic Pressure Transducer," Journal of Lightwave Technology, Vol LT-5 No. 7, July 1987

(2) D. Varshneya and J. W. Berthold, "Fiber-Optic Noncontact Temperature Probe System," SPIE Proceedings 1986, Boston, MA

(3) D. Varshneya, D. Raj, and D. Miers, "Fiber-Optic Microbond Accelerometer", Patent Pending; SPIE Proceedings, 1987, San Diego, CA

(4) Laser Reliability, Report No. LT86-2, Jan 1987, Lasertron, Inc.

(5) S. A. Pappert, "Ultra-Wideband Direction Finding Using Fiber-Optic Transversal Filters", Report No. 1161, March 1987, pg. 57

(6) R. H. Kingston, "Detection of Optical and Infrared Radiation," Springer-Verlag, NY 1978

APPENDIX C

ELDEC ELECTRONIC AND ANALOG OPTIC EOA'S

FINAL REPORT

ELECTRO-OPTIC ARCHITECTURE STUDY

FOR

ADVANCED AIRCRAFT SENSING SYSTEMS

ELDEC Document No. 011-0880-701

Prepared by: Thomas A. Lindsay 11/20/88
Thomas A. Lindsay

William R. Little 11/23/88
William R. Little

Approved by: Randall E. Morton 11/21/88
Randall E. Morton

Date: November 21, 1988

EXECUTIVE SUMMARY

This study presents comparative information on several different electrically active and passive fiber optic sensors and sensing system architectures for future advanced aircraft applications.

The characteristics presented for architectures based on electrically active sensors with fiber optic signal communication are derived from ELDEC development of EL-OPTIC™ sensors, which have been undergoing in-flight evaluation since January of 1987.

The characteristics presented for architectures based on passive fiber optic sensors are derived from development of various intensity modulated multimode sensors incorporating our patented TDIN (time domain intensity normalization) technique.

Tradeoffs are summarized in an Architecture Characteristics Matrix that references specific portions of the text for further elaboration. Finally, significant sensor and system development issues relevant to practical implementation of sensing system architectures in advance aircraft are discussed.

TABLE OF CONTENTS

LIST OF TABLES AND FIGURES

1. ORGANIZATION OF THIS REPORT

Information on designs for candidate fiber optic sensor systems, as requested by ATTACHMENT "A" of the letter subcontract, (P.O. no. 153664), are presented in the beginning of section 2 of this report. This information has been assembled in matrix format to assist in identifying and characterizing the system options.

In addition, ELDEC is pleased to present more detailed information in the balance of section 2 and section 3 relating to our preferred sensor concepts and their implementations.

2. CANDIDATE FIBER OPTIC SENSOR SYSTEMS

A matrix of the characteristics of the ELDEC EL-OPTIC™ and TDIN™ sensor concepts is presented in Tables 1a and 1b respectively which include references to sections of this report in which more detailed discussions are presented.

ELDEC has investigated many sensing concepts and considers two of them most likely to satisfy the overall industry needs, particularly those related to interface commonality combined with practicality. We believe that these concepts are more likely than other alternatives to result in cost-effective devices for near term deployment. An ongoing IR&D program is developing these two techniques into families of fiber optic based sensors suitable for the aerospace environment. The first of these to reach flight test status is the ELDEC EL-OPTIC sensor concept. One unit has been flying since February of 1987 as an operational device in scheduled commercial service and a second since January of 1988. This concept employs a battery powered electrical transducer element with an optical fiber signal line.

The second concept, now being prepared for delivery, is the ELDEC TDIN sensor concept. It employs an analog optical intensity modulation transducer with ratiometric normalization and is an electrically passive opto-mechanical device. Each of these schemes provides the advantages of versatility and interface circuit commonality; that is, a single interface module design will operate with various transducers designed to detect many different physical phenomena.

The initial development has been concluded for each program

and we are now in position to proceed with extending these concepts to other sensed parameters. Both concepts support the multiplexing of sensor signals.

Table 1a

EL-OPTIC Sensor System Characteristics - Summary

n = # of sensors within channel

Characteristic	No Mux 2.1.1	SDM 2.1.3	TDM 2.2.3
1. Sensor types	see 2.1	see 2.1	see 2.1
2. Sig. Compens.	/1	/1	/1
3. # Sensors /2	1	1	several
4. #Sources (LEDs) /2 /3	none	2	2
5. # Detectors /2	1	2	2
6. # Fibers /2	1	1	(2n-1) segments
7. #I/O pins /2	1	1	1
8. Power margin	30 dB	poorer	poorer
9. Proc. time	/4	/4	/4
10. Complexity	simple	more complex	more complex
11. Elec. power	0.07 watts	much larger	larger
12. I/O ckt area /2	<1 sq. inch	<1 sq. inch	1 sq. inch
13. Weight /2	0.4 ounce	0.4 ounce	—
14. Reliability (MTBF, hrs)	high 2.1.2.2	lower	lower
15. Redundancy	dual output	yes	yes
16. Maintainability	good	lower	lower
17.1 Development Risk	lowest	moderate	low
17.2 Devel. Schedule	2 years	3 years	3 years
17.3 System Cost Relative to conventional electric sensors as 1.0	1.1x	2x	1.3x

/1 Compensation and calibration is accomplished within the sensors.
/2 Per channel
/3 The sensors each have an output LED
/4 Less than 100 microseconds processing time, less than 5 milliseconds update rate.

Table 1b

TDIN System Characteristics - Summary

n = # of sensors within channel

Characteristic	No Mux 2.2.1	SDM 2.2.2	TDM 2.2.3	WDM 2.2.4
1. Sensor types	/1	/1	/1	/1
2. Compensation method	TDIN	TDIN	TDIN	TDIN
3. # Channels /2 (see #8)	No limit	18/49	7/15	4/10
4. # Sources (LEDs)	n	n	1	n
5. # Detectors	n	1	1	1
6. # Fibers /3	2n	n+1	2	2
7. # I/O pins	2n	n+1	2	2
8. Power margin (db) /2	29.4/36.5	11.1/11.0	11.0/11.2	12.5/11.3
9. Process time (eff.)	1.67 msec	1.67 msec	1.67 msec	1.67 msec
10. Complexity	n x (1 LED + 2 ICs)	n LED + 3 ICs	1 LED + 3 ICs	n LED + 3 ICs + WDM
11. Elec. power	n x 1.5 watts	2 watts	2 watts	2 watts
12. I/O ckt area	n x 4 sq.in.	4 + (n x 0.5) sq.in.	4.5 sq.in.	4.5 + (n x 0.5) sq. in.
13. Weight /4	n x 4 ounces	4 + (n x 0.5) oz.	4.5 ounces	4.5 + (n x 0.5) oz.
14. Reliability /8	53,000/n	53,000 - (n x 1000)	53,000	53,000 - (n x 1000)
15. Redundancy	5/	5/	5/	5/
16. Maintainability	6/	6/	6/	6/
17. Availability	7/	7/	7/	7/

Notes:

/1 All position, temperature, pressure. Others possible with alternate post-processing.
/2 With PIN/APD detector, LED source(s) @ 125°C
/3 At FADEC. See text for fiber specifications
/4 Electronics only
/5 Best to multiply entire system
/6 Automatic BITE, replaceable sensors and sensor mux, standardization electronics. TDM approach is installation dependent.
/7 Reduced systems available, 1 yr; miniature electronics, 4 yrs; full capability by late 1990s. Improvements sought in power budget, connector and coupler performance, and electronic miniaturization.
/8 @125°C

2.1 EL-OPTIC™ description

The EL-OPTIC concept involves micro-powered, electrical sensing elements (ie. transducers) with fiber optic signal lines but without any other attachments; no electrical power lines or electrical bonding. This concept facilitates the development of sensors incorporating the benefits of fiber optics that will provide state-of-the-art performance for many present electrically sensed measurands, including those listed in the FADEC sensor set. This concept facilitates use of a common architecture for all sensed parameters. The following functional blocks, shown in figure 2.1-1, comprise a single channel of this sensor concept: electrical power storage, system period generation, the transducer and its driver/interface circuit with data formatting, and output signal generation. The sensor output employs a lightly stressed LED.

Most transducers, whether optical or otherwise, measure what are basically analog phenomena. The few exceptions include on-off parameters such as RPM indication. The EL-OPTIC concept provides for suitable compensation and referencing within the sensor circuits, then formats this analog data in a standardized digitally coded optical format for transmission to a standardized receiver interface module. This concept provides a robust optical power margin.

In our EL-OPTIC Local Sensor Interface Unit (LSIU) architecture, presented in paragraph 2.1.2, each sensor output function has a single optical fiber with one-way signal transmission. This uses one connector terminus at the FADEC box feeding to a dedicated optical interface module. This electrically-multiplexed approach provides a reduction of single-point failure opportunities. The reasons that we favor this scheme for the EL-OPTIC concept are presented in later paragraphs of section 2 and elsewhere in this report. The EL-OPTIC concept is, however, compatible with optical sensor multiplexing and command-response addressing.

The EL-OPTIC concept will accommodate multiple fiber optic output lines if such an architecture is required for redundancy. It can be implemented by the addition of another LED and connector. These outputs may then connect to multiple FADEC units. Redundant batteries are also possible.

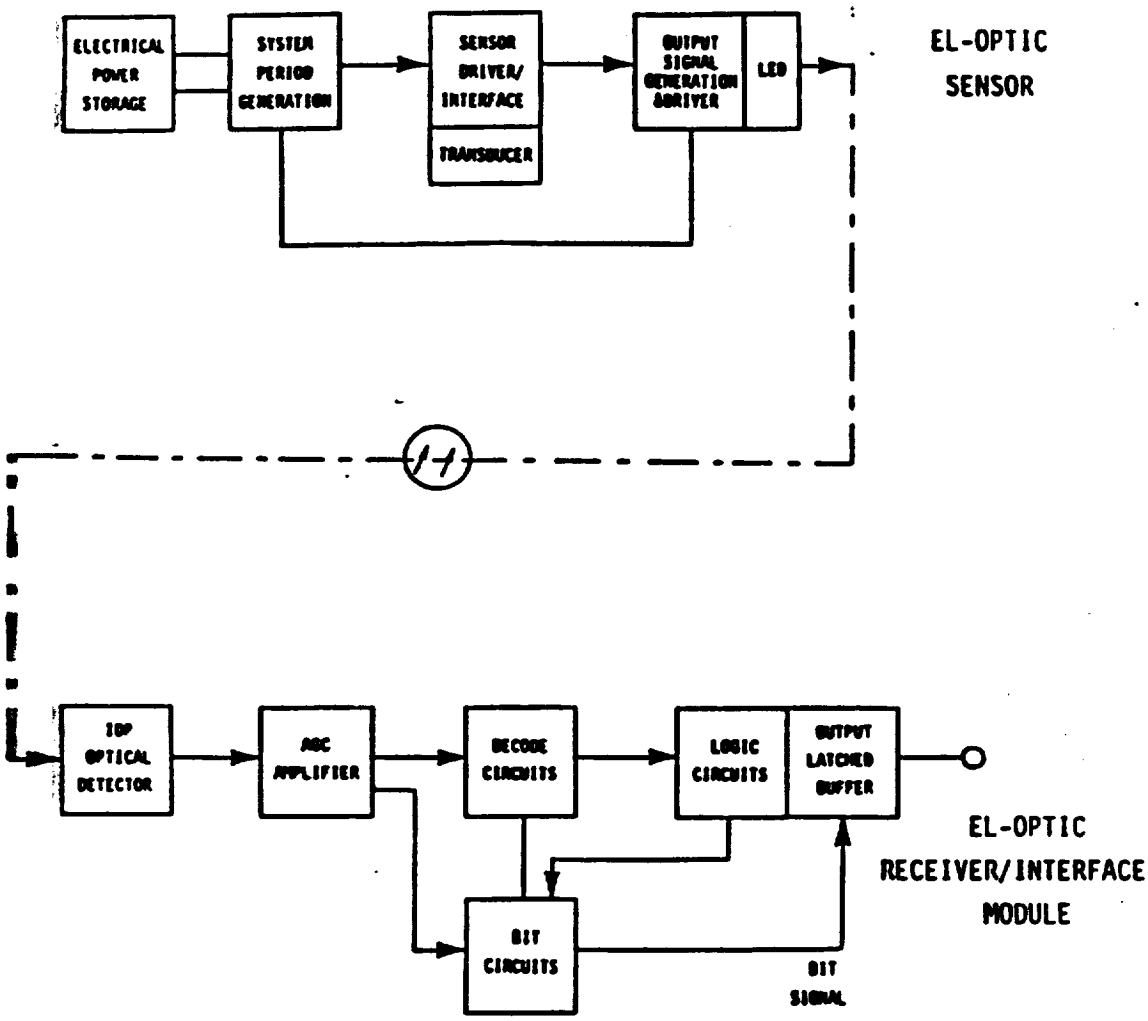

SENSOR SYSTEM BLOCK DIAGRAM

FIGURE 2.1-1

The fiber optic interface module, also shown in Figure 2.1-1, is comprised of an integrated detector preamplifier (IDP) of modest capability, an AGC amplifier section and digital detector-decoder with storage buffer. No optical source is required at the interface module.

The EL-OPTIC concept combines proven electrical sensing technology with fiber optic signalling to provide the environmental immunity expected from fiber optic technology. It features total EMI isolation, and the signal is

unaffected by lightning strike, and EMP. Our implementation is designed for operation in harsh environments. A proximity device is hermetically sealed to provide water immersion protection and enhanced survivability to fire. It has low weight as well as reduced system complexity and cost relative to many competing passive fiber optic sensing technologies and is far more forgiving of optical cabling losses and variations in loss.

This sensor format has substantial advantage in the near term (ie. 5 year time frame). Within this period, passive fiber optic technology is not likely to be competitive with respect to either non-recurring or recurring costs. El-Optic sensors are based upon known, familiar sensing technology with modest fiber optic content. Consequently, development schedules and costs, as well as production costs, may be lower and more accurately projected at program inception.

Development risk to produce proof-of-concept sensors rated to 130°C is low. Such development would meet many early test vehicle needs and would basically be an application of known technology. Research required to extend the EL-OPTIC concept to 175°C operation is expected to be modest. There is potential to further extend this concept to 300°C operation (see section 3).

The EL-OPTIC concept is compatible with most phenomena for which electrical sensors presently exist. It has been applied to non-contact proximity sensing, position sensing, and mass flow (conceptually) at this time, with pressure and temperature slated for future development. It complements micro-machined electronic sensor technology. It facilitates commonality of the sensor optical interface module independent of the nature of the sensed parameter and therefore should satisfy the desire for commonality.

The sensor output pulse train occupies a time span of less than 100 microseconds. The sensed parameter value is stored in digital form by the end of this period. This data is updated as required by the particular sensor function; for example, once every 5 milliseconds. The update rate is tied to sensor power requirements which are described in paragraph 2.1.1.1.

The interface module will be implemented in Application Specific Integrated Circuit (ASIC) form, initially as a hybrid device having 3 IC chips. The circuits are all

simple, low cost designs with very low stress levels and modest performance requirements. Presently, the IDP detector is an MFOD 2404. The output latched buffer can be a low speed device equivalent to a CMOS 54C374. The present discrete implementation of this scheme uses commercially available optical hardware of modest performance, draws 25 mA at 12 volts, and occupies 6 square inches of board area. The ultimate interface module, to be implemented in high density ASIC form, will draw less than 6 mA and occupy less than a 1 square inch area. The interface receiver module weight will depend upon the technology to be used, but should be no more than 10 grams.

The sensor environment is likely to include extremely high temperatures. However, the LED and other circuit elements will be operated in forward bias only at very low duty-cycle for which they can show good reliability in spite of this high temperature. It is reasonable to extend sensor operational capability to 175°C based on work done by Eldec Technology and Central Operations Division (TCO) on high temperature electronic circuits and packaging, and the latest information on the battery and LED capabilities. Future developments should allow extension to 300°C service temperature with reliability and service lifetime.

The EL-OPTIC concept involves micro-powered electrical circuits and sensing elements, the need for which is dictated by the realities of power availability via optical fiber, or from small batteries when a minimum 20 year continuous service life is required dependent upon update rate.

The minimum power needs are set by electrical requirements of the sensing circuit, its peripherals, and the LED signal emitter. In virtually all practical schemes, available power will be severely restricted. In order to make such schemes viable, strategies must be developed that minimize the necessary power level within the sensor. There is a tradeoff between power consumption and sensor repetition rate (data update rate) in that the average available power will be set by fixed system parameters. Several schemes are available to conserve this power. Discussion of these is beyond the scope of this report.

ELDEC has evolved a format for the digital output signal. Accuracy is not dependent upon precise time stability at the sensor or receiver and does not invoke a wide receiver bandwidth requirement. A major advantage of this EL-OPTIC

concept over passive sensing schemes is that it can provide a robust optical power margin.

There are three basic ways of providing electrical power to the sensor circuits; battery, power-by-fiber, and local power lines. The key to achieving the full benefits of the EL-OPTIC concept in the near future at competitive cost and performance is the use of the local battery power source discussed in section 3. Power-by-fiber (PBF) is discussed in paragraph 2.1.4.1. The consequences of powering a sensor by aircraft electrical power lines are:

a. EMI filter capacitors must be provided;
b. these are physically large and expensive;
c. they have relatively low electrical breakdown voltage characteristics;
d. it is difficult to obtain sufficient filtering action;
e. some EMI in the region between 40 and 100 MHz will get through, and
f. the Hi-Pot problem has not been adequately handled, consequently the sensor is not adequately protected against lightning strike.

2.1.1 LSIU Architecture

The ELDEC EL-OPTIC sensor concept is well suited for engine use. It facilitates the collection of signals from all of the sensors in a local region, regardless of the parameter being measured, through use of a small standardized sensor receiver (or interface) module. Use of the Local Sensor Interface Unit (LSIU) concept [1], [2], shown in Figure 2.1-2 can decrease overall system complexity, cut weight, improve maintainability, and control cost. The standardized interface module is a feature greatly desired by the airframe industry.

---

1. "A New Approach to Sensors for Shipboard Use", W. Little, Eldec SSD, paper presented at the SPIE symposium on FIBER OPTIC SYSTEMS FOR MOBILE PLATFORMS, 20-21 Aug. 1987, San Diego, Calif.

2. "AN OVERVIEW OF HYBRID ELECTRICAL-OPTICAL GENERAL PURPOSE SENSING", W.R. Little, Eldec Corp., paper presented at the SAE ASD meeting Nov. 1-4, 1987 at Dallas.

The LSIU formats and stores sensor data together with a sensor location identification code, fault status code and parity bit for transmission on a data bus. Continuous availability of the simple operational status code is a feature of significance to improve mission reliability. EL-OPTIC sensor operability can be flagged without need for an interactive Built-in-Test (BIT) scheme that brings inherent complexity and non-reliability.

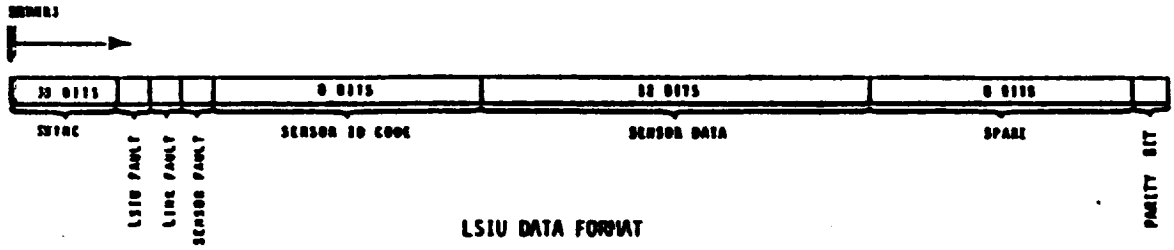

LSIU DATA FORMAT

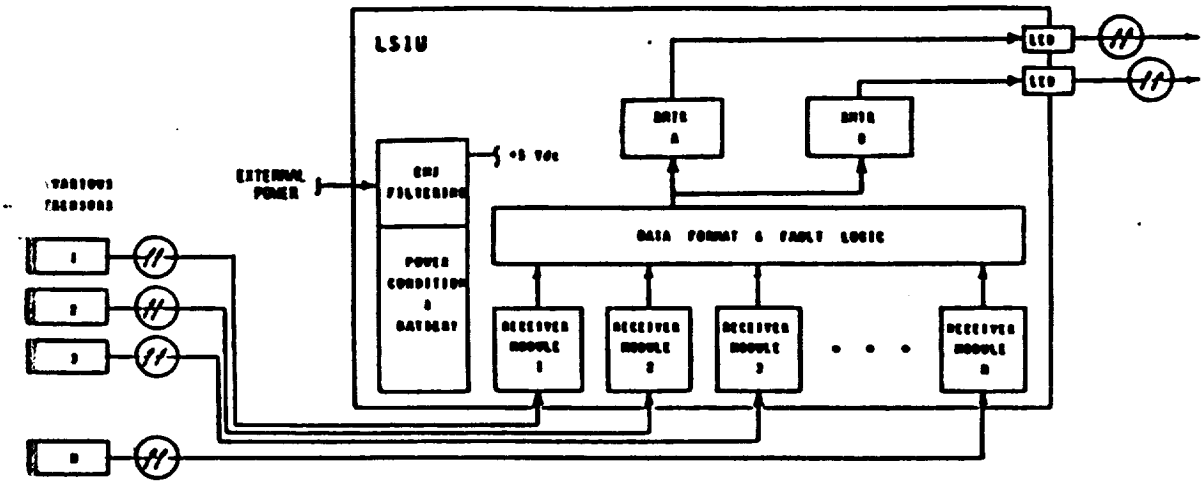

LSIU BLOCK DIAGRAM

FIGURE 2.1-2

2.1.1.1 Optical Power Budget

At the sensor, the present design uses a low emitter drive level to give 50 to 75 microwatts optical output at the end of the 100 micron core fiber optic pigtail. Future sensor versions may have a connector. The receiver threshold, to yield a stable digital output pulse train, is between 25 and 50 nanowatts measured at the box connector. These characteristics provide a full 30 dB design signal budget. These numbers also should be exceeded in well engineered production hardware using present technology. Therefore, this power margin allows normal system operation with over 20 dB of one-way cable and connector losses.

2.1.1.2 Reliability

A meaningful estimate of the sensor MTBF can not be performed at this time because of a lack of reliability data for batteries, and for the LED under the projected usage. An estimate of battery MTBF is presented in section 3. MIL-HDBK-217E projects LED numbers to 115°C, but the projection to 300°C is suspect, especially at the low duty cycle of this application. Details of packaging will play a major part in component reliability at these high temperatures.

Reliability calculations have been made for a structurally similar ELDEC product, the 8-551 proximity switch, that uses a hybrid electronic circuit. This projection is 10^6 hours MTBF for the fighter aircraft uninhabited (AUF) environment with MIL-STD-883 screening. Actual commercial airline service of our two piece proximity switch line shows 150,000 hours MTBUR (unscheduled removal does NOT necessarily imply a sensor failure). Projecting to a mature GaAs circuit technology with careful packaging it is reasonable to expect 10^6 hours MTBF for most EL-OPTIC sensors. These calculations show the transducer element to contribute only slightly to this MTBF number; the electronic circuits are the major factor.

An estimate for the interface module is again greatly dependent upon the packaging details, but a rough-order-of-magnitude is 10^6 hours MTBF based on available data for similar ASIC devices.

2.1.2 Multiplex Architecture

The EL-OPTIC concept can implement multiplexing with modestly greater complexity at the sensor. Multiplex control circuits must be added to the system and an emitter added to the interface module. It sends a coded interrogation signal that elicits a response from only one of the various (addressable) sensors on that line. Such multiplexing is not feasible with the present non-multiplexed, continuously transmitting, non-synchronized version of the EL-OPTIC sensor because of data collisions. Optical power losses are now greater by the amount lost to splitters and added connections. This arrangement also results in the need for a higher powered interface emitter and a greater electrical power drain than for non-multiplexed EL-OPTIC. This concept has the further disadvantage that each of the (addressable) sensors becomes unique when assigned an address at installation which causes a logistics penalty.

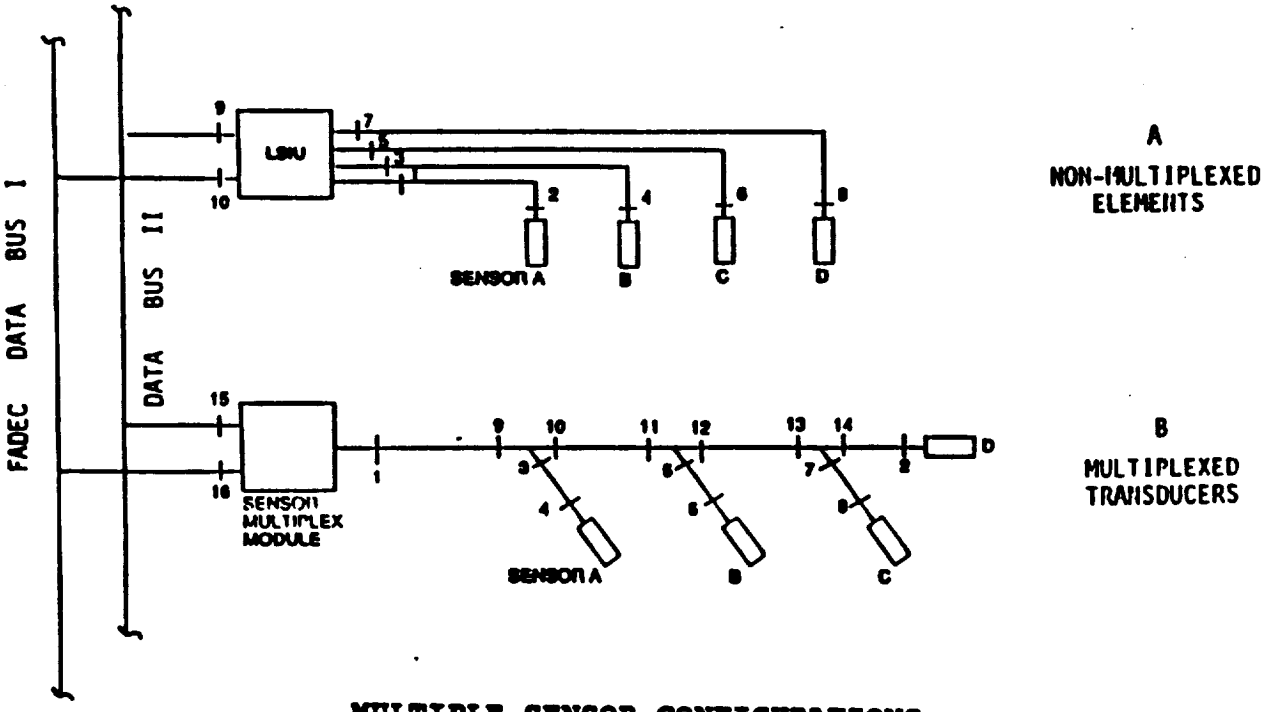

MULTIPLE SENSOR CONFIGURATIONS

FIGURE 2.1-3

Arguments of maintainability and cost support the LSIU architecture of figure 2.1-2 involving the local collection of sensor signals at an interface "concentrator" unit located at a bus node. These factors favor keeping the fiber links between transducer and interface unit short with minimal additional connections.

2.1.3 Power-by-Fiber architecture

Power-by-fiber (PBF), or Power-by-light (PBL), technology is one version of the ELDEC EL-OPTIC concept to facilitate the combining of electrical transducer advantages with those of fiber optic signal transmission. In PBL, the necessary sensor power is provided optically down the fiber, but must then be converted to suitable electrical values. The main concern is in supplying an adequate input-power level to accommodate cable losses and the opto-electric conversion efficiency. The return signal path is not technically difficult. ELDEC has an on-going program to develop this technology[3].

At the interface module the power source emitter is to be run, as a minimum, at 50% duty-cycle and must be pushed to its power limits at ambient temperatures within the module housing of 125°C for engine mounted FADEC application. It will be the most heavily stressed system component; its reliability may be a significant limiting factor to the overall system reliability.

There is a strong desire for simplicity, both within the electrical components and the cabling, in order to achieve full benefits as compared with existing electrical sensing hardware. In reference 3, five major cable architectures were identified for PBF use. From this, ELDEC has developed means to optimize the PBF function that uses only one connecting fiber line. This scheme avoids use of fiber splitter/combiner elements yet shows good overall conversion efficiency and results in lower complexity and cost than other schemes. The trick is to balance all aspects of the system for best advantage and to achieve the minimum possible electrical load.

---

[3]. Eldec doc. 011-0871-001 "Optical Fiber Transmission of Power for Electric Circuits (Power-by-Fiber), prepared by Diane Stong, Oct. 27, 1987.

At the sensor, additional circuits are needed for opto-electric power conversion. Although these are not complex, they will increase cost.

Although the EL-OPTIC concept is compatible with Power-by-Light as an alternative power source, it does not yield the same advantages as battery power. Specifically, PBL is limited by power conversion inefficiencies, cable/connector losses, and a tight optical power budget. Most such work to date has depended upon laser diodes to provide an adequate power budget but these are presently poorly suited for use at high ambient temperatures. Compared with the battery powered EL-OPTIC version, the PBL concept needs more components, and will necessarily have lower predicted reliability. Overall system development time and costs may be larger and sales price higher. However, there may still be applications for which it is an appropriate solution.

2.1.4.1 Optical Power Budget

The largest concern for PBL, the level of electrical power available to the sensor, is greatly influenced by the fiber optic cable losses. In this case, these losses are for a one way path and result mainly from the connectors. Assuming average quality 1.0 dB loss connector hardware, degraded by time, temperature and other effects, it is conservative to budget an average 2 dB loss per connection. To this must be added component service-lifetime degradation, plus system operational margin. Unfortunately, past industry experience has shown that there are likely to be excessive cabling losses, perhaps a result of cable routing, cable-ties and the like, and that in-service conditions can result in significant maintenance problems when optical power budget margins are figured too closely. The truth is that the industry does not, at this time, know what excess power budget allowance will result in a satisfactory field-maintenance experience.

Because of the power budget issue and architectural considerations, the PBL scheme will be much more difficult to configure than the battery powered version of the EL-OPTIC concept.

2.2 Candidate TDIN Sensor Systems/Architectures (Passive)

ELDEC has developed and patented (U.S. patent #4,681,395) a fiber optic sensor referencing scheme titled Time Domain Intensity Normalization (TDIN), which is capable of serving as the key ingredient or building block to numerous system architectures.

Basic TDIN Description

All sensors operating within the TDIN concept analyze the intensity of light returned from the sensor to determine the measurand; that is, all are forms of intensity modulated sensors.

ELDEC has chosen to focus its passive fiber optic sensor development efforts on analog intensity sensors for a variety of reasons. The most important is the potential for simplicity with attendant low cost, high reliability, easy maintenance, small size and low weight. Second, intensity sensors work well with low cost, broadband LED sources and large core, step index multimode fibers. Expensive, lower reliability laser diodes are not required in most cases. The use of multimode fibers in turn provides for better source-fiber coupling and simpler, more reliable connector designs. In contrast to interferometric/singlemode technology, intensity modulated/multimode technology is more mature. Third, it has been demonstrated by a multitude of investigators that essentially any conceivable parameter can be made to cause an intensity change in a multimode fiber. Through careful design, any of these mechanisms can become useful sensors. This broad applicability of intensity modulation for sensing various measurands brings forth the possibility that a single (or small set) of standard electrical interfaces can serve a large family of fiber optic sensors. Finally, unlike their digital counterparts, analog intensity sensors degrade gracefully in the presence of adverse conditions, allowing continued use.

The central significance of TDIN is that it isolates the sensor response from variations in the source power, connector losses, fiber attenuation, and receiver sensitivity. A block diagram of a fundamental single channel TDIN analog sensor is shown in Figure 2.2-1.

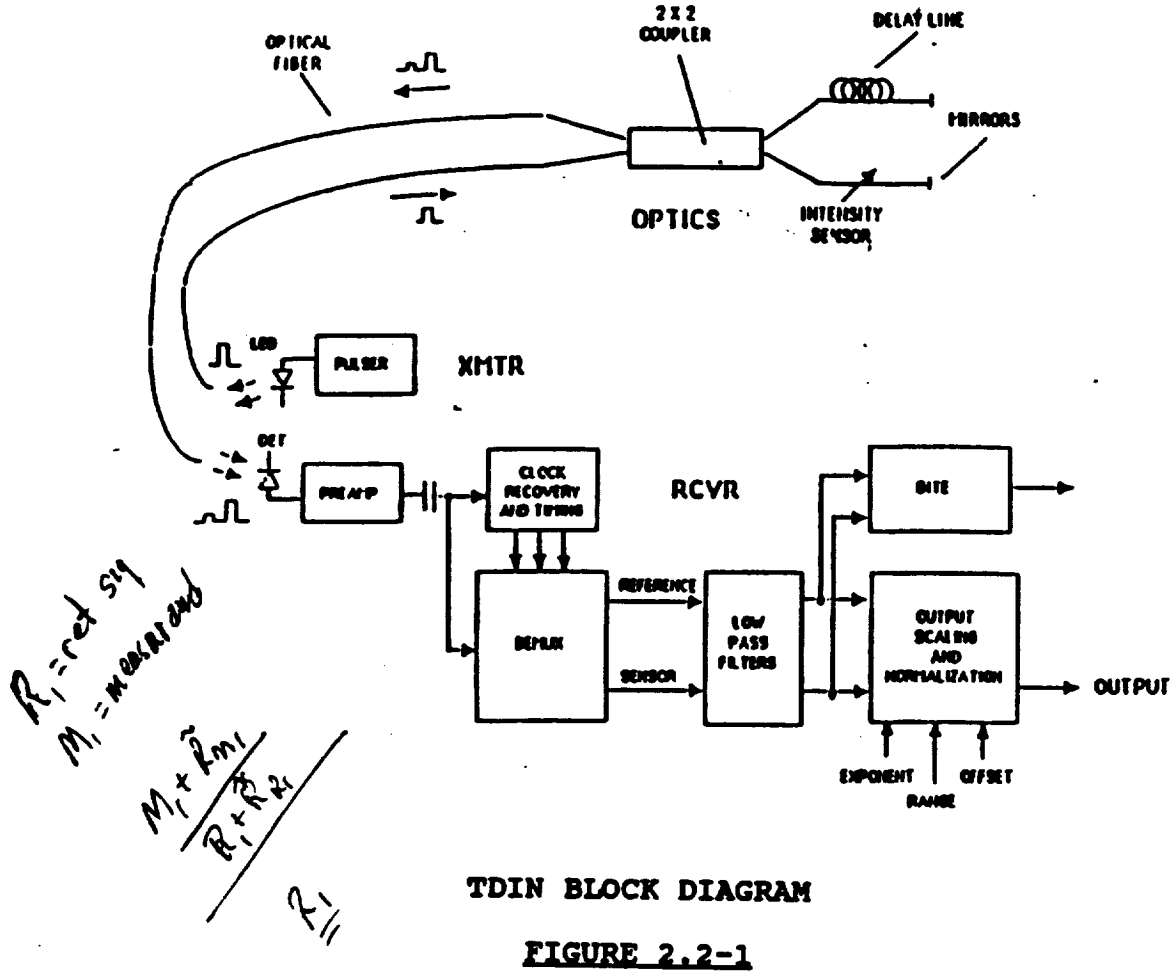

TDIN BLOCK DIAGRAM

FIGURE 2.2-1

Notice the simplicity of the concept, especially the small number of optical components. In operation, a pulse is transmitted along a fiber to the sensor, where a coupler is used to separate the pulse into two legs: a sensor leg and a reference leg. A single delay line is used to generate a delay in one of the legs. When the pulses are reflected and recombined by the coupler, two pulses propagate back to the electronics where they are separated for processing. Since both pulses are emitted from the same source, travel the same fibers and connectors out and back, and are received by the same photoreceiver, signal strength variations caused by these items are common to both pulses and are compensated when the signals are separated and divided. The ratio of the pulse amplitudes contains the sensor information.

Not only does TDIN compensate for the unwanted variations, it is an excellent solution as a common interface technique

for all analog intensity sensors. With it, a single electronics design/module can be used for numerous parameters. Integrated circuit techniques can reduce the circuitry down to one to three chips, making the circuits very simple and low cost, especially in mass production. Commonality allows greatly simplified logistics support for the sensor electronics. Also, since much of the optics is common, it too can made into a standard module. Sensor design would then be reduced to design of the sensing mechanism and packaging.

Furthermore, due to the ever-present reference pulse, TDIN has a natural built-in-test capability.

ELDEC has reduced TDIN to practice and obtained excellent performance. The delay line, coupler, and mirrors have been proven in both performance and producibility. Stability in the pulse height ratio against temperature and variations in the modal content of the multimode fiber waveguides has been designed into the system and demonstrated. Testing has shown that disconnecting and remating connectors results in a change of less than 0.1% in the output. Also, the response has been shown to vary less than 0.25% full scale range (FSR) over an optical power range greater than 12 dB, indicating good power margin and excellent link loss compensation. Because of these results, ELDEC believes that the TDIN system approach is an excellent candidate for engine control applications.

In addition to its many features, TDIN is adaptable to multiplexing. TDIN performs a sampling function of the measurements, and sampling brings the potential for (pulse-amplitude-modulation) time-division-multiplexing (PAM-TDM). Also, TDIN can be configured in combination with wavelength division multiplexing (WDM) and/or spatial division multiplexing (SDM). With appropriate attention to redundancy and reliability, multiplexing potentially offers notable benefits in weight, cost, and complexity in the FADEC box and the interconnect.

Several sensor system architectures are presented below that build upon the fundamental TDIN concept.

Overall TDIN System Architecture Description

The system configurations below are built with TDIN as the basic ingredient or building block. Seemingly, an infinite

number of system configurations are envisioned when one considers all the combinations of Spatial, Wavelength, and Time division multiplexing that are possible in transmissive or reflective "star" or "linear" configurations plus all the various modulation schemes. Many of these can be dropped due to over-complexity, poor power budget performance (loss), or other reasons of impracticality. ELDEC has attempted to filter the numerous concepts, and we believe that the following are representative.

ELDEC prefers three concepts all based on a generic "sensor multiplexer" (sensor mux) configuration. These are shown in a summary fashion by Figure 2.2-2. An electronic interface module couples the interrogation signals out to the sensor mux which directs the signals to the appropriate sensors. Each sensor is a basic TDIN-referenced sensor. The parameter-modulated signals are then returned to the sensor mux where they are combined onto a single path for return to the electronics receiver.

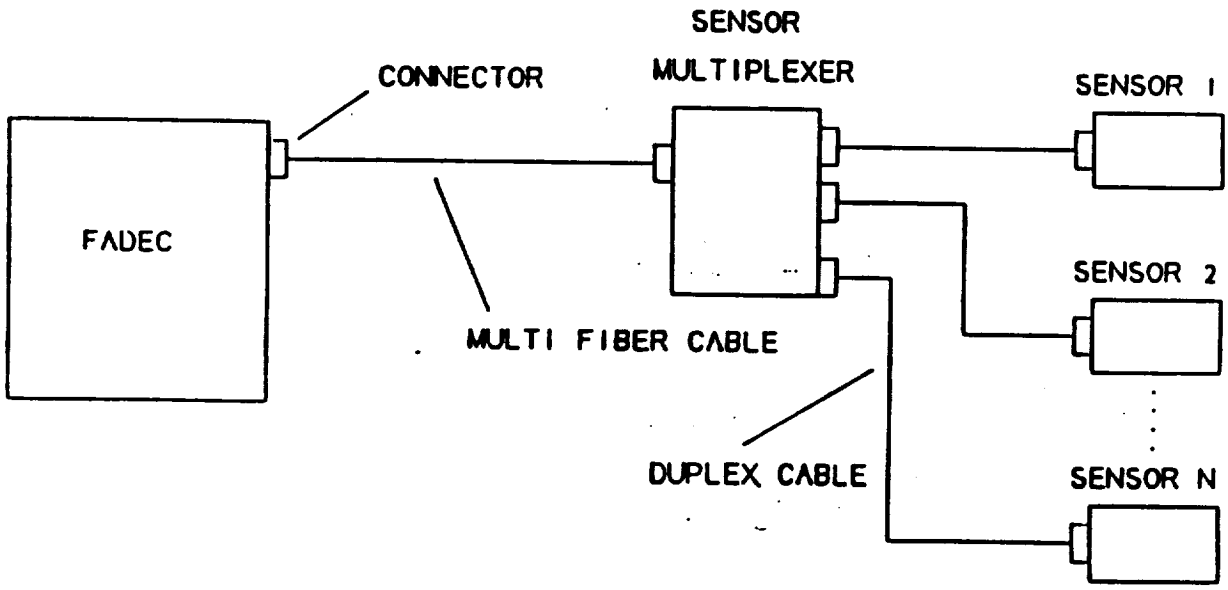

FIBER OPTIC SENSOR SYSTEM BLOCK DIAGRAM

FIGURE 2.2-2

These approaches use stand-alone TDIN sensors that are individually calibrated at fabrication and provide their own reference signal.[4] Note that the sensor mux unit can be anywhere along the fiber path - from within the FADEC, all the way to within a cluster of tightly grouped sensors such as a four-axis sidearm controller, or at any point in between.

Figure 2.2-2 is labeled to show that each fiber path to the sensors is actually two fibers - one for interrogation and the second for response. For this effort, ELDEC is describing two-fiber systems due to the problems caused by connector reflections. As connector reflections are eliminated with technology developments, then single fiber configurations are possible, with a slight penalty in optical flux budget.

As a baseline for comparison, a non-multiplexed configuration is also included in this discussion. In this case, the sensor mux is simply a fiber breakout box which only collects and distributes the signals; there is no multiplexing of any sort, and the performance as a system is that of numerous but individual sensors.

The three multiplexed configurations described in sections 2.2.2 - 2.2.4 are based on spatial (SDM), wavelength (WDM), and time (TDM) division multiplexing, in which the sensor mux takes on more interesting characteristics as described below. (Note: the terms SDM, WDM, and TDM are used somewhat loosely here. As will be seen, all use a serial format to share portions of the same electronics - hence, all use TDM. Likewise, all approaches use spatial separation of the sensors, and hence, involve SDM principles. The names have been abbreviated to designate the configuration within the sensor mux: SDM uses separate interrogation paths (separate fibers within a common cable) from the FADEC to the sensors; WDM shares the same fiber path but determines direction to the sensors based on color; TDM also shares the same input fiber path, but separates the signals in time with unique

---

[4]It is also possible to combine multiple sensors with a single reference signal using TDM. Implementation would involve an (N+1) x 2 coupler and a unique delay for each sensor. This approach would be used only with a tightly related, closely situated group of sensors, such a side-arm controller where a single package is reasonable.

time delays built into the individual paths to the sensors.)

The maximum number of sensors that can be combined into multiplexed TDIN systems is typically limited by the optical flux budget. All system discussions and characteristics below assume that "n" sensors are connected into the system, with "n" being determined by power budget calculations.

Laser diodes can be used with TDIN, provided the required signal to noise ratio (SNR) is not over a few hundred to one. Certainly the power budget over normal receiver noise will be increased and more channels can be multiplexed. However, due to modal noise with multi-mode fibers, the SNR will be limited on the other end to a few hundred. This will be the case with any analog sensor using laser diodes. For purposes of this report, specific analyses with laser diodes are not included. LEDs for which modal noise is negligible are assumed for all sources.

Overall TDIN System Architecture Characteristics

A summary of the characteristics requested in the statement of work is presented in the Architecture Characteristics Matrix table in section 2.0.

Some of the 17 characteristics can be addressed globally for all the concepts. A set of assumptions (for a single TDIN channel) for the late 1990's for all calculations is:

- o LED coupled power = +6 dBm (peak) into 100/140 micron, 0.27 NA step-index fiber, at 298 °K
- o RCVR equiv. noise resistance = 50K ohm, 50 MHz BW
- o Resolution = 100 (SNR)
- o Bandwidth = 200 Hz (noise bandwidth)
- o Connector loss = 1 dB each x 6 connectors
- o Two-fiber paths, 100/140 step-index to/from sensors
- o Customized electronics design/packaging

1. Types of Sensors - TDIN is applicable to all sensors for which a "DC" or absolute response is required. From the list in Attachment A, these include all position, temperature, and pressure sensors. The one exception is the turbine blade temperature, which may be better sensed with an approach other than intensity due to the extreme temperature. Other parameters may be possible with aspects of the TDIN interface, but would require different post-processing electronics (see section 3.2) Present status of

Eldec's sensors, in terms of meeting the requirements of Attachment A, are also presented in section 3.2.

2. Signal Compensation - As described in section 2.2, all sensors use the TDIN scheme for referencing against unknown intensity variations.

5. # of Detectors - All three multiplexed approaches use only one detector per "n" sensors due to the serial sensor/sensor-data format. The non-multiplexed baseline approach, of course, would require one detector for each sensor.

8. Power Margin - Optical power margin is a function of the number of channels combined, the response times required, plus the basic coupled power, losses, and receiver sensitivity considerations. To manage the number of variables, all calculations are based on a target power margin of 11 dB[5] at 125°C (worst case), with the result being the maximum number of sensors or channels that are possible.

9. Signal Processing Time - As suggested in the SOW, an effective time constant of tau=(1/3)*5msec is used as a typical value for all calculations. Using the approximation of bandwidth = 1/(2pi*tau), the resulting effective signal bandwidth is near 100 Hz. (The time required for A/D conversion is typically around only 40 microseconds, and is neglected.) In all calculations, we have assumed an effective noise bandwidth of 200 Hz.

It should be noted that the various mux approaches perform processing in different manners, the specific signal and noise bandwidths allotted to a specific channel may be changed. However, from a system viewpoint, the effective output signal bandwidth in all cases will be 100 Hz.

With dynamic signals (changing measurands), errors will occur from multiple causes. Their effects are additive.

> Simple analog filters will cause a dynamic error. Assuming a parameter ramp input of rate twice full scale range per second, a 100 Hz BW results in a dynamic ramp or slew error of 0.33%.

---

[5]11 dB = 3 dB repair splices + 2 dB added connectors + 3 dB connector aging + 3 dB source aging.

In the WDM and SDM cases, where each parameter is sampled once in every 5 msec. frame, the individual response times must be sped up to compensate for the increased number of channels that share the frame. Within such a frame, the parameter may have changed up to 1.0% (using the same rate example as above) between interrogations, worst case, in highly multiplexed systems. Here, the processing BW imposes a dynamic step error. For example, a time constant of 1/3 of the allotted dwell time causes a step error of 5% (exp(-3)) of the 1% step (this assumes that the previous value is retained as a starting point for the next value), or 0.05%.

Such step error is the dominant error in highly multiplexed systems; in low-level multiplexing, ramp error dominates.

This error is worsened if a sensor is the first one (worst case) interrogated in a serial group, and it has to hold its value until the whole group is interrogated, causing further lag. This lag could be as much as 1% peak for this example.

A final error is the error resulting from the time lags from the host sampling; this too could be up to 2% peak for this example. This latter error term can be reduced by more rapid sampling. This term is not considered in any response time discussion below, since it is beyond the control or the effects of the mux design.

In TDM, step error is minimized, since a new sample is taken every 1/6 MHz (6 MHz is the present repetition rate), and thus ramp error dominates.

11. Elec. power consump. - 2 watts. Due to the time-sequenced (serial) format of the sensor interrogation and the use of a single receiver (for the multiplexed systems), the power consumption is essentially constant regardless of the mux system configuration or the # of sensors. In the TDM case, as the transmitted pulse train is spread out to allow more sensors, the peak power will be increased in an attempt to maintain a constant average drive level. With the narrow pulses in the TDIN approach, the heating from individual pulses is negligible, and thus the LEDs can be average power limited without a sacrifice in reliability. This is not the

case for wide, pulse baseband schemes, for which reliability will be limited more by peak power.

For the non-multiplexed configuration, the consumption is 1.5 watts per each sensor.

15. Redundancy - This a major issue for critical flight systems, and can be handled in a number of ways. The probable best approach is to simply duplicate (triplicate, etc.) the system configurations as shown, including the FADEC, fiber paths and sensor mux, and the sensors.

16. Maintainability - TDIN, as the fundamental ingredient of a system, has excellent system maintainability features:

    1. TDIN provides a constant amplitude reference signal for each sensor that can be used for failure monitoring. Its amplitude can provide a reading of the general state of the losses through the system, and therefore, system health. Secondly, the normal intensity range of the sensing mechanism would not go to zero, allowing detection of a failure in either of the TDIN legs. Failure and/or "out of range" are easily monitored.

    2. Since each sensor is individually calibrated at the factory, sensor replacement is accomplished with a simple swap (a mechanical rigging adjustment may be required).

    3. The FADEC electronics is a standard interface that works identically for all "DC" intensity sensors. A set of offset and/or slope and # of sensors adjustments may be needed depending on the variety of sensors that are attached to it, although ideally, all sensors would have common characteristics. The benefit is simplified logistics support.

    4. The sensor mux is configured with connectors such that it can be a replaceable unit although the elimination of these connections would improve the power margin.

17. Availability of Components - The status of the ELDEC TDIN concept and intensity sensors is described in more detail in section 3.2. In summary, improvements are needed in source power, receiver sensitivity, connector losses and reflections, electronics bandwidths, fiber NA, and coupler performance to fully take advantage of the strengths of TDIN. Not surprisingly, the status of TDIN components is

heavily dependent on the status of the technology of the parts that we have available to use in our designs, which in many cases, is the same for all sensors approaches.

The status of the components needed for configuration in the three suggested systems is much the same as for a single sensor. The additional components required are the couplers in the sensor mux units (broadband in two cases and spectrally selective in the WDM case). Also, in the WDM configuration, wavelength stable LED-type sources are required that are suitable for the aerospace environment. It is important that these components exhibit low loss and high power, and are built to withstand the environment.

The characteristics given/used represent the late 1990's time frame. At this writing, the basic TDIN and additional system components (sensors and sensor mux units) could be available within a year or two, although the number of sensors that could be multiplexed would be slightly reduced from the 1990's estimations due to power margin considerations. Errors achieved would also be increased slightly due to coupler drift and connector reflections. ELDEC plans to develop a custom IC chip-set for the electronics by the early 1990's.

The specific system configurations are described in the following sections. The 17 characteristics questions that were not addressed globally above are addressed in the specific sections below.

2.2.1 Baseline Configuration

Description

The baseline configuration, as mentioned previously, is envisioned as the sensor mux box being a "breakout box" which serves only to pass the fiber paths directly to the individual sensors. Each sensor communicates with its unique FADEC interface and has its own fiber path. This configuration is included in this report only for comparison purposes; no figure is shown. In actuality, the "breakout box" may not exist; the paths could route directly to sensors. (For analysis, the "breakout box" is assumed to have no connectors.)

Refer to Figure 2.2-1 for a single optical channel of such a system. 100/140, 0.27 NA fiber is assumed for the interconnect.

Characteristics

3. # of Channels - 1 sensor per electronic interface.

4. # of Sources - 1 per sensor

6. # of Fibers - 2 per sensor

7. # of I/O pins - 2 per sensor

8. Optical power margin (@125 °C) - 29.4 dB PIN, 36.5 dB APD

10. Complexity - per sensor: 1 transistor (LED driver), 1 LED, 2 custom IC's, plus misc. R's and C's

11. Elec. power consump. - 1.5 watts per sensor

12. I/O area - 4 sq. in. per sensor

13. Weight - Electronics: 4 ounces per sensor. Cable weight is to be based on (duplex) 100/140 fiber for each sensor.

14. Reliability - approx. 53,000 hrs. MTBF -- per sensor, including the LED. This value will be reduced for this approach and all those below if an APD is used due to the high voltage stresses.

2.2.2 Spatial Multiplexing (SDM)

Description

The spatial multiplexed configuration is depicted in Figure 2.2-3. Separate fibers are coupled to the sensor mux, one for each sensor. Within, they are coupled straight through to the individual sensors. The parameter-modulated signals are returned from the sensors to the sensor mux where they are passively recombined in a broadband coupler and sent back to the electronics receiver.

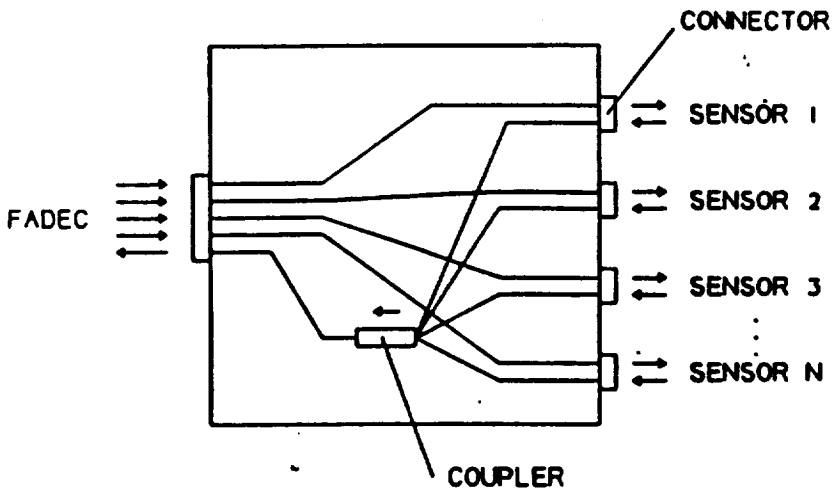

TRANSMISSIVE CONFIGURATION

SDM SENSOR MULTIPLEXER

FIGURE 2.2-3

Within the frame of the system update rate, each sensor's source transmits TDIN pulses for approximately the system rate divided by the number of sensors that are combined. Each sensor is sequentially scanned in this manner. Note that a single transmitter clock, detector and receiver front-end are multiplexed through all sensors within the system. In the electronics, the controller that switches the sources also switches the A/D and respective receiver output drivers or latches. The electronics can be switched quickly and the TDIN receiver can lock onto a new sensor pulse train in approximately 10 microseconds. Thus, very little percentage of SNR is lost due to overhead. The receiver dwells on (filters) the pulse train for each sensor's time interval, converts, and then places the data into the respective sensors's output latch.

The response time of the receiver for the individual channels is a function of the number of channels that are processed. For example, if "n" sensors are sequenced within a 5 msec. frame, then the response time of the electronics must be no greater than (1/3)*(5msec/n) for the signals to settle before performing a conversion. However, considering the sensors as a group, the overall effective response time remains unchanged.

Note that an option to the sequencing of sensors within a system frame is the interposition of pulses within a TDIN sample frame (presently approx. 6 MHz / # of channels). This is what is being done necessarily in the TDM approach below. Synchronization of the transmitter LEDs must consider the path delays within the installation, which is a compromise with logistical flexibility. The analysis results below assume this method is not used.

This approach assumes the use of 100/140 fibers to the mux unit and to/from the sensors. The fiber returning from the mux unit to the receiver is assumed to be 200/230, 0.37 NA fiber. The mux unit uses an asymmetric coupler.

Characteristics

3. # of Channels - (@ power margins below) with PIN: 18
   with APD: 49

4. # of Sources - 1 per sensor

6. # of Fibers - at FADEC: # of sensors + 1

7. # of I/O pins - # of sensors + 1

8. Optical power margin (@125 °C) - 11.1 dB PIN, 11.0 dB APD

10. Complexity - (# of sensors)*(1 transistor + 1 LED) + (3 custom IC's + misc.)

12. I/O area - (# of sensors)*(0.5 sq. in.) + 4 sq. in.

13. Weight - Electronics: (# of sensors)*0.5 ounce + 4 ounces; Cable weight: to be based on duplex 100/140 cable.

14. Reliability - MTBF estimation based on parts count increase: 53,000 hrs. - (# of sensors) * 1000 hrs. (See section 2.2.1)

2.2.3 Time Division Multiplexing (TDM)

Description

The time division multiplexed configuration is shown in

Figure 2.2-4. It is different from the spatial case in that here there is only one source that powers all the sensors. Its pulsed power is sent to the splitter in the sensor mux, where the power is split into the individual sensor's interrogation path. Each path has a delay built into it that delays the respective pulses into time-spaced time slots. These delayed pulses are finally modulated by the sensors and returned to the sensor mux, combined in a broadband passive coupler, and sent to the receiver for processing.

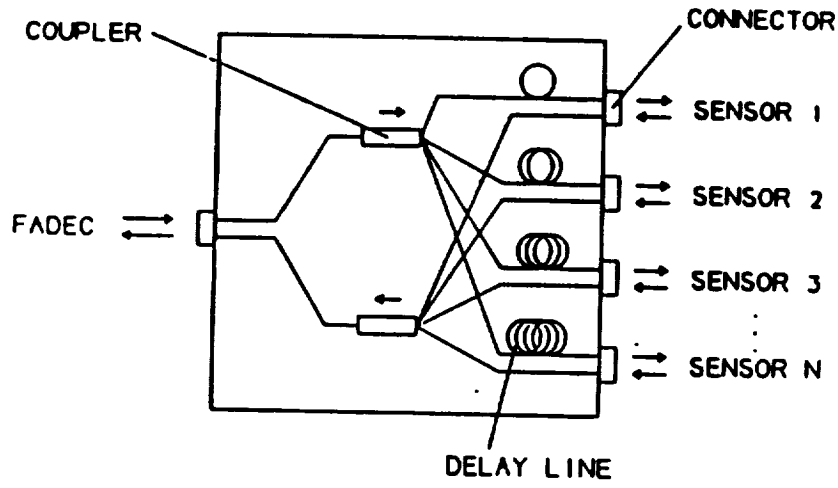

TRANSMISSIVE CONFIGURATION

TDM SENSOR MULTIPLEXER

FIGURE 2.2-4

Of the three concepts, this system approach is the most similar to a basic TDIN scheme. The transmitter is identical, the only change being that the duty cycle is reduced to allow the interposition of multiple time slots for the increased number of sensors. The receiver is also similar, except that more waveform sampling gates are needed, two for each sensor in the system.

The pulses are a serial train of the various sensor's reference and measurand signals. Data synchronization is based on the same principle for multiple sensors as for a single sensor. Following the input amplifiers, the clock is recovered and used to demultiplex the signals into their respective time slots for processing.

The response time required for this approach is a little different than the SDM approach above. Since all the channels are interposed within the TDIN repetition rate (presently 6 MHz / # of channels), there is no significant intra-frame dynamic step error problem from sampling; the primary limitation will be dynamic ramp error.

To assure the pulses fall into the correct time slots, the length of the delay lines must consider the delays of the existing fiber paths within the installation; the sensor mux is therefore installation dependent. This is a potential disadvantage of the TDM approach.

This approach assumes the use of 200/230, 0.37 NA fibers to/from the mux unit, and 100/140 fibers to/from the sensors. The mux unit uses asymmetric couplers.

Characteristics

3. # of Channels - (@ power margins below) with PIN: 7
   with APD: 15

4. # of Sources - 1

6. # of Fibers - at FADEC: 2

7. # of I/O pins - 2

8. Optical power margin (@125 °C) - 11.0 dB PIN, 11.2 dB APD

10. Complexity - (1 transistor + 1 LED + 3 custom IC's + misc.)

12. I/O area - 4.5 sq. in.

13. Weight - Electronics: 4.5 ounces; Cable weight: to be based on 200/240 duplex cable.

14. Reliability - MTBF approx. 53,000 hrs, including the LED. (See section 2.2.1)

2.2.4 Wavelength Multiplexing (WDM)

Description

Referring to Figure 2.2-5, an approach is shown for the combination of sensors using wavelength division multiplexing in the path to the sensor mux. Within the sensor mux, this approach appears to be similar to the time domain approach with the passive couplers replaced with wavelength-tuned devices and the delay lines removed. In terms of FADEC operation, however, this approach is actually more similar to the spatial approach. Within a frame, multiple LED sources at different wavelengths are activated in sequence at approximately the system rate divided by the number of sensors. During each transmitter's interval, that transmitter emits a train of TDIN-type pulses that are coupled out through a combiner in the electronics to the sensor mux. There, the respective color is directed to the appropriate sensor, parameter modulated, and returned to the sensor mux for combination to the return fiber and sent to the electronics receiver. The receiver operation is identical to that of the spatial approach, including the response times required.

This approach assumes the use of 100/140 fibers to/from the mux unit and to/from the sensors.

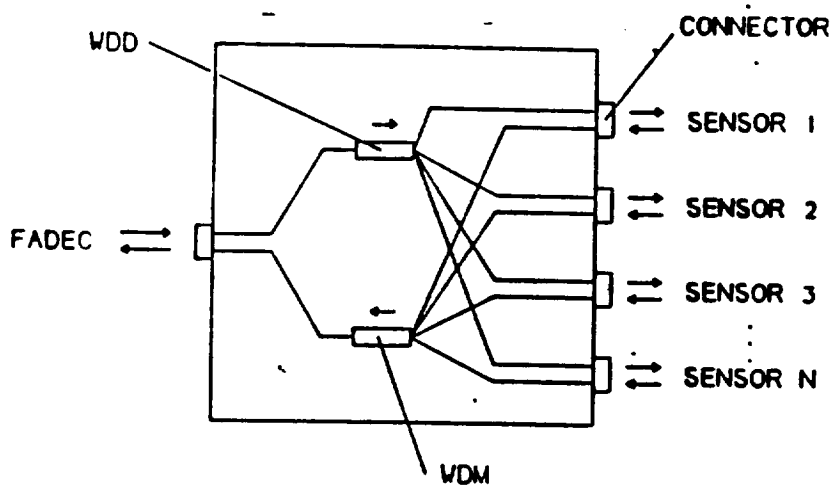

TRANSMISSIVE CONFIGURATION

WDM SENSOR MULTIPLEXER

FIGURE 2.2-5

Characteristics

3. # of Channels - (@ power margins below) with PIN: 4
   with APD: 10

4. # of Sources - 1 per sensor

6. # of Fibers - at FADEC: 2

7. # of I/O pins - 2

8. Optical power margin (@125 °C) - 12.5 dB PIN, 11.3 dB APD

10. Complexity - Optical WDM + (# of sensors)*(1 transistor + 1 LED) + (3 custom IC's + misc.)

12. I/O area - (# of sensors)*(0.5 sq. in.) + 4.5 sq. in.

13. Weight - Electronics: (# of sensors)*0.5 ounce + 4.5 ounces; Cable: to be based on 100/140 duplex cable.

14. Reliability - MTBF estimation based on parts count increase: 53,000 hrs. - (# of sensors) * 1000 hrs. (See section 2.2.1)

3. SENSOR AND SYSTEM DEVELOPMENT ISSUES

3.1 EL-OPTIC

The present flight service implementation of the EL-OPTIC concept is a non-contacting limit switch function called a "proximity" switch. This device weighs 67 grams plus 12 grams of mounting hardware. Present cable per Boeing specification BMS 13-59 weighs 3 grams per meter.

3.1.1 Development Risk

Each of the sensors for position, pressure, temperature, and fuel flow has been developed through proof-of-concept demonstration. Also a sensor for detecting lubricant debris (chip detector) has been demonstrated. These sensors will be modest extensions of familiar technology, mainly a repackaging effort, and therefore the risks of successful development to meet all specification requirements are quite low.

To take these sensors to flight-quality brassboard form for operation up to 130°C will realistically require about a two year effort, given suitable funding. At this temperature level, all necessary components are available today in flight quality. Development of each product with little further research is required. We would probably choose to design the circuits in ASIC form.

The EL-OPTIC sensors are expected to have development and production costs modestly greater than equivalent present day electrical sensors. In addition, the sensor interface module should be modestly more expensive than similar present hardware. In both cases, additional components compared with traditional sensing are the LED and IDP, but the usual electrical line driver/receiver protection devices have been eliminated.

3.1.1.1 Battery issues

A suitable battery is critical to the EL-OPTIC concept. A survey of the technology has highlighted the lithium thionyl-chloride cell as the most promising candidate for immediate applications to 130°C. Advanced solid-state cells

are also becoming available that are useful to 200°C.

ELDEC Sensing Systems Division has an ongoing test program designed to evaluate and apply this lithium cell technology to advanced sensor concepts. A 5500 hour continuous exposure test at +130°C under service load has been completed on a limited sample size. An 80°C continuous exposure test has logged 11,000 hours. Other tests are planned. Data from these tests provide information required for detailed specification of these cells and define the operational envelope for the advanced sensors. Cell quality assurance provisions and source inspection requirements are also being determined during this program.

Test results support the prediction that these lithium cells will operate in this type of application for over 20 years without maintenance [6].

The lithium primary (non-rechargeable) battery cell has gained acceptance with commercial aviation and military customers where it is used for computer-memory backup power and as primary power for diverse applications such as field communication sets and missiles. The lithium cell contains no strategic materials and uses only a small amount of lithium, which is both inexpensive and abundant. This technology, new in the last twenty years, is being aggressively developed by a dozen manufacturers. There are many types of lithium cells distinguished by internal chemistry, size and construction. The type proposed for sensor use is a small cell with the lithium thionyl-chloride couple. This cell supplies a constant 3.5 to 3.7 volts throughout its life and over the -55 to +130°C temperature range. Among its important features are a high capacity and high performance, very low rate of self discharge leading to very long storage life, hermetically sealed package with no leaking or venting, and safety when damaged, crushed, shorted or heated.

This cell design has been extensively tested by the manufacturers, the Military and Underwriters Laboratory, Inc. and proven to be safe and reliable. ELDEC has also developed a method of prolonging useful life in low power applications beyond industry expectations.

---

6. ELDEC Doc. No. 011-2870-308, "Application of the Lithium Battery to Self-Powered Sensors", Jan 1987

An analysis of military aircraft, missile, shipboard and other similar potential applications shows these environments to be less severe in some ways than commercial aviation where total flight hours are much greater. The new generation of solid-state battery designs will extend the useful temperature limits as the technology matures and can be expected to keep pace with the capabilities of electronic circuits.

Battery MTBF calculations per MIL HDBK-217E can not be made because batteries are not listed in that document. Such calculations would require extensive performance history from the specific type of battery and environment anticipated by the subject application; such data are not available. However, to provide some indication of MTBF, a rough model of the lithium electrochemical system was developed based on the hermetically sealed solid tantalum capacitor per MIL-C-39003, style CSR. The result, reported in reference 5 (presented without comment on its validity), showed 4.6×10^6 hours MTBF for the fighter aircraft environment (AUF).

3.1.1.2 High Temperature Circuit and Transducer Development

Several sources detail the need for development of electronic circuits and of various sensors which are operable at much higher temperatures than are presently achievable.[7] [8] [9] [10] [11] [12] Operation over the range -60°C to

---

[7]. L.J. Palkuti, et al.," Integrated Circuit Characteristics at 260°C for Aircraft Engine-Control Applications," IEEE Trans. on Comp. Hyb. and Manuf. Tech., Vol CHMT-2, No.4, Dec '79, pp 405.

[8]. W.C. Nieberding, et al.," High Temperature Electronics Requirements in Aeropropulsion Systems," IEEE Trans. on Industrial Electronics, Vol IE-29 No. 2, May '82 pp 103.

[9]. M.D. Marvin," High Temperature Electronics Technology, Phase II - Final Report," GE Aircraft Engine Business Group, R83AEB637. Contract No. N00173-79-C-0010, May '84, pp 1-4.

+300°C is needed within 10 years, with some specialized sensor-heads operating to much higher temperatures. Several ELDEC studies[13], have centered on high temperature electronic and packaging technologies.

It is reasonable to extend the present EL-OPTIC sensor temperature limit to 175°C based on work done at ELDEC TCO on high temperature electronic circuits and packaging, and the latest information on battery and LED capabilities. Future developments are expected to facilitate extension to 300°C service temperature without great compromise of reliability or service lifetime. Research required to develop circuits suitable for use at higher temperatures would include the following areas of concern:

- Electronic circuits: dielectrically isolated silicon circuits can be developed for up to 200°C use. Gallium

---

[10]. Kreitinger, et al., "Full Authority Digital Electronic Control, Phase II - Final Report," R82AEB435, Contract No. N00019-76-C-0423, Oct '83.

[11]. G.L. Poppel et al., "Fiber Optic Control System Integration - Final Report," NASA CR-179568, R87AEB111, Contract No. NAS3-24624, Feb '87.

[12]. Problem Statement: "Fiber Optic Sensor Development With Standard Sensor Interface," 7J7 Fiber Optic Design Build Team, BCAC, Feb 4, 1987.

[13]. Eldec Memoranda; GAK85-23, "High Temperature Electronics Study Report," June 23, 1985.

GAK85-33, "High Temperature Electronics Study Report Part II," Sept 25, 1985.

TDR85-10, "Additional Information on High Temperature Electronics," Oct 1, 1985.

LCW87-4, "High Temperature Gallium Arsenide Packaging," Feb 6, 1987.

LCW87-7, "High Temperature Hybrid Circuit," Mar 20, 1987.

arsenide, needed for reduced leakage current at higher temperatures, is suitable to at least 350°C and has been proposed for ELDEC use to 300°C. Silicon carbide shows promise to 650C[14], but is a long way from practical reality.

- Hermetic enclosure: a concept suitable for a connectorized sensor enclosure format is being developed. This concept is compatible with development for high temperature applications.

- LED: extrapolation of published data shows satisfactory operation (for the EL-OPTIC application) to 200°C. Use at temperatures to 300°C is promising but must await further packaging development and testing.

- Magnetic materials: Curie temperature limits apply. Most projected designs avoid the use of any magnetic materials, or employ only those having capability above 300°C.

- Wire: the HML nickel coated copper magnet wire is rated to 220°C continuous and has been tested to as high as 300°C. For use with the EL-OPTIC concept (no self heating), 300°C seems acceptable.

3.1.2 Position Sensing

Recent proprietary advances in our present proximity switch technology will assist ELDEC in development of the desired higher temperature transducers for limit switch and proportional position sensing. With these advances, temperature effects become of second order importance, thus extending the useful temperature operating range. This concept accommodates rotary position as well as linear position sensing over both short and long ranges and can be applied to many actuator and valve position sensing applications. It is a viable replacement for the LVDT position transducer.

---

[14]. SCIENCE NEWS, vol. 132, page 390, article discussing high temp semiconductor limitations of 200°C for silicon circuits, 250°C for silicon sensors, and 650°C for silicon carbide.

An EL-OPTIC 6 inch stroke linear position sensor will weigh about 200 grams. The target and associated rod weigh 20 grams.

3.1.3 Pressure Sensors

An ELDEC subsidiary, Transducers Inc., is presently manufacturing pressure transducer elements in the ranges from 700kPa up to 8000kPa which operate to above 150°C. Since these devices are exposed to 500°C during their fabrication, there is not thought to be any fundamental technical reason that they can not be further developed to meet the top temperatures required by the subject applications. This technology fits well with the EL-OPTIC concept; no technical obstacles are foreseen.

3.1.4 Temperature Sensors

The standard RTE temperature elements per MIL-T-24388B are compatible with the EL-OPTIC concept for use over the range -54°C to +500°C.

The turbine blade temperature measurement is best done with a pyrometry technique. This can be accomplished by means of a suitable optical fiber probe connected to an EL-OPTIC sensing element having a bandpass optical filter.

The light off detector requires an optical fiber probe (sapphire) feeding the ultraviolet light to a special filtered detector.

3.1.5 Fuel flow Sensors

Eldec Corp. builds a full complement of true Mass Fuel Flow systems. The advanced, motorless versions are compatible with our EL-OPTIC concept, with improved EMI performance. A proof-of-concept model of suitable sensor electronic circuits has been built and no technical problems were found.

3.1.6 Other Sensors

Our lubricant debris "chip detector" is a proportional readout device capable of responding to and grading the presence of permeable chips (and chromium flakes) down to 10 milligrams in size. It has 100% coverage of the flow through a 1/2 inch tube, and operates in a high temperature environment. This device does not remove or trap the chips,

but performs only the sense function.

Eldec Corp. has not yet investigated EL-OPTIC versions of rotary speed, vibration, or fluid level sensors.

3.2 TDIN

This section discusses the status of TDIN and presents technology improvements required by the 1990's time frame to achieve its full capability as a building block for enhanced system configurations.

In the late 1980's, TDIN is showing promising results as a high accuracy reference scheme for analog intensity sensors. Testing has shown that accuracies of better than 1% are possible over greater than 10 dB of optical signal range. A sensor temperature range of -55°C to +200°C (for a short interval) has been demonstrated with small temperature coefficients. The electronics is operational from -55°C to 125°C with approx. 15 sq. inches of board area using standard components. However, improvement is still envisioned, and it is the technology as a whole (its components, standards, etc.) that must be given attention.

Fiber optics technology is maturing nicely for the telecommunication sector, but is not yet mature for the aerospace sector. Many performance needs are related to harsh environmental issues. To meet all the objectives of the late 1990's, technology developments are needed to address a few fundamental issues:

3.2.1 Optical Power Margin

Higher power LED-type sources are needed to provide more power margin for increased versatility in system configurations. Sources with broad spectral width (>10 nm) are necessary to minimize modal noise to better than (the equivalent of) 12 bits.

Receiver configurations and sensitivities need to improve. The aerospace industry needs an integrated PIN detector/preamp that has a wide thermal range and also has high sensitivity on the order of 50K ohms or better NEP in a 100 MHz or greater bandwidth.

Correspondingly, connector losses must be reduced. Aerospace installations are (so far) connector-intensive and

connector losses have been the dominant source of loss. In every case, power budget is a critical issue, and interactively limits resolution, response time, configuration versatility, temperature range, power consumption, etc.

Multimode fibers need to have higher NA's to allow higher source coupling and better resistance to bending losses. As a closely related issue, TDIN uses a delay coil, and to design smaller sensors, a smaller diameter is preferred. However, bending losses are temperature-dependent, and a tighter coil will have a higher temperature coefficient unless a corresponding higher NA is used.

3.2.2 Connector Reflections

Low-reflection connectors are required to attain full accuracy over any possible variation of interconnects. TDIN has a slight sensitivity to connector reflections in that the resulting small spurious signals act as error or noise sources. A pair of normal-reflection connectors can contribute as much as 0.5% of steady-state error.

If connector reflections are reduced sufficiently, single fiber architectures are conveniently possible, reducing interconnect complexity by 50%.

3.2.3 Couplers

TDIN presently uses a coupler to establish a separate path for the generation of the reference signal. In the future, such a reference could come from an in-line partial reflection, but much development is necessary for this technique to approach the performance of the coupler method.

TDIN performance at this time appears to be limited by the fused coupler's splitting ratio sensitivity to temperature and modal input variations. To maintain 1% accuracy, the coupler's contribution must be a fraction of this -- but some types have shown splitting ratio drift of close to 5%. Modal conditioning can solve the modal sensitivity, but this is invariably achieved at the cost of optical power loss. Both modal and temperature response can potentially be improved with more "geometrically" based coupler designs.

The present size of fused couplers is also a problem. Their packaged length of 1 to 1.5 inches is restrictive in the design of small sensors.

The long term temperature range of couplers (approx. -55°C to 125°C) is the limiting factor in the capability of the TDIN optics. (The fibers and other optics are capable of operation near 400C). With fused couplers, the limitation is a result of the epoxies used. To attain 200°C or higher operation, packaging must be improved.

For system configurations, a wider range of couplers is required. These should include symmetric and asymmetric couplers with ranges of 1x2 up to NxN. Presently, the best couplers are fused 2x2, although new approaches are appearing.

3.2.4 Electronics

A custom chip-set is needed for TDIN to reduce the electronics area. It is important that these chips be designed to operate at the +125°C temperature found on engines. A vision of two custom IC's shows one analog chip for the receiver front-end and one for the transmitter and other digital/switching functions. A third chip may be appropriate as a controller for multiplexing functions. The present TDIN electronics is capable of 125°C operation, but uses discrete IC's and occupies approximately 15 square inches (one sided).

The source/detector/preamp issues were mentioned above. In addition, TDIN performance will be improved with higher bandwidth circuits. Higher bandwidth results in better immunity in all aspects of timing error including delay line length mismatch. Also, as frequency capabilities improve, shorter delay lines are possible, resulting in better sensor thermal stability and smaller size.

3.2.5 Interconnect Reliability

A serious limitation to any fiber optic installation aboard aircraft will be the reliability/maintainability of the connectors and the cable. See section 3.3.

3.2.6 TDIN Summary

In response to the specific requirements listed in Attachment A of the 50W, 1% or better accuracy over temperature is presently a challenge, but we are optimistic that it can be improved with time. The primary present cause of this difficulty is coupler stability over

temperature. +/-2% is achievable now with careful selection of components.

3.2.7 Position Sensors

To date, ELDEC has concentrated its TDIN efforts on position sensors, and two approaches have been used with different advantages. The first, Macrobending, is an intrinsic concept which cannot be contaminated by dirt and moisture in the optical path. Its limitations are ripple in the response (on the order of +/-1%), and some sensitivity to modal variations. The other concept uses a unique "neutral density" variable transmittance analog code plate, which is an extrinsic approach that have excellent linearity and virtual independence of modal variations.

As of this writing, both of these approaches have demonstrated good results, but optimization is still required. The main concern is sealing against environmental effects. Some improvement in linearity and power loss is still desirable.

3.2.8 Temperature Sensors (except Turbine blade)

TDIN is well suited to the measurement of temperature. ELDEC has not yet developed temperature sensors, and specific mechanisms are not chosen. Some possible concepts include using the differential change in core and clad refractive indexes to provide a NA change within a macrobending coil biased in a sensitive region, a variable gap approach with a bimetallic mirror, a temperature-dependent refractive index cladding, microbending, or fixed end gap with a variable-index gap-fill to modulate the optical distance.

The temperature ranges in Attachment A are of concern (+350C), but once solved, there is nothing inherent in the use of intensity concepts that prevents TDIN from being used. The challenge will be temperature probe design.

3.2.9 Pressure Sensors

TDIN is also directly applicable to the measurement of pressure. ELDEC has not yet developed pressure sensors, and again, specific mechanisms are not chosen. Presently envisioned concepts are the use of bellows expansion/compression against a macrobending coil, and

microbending or end-gap modulation with a diaphragm.

As with temperature sensors, the temperature ranges in Attachment A are of concern (+350C), but once achieved, there is nothing inherent in the use of intensity concepts that prevents TDIN from being used. It is a matter of pressure probe design challenges.

3.2.10 Other Sensors

TDIN is most useful with parameters that are "DC" in nature. Considering Attachment A, these are the sensors that are discussed directly above.

The other sensors on the list of Attachment A can also be configured with the TDIN approach (TDIN would provide a sampling function of the parameters), but since they are "AC" in nature or measure relative event timing or event rate, other interface approaches are more suitable, at least as far as single channel sensors are concerned. However, when considering system issues, it may make sense to modularize the interface to allow aspects such as the transmitter and the receiver detector and amplifiers to be common and shared by any and all similar and non-similar sensors but have different post-processing units. This approach would allow the use of multiplexed fiber paths as well as the electronic front-end sections for any variety of sensor types. The post-processing units would be serially switched in conjunction with the type of multiplexing used.

This issue must be resolved by evaluation of the logistics and reliabilities involved. If non-similar sensor types are combined in this way, then the total numbers of electronic front-ends, connectors pins, and fiber paths are reduced; if separate interfaces are used, the advantage will be generally simpler (although more of them) individual interfaces.

3.3 Needed technology developments - general

3.3.1 Interconnection Development and Testing

A considerable developmental effort is necessary to arrive at better concepts for aircraft fiber optic wiring practices, especially for engine application. These concepts will need to be given a thorough shake-down by the

engine and airframe manufacturers culminating with in-service flight testing.

3.3.2 Interconnection Tool Kit

A simple tool kit is needed for handling all fiber optic interconnection tasks. This should require only low cost, uncomplicated, hand held devices requiring minimal calibration so that functional tools can and will be made available at remote locations or can be carried on the aircraft.

3.3.3 On-aircraft Repair Methods

Effective means are needed to determine the location and the nature of fiber optic cable/harness/connector defects. Present OTDR devices have been designed for telecommunications use and are unsuited, as well as being much too expensive, for aircraft use.

APPENDIX D–1

LITTON POLYSCIENTIFIC WDM EOA

FIBER OPTIC WAVELENGTH DIVISION MULTIPLEXING SENSOR TECHNIQUES IN AIRCRAFT ENGINE CONTROL SYSTEMS

Preliminary Report

Presented to

United Technologies Research Center

by

Poly-Scientific Division
Litton Systems, Inc.
1213 North Main Street
Blacksburg, VA 24060

9 August 1988

TABLE OF CONTENTS

1.0 INTRODUCTION

This report covers information pertaining to the design of fiber optic sensors that are based upon wavelength division multiplexing (WDM) techniques. Information is provided for rotary and linear position sensing, rotary speed sensing, and pressure and temperature sensing. Rotary position, linear position and rotary speed sensing design information is outlined in detail. The design of the devices for measuring temperature and pressure is not shown for proprietary reasons. However, adequate detail such as power budget, required spectral bandwidth, sensitivity, and certain electronic interface detail is given.

The relationship between sensor and electronic interface design is discussed. Several concepts for sensor multiplexing architectures are also presented.

The list of 17 questions presented as a part of the data requirements has been addressed.

2.0 SENSOR CONCEPTS

Rotary and linear position, rotary speed, pressure and temperature sensors will be considered here. Fluid level sensing does not seem tractable using the proposed system, and although it may be possible to attack the problem of light-off detection and fluid flow, implementation using an interface of the type discussed here seems nontrivial.

2.1 Rotary & Linear Position Sensor Design

One way of accommodating variations in optical power level due to source degradation, fiber loss variation, connector variations, and so forth, is to use a digital system which allows fluctuations in signal level so long as the levels corresponding to "on" and "off" states straddle the line representing the comparator threshold. Litton proposes use of such technology for rotary and linear position and rotary speed.

2.1.1 Reflective Approach

In Litton reflective position sensor systems, one optical fiber serves as both injection and pickup for the optical system. The injected light is collimated by the GRIN lens and dispersed by the grating. A chromatically dispersed stripe of light is then focused onto the code tracks by the same lens. Where there is a reflective track, the light is reflected back into the lens. It then propagates back through the optical system to be refocused into the fiber. The returning light contains wavelength band digital information concerning the relative position of the lens and code plate.

Figure 2-1 shows the elements of a reflective position sensor system. This system consists of a broadband source, a power splitter, an optical demultiplexer, and the detection and decoding circuits. The interface is

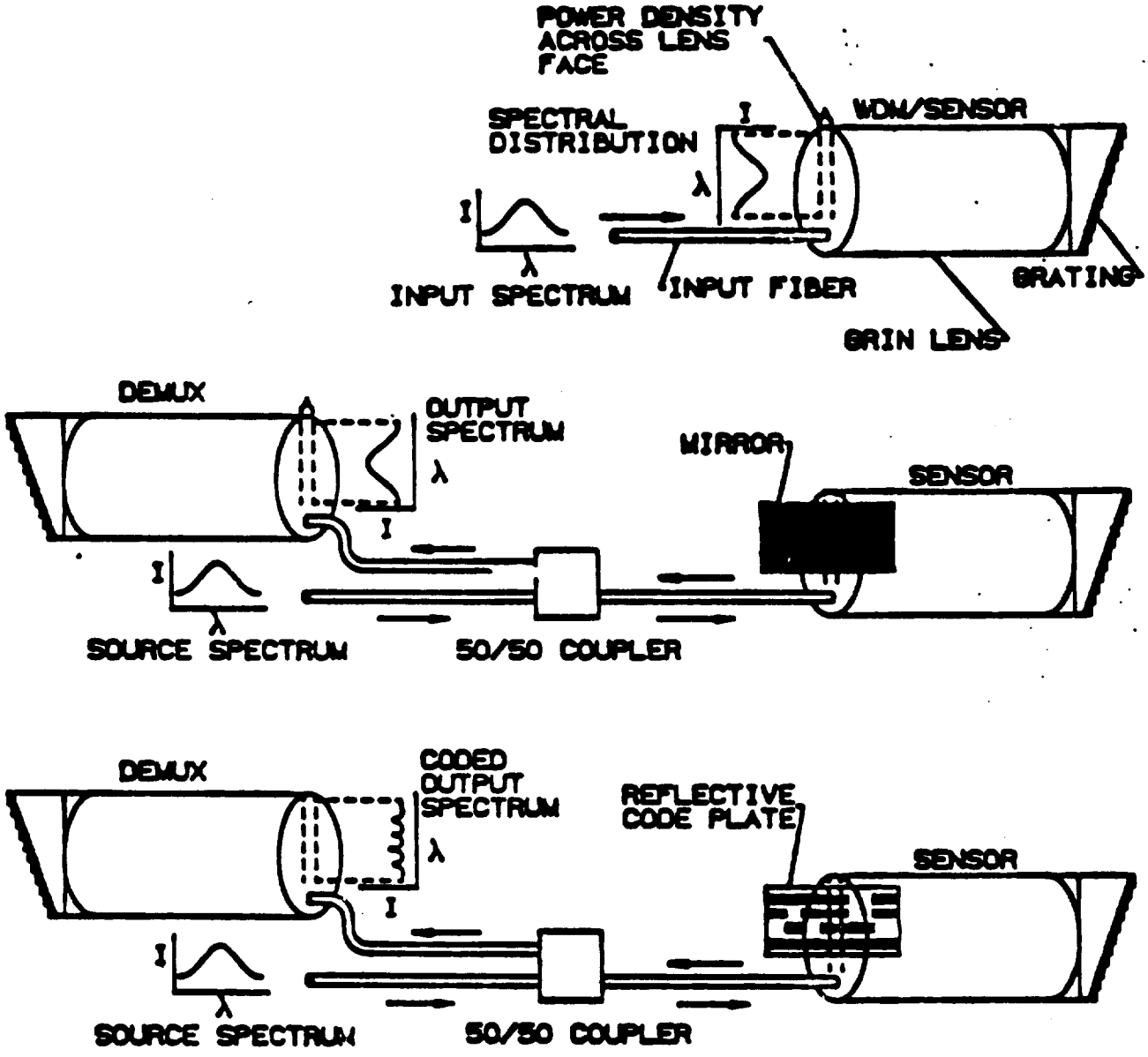

SCHEMATIC ILLUSTRATION OF BROAD BAND ENERGY BEING TRANSMITTED THROUGH A WDM SYSTEM

FIGURE 2-1

generally located some distance from the sensor. In the configuration shown, the power splitter is located with the interface electronics and a single fiber connects the sensor. In some cases, it may be desirable to use two fibers to connect the sensor to minimize connector back-reflections, in which case the power splitter wouuld be packaged with the sensor.

Figure 2-1 also illustrates in a stepwise fashion the manner in which broadband energy is transmitted through the system. One method of producing a broadband (700 nm to 900 nm) source is to combine the output of multiple LEDs. A white light source is another means of providing energy in the 700 to 1000 nm region. However, serious consideration may not be given to this type of source for applications that require the sensor interface to be mounted in a high vibration and high temperature environment.

It can be seen from the diagram that the source spectral width must be adjusted to accommodate the number of reflective tracks and guard bands on the code plate. More than one LED may be required to illuminate a ten bit code plate with guard bands. When considering the design of a code plate, a minimum track width must be maintained to insure that a detectable power level is reflected to the demultiplexer. Guard bands must be scaled to minimize crosstalk between channels while holding excess loss to a minimum.

Photodiode arrays or discrete photodiode receivers with the appropriate pre-amplifier and post-amplifier circuits are used to detect signals coming from the optical demultiplexer. Trade-offs between detection techniques are made in terms of size, sensitivity, stability with temperature, dynamic range, and circuit complexity. Standard decoding circuitry is used to translate the Gray code pattern into a binary output.

Figures 2-2 and 2-3 show current Litton linear and rotary sensor designs.

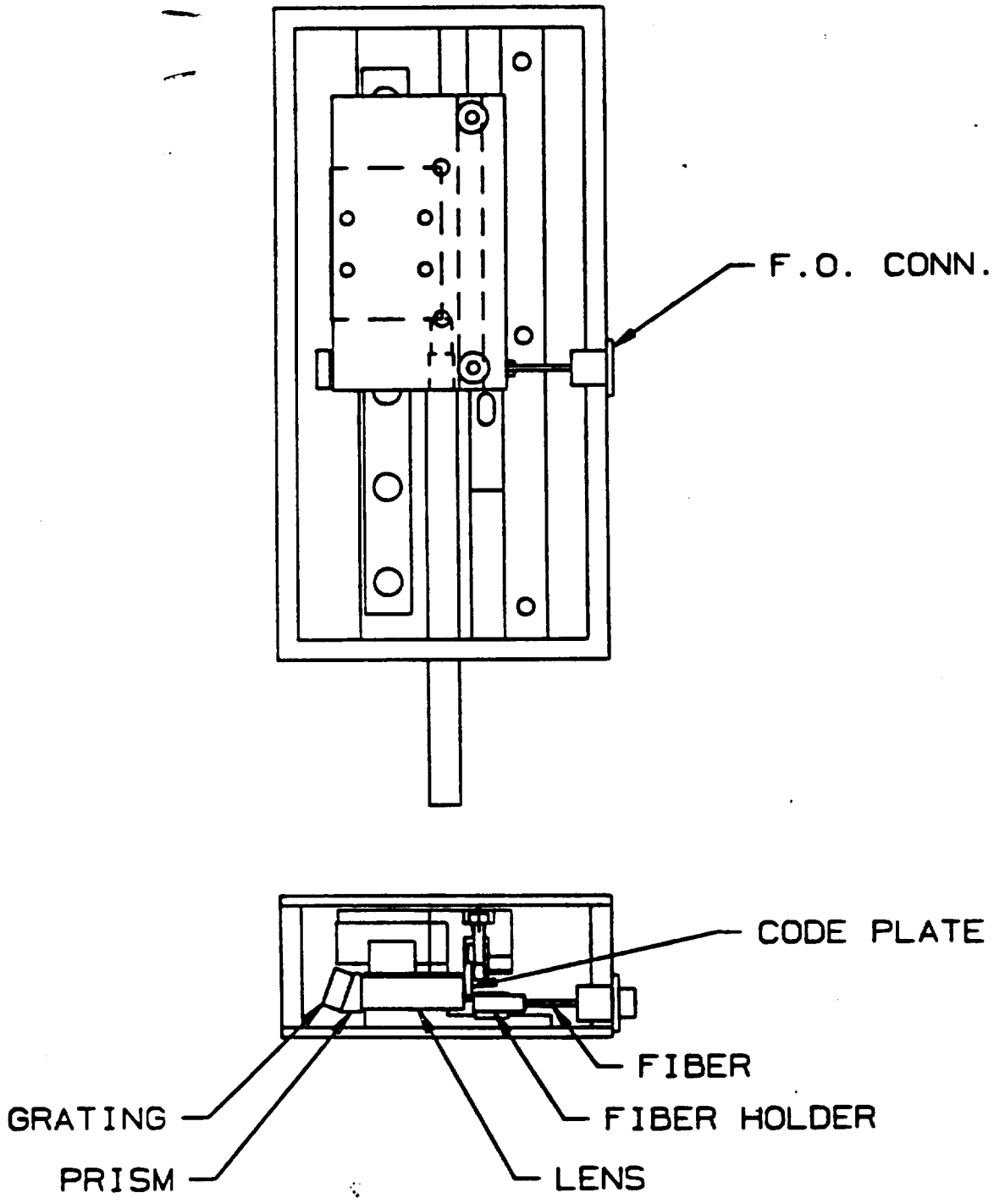

FIGURE 2-2 Litton Linear Position Sensor

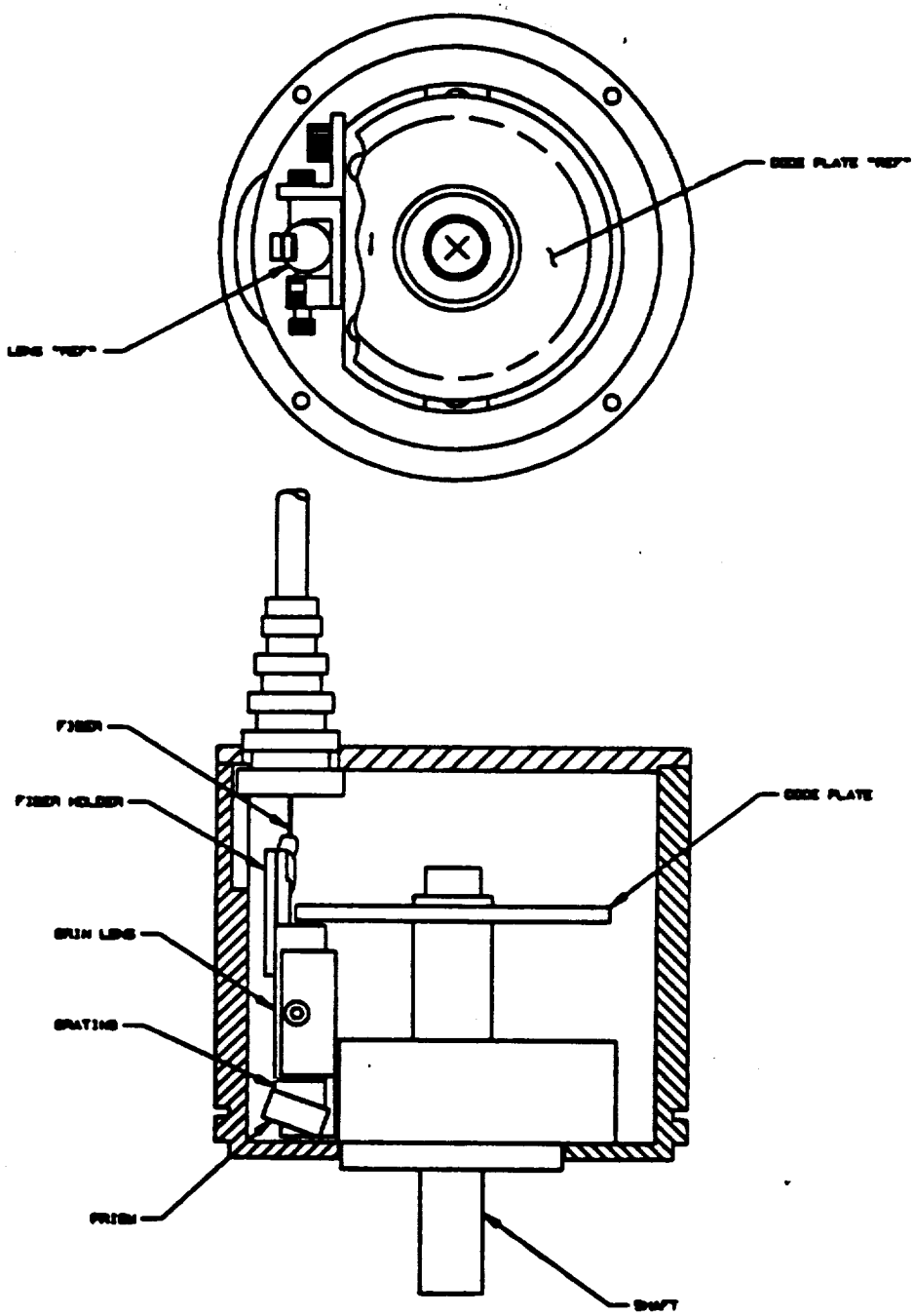

FIGURE 2-3 Litton Rotary Position Sensor

2.1.2 Transmissive Approach

A disadvantage of the single fiber position sensor concept is the sensitivity of the system to light reflected back through the fiber by connectors and the internal optical surfaces of the sensor. This problem may be overcome by using a transmissive code plate and a two fiber system, as shown in Figure 2-4. Rather than reflecting the light, the code plate allows the light of interest to be transmitted into another lens-prism-grating assembly, which refocuses it into a second fiber. This approach will increase the on-off ratio from 10 dB to over 20.

2.2 Rotary Speed

Rotary speed is sensed using a simple concept (see Figure 2-5). Light is transmitted from an optical fiber through a lens and onto a rotating surface. As the surface rotates, reflective areas pass through the focused spot causing intermittent reflection. The frequency of the returning waveform is proportional to the speed of the wheel.

A two fiber rotary speed sensor is constructed using two lenses and a transmissive wheel with intermittent opacity which causes the light path to be interrupted at a rate proportional to the rotation of the wheel. This output signal may be interpreted by an interface identical to that used for the reflective approach.

2.3 Pressure, Temperature (Analog Sensing)

The greatest difficulty encountered in multimode analog sensing is how to deal with source and system degradation without suffering loss of accuracy. Once a calibration curve is established, any change that occurs in connector and fiber loss, any change in LED output power, or a change in detector Figures

FIGURE 2-4
Transmissive Encoder Concept

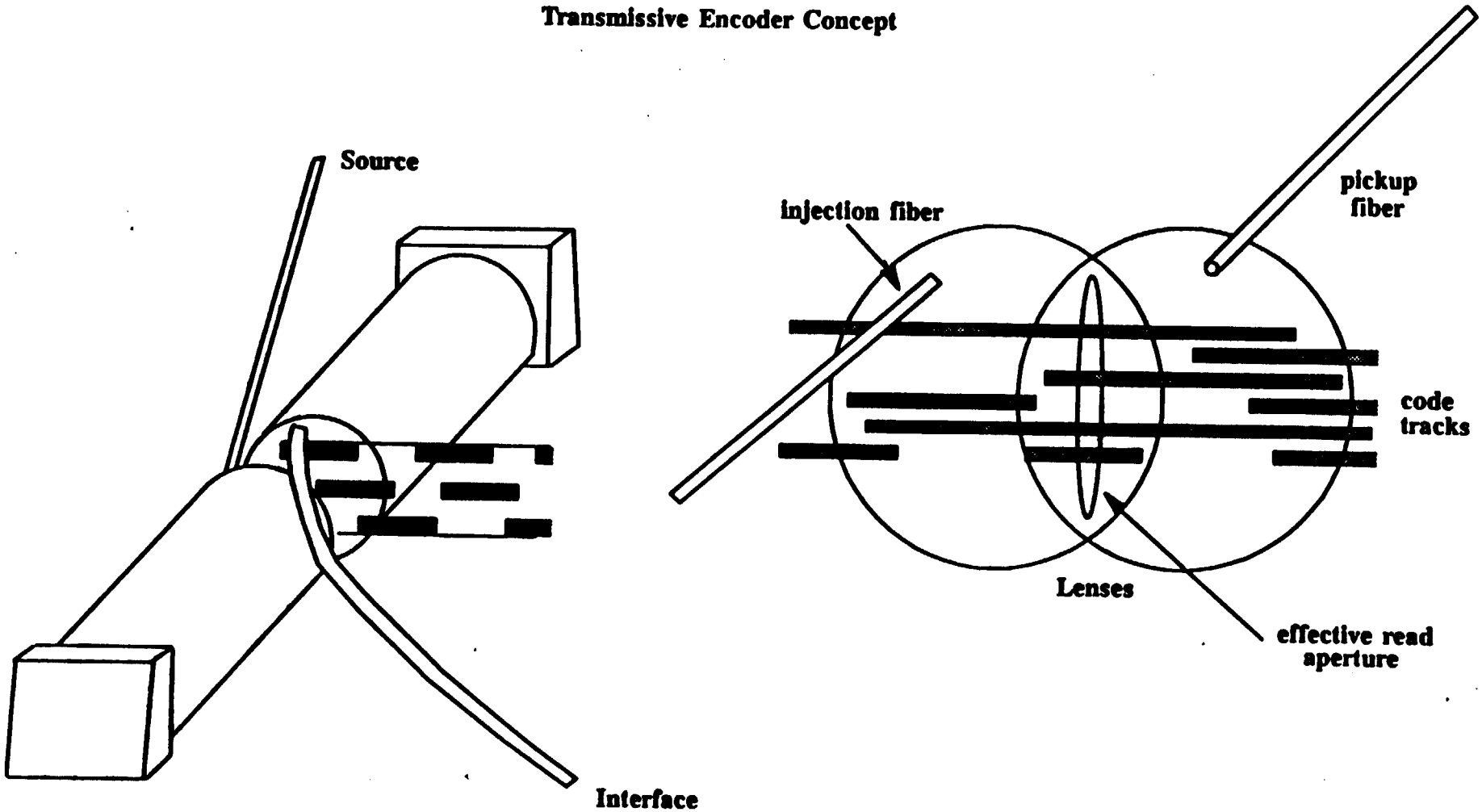

Light is injected by a fiber into the first lens prism grating assembly, which focuses a dispersed stripe into the code plate. The light of interest is then transmitted rather than reflected, and encoded information is launched into the pickup fiber.

FIGURE 2-5
Rotary Speed Sensor

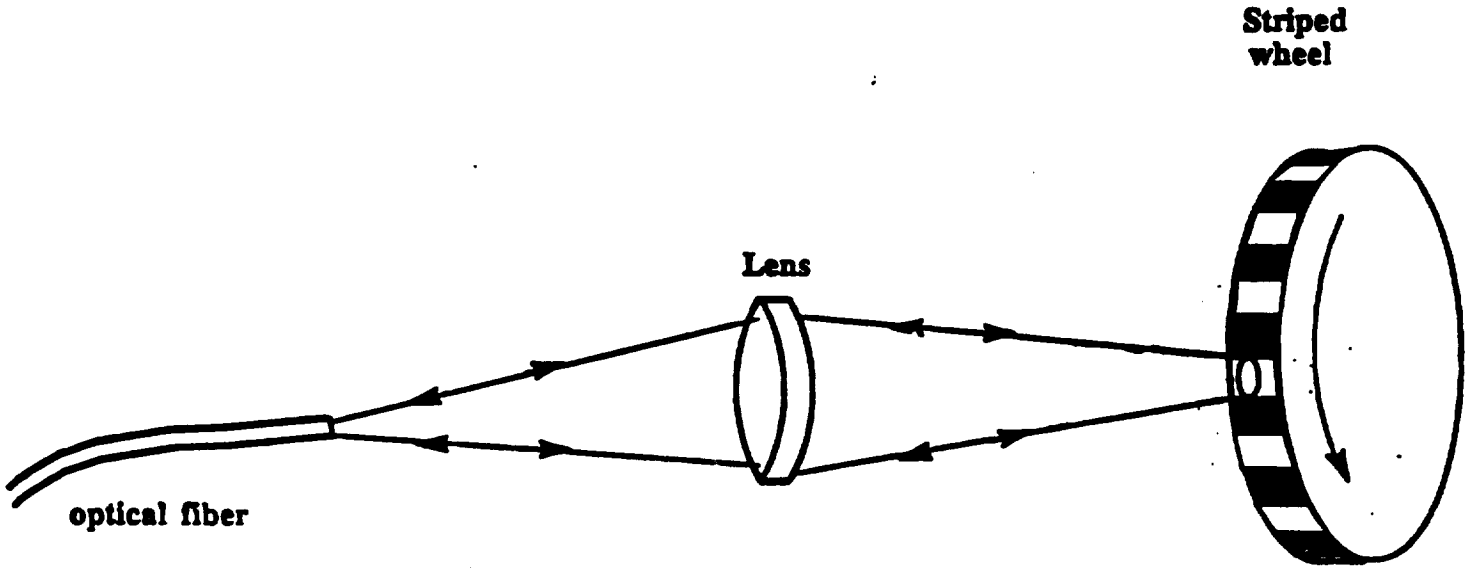

When the light focused onto the wheel encounters a reflective area, it is returned to the fiber and propagates through it.

sensitivity, is interpreted as a change in the measurand. However, it is possible to deal with this problem by using an appropriate reference scheme.

Most of these problems result in a multiplicative effect on the signal - a signal twice as great suffers twice as great a change in power level. This problem may be remedied by using sensors which output two optical levels to compensate for system changes.

The information provided in Figure 2-6 was collected from a WDM based device that addresses the problem of component drift. This device is based on a technique that compensates for LED drift in output power, changes in detector sensitivity, and changes in system optical attenuation. A translation of about one half core diameter yielded a change in output of approximately 40 dB. By modifying the device slightly, this output range can be made to correspond to a movement of one core diameter, or about .002" for 50 micron fiber. This is roughly the linear range of the device, and pressure and temperature changes must be transformed into linear motion of this magnitude.

In one-fiber systems, problems associated with connector backreflection are to be minimized.

2.3.1 Pressure

The sensor concept described above may be used to sense pressure, if a diaphragm is used to actuate the device, as shown in Figure 2-7. The mass of the linkage used to connect the diaphragm to the sensor device should be minimized.

2.3.2 Temperature

The fiber optic temperature measurement techniques discussed here take three forms: optical pyrometry, sensing thermal expansion of some material,

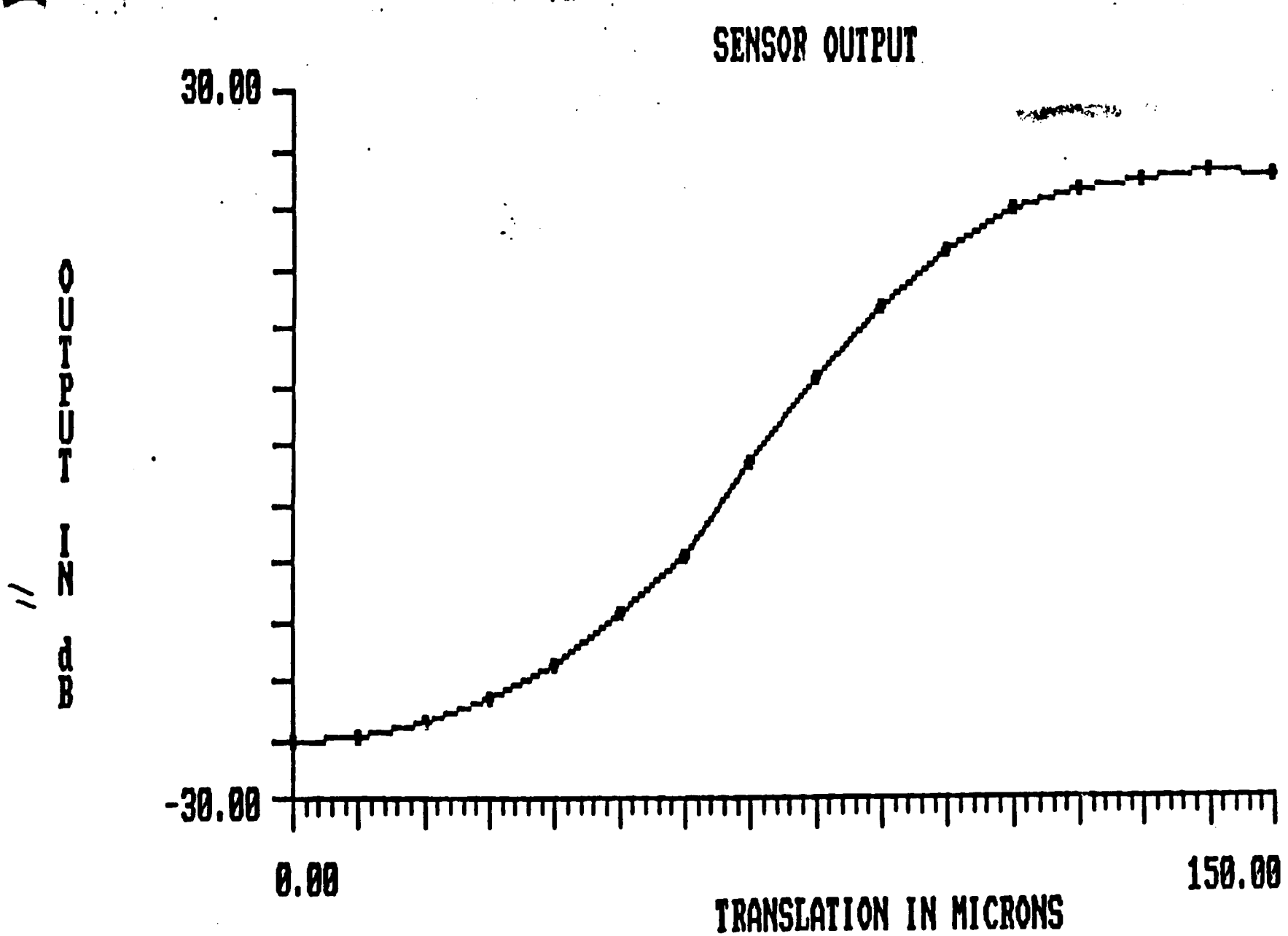
SENSOR OUTPUT
30.00
-30.00
OUTPUT IN dB
0.00
150.00
TRANSLATION IN MICRONS

FIGURE 2-6

FIGURE 2-7
Pressure Sensor Concept

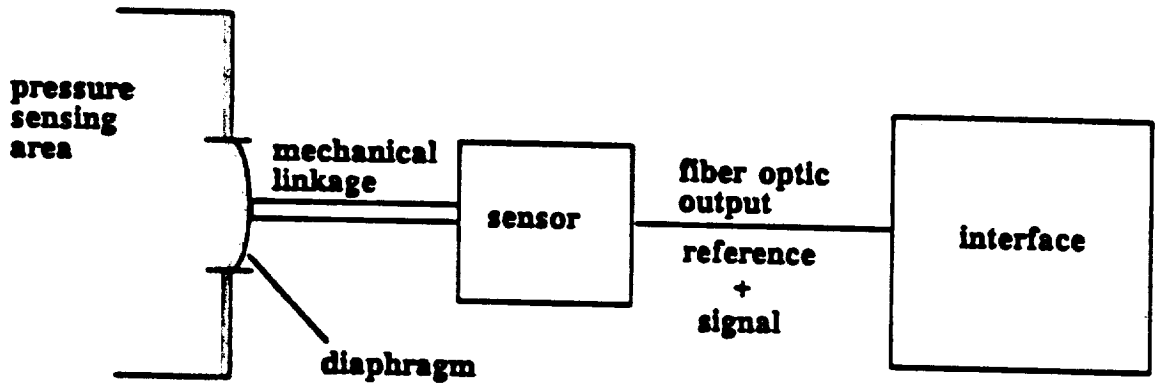

A pressure sensitive diaphragm provides the .002" to .004" movement required by the sensor system depicted in Figure 9A.

and temperature dependent optical properties of thin films. Each of these techniques is best suited to its own temperature range.

Optical pyrometry is shown in Figure 2-8. The relative intensities at different temperatures is given by Planck's blackbody radiation laws, modified by the specific nature of the materials involved.

Figures 2-9 and 2-10 show temperature sensors which operate using thermal expansion of some material. The setup pictured in Figure 2-9 uses the expansion of a rigid rod. The amount of movement which results is dependent on the length of the region subjected to the temperature and the thermal expansion coefficients of the materials involved.

The system pictured in Figure 2-10 uses an hydraulic system to provide the actuation. These hydraulic systems can be designed to provide movement of up to .050" or so over a couple of hundred degree range. The device required in this sensor system needs to have a travel of only .002" to .004".

2.4 Meeting UTRC Requirements

2.4.1 Linear Position

All of the linear position sensing requirements specified by UTRC have $\pm$ 1% accuracy. This translates into a total accuracy range of 2%. Code tracks are added for each binary bit of accuracy required. The 2% range requirement falls between 5 bits (2.125%) and 6 bits (1.5625%). Therefore each linear transducer can be accommodated using a 6 track code plate. It should be noted that the code plate has a better resolution than required by the application. This difference can be used to add stability to the interface circuit. The difference between the code plate accuracy (1.5625% and the accuracy required by the application (2.0%), or 0.4375%, can be used to set a differential electrical threshold between a state coming on and a state going off. Rather

FIGURE 2-8

Fiber Optic Pyrometry

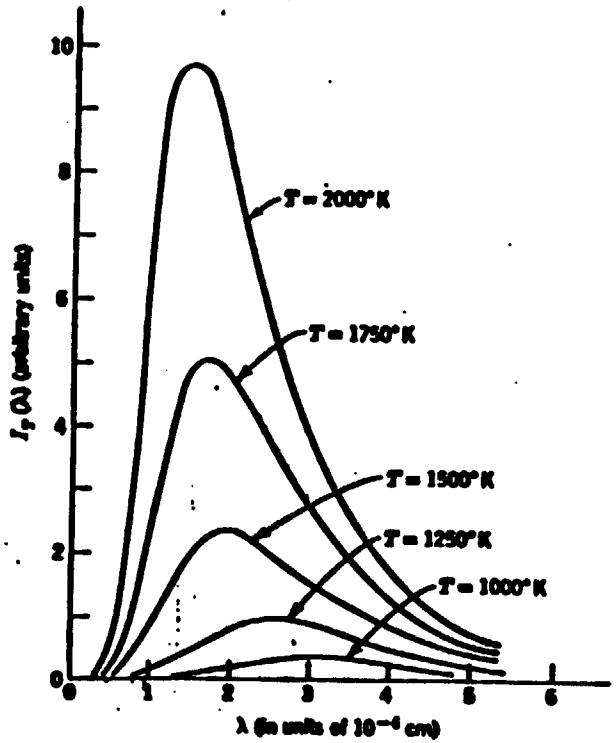

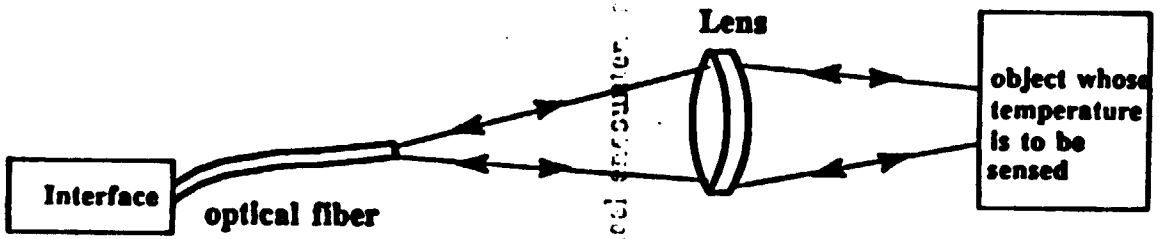

Radiant energy emitted by the object is collected by a lens system and transmitted through an optical fiber, where an interface system compares the power levels at two different wavelengths (pictures λ_1 and λ_2 - 1.1 and 1.8 microns).

FIGURE 2-9
Thermal Expansion of Rod

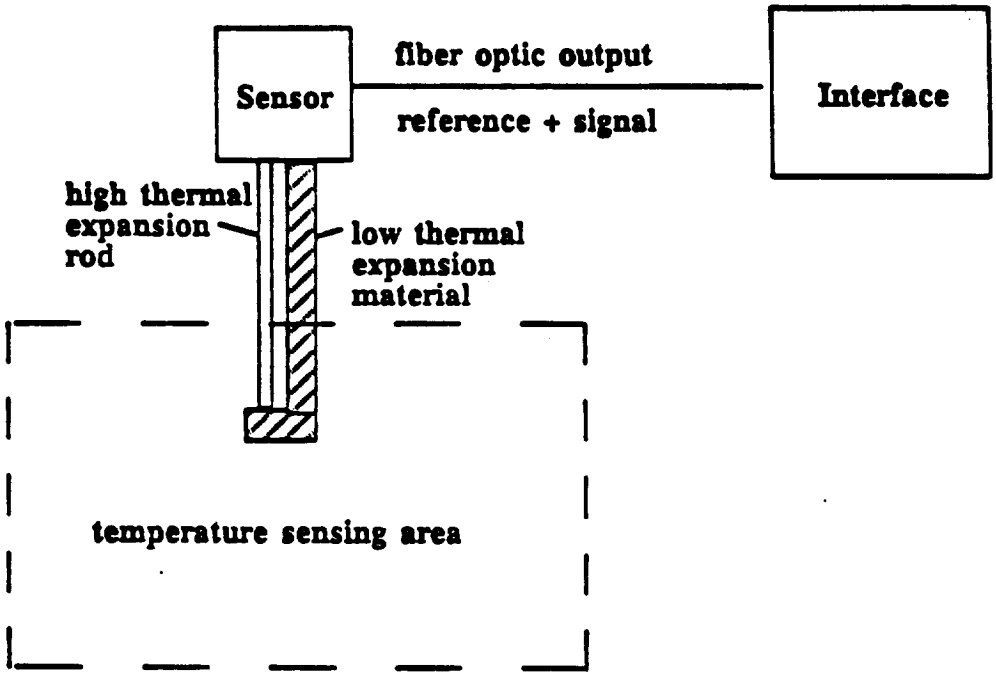

A movement of .002" can be expected to result from a sensor bar length of 1", given a 200C range. The resulting output can be analyzed in the interface by ratio of power at λ_1 to that at λ_2 .

FIGURE 2-10

Fluid Reservoir-Type Temperature Sensor

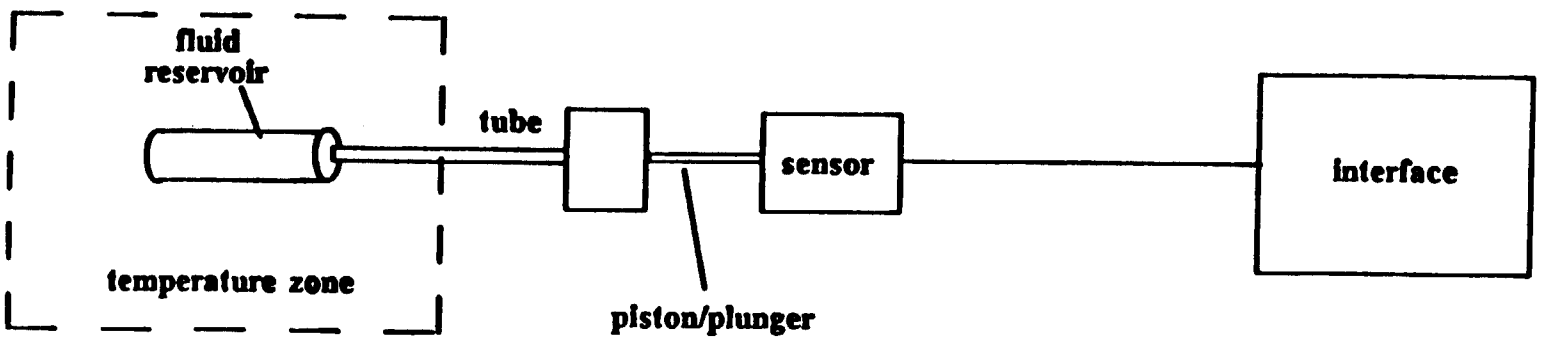

Thermal expansion of a fluid causes movement of a piston, which is attached to the output fiber. The resulting wavelength shift can be sensed in the interface by taking the ratio of the power at two different wavelengths λ_1 and λ_2 .

than having a single threshold which makes the least significant bit indeterminant for sensor positions right on the threshold, a differential threshold creates a range which must be traversed in order to change states. As long as this traversed range is less than 0.4375% the accuracy required by the application (2%) is not degraded.

The minimum length of a reflective code track in the position sensor is 1.5 core diameters. Shorter tracks result in poor optical modulation, compromising the function of the device. Without the use of a multiplier technique (see Section 3.2), this minimum track length is the same as the minimum state length.

The tightest accuracy specification indicated in the FADEC sensor table (Appendix 1) is $\pm$ .05 cm, or 500 microns. Full accuracy is therefore 1 mm. This poses no problem with either 100 micron or 50 micron core fiber.

Six tracks require a source spectral width of 80 nm using 50 micron core fiber, and 155 nm using 100 micron core fiber.

2.4.2 Rotary Position

The accuracy required of this sensor is $\pm$ 0.15%. This can be accommodated by a 9 bit device. Such a 9-bit device may be obtained in two ways.

The first way is to use 9 code tracks. Assuming 50 micron core fiber, this requires a code plate radius $\geq$0.666 inches. The optical bandwidth requirement is 110 nm.

The second way involves the use of a multiplier technique. By making two duplicates of the finest track and reproducing each out of phase with the original, the resolution can be increased by a factor of 8. This increases the number of tracks required to 10, but allows the reduction of the code plate

radius to 0.333". The optical bandwidth required with this technique is 115 nm, assuming 50 micron core fiber.

2.4.3 Pressure

A stainless steel diaphragm can easily give the required 2-4 mil. movement over the given ranges, as shown in Figure 2-7. A 40-50 dB range of output must correspond to the full pressure range. This is no problem, given the sensitivity of the wavelength modulation device and the pressure ranges specified in the table. The accuracy specified (best = $\pm$ 0.4%) requires recognition of a .15 dB change in ratio.

The time constants indicated by the table (some as fast as 3 ms) do not appear to be a problem. Manipulating the diameter and thickness of the diaphragm to obtain fast response time must be combined with damping to minimize ringing.

2.4.4 Temperature

Both of the thermal expansion based sensors discussed here have the disadvantage of high thermal mass. Time constants on the order of a second are to be expected from such devices, and it is not obvious how to decrease this value to the 7 to 40 ms required here.

Optical pyrometry is suitable for the turbine blade temperature sensor (500-1500°C) requirement. Accuracy may or may not be a problem - further testing is required to determine this.

Another possible method of sensing temperature involves the use of thin films whose optical properties vary over the temperature range of interest. These films would be amenable to the same analog technique to eliminate dependence on connector loss and/or source degradation. Such sensors would

require the development of special materials having optical properties tailored to the specific sensing application. If such technology were used, the sensor could be remoted from the high thermal inertia optical systems, and much faster time constants could be expected.

2.4.5 Rotary Speed

If 10 reflective zones per revolution are used, a device capable of registering 650 to 19000 $\pm$ 7 rpm with an update time of 10 ms is no problem. Discrete detectors are required, however, as the CCD circuitry is unsuitable for applications involving frequency counting.

3.0 INTERFACE

The interface system consists of an optical system and an electronic system. The two will be considered separately below.

3.1 Optical System

The optical system consists of a light source subsystem and a detection-demultiplexing subsystem.

3.1.1 Light Source

LED's, either alone or in banks, are believed to be the most promising light source to be used with these sensor designs.

Optical power budgets (see Section 4) are the major determining factor in the selection of fiber diameter for use in these devices. Fiber diameter, in turn, determines the required spectral width of the sources to be used in these systems.

Six bit digital sensors using 100 micron core fiber require about 155 nm of optical spectral width per device to function. At least two LED's must be combined to give such a width.

If fifty micron core fiber can be used in these sensors, however, only about 80 nm is required. This can be supplied by a single LED.

Analog sensors require only about 30 nanometers each if they are 100 micron core devices, and 15 if they use 50 micron fiber. A single LED can power two to five of these devices.

3.1.2 Optical Detection

The optical detection system may be one of three different configurations, two of which involve the use of a CCD array and the other of which uses a WDM

with discrete detectors. The simplest CCD system uses a single fiber, lens-prism-grating assembly, achromatic lens assembly (1:1 projection system), and a linear CCD array (see Figure 3-1). A sort of optical spectrum analyzer is formed when a chromatic stripe created by the fiber-lens-grating assembly is projected onto the CCD array.

The following power budgets depend heavily on the performance of CCD detector devices. Experiments at Litton Poly-Scientific have yielded figures for Thompson CSF model TH78062 linear CCD array. This array consists of 256 13 X 13 micron pixels in a linear arrangement. More research on other devices needs to be done to find an optimum device for these applications.

The responsivity of the CCD array has been determined to be linear with the integration time over the range 2.5 ms to 27 ms. With the integration time set at 27 ms, a responsivity of 70 V/nW/pixel was measured. This gives the following responsivities given the UTRC update time requirements:

Update Time (ms)	Responsivity (V/nW/pixel)
5	13
10	26
20	52
40	104
120	312

It is believed that a minimum signal of 0.5V is required for reliable detection. This corresponds to:

FIGURE 3-1
Optical Interface (Single Fiber CCD Type)

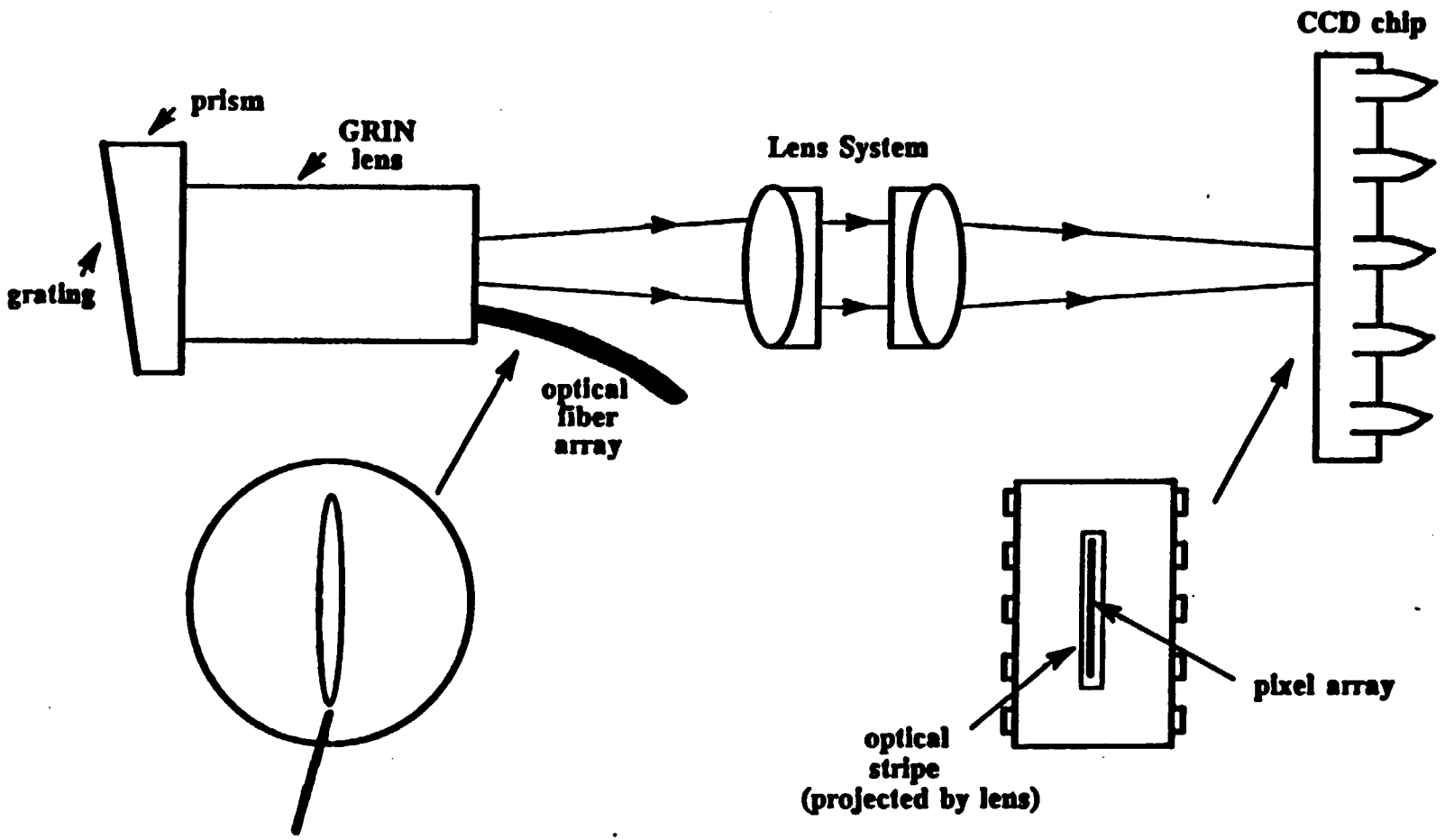

A spectrally dispersed optical stripe, formed on the surface of the GRIN lens, is projected onto the pixel array of the CCD chip. The output of the linear array can then be used as a set of discrete outputs would be. The position of the pixels determine the respective wavelengths incident upon them.

Update Time (ms)	Min. Signal Req'd (pW/pixel)
5	38
10	19
20	10
40	5
120	2

Although the linear dispersion remains constant regardless of the diameter of the fiber used to inject light into the optical system, the width of the chromatic stripe projected onto the CCD array is proportional to the fiber diameter. Since the pixels on the CCD device used in these tests are smaller than the diameter of any of the fibers used, the power intercepted by each pixel is roughly inversely proportional to the fiber diameter.

Calculating the resultant sensitivity in terms of power/wavelength, we get the following:

Sensitivity of CCD Array (pW/nm)

		5	10	20	40	120	Update time(ms)
	50	94	47	25	12	4	
	100	187	94	47	24	8	
fiber diameter (microns)	200	374	187	94	48	16	

NOTE: Use of a CCD with greater pixel width (dimension perpendicular to the direction of the chromatic stripe) will certainly result in better performance and reduced sensitivity to increase in fiber diameter. Exact (or even reasonable) estimates of these effects are difficult without testing such devices.

A more complex system is pictured in Figure 3-2. Several fibers may have the same spectral content and still be dispersed by the same optical system. If a linear CCD with elongate pixels is used, only one fiber may transmit light at one time, complicating the light source scheme and making it more difficult to empower more than one leg with a given light source. However, if a CCD area array were used, all fibers might be on simultaneously without compromising the device.

On the other hand, if a reliable electro-optic or other switch could be found, it might be possible to use the same LED source for a multiplicity of sensors, making simultaneous reading of sensors unnecessary. Further research in this area is planned for the future.

Figure 3-3 shows an interface concept which uses a fiber optic WDM and discrete detectors. Although six or seven of these detectors would be required to decode only one digital position sensor, only two are necessary for an analog sensor of the type discussed in 2.3.1.

Litton has built a prototype rotary/linear position sensor system using a WDM and discrete detectors. The receiver sensitivity was about -70 dBm, but some problems with stability were noticed. At present, it seems necessary to reduce the amplifier gain in this type of receiver to combat these instabilities, so a sensitivity of -55 dBm is anticipated for this type of receiver.

Fiber optic WDM's made with different fiber sizes have similar insertion losses at peak wavelengths, but their channel spectral widths differ. These values are approximate (using standard Litton components).

FIGURE 3-2
Optical Interface (Single Fiber CCD Type)

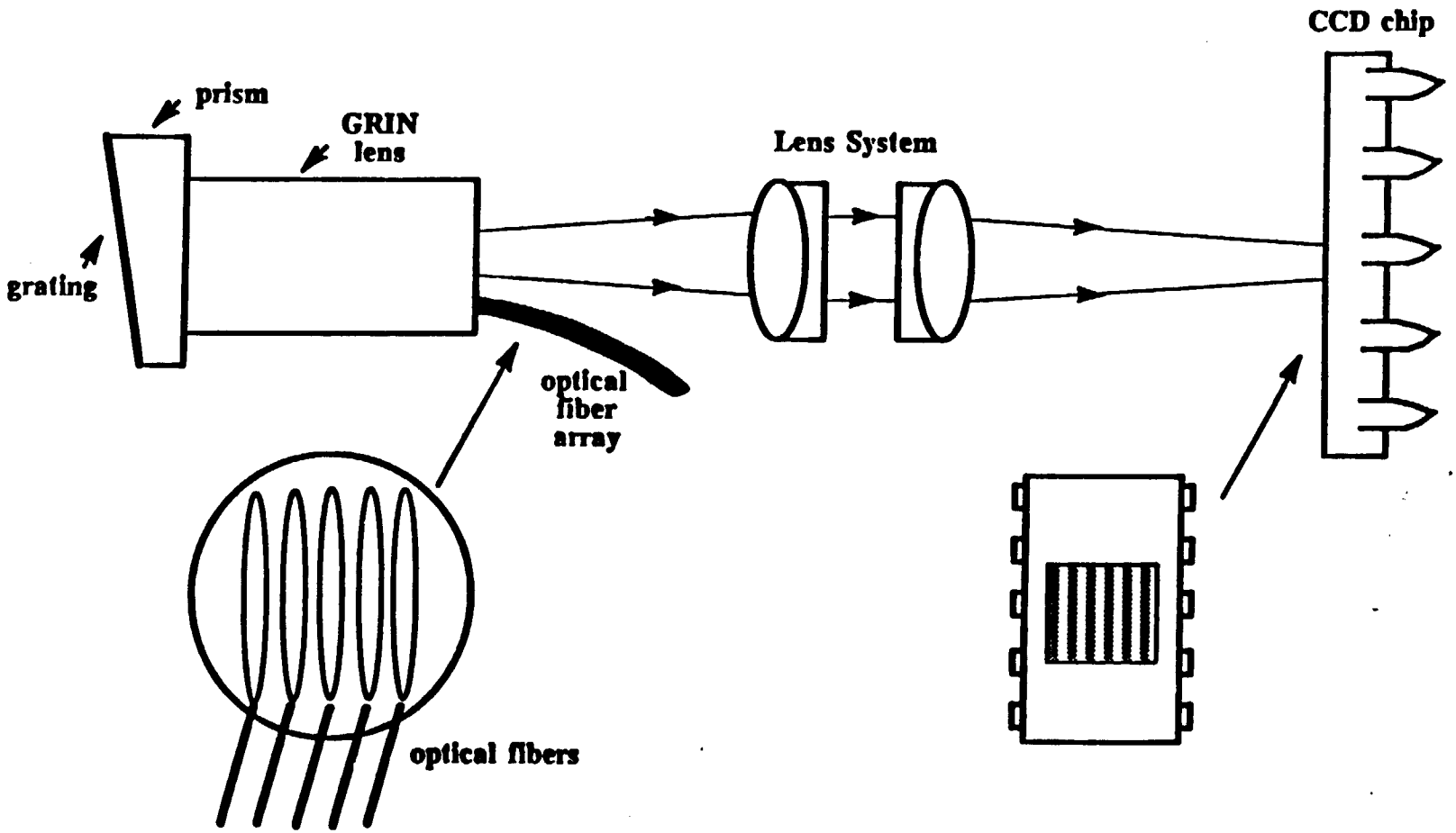

Up to 20 spectrally dispersed optical stripes, formed by the GRIN lens, are projected by a lens system onto either an area CCD array or a linear one with long pixels .

FIGURE 3-3
Discrete Detector Interface

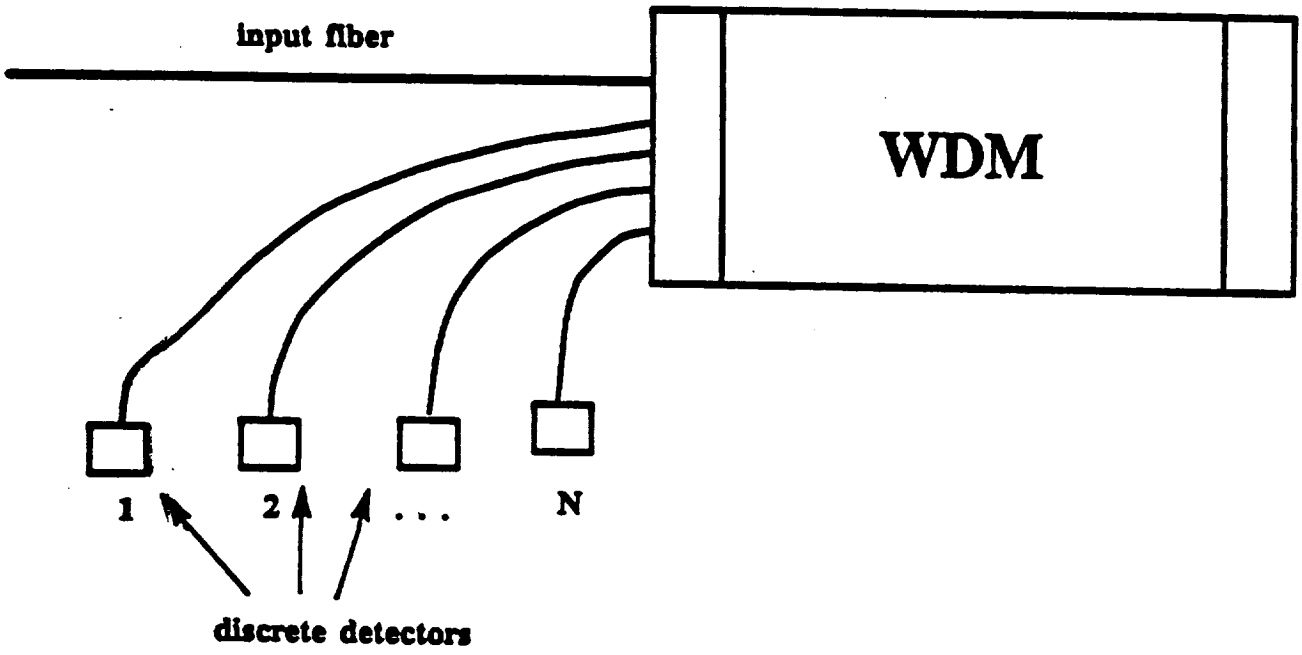

Although it is not recommended to attempt to multiplex multiple digital sensors using this concept, up to N/2 analog sensors may be multiplexed in this way.

Fiber Size	Channel Width
200 micron	18 nm
100 micron	9 nm
50 micron	4.5 nm

The sensitivity of systems using discrete optical detectors and differing fiber diameters is given below.

Fiber Diameter (microns)	Sensitivity (pW/nm)
50	700
100	350
200	175

The spectral range of all three of these optical systems is approximately 300 nm, limited by the use of a 5 mm GRIN lens with a 1200 groove/mm grating. Other optical systems might be used if this range is found wanting, or if greater resolution is desired.

3.2 Digital Sensor Interface Circuits

A digital interface circuit is used with rotary and linear position sensors as well as rotary speed sensors. As previously discussed, the code plate has tracks which have reflective and non-reflective regions. The two optical properties correspond to the two binary states, on and off. These tracks are aligned such that at any given position the state of each track can be detected and compiled to resemble some sort of code, whether it be Gray code or binary code. There are several electronic configurations that can be used for digital systems. They are discussed in the following sections.

3.2.1 Single Sensor Digital Interfaces Using a CCD Array

The circuitry required for a single sensor digital interface using a linear CCD array is shown in Figure 3-4. A breadboard version of this circuit is scheduled for completion in September 1988. The code plate has tracks, each corresponding to a Gray code channel. Each track has reflective and non-reflective surfaces which correspond to "1's" and "0's". A broadband light source is chromatically dispersed and then focused onto the code plate. Each Gray code channel reflects a unique wavelength band of light back to a single fiber. A lens-prism-grating assembly then separates the light on that fiber back into individual channels of light which are projected upon a CCD array as shown in Figure 3-1.

A CCD array can be thought of as a row of detectors, each of which has a small active area (13 by 13 um in the present device). The CCD array presently under consideration has 256 detectors (pixels). Since it would require a very large package to have a connection to each pixel, the information from each pixel is read serially. Within the CCD, this is done by putting each detector in series with a capacitor. At the beginning of an integration cycle, the CCD circuit charges all the capacitors to a certain voltage. During the integration cycle, each detector discharges its respective capacitor at a rate determined by the amount of light hitting the detector. At the end of the integration cycle, the voltage on each capacitor is stored so that a sequential read of these voltages can take place. A shift register then sequentially shifts out these levels.

Each channel reflected from the codeplate takes up several pixels of the CCD array. In this design, we have chosen to look at only the pixel which falls in the center of each channel. Thus, if we had 15 Gray code channels, only 15 of the 256 CCD pixels would be used. Since the responsivity of the CCD

FIGURE 3-4
Single Sensor Digital Interface with CCD Array

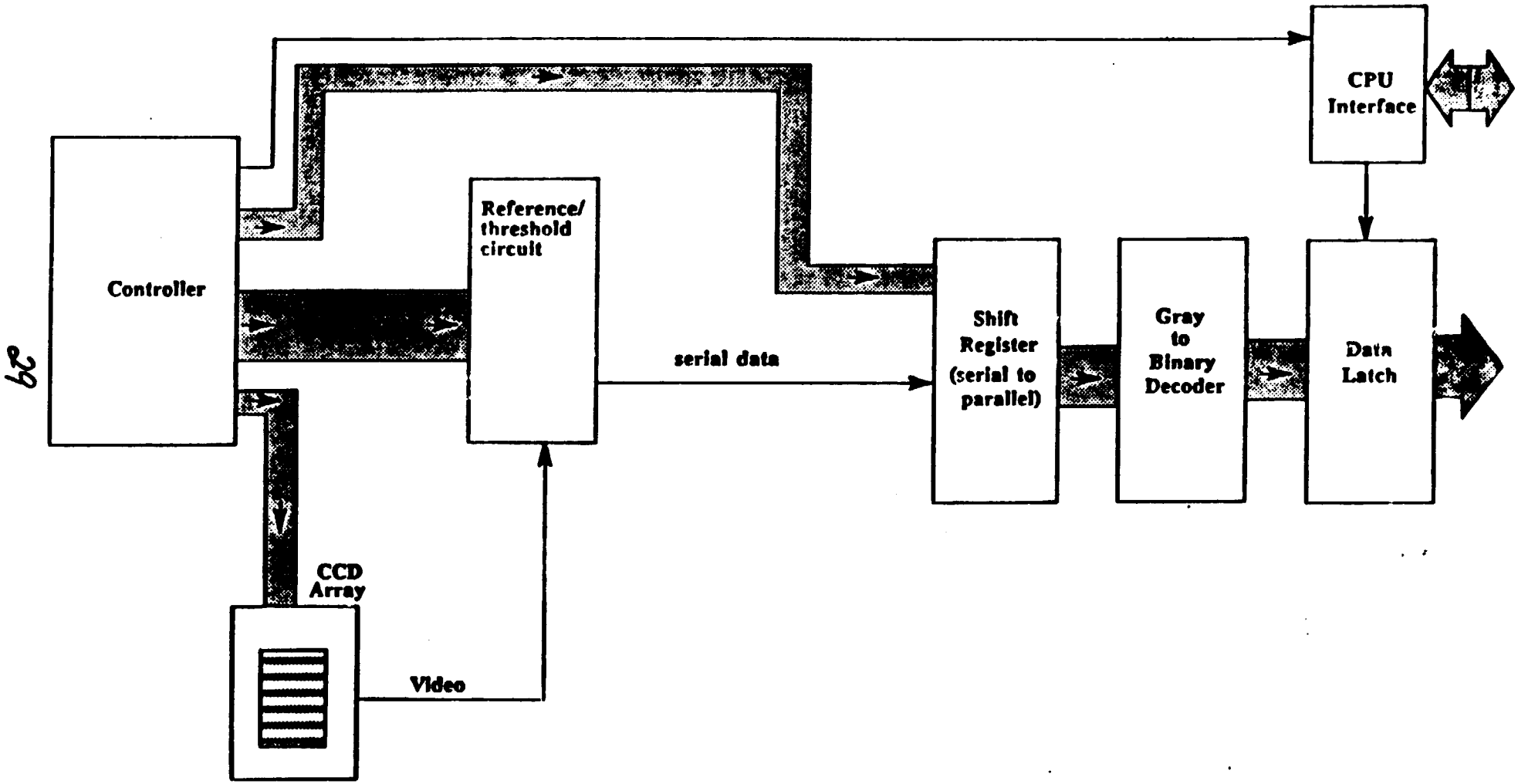

array changes across the broad light spectrum, and the light spectrum itself is not "flat" with respect to power, the reference/threshold circuit employs a reference scheme which assures that each channel's state (1 or 0) can be determined. A shift register converts the serial Gray code output of the reference/threshold circuit to a parallel output for the Gray to binary code converter. The CPU interface and data latch circuits permit the user's CPU to read data asynchronously. The controller functions as a timing and command generator for the interface.

A potential problem with this configuration could be that fixed reference levels are used in deciding whether a pixel is on or off. If the CCD has significant dark current increase over temperature, or the LED spectrum shifts over temperature, the reference level may no longer reside between the on and the off state. A large optical on-off ratio at the CCD array may allow for substantial shift in on-off levels without violating the reference requirement.

Signal processing time may be another area of concern. The output signal amplitude of a CCD array is directly proportional to the integration time. Therefore, if greater signal amplitude is required, a long integration time will be necessary, resulting in slow processing times.

Since this circuit has already been designed and a breadboard is being built, an accurate parts count and area calculation was possible. The following parts are necessary for this design:

(9) Integrated Circuits
(2) Transistors
(2) LED's
(4) Diodes
(53) Resistors
(18) Capacitors
(1) Linear CCD Array

With present technology, the calculated power consumption of the electronic interface is 6.6 watts. Three IC's in the circuit consume the

greatest percentage of this power. At present, these particular IC's are not available in CMOS with extended temperature range. One of them will be available in CMOS by December 1988. This will reduce the power requirement by 1.5 watts. If the other IC's were to go to CMOS, a reduction of another watt could be realized.

With standard size parts (DIP packages and leaded components) and a two sided circuit board, the estimated board area required by the circuit is 23.8 square inches. With surface mount technology (leadless chip carriers, chip resistors, etc.), and multilayer copper-invar-copper boards, the required area would only be about 12 square inches.

Using the procedures outlined in MIL-HDBK-217E, the mean-time-between-failure of this circuit was calculated to be 2.2 years. If the CCD array were left out, the MTBF would be 93.2 years. Since there was no established procedure for calculating the reliability for a CCD array, it was assumed that the CCD array was made of 13 individual PIN diodes, since only 13 pixels are used in a 12 bit system.

3.2.2 Single Sensor Digital Interfaces with Discrete Detectors

The circuitry required for a single sensor digital interface using discrete detectors is shown in Figure 3-5. Litton Poly-Scientific has built a prototype of this system excluding the CPU interface and data latch circuitry.

A broadband light spectrum is projected upon a code plate as previously described. The returning light from the codeplate is demultiplexed by a WDM such that the WDM has a separate output fiber for each channel. Each output fiber is routed to a separate receiver. The receiver outputs are then sent to comparators with fixed reference voltages. A TTL level is seen at the output of each comparator, corresponding to the state of a Gray code channel.

FIGURE 3-5
Single Sensor Digital Interface with Pin Diode Detectors

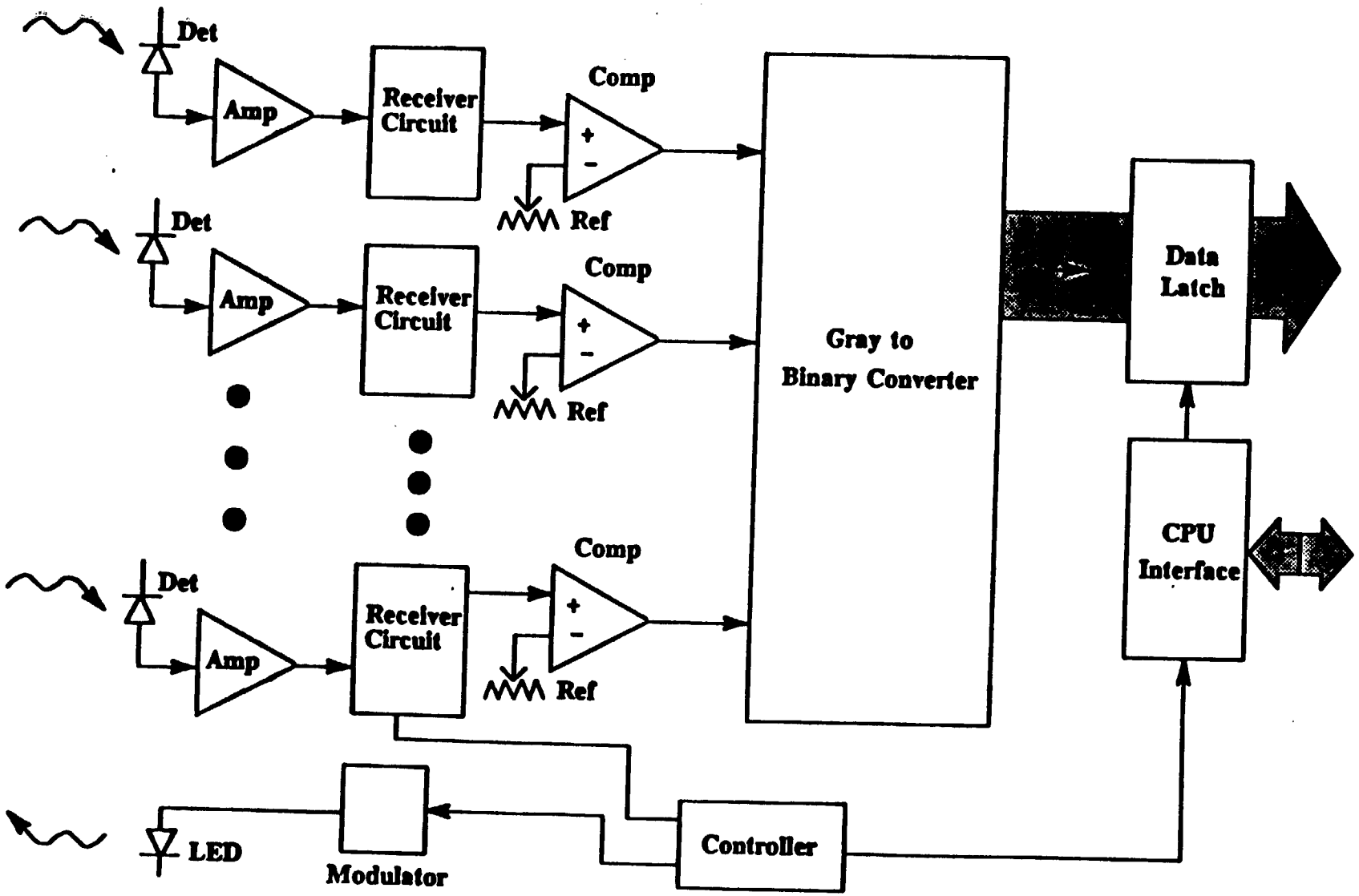

The comparator outputs are routed to a Gray-to-binary code converter, and then on to a data latch. The CPU interface makes sure that no data is read during the sample period and that the latch is not updated during a read.

An advantage of this configuration is that its data refresh rate is faster than that of a CCD configuration because a serial-to-parallel conversion is not necessary. A drawback of this configuration is the size. Currently, the electronic circuitry and optics fit into a 8.5" x 10" x 3.5" box. Also, as before, the reference voltages are fixed, perhaps making temperature stability difficult to achieve. Multiplexing the detectors and reference voltages could help reduce the size. At first glance, this would appear to be much like the CCD configuration. However, in this case the detector circuitry is accessible for temperature compensation, whereas in the CCD circuitry the pixel multiplexing circuitry is in the chip, making it inaccessible.

Some development work is necessary in order to put an array of detectors on a substrate with multiplexing and temperature compensation capabilities. It is likely that the power consumption on the present prototype would drop from 10 watts to about 5 watts using such an array. The size requirement would be similar to that of the CCD system.

3.2.3 Rotary Speed Sensor Interfaces

An interface circuit for a rotary speed sensor could be configured as shown in Figure 3-6. It is assumed that this interface would have an update time of 10 ms, a maximum speed of 19000 rpm, a minimum speed of 650 rpm, and a maximum error of 7 rpm. The 10 ms update time and minimum speed requirement mandate that the code plate have one track with 10 on/off states around the circumference as shown in Figure 2-5. As shown in Figure 3-6, the reflected signal from the code plate would be detected with a pin diode detector,

FIGURE 3-6

Speed Sensor Interface

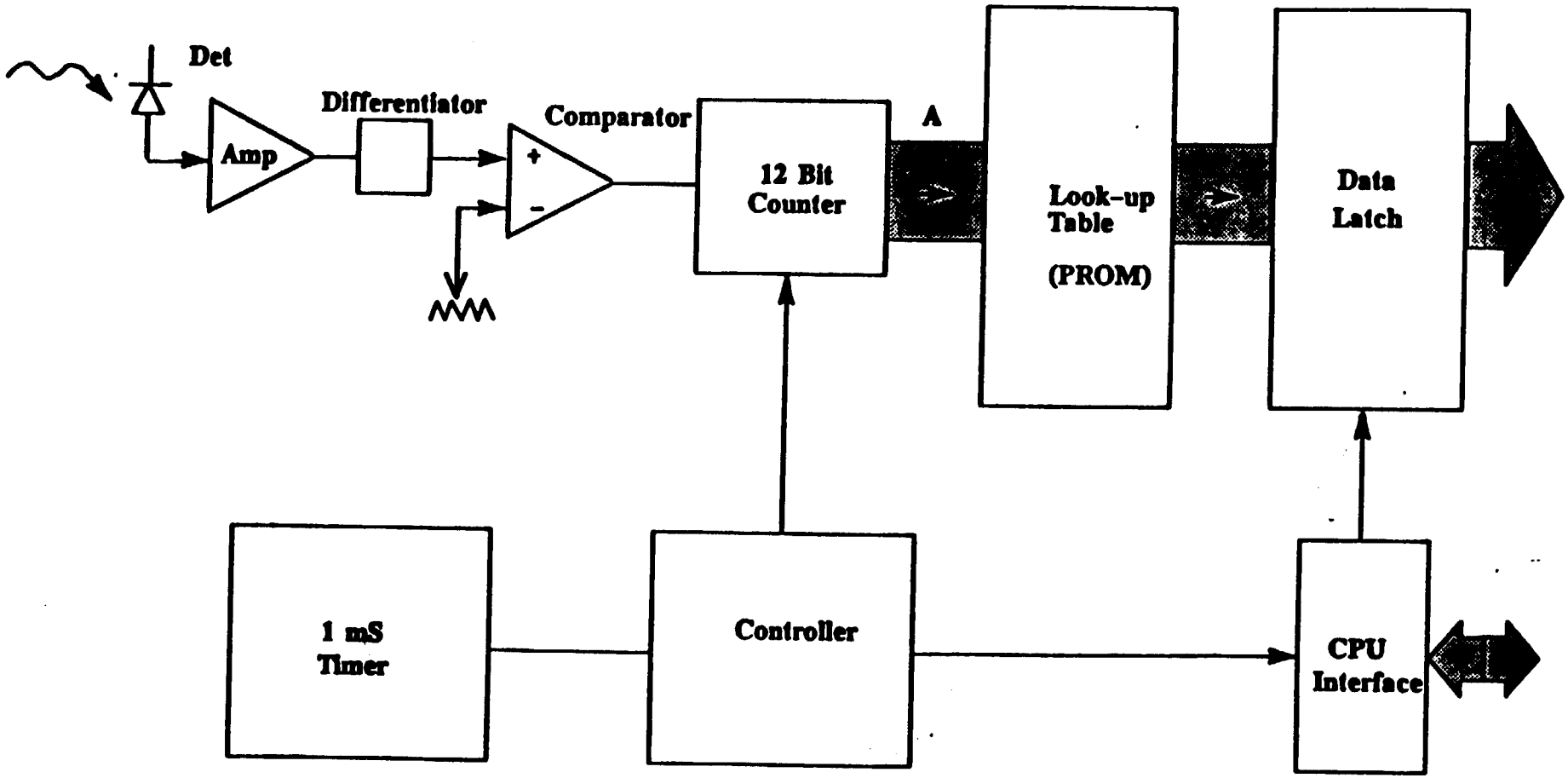

amplified, and differentiated. The differentiated signal would show up as spikes. The comparator would determine a valid leading edge in the waveform.

The digital output of the comparator would be sent to a 12 bit counter which would count the number of pulses detected due to the movement of the code plate. There will be 10 pulses counted for every rotation of the code plate. If an update time of 1 ms is used, a 12 bit counter is necessary to count the number of pulses at the highest rotational speed, 19000 rpm. The controller resets this counter every 1 ms.

A maximum error requirement of 7 rpm at 19000 rpm mandates that the maximum error of the timer must be less than +/- 1 us.

The lookup table converts the counted pulses to RPM in a format determined by the user. The CPU interface controls the data latch according to the read instructions from the CPU and the data ready instructions from the timing circuit.

The circuit area required by this interface would be approximately 12 square inches with surface mount technology. Power consumption is predicted to be about 3 watts.

3.3 Analog Sensor Interface Circuits

Analog sensor systems perform analog operations on one or more light channels. The analog systems discussed in this paper generally process two analog signals per sensor. This analog information is converted to a digital word for input to a CPU. The following sections outline two electronic means for processing this analog information.

3.3.1 Single Sensor Analog Interfaces using CCD Arrays

A block diagram showing the circuitry required for a single analog sensor using a CCD array is shown in Figure 3-7. The signals that are to be processed are projected onto a linear CCD array. A controller generates the integration and readout timing signals for the CCD array. Since the two signals are serially shifted out of the CCD, a sample and hold circuit is necessary for both channels to be processed simultaneously.

The analog signal is converted to a digital word which is used to select a value from a lookup table. The lookup table is used to customize the interface for a specific application.

The physical size of this circuit is estimated to be 9 square inches using surface mount technology. Power consumption is predicted to be 3.5 watts.

3.3.2 Single Analog Sensor Interfaces Using Discrete Detectors

The circuitry required for a single analog sensor using discrete detectors is shown in Figure 3-8. Discrete detectors simplify the circuit requirements.

In this system, the two signals are separated and directed via individual fibers to individual detectors and amplifiers as shown in Figure 3-8. Since the two signals are read simultaneously, no sample and hold circuit is necessary. Instead, the two signals are continuously processed by the analog processor. The controller insures that the A/D conversion time restraints are not violated. The lookup table and CPU interface functions were described in the previous section.

This design shows more promise than the CCD version since it allows access to the detectors for possible dark current compensation. Also, the update speed could increase, since there would be no sensitivity vs. integration time tradeoff.

FIGURE 3-7

Single and Multiple Sensor Analog Interface with CCD Array

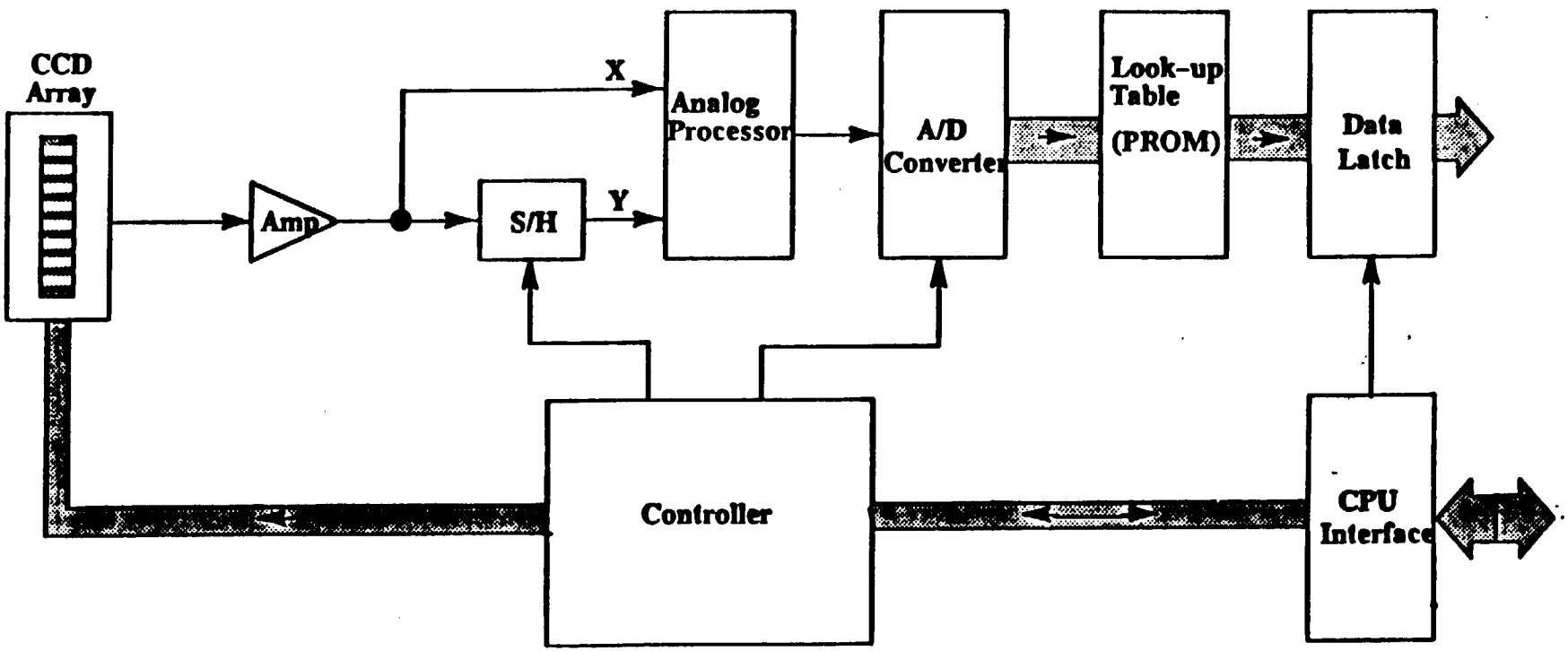

FIGURE 3-8
Single Sensor Analog Interface with Pin Detectors

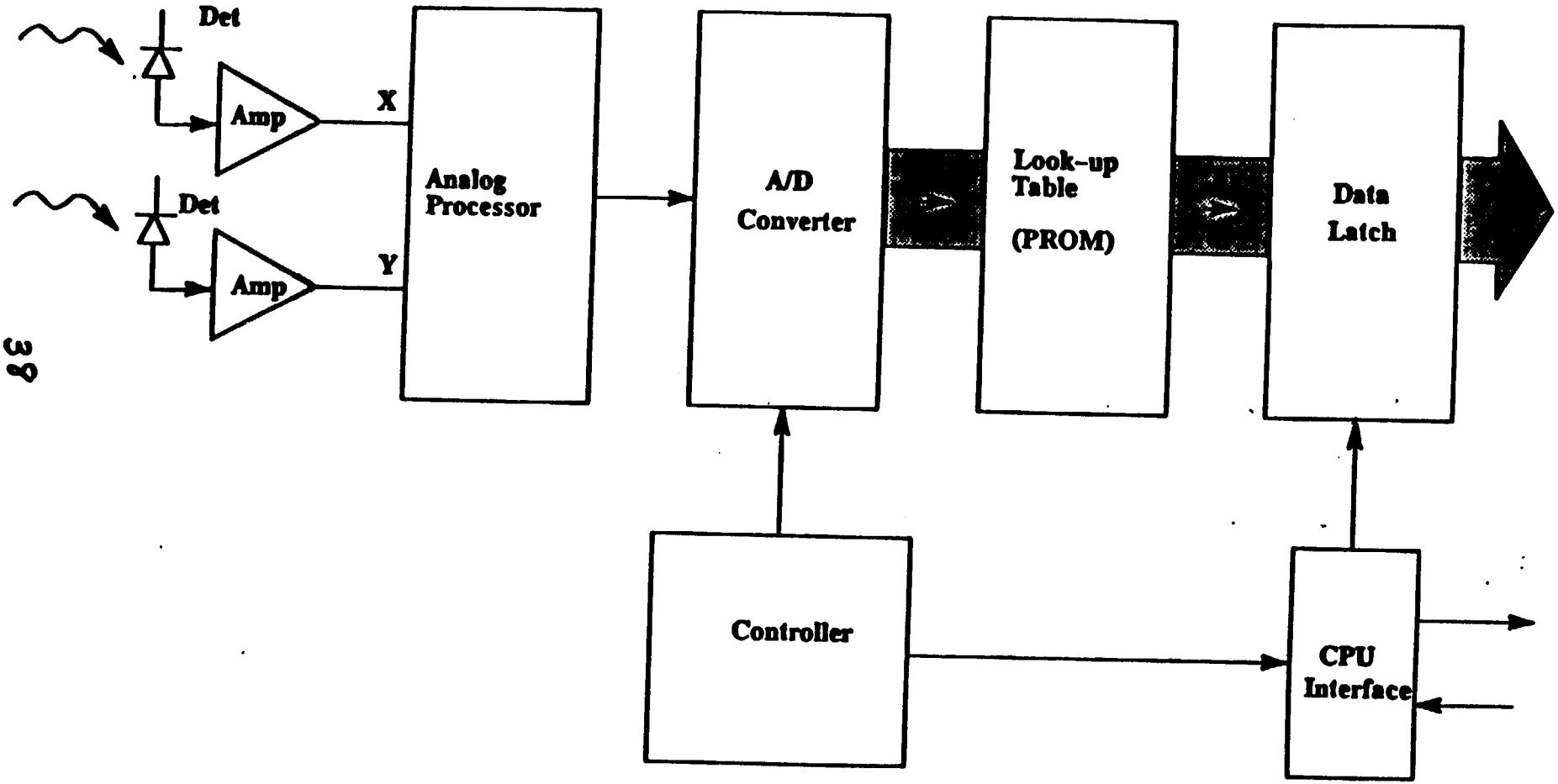

The board area requirement for this design is predicted to be 7 square inches with a power requirement of 2.5 watts.

4.0 MULTIPLEXING

There are many possible topologies for multiplexing these sensors onto one interface. The basic configurations are pictured in Figure 4-1.

4.1 Optical System

4.1.1 Loss Values for the Various Optical Components

Optical losses encountered in the use of some optical components are listed below.

Component	Loss
Linear, rotary digital position sensor	11 dB
50:50 Coupler	4 dB each pass.
WDM	4 dB
Analog Sensor	
Moving mirror type	11 dB
Moving fiber type (2-fiber design)	5 dB

NOTE: Moving fiber type analog sensors and transmissive (2 fiber) linear and rotary transducers do not require a 50:50 coupler.

4.1.2 Loss Budgets for the Topologies Pictured in Figure 4-1

For each of the figures, a specific set of fiber sizes was chosen and the loss budget calculated for each of 3 applications - position sensors, rotary speed sensors, and analog sensors (pressure or temperature). These figures are to be used with spectral power densities corresponding to light source strength and receiver sensitivity, as no filter factors are included to account for channel spectral width.

FIGURE 4-1

Schematic Diagram of System Composed of Several Sensors Sharing a Common Interface

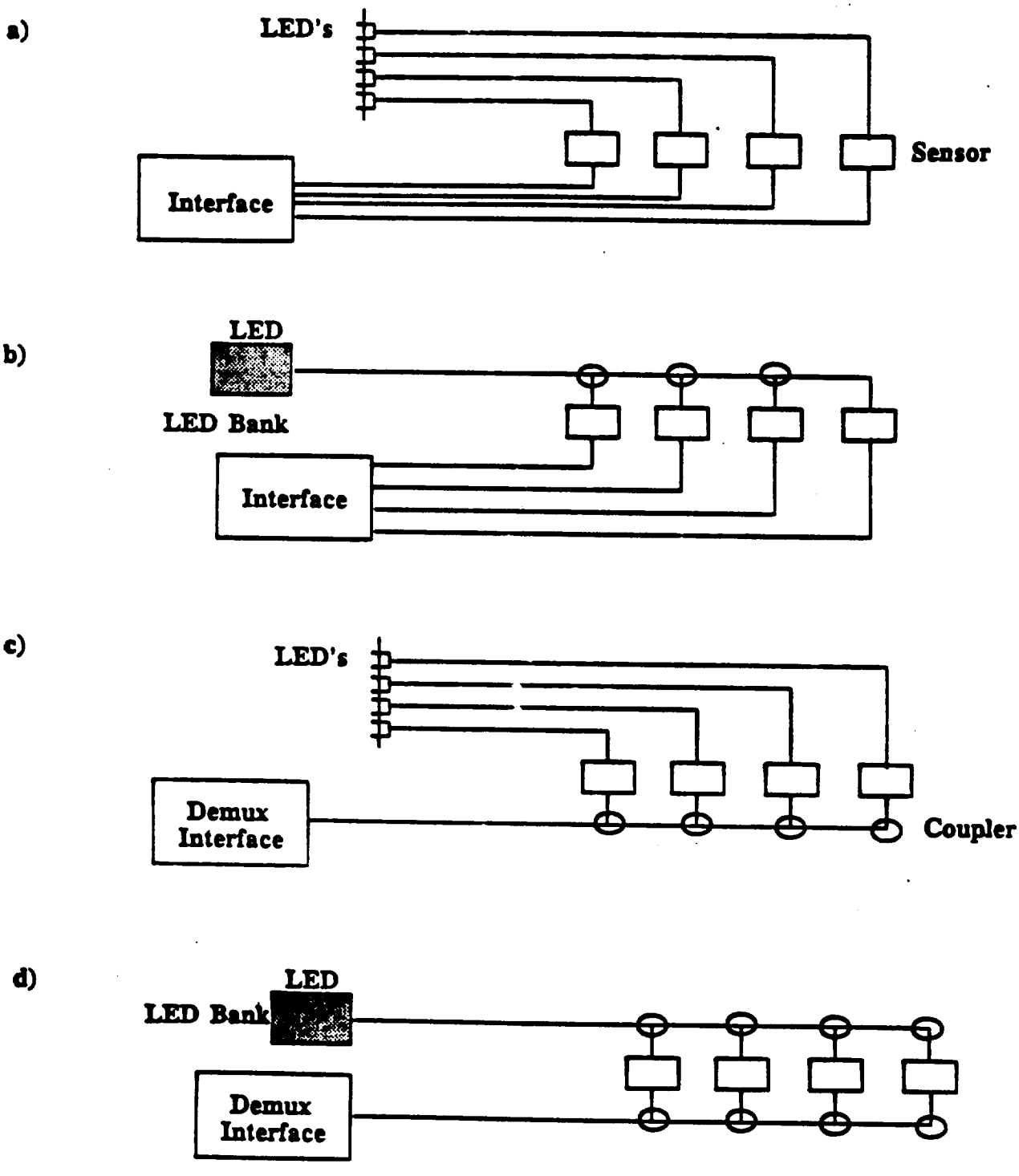

FIGURE 4-1 (Cont.)

Schematic Diagram of System Composed of Several Sensors Sharing a Common Interface

e)

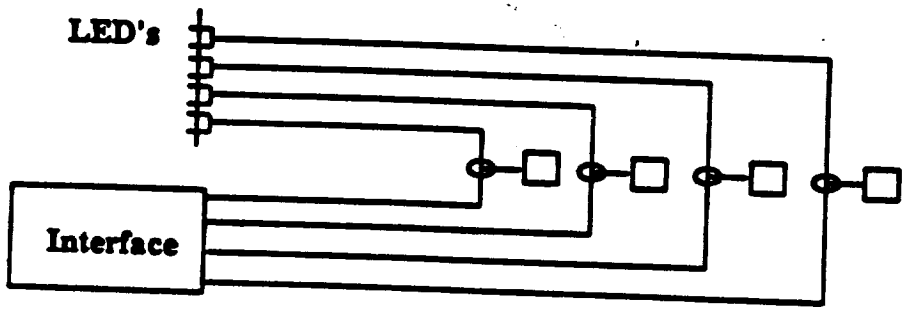

f)

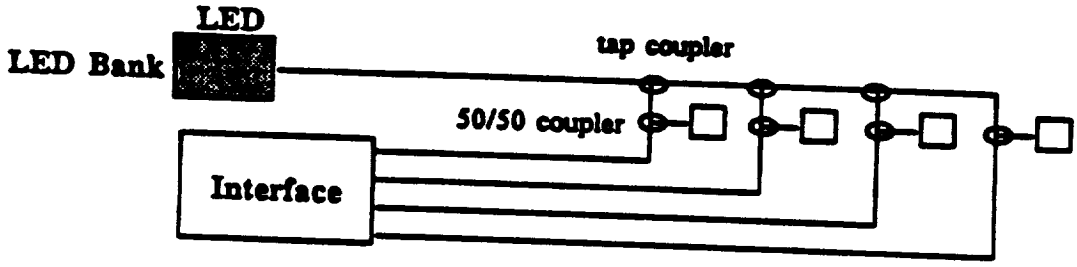

g)

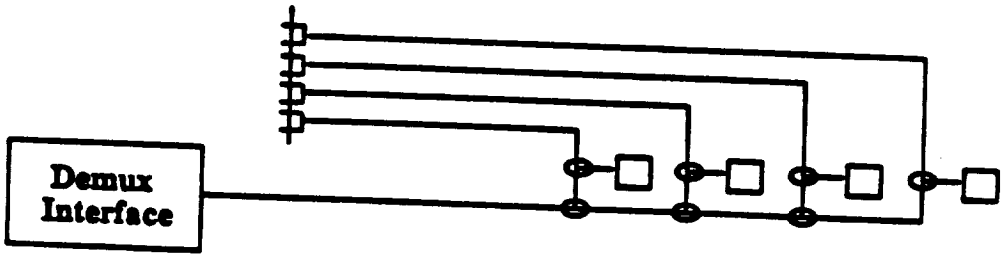

h)

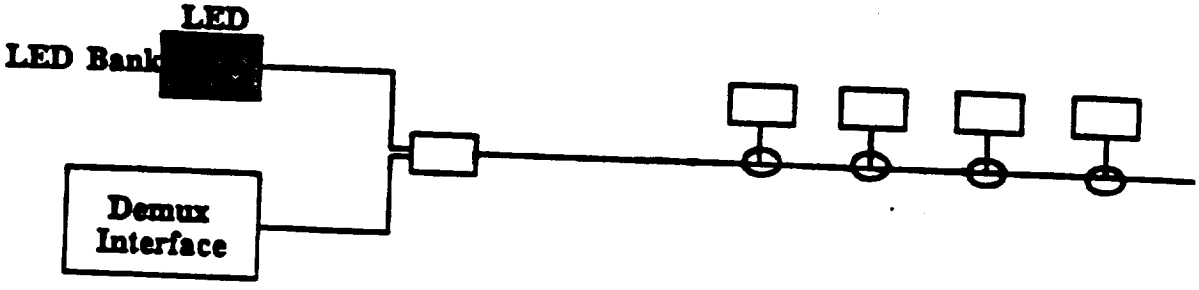

4.1.2.1 Transmissive (2 Fiber) Systems

Figure 4-1(a) Multiplexing: multifibers onto 1 CCD
no effect on receiver sensitivity

Loss Budget

	Digital Position	Rotary Speed	Analog
1 sensor	11 dB	4 dB	5 dB
TOTAL	11 dB	4 dB	5 dB
dynamic range*	0	0	0

NOTE: Any fiber diameter may be used in a system of this simplicity, as loss is small and no couplers are present.

* Dynamic range is the maximum signal from the brightest sensor minus the maximum signal from the dimmest.

Figure 4-1(b)

An array of couplers is used to split light from a single LED or bank of LEDs into N sensors, each of which uses its own return fiber.

LOSS BUDGET

	Digital Position	Rotary Speed	Analog
Power Split (rough)	-10log(1/N)+2dB	-10log(1/N)+2dB	-10log(1/N)+2dB
1 sensor	11 dB	4 dB	5 dB
TOTAL	13-10log(1/N)	6-10log(1/N)	7-10log(1/N)
Dynamic Range	0 dB	0 dB	0 dB

NOTES: As asymmetric couplers are not required in this topology, no fiber diameter restriction exists other than those which may be dictated by lower launch considerations. As a tapered bus can be used, equal power can be delivered to each sensor.

Figure 4-1(c)

N sensors, each with its own LED, coupled onto a single return fiber.

LOSS BUDGET

	Digital Position	Rotary Speed	Analog
1 sensor	11 dB	4 dB	5 dB
Asymmetric coupler tap-on	3 dB	3 dB	3 dB
Loss due to use of 200 micron fiber with CCD array	6 dB	6 dB	6 dB
TOTAL (closest node)	20 dB	13 dB	14 dB
Dynamic range	(N-1) (0.35 dB)*	(N-1) (0.35 dB)	(N-1) (0.35 dB)

*Asymmetric coupler transit loss.

Figure 4-1(d)

N sensors sharing a common LED and return fiber.

LOSS BUDGET

	Digital Position	Rotary Speed	Analog
Power split	-10log(1/N)+2dB	-10log(1/N)+2dB	-10log(1/N)+2 dB
1 sensor	11 dB	4 dB	5 dB
Asymmetric coupler (tap-on)	3 dB	3 dB	3 dB
Loss due to use of 200 micron fiber with CCD	6 dB	6 dB	6 dB
TOTAL	22-10log(1/N)	15-10log(1/N)	16-10log(1/N)
Dynamic range	(N-1) (0.35 dB)	(N-1) (0.35 dB)	(N-1) (0.35 dB)

Figure 4-1(e)

N sensors, each with its own LED and return fiber.

LOSS BUDGET

	Digital Position	Rotary Speed	Analog
2X 50:50 coupler	8 dB	8 dB	8 dB
1 sensor	11 dB	4 dB	8 dB
TOTAL	19 dB	12 dB	19 dB
Dynamic range	0 dB	0 dB	0 dB

Figure 4-1(f)

N sensors, sharing a common LED but each with its own return fiber.

LOSS BUDGET

	Digital Position	Rotary Speed	Analog
Power split	-10log(1/N)+2dB	-10log(1/N+2dB	-10log(1/N)+2dB
2X 50:50 coupler	8 dB	8 dB	8 dB
1 sensor	11 dB	4 dB	11 dB
TOTAL	21-10log (1/N)	14-10log (1/N)	21-10log(1/N)
Dynamic range	0 dB	0 dB	0 dB

Figue 4-1(g)

N sensors, each with its own LED, but sharing a common return fiber.

LOSS BUDGET

	Digital Position	Rotary Speed	Analog
2X 50:50 coupler	8 dB	8 dB	8 dB
1 sensor	11 dB	4 dB	11 dB
Asymmetric tap-on	3 dB	3 dB	3 dB
Loss due to 200 micron with CCD	6 dB	6 dB	6 dB
TOTAL	28 dB	21 dB	28 dB
Dynamic range	(N-1)(0.35 dB)	(N-1)(0.35 dB)	(N-1)(0.35 dB)

Figure 4-1(h)

N sensors sharing a common LED and return fiber.

LOSS BUDGET

	Digital Position	Rotary Speed	Analog
Power split	-10log(1/N)+2dB	-10log(1/N)+2	-10log(1/N)+2dB
2X 50:50 coupler	8 dB	8 dB	8 dB
1 sensor	11 dB	4 dB	11 dB
Asymmetric tap-on	3 dB	3 dB	3 dB
Loss due to use of 200 micron fiber with CCD	6 dB	6 dB	6 dB
TOTAL	30-10log(1/N)	23-10log(1-N)	30-10log(1/N)
Dynamic range	(N-1)(0.35 dB)	(N-1)(0.35 dB)	(N-1)(0.35 dB)

4.1.3 Sample Calculations Involving Digital Code Plate Systems

Single fiber linear, rotary sensors

Topology: Figure 4-1(e)

2 X 50:50 coupler	8 dB
1 sensor	11 dB
	19 dB

	100 micron	50 micron
Min. launch density (Texas Optoelectronics TOX 0001)	0.78 uW/nm	.125 uW/nm
Min. peak density into interface	10 nW/nm	1.6 nW/nm
Sensitivity of interface (integration time = 5 ms)	187 pW/nm	94 pW/nm
Margin (dB)	13	12

Transmissive code plates (2 fiber systems) give 8 dB better performance (see Figure 4-1(a)).

According to the above, ten 100 micron core encoders can be powered by one light source (see Figure 4-1 (f)). These calculations need to be verified by direct testing. Such tests are planned for the near future.

If one were to use two fiber (transmissive) digital encoders, the reduction of the loss by 8 dB would increase the devices's multiplexibility. In the topology pictured in Figure 4-1(b), 15, 100 micron or 50 micron core encoders can be powered with a single light source. Figures 4-1(c), (d), (g), and (h) show multiple encoders multiplexed onto a single return fiber. It was stated in Section 3.1.1 that the required spectral width for a 6 bit digital encoder is 155 nm for 100 micron core devices and 80 nm for 50 micron core. This prohibits the multiplexing of more than one of the former or two of the

latter onto one return fiber. However, in order to have sufficient power margin in this configuration, the update time must be increased.

4.1.4 Sample Calculations Involving Analog Systems

Topology: Figure 4-1(e)

2 X 50:50 coupler	8 dB
1 sensor	11 dB
	19 dB

	100 micron	50 micron
min. launch density	0.78 uW/nm	0.125
min. peak density into interface (excluding additional system loss, such as from multiplexing)	9.8 nW	1.5 nW
sensitivity of interface	187 pW/nm	94 pW/nm
margin	17 dB	12 dB

Current Litton asymmetric couplers have the following characteristics:

50 micron fiber to 200 micron fiber loss	3 dB
transit loss (including splice)	0.35 dB
200 micron fiber to 50 micron fiber loss	16 dB

Moving fiber type: Figure 4-1(a)

1 sensor		5 dB
	total	5 dB
	100 micron	50 micron
Launch density	.78 uW/nm	.125 uW/nm
Min. peak density into interface (excluding additional system loss, such as from multiplexing)	250 nW/nm	40 nW/nm
Sensitivity of interface	187 pW/nm	94 pW/nm
Margin (dB)	31	26

Analog sensors of the type described above use 30 nm (100 micron core devices) and 15 um (50 micron) each. This permits multiplexing 7 of the former and 15 of the latter onto one return fiber (Figures 4-1(c), (d), (g), and (h)).

4.1.5 Rotary Speed (see Figure 2-5)

The rotary speed sensor may have an insertion loss as low as 2-3 dB. However, multiplexing a number of these onto one return fiber requires a wavelength bandpass filter, which increases the insertion loss by another 2-3 dB. If the bandpass filter were approx. 10 nm wide, approx. 20 of these can be multiplexed onto one return fiber.

4.1.6 Multiplexing Onto One Return Fiber

When one increases the size of the return fiber in a system using this CCD detection device, a price is paid in sensitivity of the interface. Because a 1:1 imaging condition is required to match the numerical aperture of the fiber with a lens system, and because the CCD pixels are smaller than the chromatic stripe width, an increase from 50 to 200 microns causes a decrease in

sensitivity of 6 dB, as well as a decrease in resolving ability, necessitating an increase in spectral width required for each sensor to 60 nm for analog sensors and ~270 nm for digital 6 bit devices, and ~400 nm for the rotary position encoder, given the present optical system. An optical system using 200 micron fiber but giving resolution similar to that obtainable with the present design using 50 micron fiber is possible, but would take up 16 times as much board area.

NOTE: CCD devices with larger pixel sizes should result in a greater usable signal, as switching noise, a large part of the noise level in the device, does not increase with pixel size. In this case, an increase in fiber diameter should have an effect on the sensitivity of the device which is only related to the dark current of the pixels, which is generally less significant than switching noise. The only effect should be a decrease in resolving ability.

On the other hand, using 50:50 or other couplers to combine returning signals onto one smaller fiber is painful as well. Four dB loss per coupler is to be expected in this scheme. If more than two sensors are multiplexed in this way, it makes more sense to take one's lumps with the larger fiber in an asymmetric coupler-based data bus format.

4.2 Interface Circuits for Multiplexing Sensors

There are a variety of ways to electrically interface to multiplexed optic sensors. Several configurations are outlined in the following sections.

4.2.1 Multiple Sensor Digital Interfaces Using CCD Arrays

The circuitry for a multiple sensor digital interface using CCD array technology is similar to that of the single sensor version shown in Figure 3-4 with a few exceptions.

Since there would be up to 15 pixels per fiber and many fibers in the system, a large number of reference voltages are required. The controller would be more complex because it would require additional circuitry for generating reference voltages.

The communications between the controller and CPU interface have to be bi-directional in this configuration. This is necessary so that the CPU can request which sensor it would like to look at. The controller would make sure that the information from the desired sensor would shift into the register. Upon conversion, the controller would tell the CPU interface that data is ready.

The CCD array could be an area or linear array. If an area array were used, one dimension could divide the channels while the other dimension could divide the light spectrum within each channel as shown in Figure 3-2. If the same integration time was used as that used in a single sensor interface, the readout time on each pixel of the CCD array would decrease because of the increased number of pixels. This requires faster circuitry at the output of the CCD array. A linear array could also multiplex the channels if it had elongated pixels that formed a one-dimensional array with the same area as an area array. In this case, there would have to be a separate LED bank for each sensor and the controller would have to switch on one bank at a time so that only one sensor would use the CCD array at any given time. As previously discussed, the number of LED's in a bank could range from one to several, depending on the power budget. The circuit board area requirement for a linear

CCD approach would depend on the number of multiplexed sensors. This is because the LED bank count equals the sensor count. For each additional sensor, add approximately 1.5 square inches for LED bank space. The current consumption is estimated as 7 watts since only one LED bank is on at a time.

If a two-dimensional CCD array were used, the estimated circuit area is 15 square inches. The power requirement would be slightly more than the single sensor version, probably 7 watts total.

4.2.2 Multiple Sensor Analog Interfaces Using CCD Arrays

The circuitry required for multiple analog sensors is similar to that required for single sensors as shown in Figure 3-7. Linear or area arrays could be used as described in the previous section. The CPU interface would communicate to the controller to let it know which analog data to pass through the sample and hold and A/D circuits. This configuration assumes that the PROM lookup table would be the same for all the sensors, hence, all the sensors would be the same type. Power consumption and size would be the same as that for a single sensor interface. The only exception would be that if a linear CCD array with elongated pixels were used, 1.5 square inches would be required for each LED bank, necessary for operation for each additional sensor.

4.2.3 Multiple Sensor Interfaces Using Discrete Detectors

Multiple sensor interfaces using discrete detectors would only be practical for analog schemes. Digital schemes require separate receiver circuitry for each bit in each sensor. This would make the size prohibitively large.

As stated previously, the analog scheme requires only two detectors per sensor. The multiple sensor interface architecture is shown in Figure 4-2. It

FIGURE 4-2
Multiple Sensor Analog Interface with Discrete Detectors

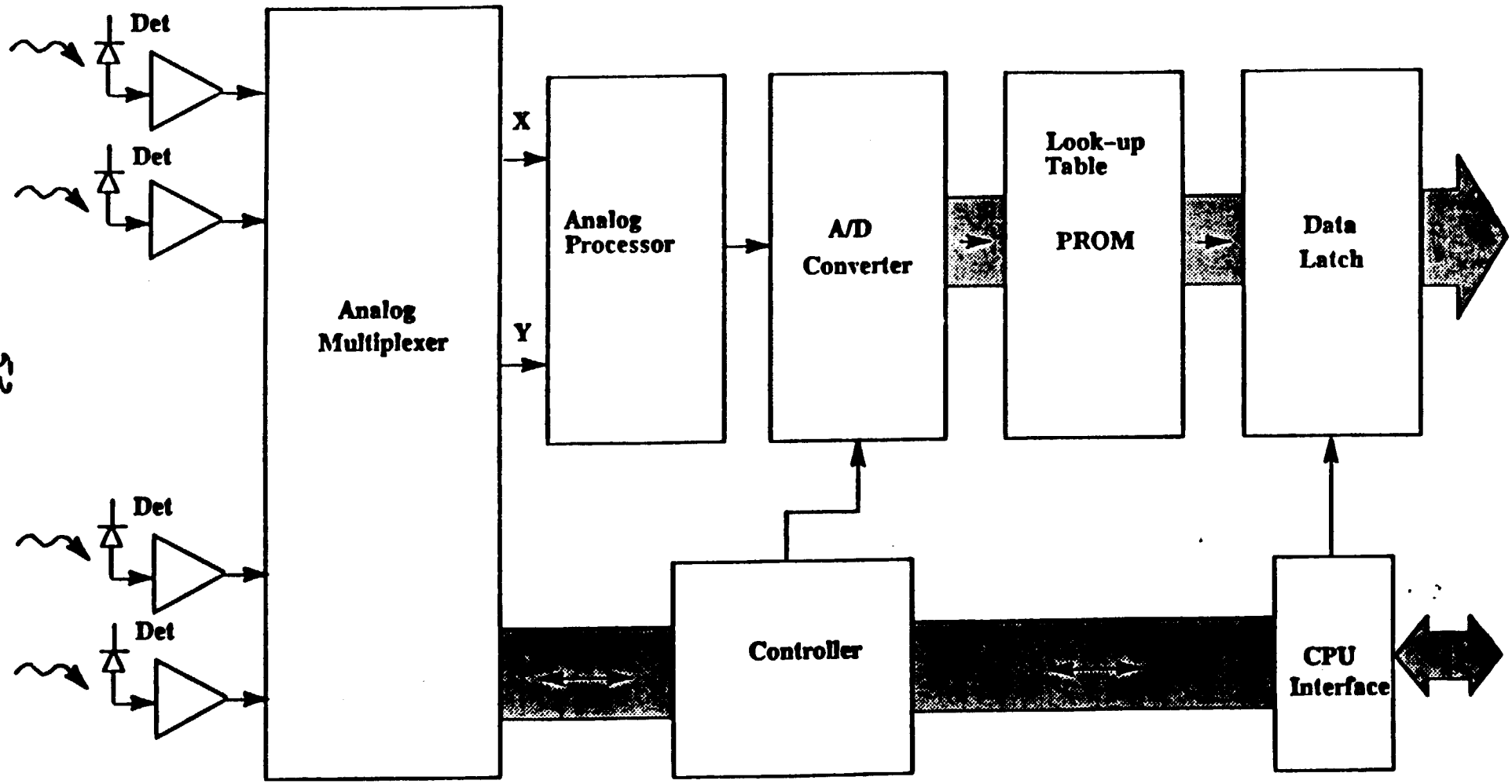

would require a two channel analog multiplexer whereby the controller determines which detector pair outputs will be connected to the analog processor.

The board space required for this interface would depend on the number of multiplexed channels. For a four sensor system, the estimated board area is 16 square inches with a power requirement of 4 watts.

5.0 UTRC Questions

1. Types of sensors: Which of the sensors listed in Table 1 can be accommodated in the design? Which cannot? What optical sensing mechanism is employed for each quantity?

   Refer to Section 2.0.

2. Signal compensation or calibration: Is the sensing mechanism digital or analog? If analog, then what compensation or referencing method is employed?

   Refer to Section 2.0.

3. Number of channels: How many sensors can share a single optical source or receiver?

   Refer to Section 4.0. (All sections)

4. Number of distinct sources: How many optical sources, light emitting diodes or laser diodes, are required to service all of the sensors shown in Table 1?

   See Section 4.0 Digital encoders 2/LED, Analog sensors 10/LED

   - All position sensors @ 1 LED/1 sensor — 20 LED's
   - Assume 1 LED/10 analog sensors + 2 rotary speed sensors (pressure, temperature) — 2 LED's

   22 LED's

5. Number of detectors: How many optical detectors are required to service all of the sensors shown in Table 1?

   See Sections 3.1.1, 4.2

   - 1 CCD/20 position encoders (20 fibers x encoders/fiber) — 1
   - 1 CCD/100 analog sensors (20 fibers x 5 sensor/fiber) — 1

   2

6. Number of fibers: How many parallel optical fibers are required to service all of the sensors shown in Table 1?

   See Section 4

2/position encoders		.3/analog sensor	
x 20		x 14	
40	+	4.2	= 45

7. I/O pincount: How many optical connector contacts are required to connect the FADEC to the optic sensors?

   See Section 6

8. Optical power margin: What is the optical power level of each source in the design? What is the receiver noise level? What are the sensor and link losses:

   See Section 4.0.

9. Signal processing time: How much time is required for the electronic interface to compute the sensor value? What is the bandwidth of the analog portion of the receiver?

   See Sections 3.1.2 & 3.1.3

10. Complexity: How many circuit elements (transistors, amplifiers, logic elements) are in the electronic interface?

    See Sections 3.1.2 & 3.1.3

11. Electrical power consumption: How many watts of electrical power are required for the interface circuitry?

    See Sections 3.1.2 & 3.1.3

12. I/O circuit area: Estimate the circuit board area required for the electro-optic interface. Specify where electro-optic hybrids or custom monolithic integrated circuits could be used to minimize the size of the interface.

    See Sections 3.1.2 & 3.1.3

13. Weight: Estimate the weight of the electro-optic interface and the fiber optic cable in the system.

    Cable: 10g/meter Interface: 50 g not including box

14. Reliability: Estimate the mean time to failure of the electro-optic interface based on the number of electronic circuit elements and electro-optic components.

    See Sections 3.1.2 & 3.1.3

15. Redundancy: How would redundancy be implemented for the sensor network?

    Combining 2-3 LED's via a coupler to obtain a single source bank would give a certain redundancy for some of the sensors (rotary speed, analog sensors).

16. Maintainability: When the system fails, how are faults isolated? What components would be repaired or replaced?

TBD

17. Availability or development schedule: Are all of the components in the system available today in flight quality? What components are lacking? What new dvelopments are needed for this design?

Information pertaining to the development status of each component appears in various sections of this report.

APPENDIX 1

Table 1. FADEC Sensor Set
with uniform temperature specifications

Number of Sensors	Measurement	Update Time	Accuracy	Range	Ambient
4	Linear position	5 ms	+/- 0.36 cm	0 to 36 cm	-54 to 200 C
2	Linear position	10 ms	+/- 0.26 cm	0 to 26 cm	-54 to 200 C
4	Linear position	5 ms	+/- 0.18 cm	0 to 18 cm	-54 to 200 C
2	Linear position	10 ms	+/- 0.09 cm	0 to 9 cm	-54 to 200 C
5	Linear position	5 ms	+/- 0.05 cm	0 to 5 cm	-54 to 200 C
2	Linear position	10 ms	+/- 0.05 cm	0 to 5 cm	-54 to 200 C
1	Rotary position	10 ms	+/- 0.2 deg	0 to 130 deg	-54 to 200 C
1	Gas temperature	120 ms	+/- 2 C	-54 to 260 C	-54 to 200 C
4	Gas temperature	20 ms	+/-11 C	0 to 1500 C	0 to 350 C
1	Fuel temperature	120 ms	+/- 3 C	-54 to 180 C	-54 to 200 C
1	Turbine blade temperature	20 ms	+/-10 C	500 to 1500 C	-54 to 350 C
1	Light off detector	20 ms	+/-5 %	< 290 nm (optical wavelength)	-54 to 350 C
3	Fuel flow	10 ms,	+/-100 kg/hr,	200 to 6000 kg/hr,	-54 to 200 C
3	Fuel flow	40 ms,	+/-100kg/hr,	5000 to 16000 kg/hr, (1 inch diameter)	-54 to 200 C
1	Gas pressure	10 ms	+/-4.0 kPa	7 to 830 kPa	-54 to 350 C
1	Gas pressure	120 ms	+/-1.0 kPa	7 to 280 kPa	-54 to 200 C
1	Gas pressure	10 ms	+/-40 kPa	35 to 5000 kPa	-54 to 350 C
1	Hydraulic pressure	40 ms	+/-40 kPa	500 to 8000 kPa	-54 to 200 C
1	Fuel pressure	120 ms	+/-40 kPa	0 to 690 kPa	-54 to 200 C
1	Rotary speed	10 ms	+/- 7 rpm	650 to 16000 rpm	-54 to 200 C
1	Rotary speed	10 ms	+/- 7 rpm	1600 to 19000 rpm	-54 to 200 C
1	Vibration	120 ms	+/- 2.5g	0 to 50 g (10 Hz to 1 kHz)	-54 to 350 C
1	Fluid level	120 ms	+/-2%	0 to 15 cm	-54 to 200 C

APPENDIX D–2

LITTON POLYSCIENTIFIC WDM EOA ADDENDUM

FIBER OPTIC WAVELENGTH DIVISION MULTIPLEXING SENSOR TECHNIQUES IN AIRCRAFT ENGINE CONTROL SYSTEMS

FINAL REPORT

By:

LITTON POLY-SCIENTIFIC
1213 North Main Street
Blacksburg, Virginia 24060

TABLE OF CONTENTS

1.0 Introduction

This report deals with possible avenues to pursue in improving the state of the art of WDM sensor technology as it applies to aircraft. The basic techniques of WDM based sensors have been detailed in another report.

2.0 Overall System Considerations

In WDM based sensors a critical relationship exists between source launch power spectral density, system loss, sensor performance, demux dispersion and receiver sensitivity. Improvement in any of these components not only enhances overall system performance, but can also relieve requirements on other components.

Improvements are possible in each of the system elements. It is not clear in advance, however, how much improvement can be realized in any individual system component. Therefore, in each of the following sections, elements will be considered independently from one another.

3.0 System Configuration - Single Fiber versus Dual Fiber

Most of the sensors currently under consideration may be configured either as transmissive or reflective devices. System diagrams corresponding to these sensor types are compared in Figure A-3.1.

Systems involving reflective (single fiber) sensors have couplers in them which are not present in those involving transmissive sensors. This causes about 8 dB of additional system loss which may be eliminated by the use of a two fiber transmissive system.

Backreflection can also be a problem in reflective systems. Bidirectional connections (those appearing in the single fiber portion of the link) can be a source of back reflections which decrease the optical signal-to-noise ratio in these systems.

Transmissive systems, on the other hand, may have up to twice as much fiber as equivalent reflective systems, and twice as many connectors. In addition, the transmissive sensors themselves are generally optically somewhat more complex, requiring more optical elements. However, transmissive systems eliminate the coupler and the sensitivity to connector back reflections.

Further trade studies for specific applications should be performed to determine where single or dual fiber configurations are most appropriate.

4.0 Light Source

Since WDM based sensor devices operate over a large spectral band, light sources having a large spectral width and high output power are required to provide adequate optical power in each channel over the spectral range of the system. In addition to being broad, the light source spectrum must be reasonably smooth, having only gradual changes in spectral density over the operating range. This provides for a more relaxed dynamic range requirement at the receiver. Lasers and SLEDs are devices with FWHM's of less than twenty nanometers, and are therefore probably not suitable for these applications.

Two emitter types have sufficiently large spectral widths: LEDs and light bulbs. LEDs with FWHM's of up to 50 nm are available. Light bulbs have FWHM's in excess of 1000 nm, but suffer in other areas, notably the low spectral power density which can be coupled into a fiber and low reliability.

LEDs have far better reliability (approximately three orders of magnitude better), and can launch spectral power densities one to two orders of magnitude greater than those possible with light bulbs. Although greater LED spectral widths are needed, LEDs are the best existing broadband light source available for this application.

Texas Optoelectronics TOX0001 LEDs launch 125 uW into 100 um core fiber and 20 uW into 50 um fiber at 100 mA. This is a relatively low launch power, but is compensated for by these LED's large (40 nm) FWHM. This gives a minimum launch spectral power density of about 1.5 uW/nm into 100 um fiber and 0.4 uW/nm into 50 micron fiber, if the spectrum is used inside the 40 nm window.

Research into the possibilities of creating broadband LED devices is currently being carried out. The use of dopants to create a multiplicity of adjacent bandgaps is being considered. This technique may result in some decrease in output power, but should also result in a significant increases in spectral width.

5.0 Sensor

In a spectrally dispersive optical system, such as the one used in Litton sensors, the diffracted light forms a band in which a given photon's position within the band is determined by its wavelength. Since this relation is linear, the term "linear dispersion" has come to mean the constant given by $d\lambda/dx$, λ being wavelength, x distance.

Figure A-5.1a shows a transverse section through three code tracks, two of which are in the "on" state while one is in the "off" state. The height of the graph indicates the ratio of reflected power to power incident on the code plate. Note that the code tracks are one core diameter wide.

Figure A-5.1b shows the smoothing effect of the nonzero fiber size on the spectral content of the output light.

Figure A-5.1c shows the output of the optical system (that incident on the CCD array). Notice that the illuminated width has increased from one core diameter (width of code track) to three core diameters. In order to avoid crosstalk (in this approximation), the detector size must be smaller than the length of the dark area shown in Figure A-5.1c (here 1/2 core diameter).

The current performance limitations of the optical assembly revolve around the spectral width requirements of the sensor. Currently, a 6 bit, 50 micron system requires a significant power density over a 110 nm range, when LED spectral shift over temperature is considered. Increasing the number of bits to 12 causes this value to change to 165 nm. Some possible remedies for this problem are considered below.

Some decrease in spectral range requirements might be realized by partial temperature control of the LED junction. An investigation into the trade-offs between minimizing temperature control circuitry and minimizing thermal spectral shift is indicated.

At present, the optical assembly which forms the basis for the rotary and linear position sensors (digital code plate devices), the analog sensors, and the demultiplexer is built around a 5 mm GRIN lens. The focal length of this lens is a constant, invariable parameter which, when coupled with the system fiber diameter and the grating pitch, determines the spectral width required of the light source system.

The fact that this required source spectral width is for the digital position sensors wider than that which can currently be provided by a single LED has caused Litton to go through elaborate gyrations involving couplers and multiple LEDs. Each additional LED has the effect of decreasing the resultant

output spectral power density, because an increase in the number of legs on a given coupler increases the loss of that coupler. The tradeoff is shown in Figure A-5.2.

If one were to decrease the spectral width of each bit to the extent that one LED would have enough spectral width for the whole sensor, a 4 dB increase in source power density would be realized. This increase should offset the decrease in power used per bit which is due to the decreased spectral bit width.

One can also reduce the spectral width required by decreasing the grating pitch. Currently, a practical minimum of 1/1800 mm exists, as more closely spaced grooves generally are more difficult to configure with the correct blaze angle, resulting in decreased grating efficiency. However, with holographic and electron beam techniques combined with ion milling, it is possible that high-efficiency gratings with much finer rulings may be obtained in the future.

Another alternative is to decrease the fiber diameter. Although this results in the freedom to use tracks which are narrower and closer together, requiring a smaller spectral width, there are disadvantages as well. Less launch power can be coupled into smaller diameter fibers. Connector losses also tend to increase. And finally, the use of nonstandard fiber may make the system more difficult to repair, should the need arise.

The third option is changing the effective focal length of the focusing element. There are many possible dispersive optical system designs which could accomplish this, enabling a single LED to be used as a light source for a digital position sensor using any fiber diameter, even allowing for wavelength shift of 30 nm or so.

A method of increasing the maximum operating temperature of the optical system to 200°C is currently being tested. If the jacket assembly problems (see Section 7.0) can be overcome, the entire optical system will be capable of 200°C operation.

Another possible improvement of the system is related to the code plate itself. Gold has a reflectivity about 1 dB better than aluminum in the 850 nm region, so code plate systems having gold code tracks would increase in on-off ratio by that amount.

The reflectivity of the non-reflective areas of the code plate is currently between one and two percent. A decrease of this value by 3 dB or so can be achieved by the use of state-of-the-art multilayer dielectric coatings, again resulting in increased on-off ratio.

6.0 Detection

Presently, there are two schemes for detecting the light returning from the sensor: discrete photodiodes in concert with a fiber optic wavelength division demultiplexer, and a CCD array onto which is projected the returning spectrum, which has been dispersed by a diffraction grating.

As light propagates through the optical system, its spectral power density (see Section 4.0) is decreased, according to the insertion loss of each device through which it passes. This quantity, which may be conveniently measured in pW/nm, may be multiplied by the spectral width of each channel to give the total optical power per channel. In systems using fiber optic demultiplexers, this quantity of power strikes the corresponding photodiode and is converted into electrical energy.

In systems using CCD arrays and optical projection, however, only part of the light contained in each channel is actually utilized by the system. Since each pixel intercepts a fraction of the light (the pixels being, in general, somewhat smaller than a fiber diameter), the quantity of light striking each one is a function of the spectral power density and the pixel size.

CCD devices are convenient for use in demultiplexer/detector systems because they are available in linear arrays with spacing roughly compatible with the output of the demultiplexer optical system. However, they have not been optimized to this application, and improvements to these devices are indicated.

The experiments performed to date have involved CCD arrays in which pixel widths (dimension perpendicular to array) have either been very large (3.2 mm for one device) or very small (13 um for another device). In the case where the pixel dimensions are large, unused pixel area contributes to the dark current, compromising the high temperature performance. When the pixel widths are small, the decrease in signal level causes high temperature amplifier drift to become a more significant factor. A CCD array with optimum pixel size (about one core diameter) would therefore improve the performance of the device.

One type of device has been tested at elevated temperature with promising results. A curve of dark current vs temperature was obtained, and indicates that if the integration time is decreased to 5 ms or so, the device has about a one volt operating range at 115°C, and with a small further decrease, 125°C operation can be expected.

The amplifiers on the chip, however, have proven somewhat less capable of dealing with higher temperatures. Several devices failed during high temperature testing. It is believed that these amplifiers are at fault.

CCD arrays which perform over the target temperature range are possible to develop, but the commercial CCD industry is reluctant to undertake the effort.

A PIN array integrated with individual preamplifiers is also possible. This device would have the advantage of being readable in parallel, rather than serially, as in the CCD.

Figure A-6.1 shows two possible types of integrated PIN circuitry. Parallel access to the PIN's is possible by using separate amplifier circuits for each channel. Alternatively, a single main amplifier may be used in conjunction with electronic multiplexing to get a serial output.

If higher sensitivity is required, the use of APD's should be considered.

7.0 Optical Interconnect

The optical interconnect is composed of the fibers, jacket assemblies and connectors used to connect the light source, sensor, and demultiplexing/decoding circuitry.

Asymmetric (non-reciprocal) couplers for use in fiber optic data buses have been extensively developed at Litton, and no major advances in coupler technology likely to improve the sensor interconnect performance are foreseen.

Connectors for use in single fiber interconnects, however, may be another story, Problems involving the use of currently available connectors with reflective sensors fall into two categories: lack of intermating repeatability and high backreflection.

The cores of multimode optical fibers, although much larger than those of singlemode fibers, are still quite small. A single speck of dust or other offensive material can cause attenuations of several dB. This effect introduces a practical repeatability problem even with keyed connectors such as FC or ST connectors. In addition, the use of these connectors results in a large fraction (approx. 10%) of the light incident on a connector-to-connector joint being reflected back through the fiber.

This backreflection problem can be dealt with by index matching or physical contact. By index matching is meant the introduction of a liquid or gel material between the fiber faces so that no backreflection can occur. Disadvantages of this are the possibility of migration of the material resulting in a loss of index matching and an increase in backreflection, and contamination of the material.

Physical contact means that the flat surfaces of the fiber ends are brought into contact so that there is no intervening gap. The light propagates through essentially as if there were only one unbroken fiber. A disadvantage of this approach is the likelihood of destruction of the fiber faces if they chatter against each other in a high vibration environment.

A possible method of overcoming these difficulties involves the use of keyed, off-center lensed connectors as shown in Figure A-7.1. This kind of connector should keep backreflections down to more than 25 dB below the signal incident on a connector-to-connector joint. In addition, the optical loss of the joint will be much less sensitive to particulate contamination, thereby improving repeatability.

The technology required to develop this connector exists, and an effort in this direction would improve the case for single fiber interconnects considerably.

Obtaining cable assemblies capable of functioning with minimum loss over wide temperature ranges has proven to be a nontrivial exercise. Although jacket materials which do not degrade at temperatures from -55°C to 125°C are available, two distinct problems have presented themselves.

The first is irreversible shrinkage when subjected to temperatures above about 70°C. This is due to the speed of extrusion of the cable. Although the manufacturer of the high temperature jacketing has expressed reluctance to

change the extrusion process, perhaps they could be induced to do so, given the proper incentive.

A second, more intractable problem is a result of the high coefficient of thermal expansion characteristic of the materials involved. Since the fiber itself has an extremely low expansion coefficient, it is difficult to match this with currently available jacket materials. As the temperature rises, then, the fiber is placed under tension, and as the temperature decreases, it is compressed. These effects lead to microbending of the fiber leading to increased loss. One possible solution to this problem, the use of service loops in splice housings and couplers, has been ruled out because of size constraints.

An alternative jacket concept using composite rods as strength members is currently under investigation. It seems promising, and may well eliminate both of the thermal problems discussed above.

A development effort in this area is necessary for any rugged fiber optic system to be used in an environment subject to large temperature swings. The effort must be carried out by fiber jacket manufacturers, who are capable of extruding jacket materials onto optical fiber.

8.0 Summary

Efforts to develop better temperature performance in fiber jacket assemblies (necessary for any fiber optic sensor type), detector circuitry capable of handling wide temperature ranges and having high reliability, and broad spectrum LEDs are currently underway. These efforts, in addition to work on alternative optical assemblies for the sensors themselves, will enable WDM to mature as an aircraft control system technology.

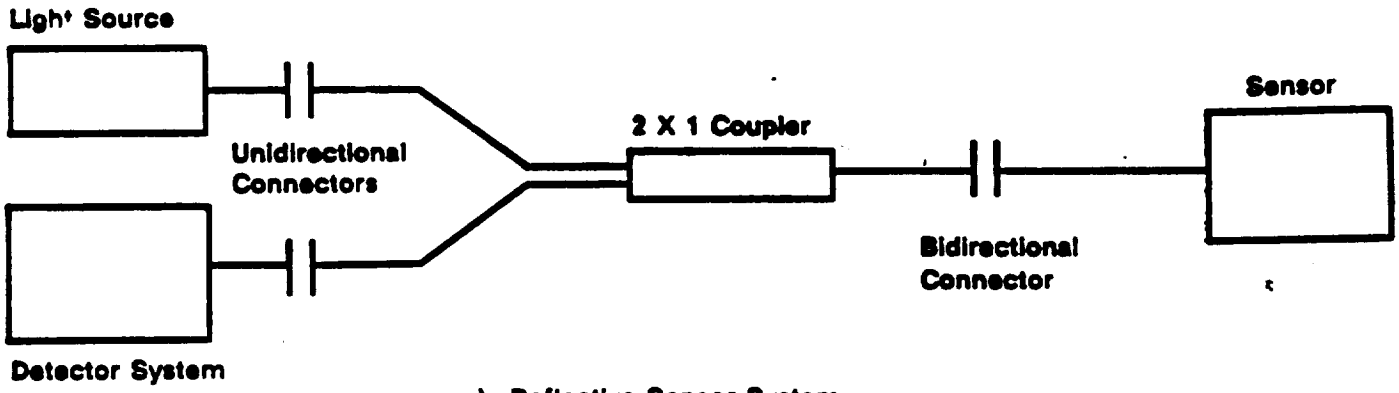

a) Reflective Sensor System

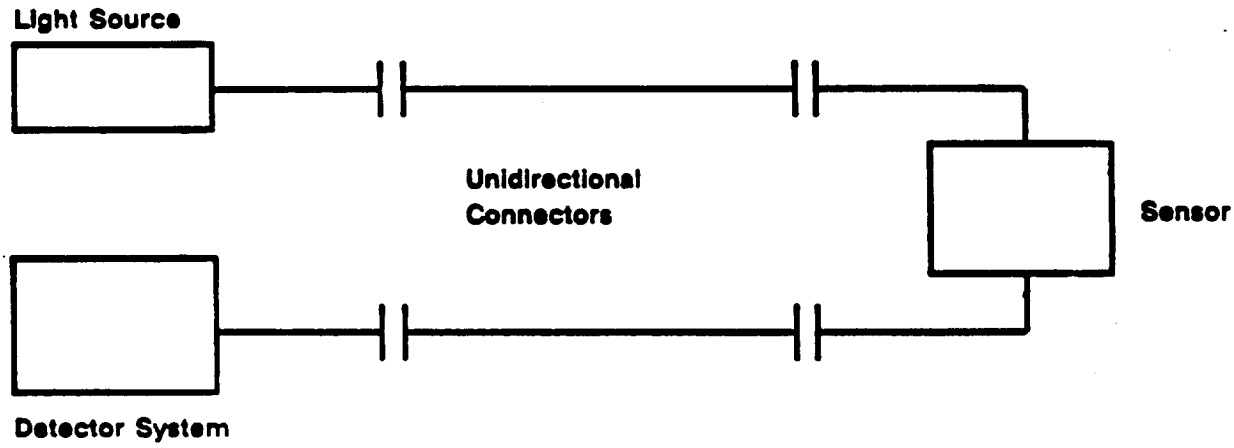

b) Transmissive Sensor System

FIGURE A-3.1 Reflective versus Transmissive Sensor Systems

Unidirectional connectors are those through which light of interest flows in only one direction. Bidirectional connectors have important light flowing in both directions, and are therefore susceptible to backreflection problems.

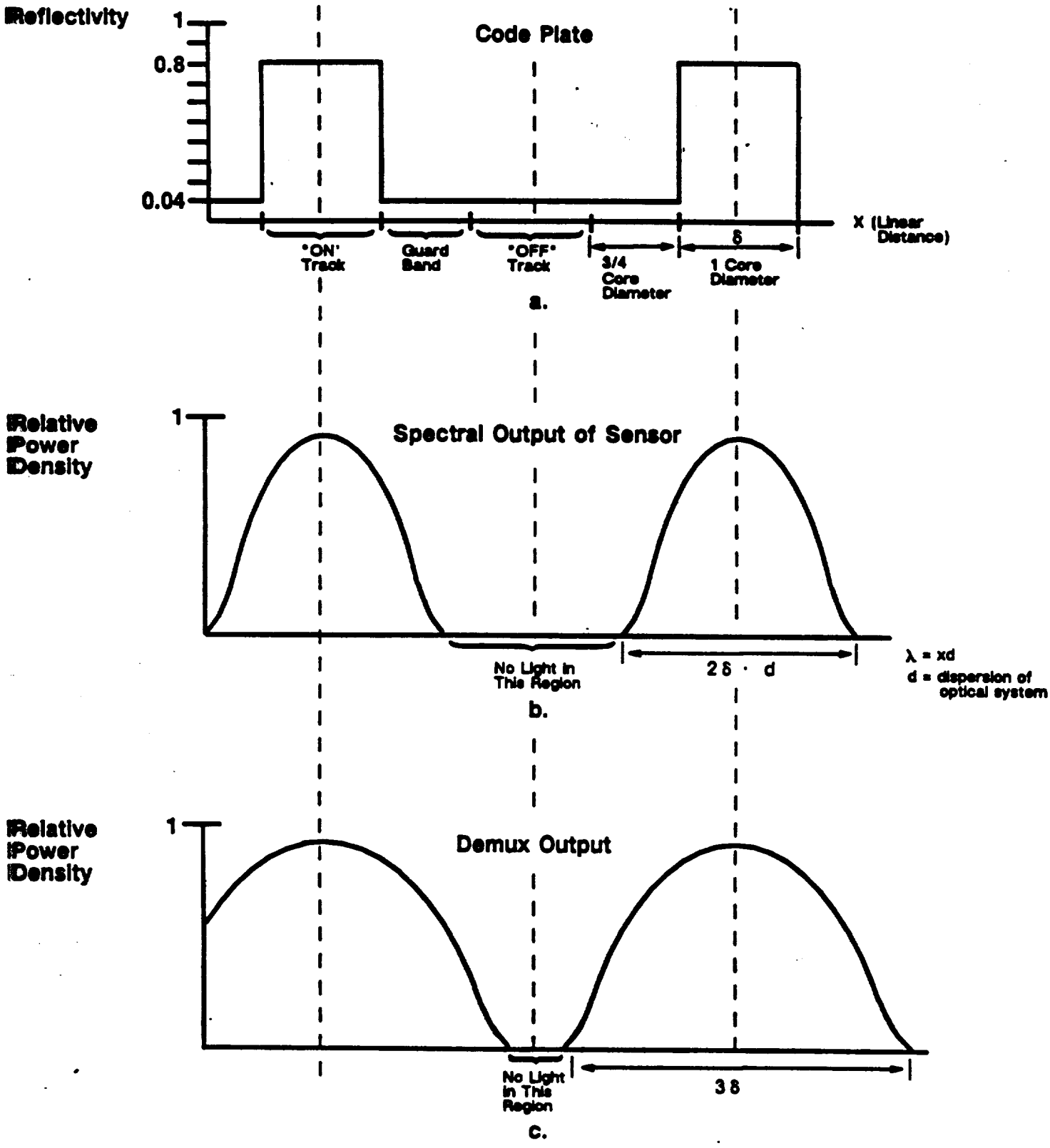
Reflectivity
1
0.8
0.04
Code Plate
X (Linear Distance)
'ON' Track
Guard Band
'OFF' Track
3/4 Core Diameter
δ
1 Core Diameter
a.
Relative Power Density
1
Spectral Output of Sensor
No Light in This Region
2δ · d
λ = xd
d = dispersion of optical system
b.
Relative Power Density
1
Demux Output
No Light in This Region
3δ
c.

FIGURE A-5.1

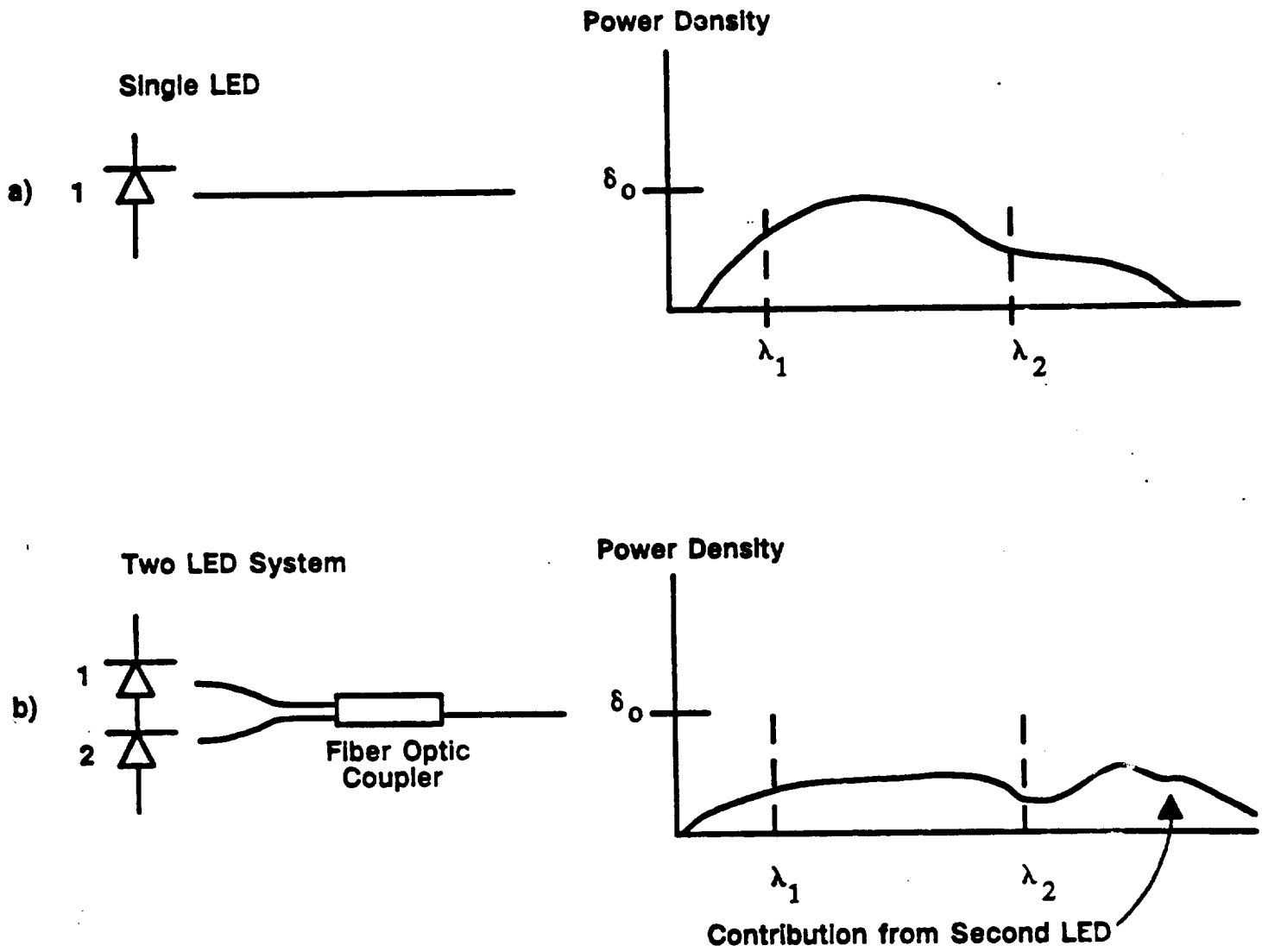

FIGURE A-5.2 Increasing the number of LED's from one to two results in approximately 4 dB decrease in system loss, the loss involved in using a coupler to combine the LED's outputs onto one fiber. Increasing the number of LED's to three results in an additional 2 dB decrease in output density.

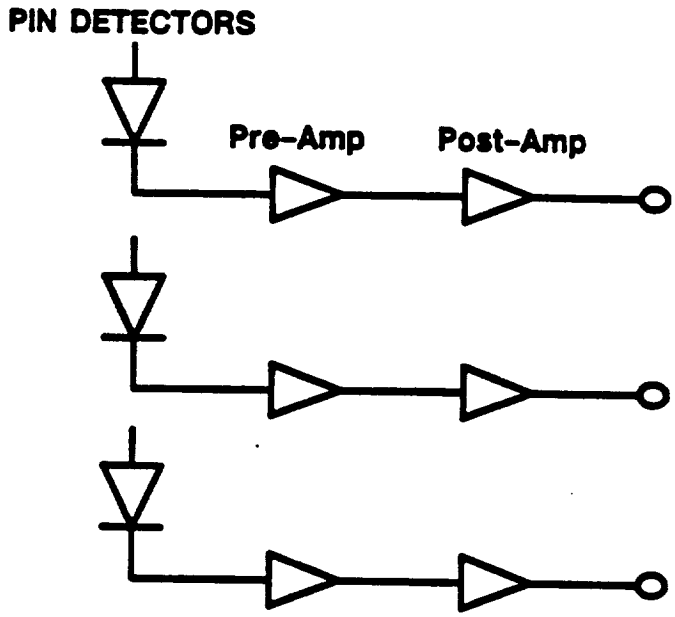

(a) Parallel Outputs

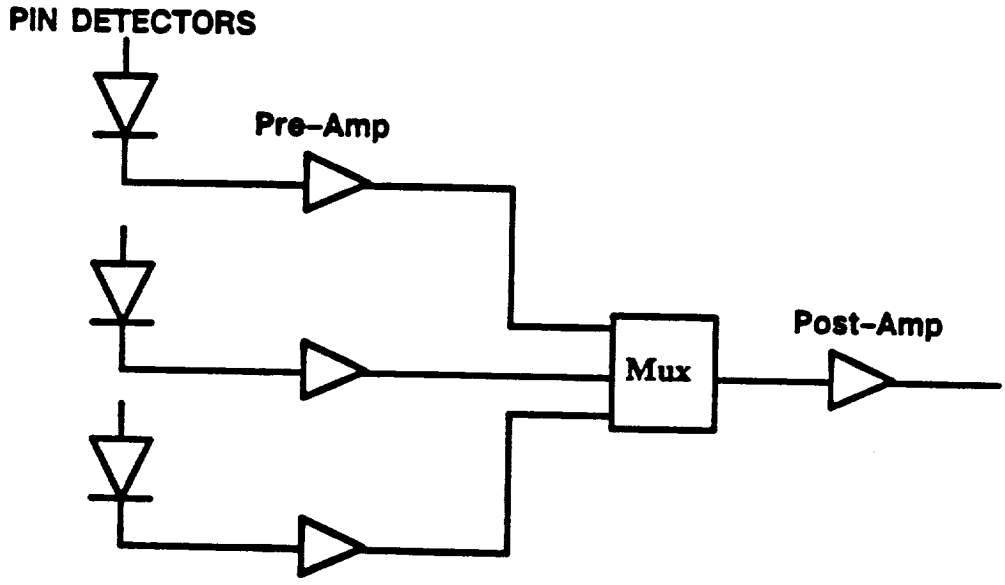

(b) Serial Output

FIGURE A-6.1 Schemes for accessing a PIN array.

(b) shows how a serial output may be obtained by means of a multiplexer between amplifier stages.

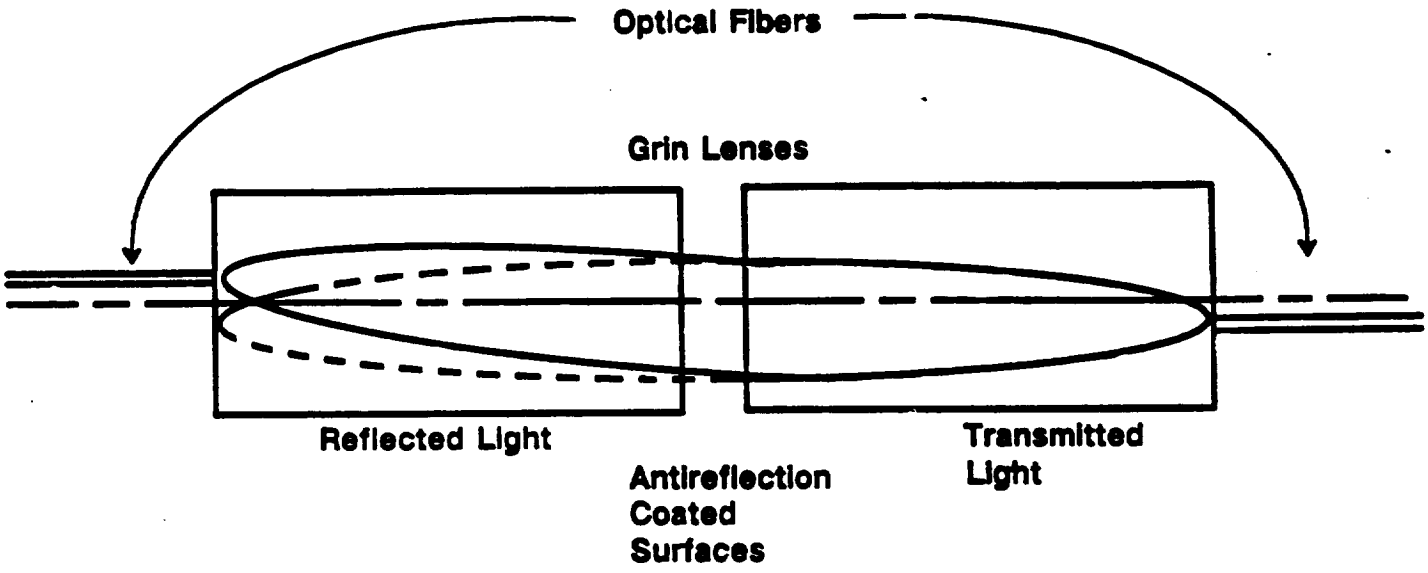

FIGURE A-7.1 Off-Center Lensed Connector Concept

In this approach, the light reflected from the lens surfaces is focused to a spot some distance away from the fiber. The two lens faces are antireflection coated to maximize transmission.

Distribution List

Robert Baumbick
NASA Lewis Research Center
21000 Brookpark Road, MS 77-1
Cleveland, OH 44135

Norm Wenger
NASA Lewis Research Center
21000 Brookpark Road, MS 77-1
Cleveland, OH 44135

Joel Terry
U.S. Army
SAVRT-TY-ATA
Ft. Eustis, VA 23604-5577

Les Small
Commander
AFWAL/POTC
Wright Patterson AFB, OH 45433

Code 933E/Andrew Glista
Naval Air Systems Command
Washington, DC 20361

Code 931E/George Derderian
Naval Air Systems Command
Washington, DC 20361

Ruso Vizzini
Naval Air Propulsion Center
1 Code PE 32
Trenton, NJ

James McPartland
Naval Air Development Center
1 Code 6012
Stoet Rd.
Warminster, PA 18974

Randy Morton
ELDEC Corp.
P.O. Box 3006
Bothell, WA 98041-3006

Gary Seng
NASA Lewis Research Center
21000 Brookpark Road, MS 77-1
Cleveland, OH 44135

Technology Utilization Office
NASA Lewis Research Center
21000 Brookpark Road, MS 7-3
Cleveland, OH 44135

D. Varshneya
Teledyne Ryan Electronics
8650 Balboa Ave.
San Diego, Ca
(619) 569-2450

Chuck Porter
Boeing Electronics
P.O. Box 24969, M/S 7J-05
Seattle, WA 98124-6269

Bruce L. McManus
Boeing Helicopters
P.O. Box 16858, M/S P31-25
Philadelphia, PA 19142-0858

Eric Henderson
Sundstrand - ATG, Dept. 740E6
P.O. Box 7002
Rockford, IL 61125

Steve Emo/Eric Arnett
Bendix-Engine Controls Division
Dept. 862
717 N. Bendix Dr.
South Bend, IN 46615

Mahesh Reddy
Boeing Electronics
Fiber Optics Product Development
P.O. Box 24969, M/S 9J-12
Seattle, WA 98124

David Griffith
Boeing Commercial Airplanes
P.O. Box 3707, M/S 6H-97
Seattle, WA 98124

Distribution List

Kausar Talat
Boeing Advanced Systems
P.O. Box 3707, M/S 32-52
Seattle, WA 98124

Stan Maki
General Dynamics, Space Systems
P.O. Box 85990, M/S DC-8743
San Diego, CA 92138

Imre Takats
Boeing Advanced System
P.O. Box 3707, M/S 33-02
Seattle, WA 98124-2207

Floyd M. Cassidy
Honeywell MICRO SWITCH
P.O. Box 681
Beverly Hill, FL 32665

Norris E. Lewis
Litton Poly-Scientific
1213 N. Main St.
Blacksburg, VA 24060

John W. Berthold
Babcock & Wilcox
1562 Beeson St.
Allison, OH 44601

Jim Findlay
Douglas Aircraft Co.
C1-E83 212-13
Lakewood Blvd.
Long Beach, CA 90846

Bob Lebduska
SAIC
10610 Campus Point Dr., M/S 45
San Diego, CA 92121